UNIVERSIDADE FEDERAL DO PARANÁ

JULIANO PIEREZAN

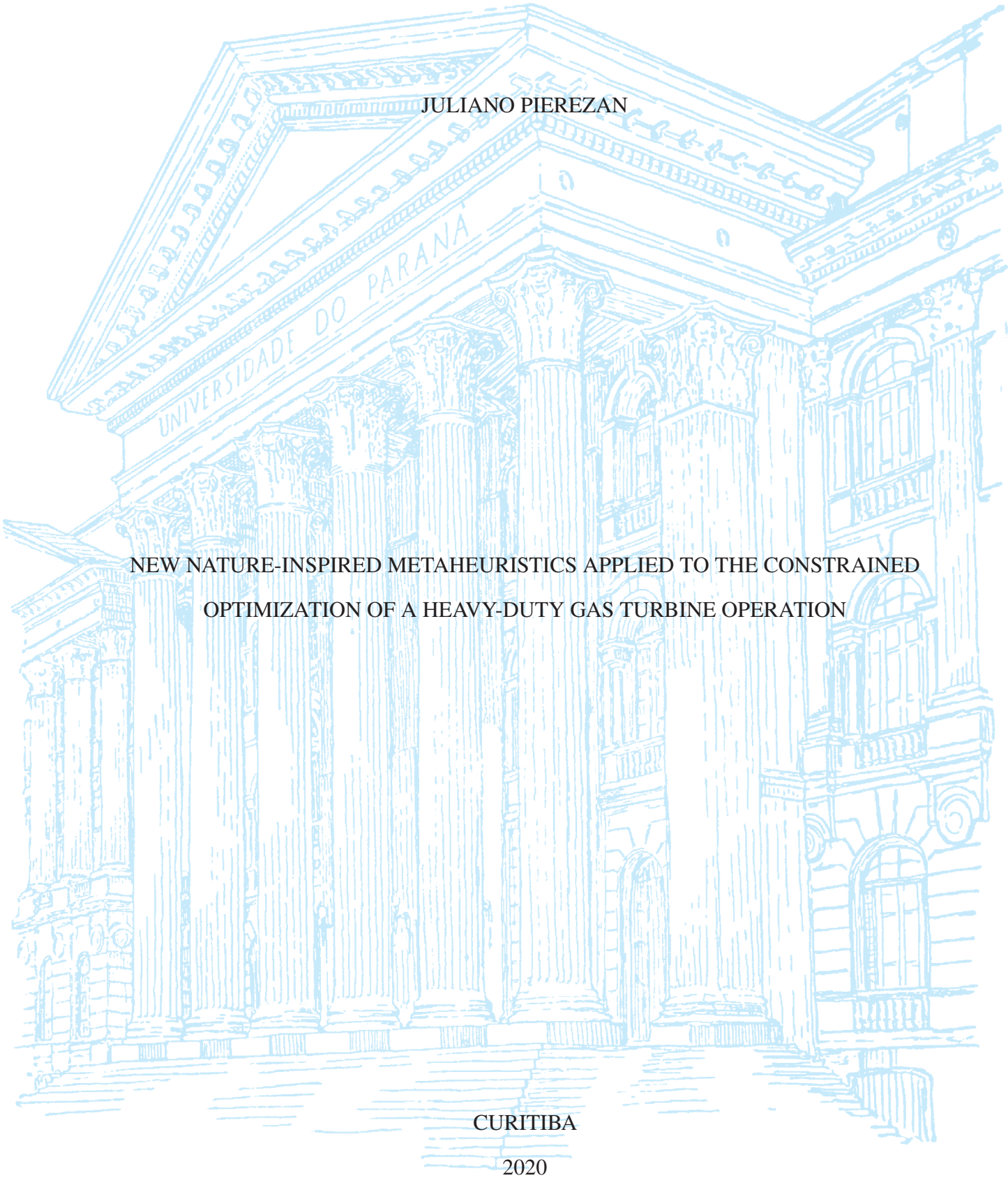

NEW NATURE-INSPIRED METAHEURISTICS APPLIED TO THE CONSTRAINED OPTIMIZATION OF A HEAVY-DUTY GAS TURBINE OPERATION

CURITIBA

2020

JULIANO PIEREZAN

NEW NATURE-INSPIRED METAHEURISTICS APPLIED TO THE CONSTRAINED OPTIMIZATION OF A HEAVY-DUTY GAS TURBINE OPERATION

Tese apresentada como requisito parcial à obtenção do grau de Doutor em Engenharia Elétrica no Programa de Pós-Graduação em Engenharia Elétrica, setor de Ciências Exatas, da Universidade Federal do Paraná.

Área de concentração: *Sistemas Eletrônicos*.

Orientador: Prof. Dr. Leandro dos Santos Coelho.

CURITIBA

2020

CATALOGAÇÃO NA FONTE – SIBI/UFPR

P618n Pierezan, Juliano

New nature-inspired metaheuristics applied to the constrained optimization of a heavy-duty gas turbine operation [recurso eletrônico]/ Juliano Pierezan - Curitiba, 2020.

Tese apresentada como requisito parcial à obtenção do grau de Doutor em Engenharia Elétrica no Programa de Pós-Graduação em Engenharia Elétrica, setor de Ciências Exatas, da Universidade Federal do Paraná. Área de concentração: Sistemas Eletrônicos.
Orientador: Prof. Dr. Leandro dos Santos Coelho.

1. Inteligência computacional. 2. Algorítmicos genéticos. I. Coelho, Leandro dos Santos. II. Título. III. Universidade Federal do Paraná.
CDD 006.3

Bibliotecária: Vilma Machado CRB9/1563

TERMO DE APROVAÇÃO

Os membros da Banca Examinadora designada pelo Colegiado do Programa de Pós-Graduação em ENGENHARIA ELÉTRICA da Universidade Federal do Paraná foram convocados para realizar a arguição da tese de Doutorado de **JULIANO PIEREZAN** intitulada: **New nature-inspired metaheuristics applied to the constrained optimization of a heavy-duty gas turbine operation**, sob orientação do Prof. Dr. LEANDRO DOS SANTOS COELHO, que após terem inquirido o aluno e realizada a avaliação do trabalho, são de parecer pela sua APROVAÇÃO no rito de defesa.

A outorga do título de doutor está sujeita à homologação pelo colegiado, ao atendimento de todas as indicações e correções solicitadas pela banca e ao pleno atendimento das demandas regimentais do Programa de Pós-Graduação.

CURITIBA, 26 de Novembro de 2020.

Assinatura Eletrônica
26/11/2020 13:27:16.0
LEANDRO DOS SANTOS COELHO
Presidente da Banca Examinadora

Assinatura Eletrônica
28/11/2020 10:47:02.0
FREDERICO GADELHA GUIMARAES
Avaliador Externo (UNIVERSIDADE FEDERAL DE MINAS GERAIS)

Assinatura Eletrônica
26/11/2020 15:41:55.0
JULIO CÉSAR NIEVOLA
Avaliador Externo (PONTIFÍCIA UNIVERSIDADE CATÓLICA DO PARANÁ)

Assinatura Eletrônica
27/11/2020 09:17:20.0
AURORA TRINIDAD RAMIREZ POZO
Avaliador Externo (UNIVERSIDADE FEDERAL DO PARANÁ)

Dedico este trabalho à minha filha
Maria Helena Quintanilha Pierezan.

ACKNOWLEDGEMENTS

Sou muito grato à minha família, pela oportunidade do estudo e pelo apoio incondicional durante todas as etapas dessa jornada.

Ao professor Leandro dos Santos Coelho, pela oportunidade de cursar o doutorado sob a sua orientação, pela sua competência em liderar as nossas pesquisas e pela compreensão nos momentos de maior dificuldade.

A todos os coautores com quem tive a oportunidade de trabalhar durante o programa, em especial à Viviana Cocco Mariani, com quem tive mais contato durante esses anos de pesquisa. Todos os resultados que obtivemos só foram possíveis devido ao trabalho em equipe.

A todos os meus amigos e colegas de trabalho, principalmente do Instituto Lactec e da Robert Bosch, que sempre me apoiaram e compartilharam conhecimento.

E, por fim, à Coordenação de Aperfeiçoamento de Pessoal de Nível Superior (CAPES) e ao Instituto Lactec pelo financiamento parcial desta pesquisa.

RESUMO

Os códigos computacionais complexos das mais diversas áreas, tais como indústria 4.0 e energia, apresentam características como não-linearidade, escala, multimodalidade e presença de restrições. Por este motivo, as técnicas clássicas Newtonianas e baseadas em gradiente não são recomendadas para problemas de otimização global, os quais contém inúmeras variáveis de projeto, restrições e simulações incorporadas. Isso incentivou novas pesquisas em metaheurísticas baseadas em fenômenos naturais, principalmente comportamentos de animais com características cooperativas ou colaborativas. Entretanto, não existe um algoritmo único capaz de ter bom desempenho para todos os tipos de problemas de otimização, o que justifica a busca recorrente por novas abordagens para solucionar esses problemas. Portanto, a presente tese introduz duas metaheurísticas com estruturas inovadoras inspiradas na natureza e nunca propostas. A primeira é baseada na espécie *Canis latrans* e denominada Algoritmo de Otimização dos Coiotes (do inglês *Coyote Optimization Algorithm*, COA). A segunda, por sua vez, é inspirada na espécie *Cebus capucinus* e denominada Otimizador dos Macacos-prego-da-cara-branca (do inglês *White-faced Capuchin Monkeys Optimizer*, WfCMO). Os algoritmos propostos são avaliados sob um conjunto de funções de benchmarks empregadas nas competições do Congresso de Computação Evolutiva (do inglês *Congress on Evolutionary Computation*, CEC) organizado pelo Instituto de Engenheiros Eletricistas e Eletrônicos (do inglês *Institute of Electrical and Electronics Engineers*, IEEE) e comparadas a outras metaheurísticas inspiradas na natureza. Além disso, a modelagem de um problema de otimização com restrições de uma turbina a gás do tipo *heavy-duty* de uma termelétrica brasileira também é proposto nesta pesquisa. Para solucioná-lo, uma versão cultural do COA é proposta e seu desempenho é avaliado e comparado com outros algoritmos do estado-da-arte. Os resultados mostram que as metaheurísticas propostos nesta pesquisa alcançaram desempenho satisfatório e superaram os outros algoritmos com 95% de confiança estatística com base no teste não-paramétrico de Wilcoxon-Mann-Whitney e também nos critérios do IEEE CEC 2017. Ainda, os resultados conquistados para problems multimodais e de alta dimensão mostram que as técnicas são promissoras para estes tipos de problema, que são usuais em problemas reais. Ademais, as análises de curva de convergência e de diversidade da população indicam um balanço adequado entre exploração e aproveitamento. Por fim, a versão cultural do COA, que se demonstrou capaz de evitar convergência prematura, superou os demais algoritmos do estado-da-arte para o problema de otimização da operação da turbina.

Palavras-chave: Indústria 4.0, Inteligência Computacional, Otimização Global, Metaheurísticas inspiradas na natureza.

ABSTRACT

The real-world applications from the most diverse fields such as industry 4.0 and energy have been formulated into complex computational codes with features as non-linearity, scale, multimodality, and the presence of constraints. Because of that, the classic Newtonians and gradient-based techniques are not recommended for global optimization applications with many design variables, constraints, and simulations embedded. It has encouraged new researches on metaheuristics based on natural phenomena, mainly animal behaviors with cooperative or collaborative features. However, there is not a unique algorithm able to perform well for all types of optimization problems, which justifies the recurrent search for new approaches. Hence, this thesis presents two never-proposed nature-inspired metaheuristics with innovative structures. The first one is based on the *Canis latrans* species and it is denoted Coyote Optimization Algorithm (COA). The second one is inspired by the *Cebus capucinus* species and receives the name of White-faced Capuchin Monkeys Optimizer (WfCMO). The proposed algorithms are evaluated under a set of benchmark functions employed in the Institute of Electrical and Electronics Engineers (IEEE) Congress on Evolutionary Computation (CEC) competitions and compared to other state-of-the-art nature-inspired metaheuristics. Besides, the design of a constrained optimization problem of a heavy-duty gas turbine operation from a Brazilian thermoelectric power plant is proposed in this research. To solve it, a cultural version of the COA is proposed and its performance is evaluated and compared to other state-of-the-art algorithms. The results show that the proposed metaheuristics achieve profitable performance and outperform some state-of-the-art algorithms with 95% of statistical confidence based on the Wilcoxon-Mann-Whitney non-parametric test and the criteria of the IEEE CEC of 2017. Also, these algorithms present promising results for multimodal and high dimensional problems, which are the most usual features of real-world problems. Moreover, the convergence and diversity curves indicate a suitable balance between exploration and exploitation. Further, the proposed cultural version of the COA outperforms other state-of-the-art algorithms for the gas turbine operation problem. Its ability to avoid premature convergence is also demonstrated.

Keywords: Industry 4.0, Computational Intelligence, Global Optimization, Nature-Inspired Metaheuristics.

LIST OF FIGURES

LIST OF TABLES

LIST OF ACRONYMS

ABC	Artificial Bee Colony
ACO	Ant Colony Optimization
AI	Artificial Intelligence
ANFIS	Adaptive Neuro-Fuzzy Inference System
ANN	Artificial Neural Networks
BA	Bat Algorithm
BCF	Bacterial Colony Foraging
BSA	Backtracking Search Algorithm
CCOA	Cultural Coyote Optimization Algorithm
CEC	Congress on Evolutionary Computation
COA	Coyote Optimization Algorithm
CFD	Computational Fluid Dynamics
CO	Carbon Oxides
CO_2	Carbon Dioxides
CSO	Cat Swarm Optimization
DE	Differential Evolution
DEc	Dolphin Echolocation
DFGT	Dual Fuel Gas Turbine
EA	Evolutionary Algorithm
FA	Firefly Algorithm
FPA	Flower Pollination Algorithm
FWER	Family-Wise Error Rate
GA	Genetic Algorithm
GD	Gas Demand
GDP	Gross Domestic Product
GSA	Grasshopper Optimisation Algorithm
GT	Gas Turbine
GWO	Grey Wolf Optimizer
HR	Heat Rate
I4.0	Industry 4.0
IEEE	Institute of Electrical and Electronics Engineers
IGV	Inlet Guide Vanes
IQR	Interquartile Range
MFANN	Multi Feedforward Artificial Neural Networks
MLP	Multilayer Perception

NARX	Nonlinear Autoregressive Exogenous
NiM	Nature-inspired Metaheuristics
NO_x	Nitrogen Oxides
NSGA-II	Non-dominated Sorting Genetic Algorithm II
PID	Proportional-Integral-Derivative
PSO	Particle Swarm Optimization
R&D	Research and Development
RBF	Radial Basis Function
SaDE	Self-adaptive Differential Evolution
SFC	Specific Fuel Consumption
SI	Swarm Intelligence
SIMPLE	Semi-Implicit Method for Pressure Linked Equations
sMAPE	Mean Absolute Percentage Error
SMO	Spider Monkey Optimization
SOS	Symbiotic Organisms Search
SSA	Social Spider Algorithm
SVM	Support Vector Machine
TOPSIS	Technique for Order of Preference by Similarity to Ideal Solution
VCS	Virus Colony Search
WfCMO	White-faced Capuchin Monkeys Optimizer
WOA	Whale Optimization Algorithm

CONTENTS

1 INTRODUCTION

Real-world problems have been formulated into computational codes from the most diverse application fields including robotics, aerospace, civil, mechanical, mechatronics, chemicals, health science, information science, and sports (Antoniou and Lu, 2007; Yang and Koziel, 2011). The combination of intelligent algorithms and digital integration to applications of these fields has generated the term Industry 4.0 (I4.0) (Muhuri et al., 2019). This term has become widespread among the researcher, especially because of the numerous applications that have been published in scientific journals during the last decade, as drawn in Fig. 1.1. A considerable set of Artificial Intelligence (AI) techniques have already been applied to complex industrial systems (Shukla et al., 2019), such as the Industrial Gas Turbines (GT).

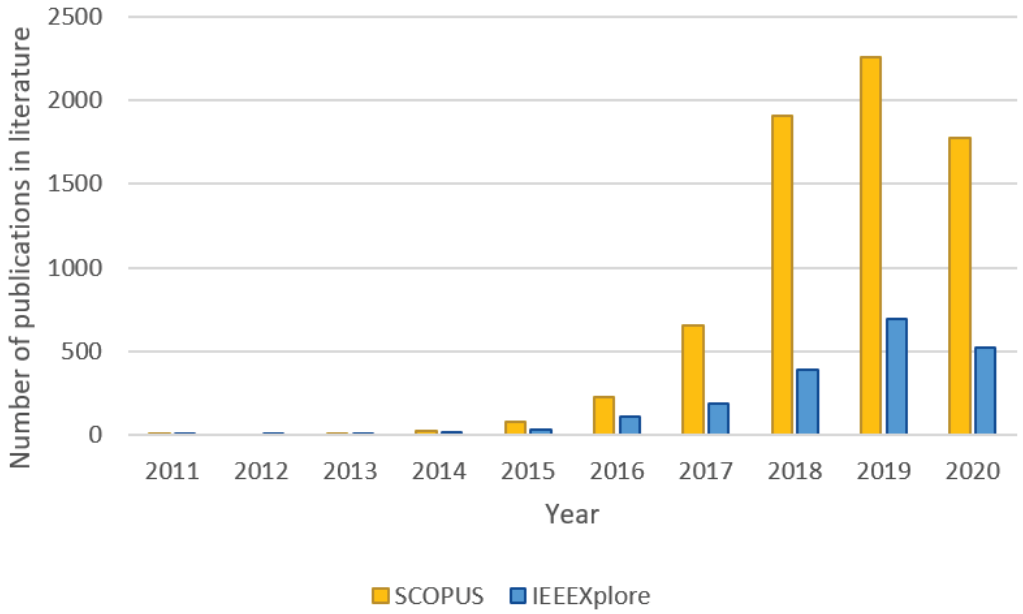

Figure 1.1: Number of papers related to Industry 4.0 over the last decade (Scopus and IEEEXplore databases).

The industrial GTs, also denoted heavy-duty GTs, have been widely used in the energy generation industry. The GTs offer high power output along with a high combined cycle efficiency, lower emissions, and also high fuel flexibility (Vyncke-Wilson, 2013). It is a consequence of the price, the environmental concerns, and the fuel diversification (Demirbas, 2009) provided by the natural gas, which has been used as fuel for power plants able to generate a couple of hundred megawatts. Unlike the advantages of this type of equipment, there are numerous problems related to the gas turbines maintenance, such as aging of gas path components, fouling in the air filter and compressor, excessive clearance due to rubbing, and malfunctions (Lemma et al., 2016). In addition, problems related to the polluting emissions and pressure oscillations in the combustion chamber that are highly complex to be mathematically written as white-box systems have been studied (Yamao et al., 2017a,b; Pierezan et al., 2017b).

Therefore, many internal and external features might be considered in order to improve a heavy-duty gas turbine effectiveness. The main topics explored are modeling and simulation, control, thermodynamic analysis, pollutant emissions, vibration, fault diagnosis, and exergy

efficiency. As example, some recent researches related to industrial GTs are summarized in Tabs. 1.1 and 1.2.

An approach suggested by many researchers is to convert mechanical, electrical, and chemical systems into optimization problems, which means to search for a set of parameters to achieve a determined objective (Yang et al., 2013). Such methodology has been successfully employed in many industrial and engineering applications in the last decades (LaTorre et al., 2015; Zelinka et al., 2013). The most challenging part of this methodology is that the resulting optimization problem usually presents non-linear behavior, multimodality, which means the presence of only one convex region or numerous local optima, non-separability, which means the minimization of the problem's cost depends on the manipulation of multiple variables at a time, and the presence of optimization constraints (Mahdavi et al., 2015; Suganthan et al., 2016).

The first optimization techniques proposed were the classic Newtonians and gradient-based (as the Hill-climbing, Conjugate Gradient, Downhill Simplex, and Pattern Search), which mathematically guarantee the convergence to an optimal solution. According to (Rao, 1996), these methods can be classified as deterministic ones and they perform well for local search problems. However, considering many recent global optimization problems with multiple design variables, constraints, and simulations embedded, other approaches are welcome to complement these methods.

Hence, the research on new algorithmic approaches for complex global optimization has begun with heuristics like the Simulated Annealing, the Tabu Search, and the GA (Goldberg, 1989). These methods are classified as stochastic and according to (Boyd and Vandenberghe, 2004) they do not guarantee the convergence to the global optimum, but they do guarantee the avoidance of the worst solutions possible due to their evolutionary feature. Based on this principle, the development of new stochastic techniques has started and some of the most widespread metaheuristics have been proposed. The Evolutionary Algorithm (EA) denoted Differential Evolution (DE) (Storn and Price, 1995, 1997), which is based on Darwin's evolution theory, and the Swarm Intelligence (SI) algorithm called Particle Swarm Optimization (PSO) (Kennedy and Eberhart, 1995), which is inspired on the synchronized flock of birds.

After the proposal of these algorithms, the exponential growth of researches on new metaheuristics for handling global optimization has been noted in the literature, as shown in Fig. 1.2. Several EA and SI methods have been proposed mainly as an improvement of the GA, the DE, and the PSO techniques (Mahdavi et al., 2015; Boussaïd et al., 2013; Das et al., 2011). Furthermore, many algorithms inspired by nature have been proposed and explored in the last decades, resulting in the creation of the Nature-inspired Metehuristics (NiM) classification (Dokeroglu et al., 2019).

Among the numerous optimization techniques, from the classic methods to the most recent metaheuristics, the nature-inspired ones have shown the most promising results in many research areas (Yang, 2014; Boussaïd et al., 2013; Salcedo-Sanz, 2016). Defined as techniques that try to copy nature, these algorithms are inspired by the most diverse phenomena. Some are based on animal movements, another on the social relations of some species. The communication, social hierarchy, and echolocation are examples of many other diverse natural inspirations found in the recent literature (Zang et al., 2010).

Several nature-inspired metaheuristics have been proposed in the last decades and the majority of them is based on some animal behavior. As example of that, there are the Ant Colony Optimization (ACO) (Dorigo et al., 2006), the Artificial Bee Colony (ABC) (Karaboga and Basturk, 2007), the Bacterial Colony Foraging (BCF) (Chen et al., 2014a), the Bat-Inspired Algorithm (BA) (Yang, 2010), the Cat Swarm Optimization (CSO) (Chu et al., 2006), the Dolphin Echolocation (DEc) (Kaveh and Farhoudi, 2013), the Firefly Algorithm(FA) (Yang, 2009), the

Table 1.1: Literature review related to industrial GTs - Part I

Year	Short description
2011	A white-box turbulence model based on the Semi-Implicit Method for Pressure Linked Equations (SIMPLE) algorithm (Wang et al., 2011).
2011	Correlation of reliability indicators, fuel consumption and carbon dioxide (CO_2) emissions of a GT cogeneration power plant (Hazi et al., 2011).
2011	Evaluation of the aerodynamic performance resulting from the fuel change on the turbine cascade of ground heavy-duty GT (Liu and Wang, 2011).
2011	White-box identification and real-time simulation of a GT (Chacartegui et al., 2011).
2012	GT heat and power identification from real data using ANN (Nikpey et al., 2012).
2013	Analysis of hybrid solid oxide fuel cells in the GT cycle (Zabihian and Fung, 2013).
2014	GT fault diagnosis system using Support Vector Machine (SVM) (Hu et al., 2014).
2014	Optimization of the performance of a GT cycle using a thermodynamic and energy study of a regenerator (Saria et al., 2014).
2014	Analysis of GT cycle NOx releases (Hajer et al., 2014).
2015	GT frequency vibration prediction using real data and ANN (Ben Rahmoune et al., 2015).
2015	Dynamic Multilayer Perceptron (MLP) networks as pattern classifier applied to GT fault detection (Sina Tayarani-Bathaie and Khorasani, 2015).
2015	Different methods of cooling the inlet air to GTs in Fars combined cycle power plants (Ghanaatpisheh and Pakaein, 2015).
2016	Analysis of the effect of ambient parameters on the performance of combined cycle GT power plants (Plis and Rusinowski, 2016).
2016	A Fuzzy Proportional-Integral-Derivative (PID) Controller for a GT power plant (Karande et al., 2015).
2016	The reliability analysis of the combined cycle GT power plant using the multi-state Markov model (Lisnianski et al., 2016).
2016	Efficiency metrics of heavy-duty GT systems using natural gas and syngas (Sorgenfrei and Tsatsaronis, 2016).
2016	GT modeling using fuzzy neural network approaches based on real data acquired and classification (Benyounes et al., 2017, 2016).
2017	Thermal performance evaluation of a GT power plant based on exergy analysis (Ibrahim et al., 2017).
2017	Optimization of Inlet Guide Vanes (IGV) position in a heavy-duty GT on part-load performance using a multiobjective approach (Mehrpanahi and Payganeh, 2017).
2017	Combined cycle efficiency optimization using evolutionary metaheuristic based on the Genetic Algorithm (GA) (Cao et al., 2017)
2017	A GT white-box model and its respective simulation (Zhang, 2017).
2017	A GT black-box dry low emissions model approach using Nonlinear Autoregressive Exogenous (NARX) model (Tarik et al., 2017)
2017	A regression-based prognostic model combined with an Adaptive Neuro-Fuzzy Inference System (ANFIS) to predict deposition and fouling in the compressor section of GT engines (Hanachi et al., 2017).
2017	A system of control and diagnostic of vibration in GTs using NARX neural networks (Ben Rahmoune et al., 2017).

Table 1.2: Literature review related to industrial GTs - Part II

Year	Short description
2018	Transient behavior of heavy-duty GTs based on a white-box simulation model optimized by a Genetic Algorithm (GA) (Chaibakhsh and Amirkhani, 2018).
2018	A multi-objective approach for Computational Fluid Dynamics (CFD) optimizations of water spray injection in GT combustors considering the Nitrogen Oxides (NO_x) emissions (Amani et al., 2018).
2018	Two-steps method to improve the robustness of GT gas-path fault diagnosis against sensor faults (Li and Ying, 2018).
2018	The modeling and simulation of a heavy-duty GT operating under temperature control mode under steady-state conditions in the popular Rowen GT model (Kim et al., 2018).
2018	Flameless combustion and its potential towards GTs (Perpignan et al., 2018).
2018	A simulation of combined cycle GT power plants (Liu and Karimi, 2018).
2018	Multiobjective Technique for Order of Preference by Similarity to Ideal Solution (TOPSIS) multicriteria decision strategy to power generation costs and exergy efficiency optimization (Entezari et al., 2018).
2018	Analysis of specific power and Specific Fuel Consumption (SFC) of open-cycle GTs using the ideal gas model with temperature-independent heat capacities (Delgado-Torres, 2018).
2018	Optimization of power generation costs in a system involving a combined cycle GT, a compressed air energy storage system, and solar energy collectors using Non-dominated Sorting Genetic Algorithm II (NSGA-II) (Wang et al., 2018).
2018	Multiobjective Artificial Bee Colony (ABC) optimizing energy cost, investment, and generators power output of an offshore GT (Zhang et al., 2018).
2019	A Dual Fuel GT (DFGT) model using natural gas and biogas (Amiri Rad and Kazemiani-Najafabadi, 2019).
2019	A modeling and system identification of gas fuel valves from real data (Omar et al., 2018).
2019	A GT fault classification method using machine learning techniques and real data acquisition (Batayev, 2018).
	2019 A numerical scheme for the thermodynamic analysis of GTs (Colera et al., 2019).
2019	A white-box simulation model of industrial GTs (Tsoutsanis and Meskin, 2019).
2019	A thermo-economic analysis applied to multi-fuel fired GT (Udeh and Udeh, 2019).
2019	A multiobjective optimization approach applied to the conceptual design of a conventional GT combustor (Saboohi et al., 2019).
2020	GT fault diagnosis using a Multi Feedforward Artificial Neural Networks (MFANN) system (Alblawi, 2020)
2020	Grey-box modelling of the swirl characteristics in gas turbine combustion system (Zhang et al., 2020d)
2020	GT signal fault isolation using Kalman filter, ANN and Fuzzy logic (Togni et al., 2020)
2020	Multi-objective-optimization of GT process parameters using Grey-Taguchi and ANN (Gul et al., 2020)
2020	GT operation characteristics design and prediction in real-time (Park et al., 2020).

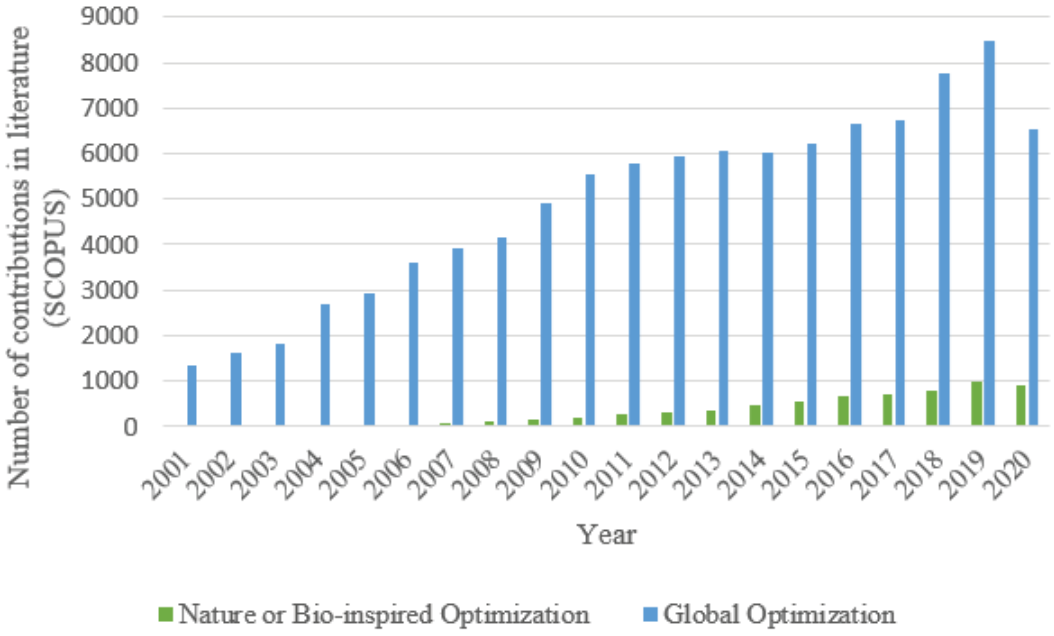

Figure 1.2: Number of papers with bio/nature-inspired optimization and global optimization in the title, abstract and/or keywords, over the last two decades (Scopus database).

Grasshopper Optimisation Algorithm (GSA) (Saremi et al., 2017), the Grey Wolf Optimizer (GWO) (Mirjalili et al., 2014), the Particle Swarm Optimization (PSO) (Kennedy and Eberhart, 1995), the Social Spider Algorithm (SSA) (Yu and Li, 2015), the Spider Monkey Optimization (SMO) (Bansal et al., 2014) and the Whale Optimization Algorithm (WOA) (Mirjalili and Lewis, 2016). There is also some NiM inspired by other natural phenomena instead of a specific animal. It is the case of the Flower Pollination Algorithm (FPA) (Yang, 2012), the Symbiotic Organisms Search (SOS) (Cheng and Prayogo, 2014), the Virus Colony Search (VCS) (Li et al., 2016) and many others (Salcedo-Sanz, 2016; Boussaïd et al., 2013). A complete review o NiM and the most diverse inspirations are presented in (Lones, 2019; Molina et al., 2020).

1.1 JUSTIFICATION

Considering the world energy scenario, the total energy supply has grown around 134% (8098 Mtoe to 14282 Mtoe) from 1971 to 2018. The share of natural gas supply has increased around 265% and it represented around 22.8% of the total energy in 2018. In the Americas, the total energy supply represented a share of 23.4% of the world energy in 2018. (IEA, 2020).

According to the Brazilian Energy Review (*Resenha Brasileira Energética*) 2020, which is written by the Ministry of Mines and Energy (*Ministério de Minas e Energia*) regarding the year 2019, the energy demand in Brazil grows above the Gross Domestic Product - GDP (*Produto Interno Bruto - PIB*). In 2019, the Brazilian energy matrix has grown around 15.5% considering both renewable and non-renewable sources (Brasil, 2020). The development of sustainable energy has become more than an international policy objective, but also an integral part of sustainable development (Gunnarsdottir et al., 2020). Moreover, the search for robust solutions to optimize different energy sources has increased (Impram et al., 2020; Iqbal et al., 2014).

The current research is based on an Research and Development (R&D) project of a thermoelectric power plant located at Araucária, Paraná state, Brazil, which generates electrical

energy using natural gas as an energy source. The power plant operates in a combined cycle and it is composed of two Siemens Westinghouse W501FD combustion turbine generators, two Aalborg unfired heat recovery steam generators, one Alstom steam turbine of condensing type, and one Alstom single-shell two-pass condenser. A photograph from the facility is shown in Fig. 1.3, where it is possible to see the exhaust tower of each gas turbine.

Figure 1.3: Exhaust towers view of the UEGA power plant at Araucária, Parana State, Brazil.

Each gas turbine has 173 MW of nominal power output with around 36% of efficiency in normal conditions, while the steam turbine has around 123 MW. Thus, the total nominal power output is 469 MW and the efficiency considering the combined cycle reaches around 50%. The performance of the power plant is measured by the Heat Rate (HR), which is calculated in Btu/kWh (the lower, the better) and it considers the individual equipment's energy conversion and the energy spent to run the operation (electrical transformers, office, etc) (Yamao et al., 2018).

Since the construction of the facility, a set of technical reports has been written to evaluate the performance after each setup procedure. It has been noticed that HR has increased significantly while the energy spent to run the operation has not increased in the same proportion. Hence, the employees of the power plant have concluded that the efficiency loss may be a result of the individual equipment's performances, mainly the gas turbine, which has a double impact on HR. Because of the dimension of the system, any small variation in the performance impacts hundreds of thousands of dollars per year.

1.2 OBJECTIVES

The objectives of the present thesis are (i) to propose a metaheuristic for global optimization inspired on the *Canis latrans* species; (ii) to propose a metaheuristic for global optimization inspired on the *Cebus capucinus* species; and (iii) to evaluate at least one proposed algorithm under a constrained real-parameter engineering optimization problem. According to the aforementioned goals of this research, the specific objectives are summarized as follows:

- To compare the proposed algorithms with the other similar nature-inspired metaheuristics from literature in terms of structure, mechanisms, and optimization strategies;
- In order to explore the advantages of the proposed algorithms, to test them on a set of continuous optimization benchmark functions with distinct features as multimodality;

- To compare the performances of the proposed algorithms with other nature-inspired metaheuristics in terms of convergence and diversity of the population;
- To design an optimization problem to improve the efficiency of a heavy-duty gas turbine respecting the physical and operational constraints;
- To applied the proposed algorithms to the designed problem of the constrained optimization of a heavy-duty gas turbine operation.

1.3 ORIGINAL CONTRIBUTIONS

The present thesis introduces two original NiM for global optimization with different inspirations. Each NiM presents an original approach to the global population structure, division, and interaction. Conceptually, each algorithm introduces a new metaphor regarding the solutions of an optimization problem and the balance between exploration and exploitation is analyzed.

The first proposed NiM is inspired by the *Canis latrans* species, which contains a distinct structure when compared to other similar state-of-the-art algorithms. The global population is divided into subpopulations with local interactions and the social exchange between the individuals of the population based on real observations of this species is introduced. The second one is inspired by the *Cebus capucinus* species, which is designed with separated groups of monkeys composed of males and females. Instead of sharing information and working as a team as most population-based and swarm intelligence metaheuristics, the social behavior employed is the fight between the groups of the same species.

Moreover, the present research contributes to the optimization of a real-world application using the proposed NiM. The optimization problem is the operation of a heavy-duty gas turbine of 173 MW from a combined cycle power plant with two of these turbines and an additional steam turbine. A computational grey-box model is proposed to simulate the power output considering constraints as the gas emissions and pressure oscillations inside the combustion chamber.

Furthermore, alternative optimization mechanisms and strategies from literature are pursued to improve the performance of the proposed NiM. The domains from the cultural algorithms and the chaotic maps are examples of possibilities for NiM improvements. Besides, multi and many-objective versions of the proposed NiM are explored during this research.

1.4 RESEARCH LIMITATIONS

Due to the numerous repetitive evaluations of an objective function, one single optimization process using evolutionary algorithms (EAs) is usually quite slow in terms of computational execution time. When a new metaheuristic is proposed, multiples EAs are compared and the total execution time increases considerably (LaTorre et al., 2015; Suganthan et al., 2016). First and evident, because the number of EAs being tested increases. Second, because the higher the number of objective functions tested, the more reliable is going to be the conclusion obtained. Third and last, because the higher the number of experiments performed, the more reliable is going to be the statistical analysis provided.

Because of that, a small number of algorithms chosen from the state-of-the-art are used for comparison, as well as a limited number, and experiments are performed. Moreover, the set of parameters for each algorithm is reduced and the state-of-the-art algorithms employed assumes only one, while the proposed NiM assumes two or three sets.

In order to reduce the total execution time, some experiments have shared experimental unity. As a consequence, the full computational execution time of each EA can not be precisely

and reliably measured for comparison. Nevertheless, the computational complexity of each can be estimated using a technique from literature (Suganthan et al., 2005; Chen et al., 2014b; Suganthan et al., 2016). As the objective of the present thesis is to evaluate the design and contributions of the proposed algorithms, this is a limitation with a low impact on this research.

Considering the engineering application, this study is focused on gas turbine performance improvement through data analysis and operation optimization. The data has been acquired from a two days operation in October of 2015 because after that the power plant has been idle for a couple of years. Because the acquisition system was still under construction, only one gas turbine data was correctly acquired and this research does not consider the second gas turbine.

1.5 OUTLINE

The present thesis is organized as follows:

- Chapter 1: In this chapter, the general introduction is presented, including the justification, the motivation, the research limitations, and the objectives;
- Chapter 2: This chapter contains the basic concepts of global optimization, and the performance analysis methods using statistical inference and convergence analysis;
- Chapter 3: The state-of-the-art nature-inspired metaheuristics used for comparison in this research are presented in this chapter;
- Chapter 4: In this chapter, the proposed algorithms inspired on the *canis latrans* and *Cebus capucinus* species are described and the performances are evaluated under a set of benchmark functions;
- Chapter 5: A cultural version of the COA is introduced in this chapter and its performance is evaluated to the constrained optimization of a heavy-duty gas turbine operation;
- Chapter 6: The discussion related to the results presented is provided, as well as the contributed publications and the future activities for the continuation of this research.

2 SINGLE-OBJECTIVE GLOBAL OPTIMIZATION

The present chapter contains the basic concepts regarding the global optimization process. The first subsection stands for the basic concepts and definitions of a global optimization problem. The following subsection contains the stopping criteria usually adopted to test the optimization methods under global optimization problems.

2.1 OPTIMIZATION PROBLEM DEFINITION

According to (Simon, 2013), an global optimization problem containing a number of constraints to be satisfied can be written as:

$$\begin{aligned} \text{minimize} \quad & f(x) \\ \text{subject to} \quad & g_j(x) \geq 0, \ j = 1, 2, \ldots, J; \\ & h_k(x) = 0, \ k = 1, 2, \ldots, K; \\ & x_d^{(L)} \leq x_d \leq x_d^{(U)} \ d = 1, 2, \ldots, D, \end{aligned}$$

where $x_d^{(L)}$ and $x_d^{(U)}$ represent, respectively, the lower and upper bound of each decision variable x_d, defining the search space of the problem $\Omega \subseteq \mathbb{R}^D$. The $g_j(x)$ and $h_k(x)$ are denoted the constraint functions with J inequalities and K equalities that might exist. A solution x must satisfy all of the $J + K$ constraints to be considered feasible; it it does not, the it is considered infeasible. If the optimization problem contains any variable bounds, equality or inequality, then it is called a constrained problem. Otherwise, it is denoted unconstrained problem.

2.2 STOPPING CRITERIA

The stop criteria are part of the structure of the iterative optimization methods and are the ones responsible for closing the execution of the experiment. According to (Engelbrecht, 2005), the most common criteria are:

1. The maximum number of iterations or evaluations of the objective function reached: if this value is too small, the experiment will end before finding a good solution; otherwise, the processing time will be very high;

2. An acceptable solution found: an error measure is defined concerning the desired global optimum; care must be taken with very high values, since they generate an unsatisfactory solution, and also with low values, which can never be reached, generating an infinite loop.

3. When the solution is not improved for a certain time: there are different ways to stop, but it means that the method has already converged, regardless of whether the value found is the global optimal.

There may be particular stopping criteria for some metaheuristics, but this approach will not be addressed in this thesis.

2.3 STATISTICAL EVALUATION OF STOCHASTIC ALGORITHMS

Unlike the mathematical and deterministic methods, the stochastic ones do not have a proof of convergence to the global optimal solution (Sergeyev et al., 2018). Hence, many statistical tools have already been used to evaluate the performance of these algorithms (Rao, 1996). This section presents the techniques used in the present work based on (Montgomery and Runger, 2011).

2.3.1 Descriptive Statistics

The descriptive statistics can be described as a set of numerical summaries of data combined with graphical views of the results. In other words, it means to convert a considerable amount of data into a reduced group of features with understandable views. In global optimization, this approach is used to compare the performance of different methods after a set of independent runs, which means different initial conditions (or seeds).

One of the most widespread approaches used to present these numerical summaries is through a table, as shown in Tab. 2.1.

Methods	**Minimum**	**Average**	**Median**	**Maximum**	**Standard Deviation**
Method 1	7.2	9.6	9.1	9.9	1.9
Method 2	6.1	7.1	7.2	9.0	1.6
Method 3	7.3	8.9	9.5	9.8	1.7
...	...	...	...	...	...
Method M	6.8	8.7	8.5	8.8	1.2

Table 2.1: Example of a table with numerical summaries (only representative values).

For a finite population with N values, the probability mass function is $1/N$ and the mean can be considered the average value among a set of observations, such as:

$$\bar{x} = \frac{1}{N} \sum_{i=1}^{N} x_i. \tag{2.1}$$

To complement the analysis, the standard deviation of a sample evaluates the dispersion of the observations. Note that, only a sample of N independent runs is taken into account. The standard deviation (std) is then computed as:

$$std = \sqrt{\frac{1}{N-1} \sum_{i=1}^{N} (x_i - \bar{x})^2}. \tag{2.2}$$

Although the combination of the sample average and standard deviation enables the comparison of two or more methods, the existence of outliers is always possible and it needs to be considered. The outliers are described as atypical/unusual observations, it means a value far from the sample average. The sample median is a metric that can be used to evaluate the performance and reduce the influence of the outliers. It happens because this feature carries the tendency of the sample. The calculation of the median begins with sorting the sample and

picking the observation of the middle. In case of even sample size, the average between the two central observations is used, such that:

$$median = \begin{cases} x_{\frac{(N+1)}{2}}, & N \text{ is odd} \\ \frac{x_{(\frac{N}{2})} + x_{(\frac{N}{2}+1)}}{2}, & \text{otherwise} \end{cases} \tag{2.3}$$

One method used to analyze the median and the outliers is the "box plot", which is composed of a box with length denoted interquartile range (IQR) drawn from reference values called quartiles. The lower edge is denoted the first quartile (q_1, 25%) and the upper one is the third (q_3, (75%)). The second quartile is represented by a line inside the box, which is denoted the 50th percentile or the median itself. A line denoted whisker is drawn from $q1$ to the smallest sample value inside the 1.5 IQR. The upper whisker is drawn from q_3 to the largest observation inside the 1.5 IQR. The representation of a box plot is drawn in Fig. 2.1, where the outliers are the observations outside the region between the end of the whiskers.

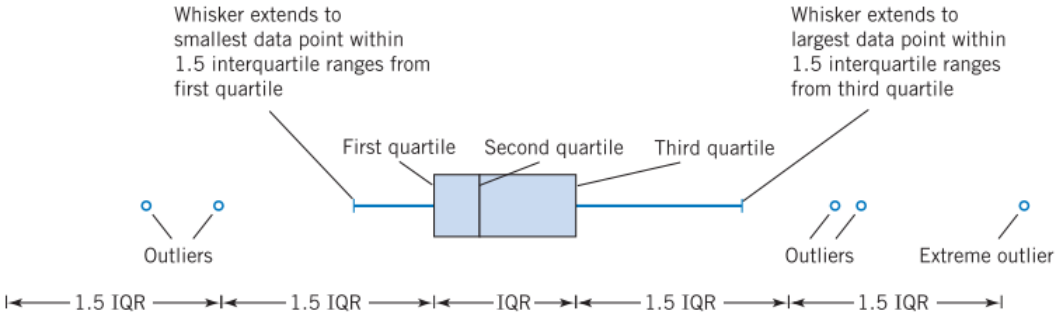

Figure 2.1: Description of a box plot (Montgomery and Runger, 2011).

Through this analysis, it is possible to evaluate the repeatability of different methods separately and compare them. Considering a minimization optimization problem, where the goal is to find the smallest costs for eh objective function, the smallest the sample average, the minimum, the median, and the maximum, the better is the result. On the other hand, for maximization problems, where the goal is to find high values for the objective function, the higher these values, the better. In both cases, the desired standard deviation is always the smallest possible, which highlights the method capacity to find solutions near the sample average.

2.3.2 Statistical inference

As mentioned in the previous section, descriptive analysis provides a compact and graphical interpretation of the observed samples. The weakness of that analysis is the lack of confidence to conclude about the difference between two or more samples. When the samples have nearly similar means, for example, how is it possible to infer if one is higher/lower than the other?

Using statistical significance tests it is possible to estimate that with a certain probability, for example, 95% (Hollander and Wolfe, 1999; Gibbons and Wolfe, 2003). Let's H_0 be the null hypothesis, which states that two samples belong to the same population, while H_1 states that the samples do not belong to the same population. A statistical test compares the sample distributions and provides an indicator denoted p-value, the probability of rejecting the null hypothesis, which is compared to the significance level α (for probability 95%, α=0.05). If the p-value is lower than α, then it is possible to say that "the samples do not belong to the same population with 95% of statistical confidence".

There are many methods on literature to estimate the p-value and it is possible to separate into two groups: the parametrical and the non-parametrical ones. The difference is that the parametrical ones assume that the probability density functions of the samples are Normal, with average equals to μ and variance equals to σ^2, as illustrated in Fig 2.2.

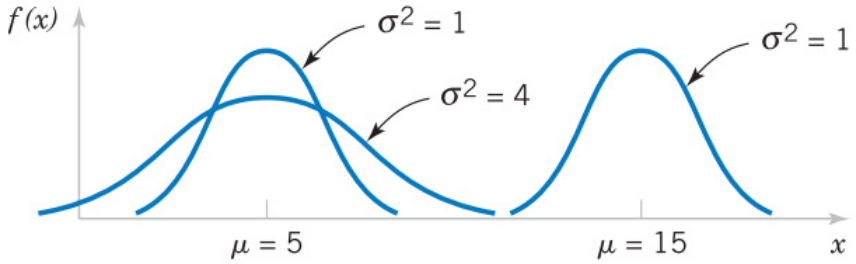

Figure 2.2: Normal probability density functions (Montgomery and Runger, 2011).

However, this assumption is not recommended when comparing the results of stochastic algorithms (García et al., 2010; Derrac et al., 2011). The samples obtained after a set of independent runs with different initial conditions can present several probability density functions, as the example shown in Fig. 2.3. The first sample has similarity with a Normal probability density, but the other samples are more similar to Beta, Weibull, and Uniform, for example (Gibbons and Wolfe, 2003).

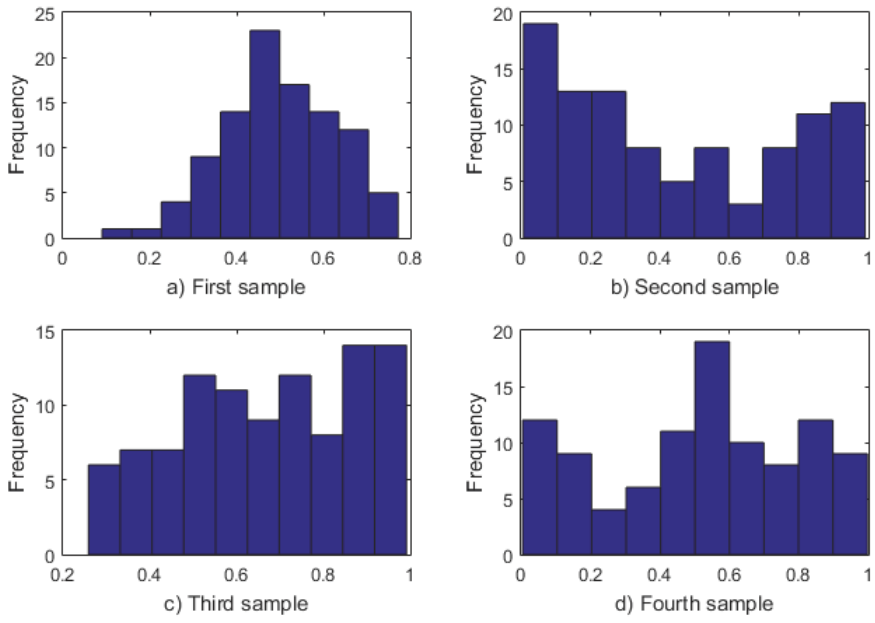

Figure 2.3: Examples of probability distributions

Therefore, the non-parametric statistical significance tests are recommended to compare the performances. The most recommended method for multiple comparisons is the Friedman Ranks test (Hogg and Ledolter, 1987), which discovers if the median errors of all algorithms belong to the same population (H_0). To perform the Friedman test, the data is arranged as demonstrated in a table as Tab. 2.2 with n rows and k columns with only one observation or c data in each of the $n \times k$ cells. The observations in the different lines are independent, while the

columns are not due to some association units. The lines represent the blocks, which contain only one subject each, and the columns represent the treatments. The k treatments are applied to the n subjects. The observation of each treatment should be replaced by its respective relative rank among the observations in the same block (Gibbons and Wolfe, 2003).

		Treatments			
		T_1	T_2	...	T_k
Blocks	B_1	$r_{1,1}$	$r_{1,2}$	...	$r_{1,k}$
	B_2	$r_{2,1}$	$r_{2,2}$	...	$r_{2,k}$
	$\vdots$				
	B_n	$r_{n,1}$	$r_{n,2}$	...	$r_{n,k}$

Table 2.2: Data arrangement for the Friedman test.

The observations of each i^{th} block are sorted in ascending order from 1 to k. The rank is then the order of the observation and in tie cases, the average rank is used. Considering $r_{i,j}$ the rank of the i^{th} block observation and j^{th} treatment, the average of the ranks of this treatment is calculated as follows (Derrac et al., 2011):

$$R_j = \frac{1}{n} \sum_{i=1}^{n} r_{i,j}. \tag{2.4}$$

$for j = 1, 2, ..., k$. The Friedman statistic is then calculated by:

$$\chi_F^2 = \frac{12n}{k(k+1)} \left[\sum_j R_j^2 - \frac{k(k+1)^2}{4} \right] \tag{2.5}$$

which is distributed according to the χ^2 distribution with $k - 1$ degrees of freedom for $n > 10$ and $k > 5$. Otherwise, the exact values should be calculated. The Kendall's coefficient (W) is then calculated to indicate a perfect concordance ($W = 1$) or no concordance ($W = 0$):

$$W = \frac{\chi_F^2}{n(k-1)}. \tag{2.6}$$

Kendall's coefficient of agreement uses the size levels of the effect suggested by (Cohen, 1988). If the null hypothesis is rejected, the Friedman test can not indicate which algorithm has achieved a different performance when the null hypothesis H_0 is reject. Thus, the multiple comparisons considering NxN or $1xN$ with a control method are recommended (Derrac et al., 2011). To perform this comparison, the Wilcoxon-Mann-Whitney method also known as the Rank sum test is recommended (Hollander and Wolfe, 1999).

When multiple comparisons are executed, there is no control over the Family-Wise Error Rate (FWER), which is defined as the probability of making one or more false discoveries among all the hypotheses when performing several $1x1$ tests. It means that, when a p-value is considered in a multiple comparison test, it reflects the error probability of a given comparison, but it does not consider the other comparisons of the group (García et al., 2010; Derrac et al., 2011).

Therefore, the denoted post-hoc methods are recommended to reduce the impact of the FWER. These methods are used to correct the p-values after the multiple comparisons using an inference method. Because of its ability to control the FWER, the Bonferroni-Holm method is recommended (García et al., 2010; Derrac et al., 2011). It works as follows (Holm, 1979):

1. All p-values are sorted in ascending order and m is the total number of p-values (it means the number of treatments compared);

2. If the first p-value is greater than or equal to $\frac{\alpha}{m}$, the procedure is stopped and no p-values are significant; Otherwise, go on;

3. The first p-value is declared significant and now the second p-value is compared to $\frac{\alpha}{(m-1)}$. If the second p-value is greater than or equal to $\frac{\alpha}{(m-1)}$, the procedure is stopped and no further p-values are significant; Otherwise, go on;

4. Go on with these logical steps until the algorithm stops.

In this research, the $1xN$ comparisons strategy with each proposed algorithm as a control method is used. More information about the NxN strategy and more details about non-parametric statistical tests can be found in (Gibbons and Wolfe, 2003).

2.4 CONVERGENCE ANALYSIS

As mentioned, the optimization process aims to find the best solution to a single-objective function. It is reasonable to consider only the final result when there is a mathematical proof of convergence, which is not the case for stochastic metaheuristics. Instead, it might result in a poor analysis not to look inside the process. That is why the researchers began to analyze the behavior of an optimization metaheuristic, from the beginning to the end of the process (Back et al., 1997).

In this context, a convergence curve can be defined as the historical values of a function cost along the optimization process, as illustrated in Fig. 2.4. At this point, it is important to remember the very common feature found in real-world optimization problems, the multimodality, which means several local optima along with the search space. The local optima can be considered a trap in the optimization process and the convergence curve is a powerful tool to evaluate the ability to avoid these traps, in other words, to avoid premature convergence (Morales-Castañeda et al., 2020).

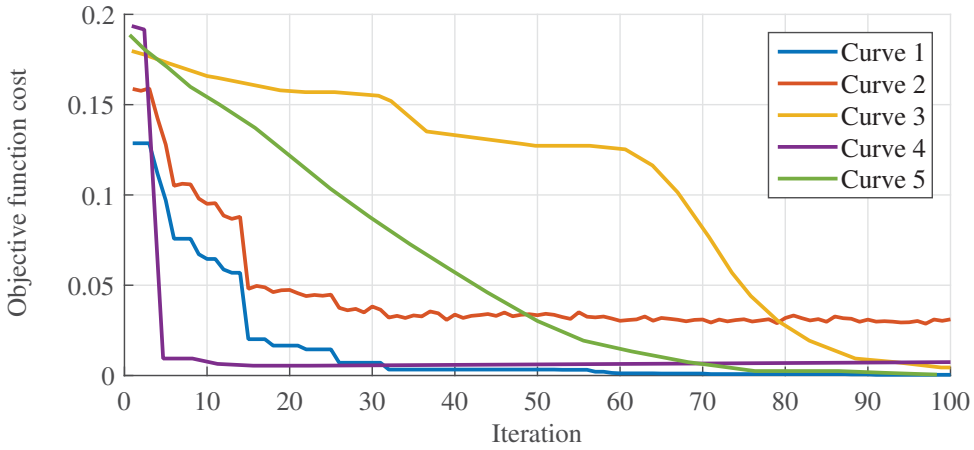

Figure 2.4: Convergence curves.

In Fig. 2.4, curves 1, 2, and 4 are good examples of premature convergence, where a local optimum is quickly found and the solution is not significantly improved until the end of the process. On the other hand, curves 3 and 5 are examples of better convergence, where the global

optimal has been discovered gradually. It is important to point out that the shape of these curves depends on the x-axis, so there is not an absolute ideal shape. The objective will always be to converge to the global optima, the faster, the better.

In this example, the iterations have been considering in the x-axis. However, other indexes can also be used, such as chronological time or the number of function evaluations. Regarding the y-axis, different values of the cost can be used: the average of a population, the average of a set of experiments, or even the raw cost, as illustrated. In cases where the global optimal cost is known, the error curve can be generated for comparison purposes. Besides, the scales in this example are linear for both x and y-axis, however, it can also be customized. For example, if the range of the costs is too high, the y-axis can be shown on a logarithmic scale to improve the view. The same idea can be applied to the x-axis and the main idea is that this setup depends on the analysis desired.

After several analyses and discoveries about the convergence of stochastic metaheuristics, a process to find out how to avoid the premature convergence keeping good results at the end of the process has started. Some researchers state that the key factor to solve this issue is to achieve a good balance between exploration and exploitation. In this context, exploration means to test new solutions from different regions of the search space, while exploitation means to investigate deeper the regions and the solutions already discovered. Some researchers denote "local search" and "global search" respectively for exploitation and exploration, but is not reliable to set a threshold to distinguish these modes of search (Xu and Zhang, 2014).

Hence, the diversity curve has been introduced to measure the exploration ability of the metaheuristics, as illustrated in Fig. 2.5. This analysis is based on a metric able to estimate the spread of the population in the search space. There are many ways to calculate the diversity and one of them is to measure the average distance of the solutions (x) to a hypothetical mean solution ($\hat{x}$) with normalized values (Chi et al., 2012). In this research, the values are normalized according to the search space maximum diagonal.

Figure 2.5: Diversity curves.

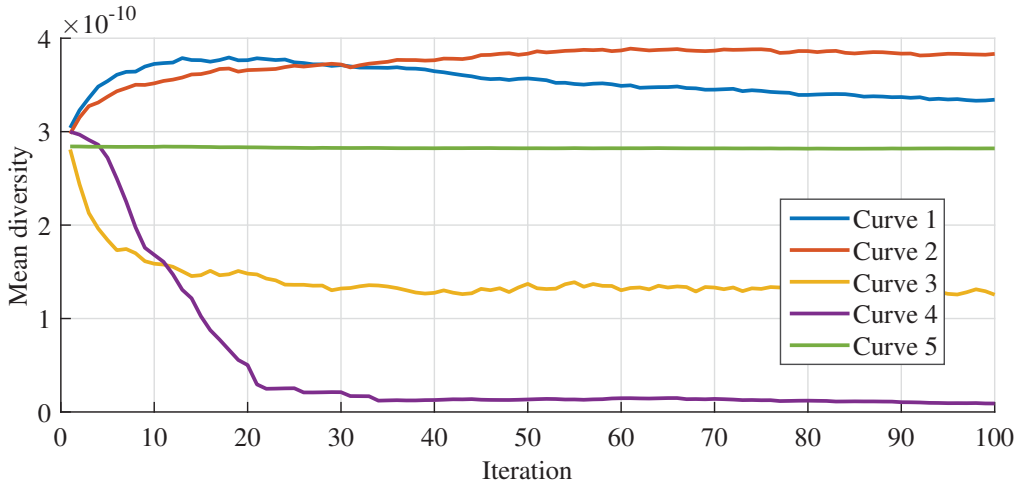

In Fig. 2.5, curves 3 and 4 indicate a concentration of solutions in the same region of the search space after iteration 20. On the other hand, curve 5 indicates that the diversity of the initial set of solutions is kept during the entire optimization process. Finally, curves 1 and 2 demonstrate an increase in diversity along with the iterations, which indicates a good exploratory ability.

Similarly to the convergence, the $x - axis$ of the diversity analysis can be set up with different indexes and scales. Combining these curves analysis, it is possible to evaluate the balance between exploration and exploitation. In general, this is a qualitative analysis and the desired result is the convergence to the global optima keeping a high diversity of solutions.

3 NATURE-INSPIRED METAHEURISTICS

The Nature-inspired Metaheuristics (NiM) perform an iterative search for the solution of a optimization problem. In the following sections, the NiM studied in this research are presented.

3.1 ARTIFICIAL BEE COLONY (ABC)

The Artificial Bee Colony (ABC) algorithm is inspired by the behavior of a swarm of bees searching for food. According to (Karaboga, 2005), bees have an intelligent behavior of communication through movements. This allows them to convey positive or negative information about explored food sources.

According to the analyzes made by Dervis Karaboga, bees can be classified as unemployed or employed (Karaboga, 2005). The employed ones are responsible for exploiting a particular food source, while the unemployed are divided into two groups: the onlooker, who stand around the hive waiting for information from the employed about the food sources, and the scouts, which go out in search of some new food sources.

The control parameters of this metaheuristic are the size of the swarm N_p, the number of scout bees N_s, the *limit* number of attempts available for the bees employed to find more food in the source, and the number of employed N_e and onlooker N_o bees. The number of employed bees defines the number of food sources S (Karaboga and Basturk, 2007).

Considering a swarm with N_e employed bees exploring a food source each (the number of food sources S is equal to N_e), for each $i = \{1, 2, \ldots, S\}$ there exists a possible solution x_i of dimension D (problem dimension) which, similarly, represents the position of the source of food. Initially, random food sources are generated to be explored within the range of the search space, such that:

$$x_{i,j}^{0} = x_j^{min} + r \times (x_j^{max} - x_j^{min}), \tag{3.1}$$

where r is a random number within the interval [0,1] and x^{min} and x^{max} are the limits minimum and maximum variables, respectively.

Each food source has a certain amount of nectar, similarly called fitness, depending on the cost f_i of the objective function, which is calculated by:

$$fitness(x_i) = \begin{cases} \frac{1}{1+f_i}, & f_i > 0 \\ 1 + |f_i| & \text{otherwise} \end{cases} \tag{3.2}$$

Onlookers wait around the hive for feedback from employed, which informs them about food sources by dancing. The frequency of this dance indicates a higher quality of the source and, consequently, more probability of an onlooker to choose such a source to explore. This probability is calculated as the normalized fitness, such that:

$$P_i = \frac{fitness(x_i)}{\sum_{k=1}^{S} fitness(x_k)}. \tag{3.3}$$

The new food sources, which are candidates to assume the positions of the old ones, are generated by:

$$v_{i,j} = x_{i,j} + \phi_{i,j} \times (x_{i,j} - x_{k,j}) \tag{3.4}$$

with random $k \in \{1, 2, \ldots, S\}$ and $k \neq i \neq j$, where $\phi_{i,j}$ is a random real value inside the interval [-1,1] generate by uniform probability density function. A clipper mechanism is adopted right after this step in order to keep the new food source inside the optimization problem search space.

The process of exploring new food sources is repeated until some of the food sources stop evolving for *limit* times, and when it happens, the food source is replaced by a new one discovered by a scout bee in a random position (in this step, the new food source is generated by the Eq. 3.1). The entire search process is repeated until the defined stop criterion is reached, as shown in Alg. 1, which contains the pseudo-code of the ABC. The process of generating a new candidate food source is shown in Alg. 2.

Algorithm 1 Pseudo code of the ABC

```
Define the control parameters
Generate S random food sources (Eq. 3.1)
Evaluate all food sources
while stopping criterion is not achieved do
    for each i employed bee do
        Search for new food sources (Alg. 2)
    end for
    Calculate the food sources fitness (Eq. 3.2)
    Calculate the probabilities (Eq. 3.3)
    Define fs = 1 and counter = 0
    while counter < N_o do
        if rand < P_fs then
            counter = counter + 1
            Search for new food sources (Alg. 2)
        end if
        Iterate fs rotatively
    end while
    for each i scout bee do
        Verify the food source i that has more attempts
        if attempts_i > limit then
            Generate one new random food sources (Eq. 3.1)
            Evaluate this new food source
            Replace the old food source by the new one
        end if
    end for
end while
The best food source is selected as the solution of the problem
```

3.2 BAT ALGORITHM (BA)

The Bat Algorithm (BA) is a nature-inspired metaheuristic developed by Xin-She Yang (Yang, 2010) and is based on the ability of microbats to use a type of sonar, called echolocation,

Algorithm 2 Generation of new food sources in ABC

1: Generate a new candidate food source (Eq. 3.4)
2: Clip the new candidate in the search space
3: Evaluate this new candidate
4: Replace the old one if the new candidate is better, increment attempts instead

for distance sensing and prey hunting. This algorithm presents advantages regarding automatic switching between exploration and exploitation, enabling a quick convergence rate at the early stages. It is based on a population of N_p bats.

The mentioned bats can emit loud sound pulses and listen for the echoes that bounce back from objects in the surrounding area (Lemma and Hashim, 2011). Each pulse in echolocation lasts up to about 8-10 ms, usually in the region of 25-150 kHz (Gandomi et al., 2013).

The basic steps of such an algorithm are shown in Alg. 3, which are based on the idealization and approximations that are taken into account in (Yang, 2010). The initial population of bats is generated randomly. After discovering the initial fitness of the population, the values are changed according to their movement, intensity, and pulse rate. All bats use echolocation to sense distances, magically differentiating between preys and background. Bats fly randomly with fixed echolocation pulse frequency, which can be adjusted given the target proximity. The echolocation loudness varies from a large positive value to a minimum constant value. (Yang and He, 2013a).

Algorithm 3 Pseudo code of the BA.

1: Initialize the position x_i and velocity v_i of each of the Np bats
2: Define the pulse frequency f_i of each bat
3: Initialize the pulse rates r_i and loudness A_i
4: **while** stopping criterion is not achieved **do**
5: **for** each i bat **do**
6: Adjust new solution (Eqs. 3.5, 3.6 and 3.7)
7: **if** $rand_1 > r_i$ **then**
8: Select a solution among the best solutions
9: Generate a local solution around the selected best solution (Eq. 3.8)
10: **end if**
11: Compute fitness of new solution
12: **if** $rand_2 < A_i$ & $f(x_i) < f(x^*)$ **then**
13: Accept the new solution
14: Increase r_i and reduce A_i (Eqs. 3.9 and 3.10)
15: **end if**
16: **end for**
17: Rank the bats and find the current best x^*
18: **end while**
19: The best bat is selected as the solution of the problem

The bats are defined by their position x_i^t, velocity v_i^t, frequency f_i, loudness A_i^t and the emission pulse rate r_i^t in a D-dimensional search space (Guo and Lihong, 2013). After

the random initialization of solutions and velocities, the new solutions x_i^t and velocities v_i^t at a specific time t are given by

$$f_i = f_{min} + (f_{max} - f_{min})\beta, \tag{3.5}$$

$$v_i^t = v_i^{t-1} + (x_i^t - x_*)f_i, \tag{3.6}$$

$$x_i^t = x_i^{t-1} + v_i^t, \tag{3.7}$$

in which $\beta \in [0, 1]$ is a random vector obtained from a uniform distribution and x_* the current global best solution after comparing the locations of all bats. At first, a random frequency f_i is assigned for each bat i in the initial population.

To perform a local search, a new local solution is generated based on one of the best solutions using a random walk, as seen in Eq. (3.8), where $\epsilon \in [-1, 1]$ is a random number in the mentioned interval and A^t is the average loudness of all bats in the respective time step.

$$x_{new} = x_{old} + \epsilon A^t \tag{3.8}$$

This local search process is controlled by the pulse rate and the loudness. For simplicity, A_0 can be defined as 1 and A_{min} as 0, assuming that this null value means that a bat has just found its prey and temporarily stops emitting sound. Then,

$$A_i^{t+1} = \alpha \times A_i^t \tag{3.9}$$

and

$$r_i^{t+1} = r_i^0 \times [1 - exp(-\gamma t)], \tag{3.10}$$

where α and γ are constants. Thus, for any α in the interval $[0, 1]$ and γ in the interval $[0, \infty]$, we have

$$A_i^t \to 0, \quad r_i^t \to r_i^0, \ t \to \infty \tag{3.11}$$

The loudness and the sound emission rates are updated only if the new solutions are better than the previous ones, which would mean that the algorithm is moving towards a better solution, which can be optimal (but not guaranteed).

3.3 FIREFLY ALGORITHM (FA)

The firefly algorithm (FA) is a bioinspired optimization algorithm developed by Xin-She Yang (Yang, 2009) that is based on the flashing characteristics of fireflies, which are used to attract mating partners and potential prey (Hackl et al., 2016). According to (Yang and He, 2013b), the main advantages of the FA algorithm include parameters that can be tuned to control the randomness as the iterations increase, making it possible to speed up the convergence; an automatic subdivision of the population in several groups that swarm around each mode or local optimum, where the global best solution can be found; and an adsorption coefficient γ (Mohammed et al., 2016), which controls the average distance of a group that allows adjacent groups to see it. The automatic subdivision is suitable for highly nonlinear, multimodal optimization problems, allowing the fireflies to find all optima simultaneously in the case of population size being sufficiently higher than the number of modes.

FA was idealized taking into account three rules (Sánchez et al., 2016; Ma and Cao, 2016): (1) fireflies are unisex and can attract to other fireflies independently of their sex; (2) the brightness or light intensity of a firefly is determined by the objective function; and (3) the attractiveness is defined proportionally to the brightness, where both decreases as the distance between the fireflies also decrease. The less bright firefly will move towards the brighter one. If there are no brighter fireflies than the one analyzed, it will move randomly in the defined search space (Khosravi et al., 2015).

The attractiveness of a firefly is determined by its brightness, which is associated with the objective function ($I_0 \propto f(\mathbf{x})$). Such a brightness varies according to the adsorption coefficient γ and distance r between fireflies, as illustrated in equation (3.12):

$$I(r) = I_0 e^{-\gamma r^2} \tag{3.12}$$

The distance r between two fireflies, i and j, at positions x_i and x_j is the Cartesian distance, which means:

$$r_{i,j} = || \, x_i - x_j \, || = \sqrt{\sum_{k=1}^{d} (x_{i,k} - x_{j,k})^2}, \tag{3.13}$$

where $x_{i,k}$ is the kth component of the coordinate x_i of ith firefly.

Equation (3.14) demonstrates another function that represents the light intensity, which decreases monotonically at a slower rate.

$$I(r) = \frac{I_0}{1 + \gamma r^2} \tag{3.14}$$

The attractiveness β can be defined given Eq. (3.15), where β_0 is the attractiveness at a distance $r = 0$, usually defined as $\beta_0 = 1$. In order to reduce computation time, Eq. (3.15) can be replaced by Eq. (3.16).

$$\beta(r) = \beta_0 e^{-\gamma r^2} \tag{3.15}$$

$$\beta(r) = \frac{\beta_0}{1 + \gamma r^2} \tag{3.16}$$

In the implementation, $\beta(r)$ can be represented as any monotonically decreasing function such as the generalized form shown in Eq. (3.17).

$$\beta(r) = \beta_0 e^{-\gamma r^k}, \quad (k \geq 1). \tag{3.17}$$

Finally, given the above values, the movement of a firefly i that is attracted to a brighter firefly is determined by:

$$x_i = x_i + \beta_0 e^{-\gamma r_{ij}^2} (x_j - x_i) + \alpha (rand - \frac{1}{2}), \tag{3.18}$$

in which the second term is related to the attraction, the third term is randomization with α parameter for scaling and $rand$ is a random number inside the range [0,1] generated by a uniform probability density function.

As a conclusion, given the mentioned rules and equations, the FA with N fireflies is demonstrated in the Alg. 4.

Algorithm 4 Pseudo code of the FA

```
Generate the initial population x with N_p fireflies
Calculate the light intensity I of all fireflies
while stopping criterion is not achieved do
    for i = 1 to N do
        for j = 1 to N do
            Compute r (Eq. 3.13)
            Compute I_j and I_i (Eq. 3.14)
            if I_j > I_i then
                Calculate β (Eq. 3.17)
                Move firefly i towards j's one (Eq. 3.18)
            end if
        end for
    end for
    Rank the fireflies according to the objective function costs
end while
Select the best firefly as the solution of the optimization problem
```

3.4 GREY WOLF OPTIMIZER (GWO)

The grey wolf optimization algorithm (GWO) is a NiM algorithm that has been recently proposed and developed by (Mirjalili et al., 2014). It is inspired by the social leadership and hunting behavior of grey wolves in nature.

Such an algorithm has a faster convergence due to the continuous reduction of the search space and to the fact that there are fewer decision variables. Moreover, it has adaptive parameters, which avoids local optima and guarantees exploitation and exploration capabilities (Mirjalili et al., 2014; Long and Xu, 2016).

The wolves groups contain between 5 and 12 wolves, counting with a dominant hierarchy where leaders are called alpha (α), followed by the beta (β) and gamma (γ), making them responsible for making the decisions (Sánchez et al., 2017; Mirjalili, 2015). The best solutions are ranked according to the social hierarchy, α, β, and γ, which are used to guide the rest of the candidate solutions, assumed to be omega (ω) (Muangkote et al., 2014), to an optimal value during the hunting process (optimization) (Hassanin et al., 2016; Mosavi et al., 2016).

As part of the hunting process, the wolves encircle the prey. Eqs. (3.19) and (3.20) model this encircling behavior.

$$\vec{D} = \mid \vec{C} \cdot \vec{X}_p(t) - \vec{X}(t) \mid, \tag{3.19}$$

$$\vec{X}(t+1) = \vec{X}_p(t) - \vec{A} \cdot \vec{D}, \tag{3.20}$$

where t indicates the current iteration, $\vec{A}$ and $\vec{C}$ the coefficient vectors, $\vec{X}_p$ the position vector of prey, and $\vec{X}$ the position vector of a grey wolf. The mentioned vectors $\vec{A}$ and $\vec{C}$ are calculated by Eqs. (3.21) and (3.22) respectively.

$$\vec{A} = 2\vec{a} \cdot \vec{r}_1 - \vec{a}, \tag{3.21}$$

$$\vec{C} = 2 \cdot \vec{r}_2, \tag{3.22}$$

where r_1 and r_2 are random vectors in the interval $[0, 1]$ generated by a uniform probability density function and the $\vec{a}$ components are linearly decreased from 2 to 0 as the iterations increase, in order to emphasize exploration and exploitation, respectively (Mirjalili et al., 2014).

The wolves will attack when the prey stops moving. To model this process mathematically, the value of $\vec{a}$ is decreased. This implies that $\vec{A}$ is also decreased, as it is a random value in the interval $[-2a, 2a]$. As soon as $\mid \vec{A} \mid < 1$, the wolves attack the prey. Therefore, the $\vec{a}$ value models the divergence ($\mid \vec{A} \mid > 1$) and convergence ($\mid \vec{A} \mid < 1$) characteristics of the optimization algorithm and determines whether the grey wolves will attack or diverge from the prey, which will determine an approach to the best solution or pursuit in the search space for a fitter solution, respectively.

Also, the $\vec{C}$ component is a factor that favors exploration. According to Eq. (3.22), it contains values in $[0, 2]$. This component provides random weights for preys to stochastically emphasize ($\vec{C} > 1$) or deemphasizes ($\vec{C} < 1$) the effect of the prey in defining the distance demonstrated in Eq. (3.19). This process favors explorations and improves local optima avoidance.

The hunting process is mainly guided by the alpha group. The beta and gamma might also participate occasionally. It is supposed that the alpha (best candidate solution), beta, and gamma have a better estimate of the location of the prey. Thus, the mentioned three results are stored and the other search agents, mainly from the omega group, update their positions according to the positions of the best search agents. These processes are demonstrated in the Eqs. (3.23), (3.24) and (3.25), in which the final position of the current solution is represented in Eq. (3.25), where:

$$\vec{D}_\alpha = \mid \vec{C}_1 \cdot \vec{X}_\alpha - \vec{X} \mid, \quad \vec{D}_\beta = \mid \vec{C}_2 \cdot \vec{X}_\beta - \vec{X} \mid, \quad \vec{D}_\gamma = \mid \vec{C}_3 \cdot \vec{X}_\gamma - \vec{X} \mid, \tag{3.23}$$

$$\vec{X}_1 = \vec{X}_\alpha - \vec{a}_1 \cdot (\vec{D}_\alpha), \quad \vec{X}_2 = \vec{X}_\beta - \vec{a}_2 \cdot (\vec{D}_\beta), \quad \vec{X}_3 = \vec{X}_\gamma - \vec{a}_3 \cdot (\vec{D}_\gamma), \tag{3.24}$$

$$\vec{X}(t+1) = \frac{\vec{X}_1 + \vec{X}_2 + \vec{X}_3}{3}. \tag{3.25}$$

The GWO algorithm is terminated when it satisfies the stop criterion and the solution that best fits is chosen (the alpha). The basic steps and methodology to implement the grey wolf algorithm are demonstrated in Alg. 5.

3.5 PARTICLE SWARM OPTIMIZATION (PSO)

The Particle Swarm Optimization (PSO) has been proposed in 1995 to treat problems in continuous search space (Kennedy and Eberhart, 1995). Its creation is inspired by the behavior of animals that live in flocks, as is the case of birds and fishes. The main factor studied is the synchronous movement that this species presents when it is in a group.

The operation of the method is based on particles that move in the search interval, whose positioning of each represents a possible solution to the problem. The position depends on the particle's own experience and also on its neighbors, an influence that happens due to the social relation in the swarm (Parsopoulos and Vrahatis, 2002).

Algorithm 5 Pseudo code of the GWO

```
Initialize the grey wolf population X with size N
Initialize a, A and C
Calculate the fitness of all grey wolves
Define the best grey wolf, X_α
Define the second best grey wolf, X_β
Define the third best grey wolf, X_γ
while stopping criterion is not achieved do
    for each grey wolf do
        Update the position (Eqs. 3.23, 3.24 and 3.25)
    end for
    Update a, A and C (Eqs. 3.21 and 3.22)
    Calculate the fitness of all grey wolves
    Update X_α, X_β and X_γ
end while
Select X_α as the solution of the optimization problem
```

It is a swarm of size N_p that moves continuously as a function of time t, for each $i = \{1, 2, \ldots, N_p\}$ there exists a particle located in x_i of dimension D (dimension of the problem) representing a possible solution for the problem. The initialization of these particles occurs randomly within the range of D variables, such as:

$$x_0 = x_{j,min} + r_j \times (x_{j,max} - x_{j,min}), \tag{3.26}$$

for $j = \{1, 2, \ldots, D\}$, where r_j is a random number generated by uniform probability distribution within the interval [0,1] and x_{min} and x_{max} are the minimum and maximum limits of the decision variables, respectively.

Each particle also has a velocity with an initial value equal to zero and is updated with each time instant. According to (Engelbrecht, 2005), there are different ways of calculating the updated value.

The basic form is calculated using a cognitive component, which depends on the best position the particle has occupied to date, and a social component, which may depend on the best position known to the neighborhood or the whole swarm. The general case is described by:

$$v_{t+1,i} = w \times v_{t,i} + c_1 \times rand_1 \times (y_i - x_{t,i}) + c_2 \times rand_2 \times (\hat{y}_{t,i} - x_{t,i}) \tag{3.27}$$

where $v_{t,i}$ and $x_{t,i}$ are respectively the velocity and position of the particle i at the previous instant, y_i is the best position that particle i has ever reached ($\hat{y}_t$) is the best position in the neighborhood of i, c_1 and c_2 are cognitive and social constants, respectively, $rand_1$ and $rand_2$ are random values generated by uniform probability density function inside the interval [0,1] and w is the inertia weight.

The neighborhood of size Nv is defined by the set V_i, such that:

$$V_i = \{x_{i-Nv,t}, x_{i-Nv,t+1}, \ldots, x_{i-1,t}, x_{i,t}, x_{i+1,t}, \ldots, x_{i+Nv,t}\} \tag{3.28}$$

and the best position will be of the particle that presents lower cost of the objective function.

The most simple case is a particularity of the general one, where the neighborhood is considered the whole swarm, i.e., $Nv = N_p$, and the inertia weight is ignored, it means that $w = 1$. The choice of the case depends on the optimization problem studied.

However, the most employed PSO case considers a linear decay of w, which is described as:

$$w_t = (w_{ini} - w_{final}) \times (\frac{t_{max} - t}{t_{max}}) + w_{final} \tag{3.29}$$

where w_{ini} and w_{final} are respectively the initial and final values of inertia and t_{max} is the number of total iterations that will be executed. The necessary condition for the decay to occur is $w_{ini} > w_{final}$.

There is also the linear decreasing method presented by (Abido, 2002), which is independent of the total execution time. The updating of inertia weight is defined as:

$$w_{t+1} = \alpha \times w_t \tag{3.30}$$

where w_t is the inertia of the previous instant and α is a decreasing constant. In this case, w_t must assume an initial value w. Other velocity limitation strategies can be seen in (Engelbrecht, 2005)

The position of each particle at the same time $t + 1$ is then calculated by:

$$x_{t+1,i} = x_{t,i} + v_{t+1,i} \tag{3.31}$$

where $x_{t,i}$ is its previous position and $v_{t+1,i}$ is its already updated velocity.

Finally, the best position of the neighborhood and of each particle is updated, such that:

$$y_{t+1,i} = \begin{cases} x_{t,i}, & f(x_{t+1,i}) > f(y_i) \\ y_i & \text{otherwise} \end{cases} \tag{3.32}$$

where $f(y_i)$ is the objective function cost of the best position of the particle thus far and $f(x_{t+1,i})$ is the cost of the updated position of the particle.

The process of updating the velocity and position of the particles is repeated until the defined stop criterion is reached. The pseudo-code of the PSO used in this thesis is described in Alg. 6, which is known as the asynchronous version (the global best is updated without evaluating all particles) and considers $N_v = N_p$ and dynamic linear decreasing w.

Algorithm 6 Pseudo code of the PSO

```
Initialize N_p particles (Eq. 3.26) with velocities equal to zero
Evaluate the N_p particles
while stopping criterion is not achieved do
    for each i particle do
        Update the local and global best (Eq. 3.32)
        Update the velocity (Eq. 3.27)
        Update the position (Eq. 3.31)
    end for
    Update w (Eq. 3.29)
end while
The best particle is selected as the solution of the problem
```

3.6 SYMBIOTIC ORGANISMS SEARCH (SOS)

The Symbiotic Organisms Search (SOS) is a population-based metaheuristic proposed by (Cheng and Prayogo, 2014) to solve numerical optimization over continuous search spaces. It is inspired by the reliance-based relationships seen in different species in nature, called symbiosis. The SOS algorithm takes into account the most common symbiotic relationships found: mutualism, commensalism, and parasitism.

The mutualism happens when both species are benefited, as the pollination. When bees fly amongst flowers, the pollen is distributed – it benefits the flowers. It simultaneously benefits bees, because during this activity the nectar is gathered for producing honey. Commensalism occurs when only one species is benefited, without causing any harm to the other species. The relation between remora fishes and sharks is an example of that because remora eats the shark's leftovers – being benefited – and the sharks are unaffected by this activity. Parasitism happens when one species is benefited and the other is consequently damaged. The plasmodium parasite is an example of that because it uses the relationship with the anopheles mosquito to pass between humans. As a result of that, the parasite is benefited by living inside the human body, while the human suffers malaria with life-threatening (Cheng and Prayogo, 2014).

In the SOS structure, each organism passes through three phases, which are represented by the symbiotic relationships. Hence, the structure of the algorithm can be written as shown by Alg. 7.

Algorithm 7 Pseudo code of the SOS.

```
Ecosystem initialization
while stopping criterion is not achieved do
    for each each organism do
        Mutualism phase
        Commensalism phase
        Parasitism phase
    end for
end while
Select the best organism of the ecosystem (in terms of objective function's cost)
```

The initialization covers the creation of N randomly positioned organisms in the search space, the evaluation of all organisms, and the verification of the best organism in terms of cost. The following subsections describe the operation of each phase previously mentioned.

3.6.1 Mutualism

In the mutualism phase, the i^{th} and j^{th} organisms of the ecosystem – where the second one is randomly selected using uniform distribution – engage in a mutual relationship to increase mutual survival advantage in the ecosystem. The mutualistic symbiosis between these organisms is modeled as follows:

$$x_i^{new} = x_i + r_1 \times (x_{best} - MutVec \times BF_1) \tag{3.33}$$

$$x_j^{new} = x_j + r_2 \times (x_{best} - MutVec \times BF_2) \tag{3.34}$$

$$MutVec = \frac{(x_i + x_j)}{2} \tag{3.35}$$

where r_1 and r_2 are vectors with D (objective function's dimension) random numbers generated inside the range [0,1] with uniform distribution of probability, x_{best} is the organism with the best fitness in the ecosystem, $MutVec$ is the mutual vector calculated from the organisms x_i and x_j, x_i^{new} and x_j^{new} are the new organisms and BF_1 and BF_2 are the benefit factor of each organism. These factors exist due to the intensity of the benefit received by each organism in the mutualism. Thus, BF_1 and BF_2 assume value 1 in case of partially benefit and value 2 in case of the full benefit. Each of these values is chosen randomly with uniform probability and is not mandatorily equal to the other.

Then, the boundaries are verified and the organisms pass through a selection operator, which keeps the solution with the best fitness. In other words, the organism x_i is replaced by x_i^{new} only if the new fitness is better than the old one. The same happens with the j^{th} organism.

3.6.2 Commensalism

In commensalism, the i^{th} organism tries to be benefited from the j^{th} organism, which is picked randomly from the ecosystem. On the other hand, the j^{th} organism neither is benefited nor suffers from the relationship. Thus, the operation is described as:

$$x_i^{new} = x_i + r_c \times (x_{best} - x_j) \tag{3.36}$$

where r_c is a vector with D random numbers generated inside the range [0,1] with uniform distribution of probability. After that, the boundaries are verified, x_i^{new} is evaluated and the selection operator is performed. The organism with the best fitness is kept. It means that the i^{th} organism is replaced only if the new fitness is better than the older one.

3.6.3 Parasitism

In the parasitism phase, a parasite organism par_k is created from the i^{th} organism using the following role:

$$x_j = \begin{cases} x_k^{min} + r_k \times (x_k^{max} - x_k^{min}), & p_k < 0.5 \\ x_{i,k}, & \text{otherwise} \end{cases} \tag{3.37}$$

for $k \in \{1, 2, ..., D\}$, where r_k and p_k are random numbers generated inside the range [0,1] with uniform distribution of probability and x_k^{min} and x_k^{max} are, respectively, the minimum and the maximum k^{th} boundary of the search space. After that, the parasite is evaluated and tries to kill the j^{th} organism – which is picked randomly with uniform probability:

$$x_j = \begin{cases} par, & f(par) < f(x_j) \\ x_j, & \text{otherwise.} \end{cases} \tag{3.38}$$

4 PROPOSED METAHEURISTICS FOR GLOBAL OPTIMIZATION

This chapter presents the proposed nature-inspired metaheuristics nature-inspired on the *Canis latrans*, which is denoted Coyote Optimization Algorithm (COA), and on the *Cebus capucinus* species, denoted White-faced Capuchin Monkeys Optimizer (WfCMO).

Experimental results from a set of boundary constrained real-parameter optimization benchmarks are provided and analyzed. The performances of the COA and the WfCMO are compared with other state-of-the-art nature-inspired metaheuristics and an extended statistical analysis is employed to prove the metaheuristics' contributions. A brief conclusion about the results is also given in this chapter.

4.1 COYOTE OPTIMIZATION ALGORITHM (COA)

The proposed COA is based on the behavior of the wild species (*canis latrans*), also known as brush wolf, prairie wolf and American jackal. This species belongs to the family Canidae and can be found from Costa Rica to northern Alaska and from coast to coast in the United States (Bekoff, 1977; Conner et al., 2008; Pitt et al., 2003).

The COA is a algorithm that can be classified as both swarm intelligence and evolutionary heuristic, once it is population-based and the coyotes that best adapt to environment are selected to "survive" along a set of iterations. In contrast with the Grey Wolf Optimizer (GWO) (Mirjalili et al., 2014), which is inspired on the *Canis lupus* species, the COA has a different algorithmic structural setup and it does not focus on the social hierarchy and dominance rules of these animals, even though the alpha is employed as the leader of a pack (as explained forward). Further, the COA focus on the social structure and experiences exchange by the coyotes instead of only hunting preys as it happens in the GWO.

In the COA, the population of coyotes is divided into $N_p \in \mathbb{N}^*$ packs with $N_c \in \mathbb{N}^*$ coyotes each. In this first proposal, the number of coyotes per pack is static and similar for all packs. Hence, the total population in the algorithm is obtained by the multiplication of N_p and N_c. For simplification purposes, the solitary (or transient) coyotes are not considered in this first version of the algorithm. To facilitate the reader's understanding, each coyote is a possible solution for the optimization problem and its social condition is the cost of the objective function.

According to (Poessel et al., 2014; Gese et al., 1996), intrinsic factors (sex, the social status and the pack that the coyote is a member) and extrinsic ones (such as snow depth, snowpack hardness, temperature and carcass biomass) have been pointed out as influences in the coyote's activities. Therefore, the COA mechanism has been designed based on the social conditions of the coyotes, which means the decision variables $\vec{x}$ of an global optimization problem. Thus, the social condition of the c^{th} coyote of the p^{th} pack in the t^{th} instant of time is written as

$$soc_c^{p,t} = \vec{x} = (x_1, x_2, ..., x_D) \tag{4.1}$$

and it implies in the coyote's adaptation to the environment $fit_c^{p,t} \in \mathbb{R}$.

The first step in the COA is to initialize the global population of coyotes. As the COA is a stochastic algorithm, the initial social conditions are set randomly for each coyote. It happens

by assigning random values inside the search space for the c^{th} coyote of the p^{th} pack of the j^{th} dimension, as follows:

$$soc_{c,j}^{p,t} = x_{j,min} + r_j \times (x_{j,max} - x_{j,min}), \tag{4.2}$$

wherein $x_{j,min}$ and $x_{j,max}$ represents, respectively, the lower and upper bounds of the j^{th} decision variable, D is the search space dimension and r_j is a real random number generated inside the range [0,1] using uniform probability. After that, the coyotes' adaptation in the respective current social conditions are evaluated:

$$fit_c^{p,t} = f(soc_c^{p,t}) \tag{4.3}$$

Initially, the coyotes are randomly assigned to the packs, however the coyotes sometimes leave their packs and become solitary or join a pack instead (Pitt et al., 2003). According to (Conner et al., 2008), the coyote eviction from a pack depends on the number of coyotes inside the pack and occurs with probability P_e, such that:

$$P_e = 0.005 \times N_c^2. \tag{4.4}$$

Considering that P_e could assume values greater than 1 for $Nc \leq \sqrt{200}$, the number of coyotes per pack is limited to 14. This mechanism helps the COA to diversify the interaction between all the coyotes of the population, which means a cultural exchange in the global population. Two random coyotes from random packs are picked to change their positions, which means that the population size remains constant along the whole optimization process, as well as the packs sizes.

In this species, the packs usually has two alphas (Gese et al., 1996; Conner et al., 2008), however the COA considers only one, which is the best adapted to the environment. Considering an minimization problem, the alpha of the p^{th} pack in the t^{th} instant of time is defined as:

$$alpha^{p,t} = \{soc_c^{p,t} | arg_{c=\{1,2,\ldots,N_c\}} minf(soc_c^{p,t})\}. \tag{4.5}$$

Due to the evident signs of swarm intelligence in this specie, the COA assumes that the coyotes are sufficiently organized to share the social conditions and to contribute to the pack's maintenance. Thus, the COA links all information from the coyotes and computes it as the cultural tendency of the pack:

$$cult_j^{p,t} = \begin{cases} O^{p,t}_{\frac{(N_c+1)}{2},j}, & N_c \text{ is odd} \\ \frac{O^{p,t}_{\frac{N_c}{2},j} + O^{p,t}_{(\frac{N_c}{2}+1),j}}{2}, & \text{otherwise} \end{cases} \tag{4.6}$$

where $O^{p,t}$ represents the ranked social conditions of all coyotes of the p^{th} pack in the t^{th} instant of time for every j in the range [1,D]. In other words, the cultural tendency of the pack is computed as the median social conditions of all coyotes from that specific pack.

Taking into account the two main biological events of life, the birth and the death, the COA computes the age of the coyotes (in years), which is denoted as $age_c^{p,t} \in \mathbb{N}$. The birth of a new coyotes is written as a combination of the social conditions of two parents (randomly chosen) plus a environmental influence, such that:

$$pup_j^{p,t} = \begin{cases} soc^{p,t}_{r_1,j}, & rnd_j < P_s \text{ or } j = j_1 \\ soc^{p,t}_{r_2,j}, & rnd_j \geq P_s + P_a \text{ or } j = j_2 \\ R_j, & \text{otherwise} \end{cases} \tag{4.7}$$

wherein r_1 and r_2 are random coyotes from the p^{th} pack selected using a uniform probability density function, j_1 and j_2 are two random dimensions of the problem also generated by a uniform probability density function, P_s is the scatter probability, P_a is the association probability, R_j is a random number inside the decision variable bound of the j^{th} dimension and rnd_j is a random number inside [0,1] generated with uniform probability. The scatter and association probabilities guide the cultural diversity of the coyotes from the pack. In this initial version of the COA, the P_s and the P_a have been defined as

$$P_s = 1/D \quad \text{and} \tag{4.8}$$

$$P_a = (1 - P_s)/2, \tag{4.9}$$

where P_a establish the same influence impact for both parents.

According to some researches, the pups have around 10% of chances of dying even before living (Conner et al., 2008) and the higher the coyote's age, the higher is the mortality probability (Pitt et al., 2003). In order to keep the population size static, the COA syncs the coyote's birth and death as described in the Alg. 8, where ω and φ represent, respectively, the group of coyotes worse adapted to the environment than the pup and the number of coyotes in this group. Note that it is possible that two or more coyotes have similar age (in line 4). In this case, the less adapted coyote is the one who dies. It is important to highlight that the age a coyotes has no limit, differently from the nature.

Algorithm 8 Birth and death inside a pack of coyotes.

```
1: Compute ω and φ
2: if φ = 1 then
3:     The pup survives and the only coyote in ω dies.
4: else
5:     if φ > 1 then
6:         The pup survives and the oldest coyote in ω dies.
7:     else
8:         The pup dies.
9:     end if
10: end if
```

In order to represent the cultural interaction inside the packs, the COA assumes that coyotes are under the alpha influence (δ_1) and the pack influence (δ_2). The first one means a cultural difference from a random coyote of the pack (cr_1) to the alpha coyote, while the second one means a cultural difference from a random coyote (cr_2) to the cultural tendency of the pack. The random coyotes are chosen by uniform distribution of probability and δ_1 and δ_2 are written respectively as:

$$\delta_1 = alpha^{p,t} - soc_{cr_1}^{p,t} \tag{4.10}$$

$$\delta_2 = cult^{p,t} - soc_{cr_2}^{p,t}. \tag{4.11}$$

Hence, the coyote's new social condition is updated using the alpha and the pack influence through the following equation:

$$new\_soc_c^{p,t} = soc_c^{p,t} + r_1 \times \delta_1 + r_2 \times \delta_2, \tag{4.12}$$

where r_1 and r_2 are, respectively, the weights of the alpha and the pack influence. Initially, r_1 and r_2 have been defined as random numbers inside the range [0,1] generated with uniform probability. It is important to highlight that a clip mechanism is included to maintain the coyotes inside the search space. The new social condition is then evaluated:

$$new\_fit_c^{p,t} = f(new\_soc_c^{p,t}), \tag{4.13}$$

and the coyote's cognitive capacity decide if the new social condition is better than the older one to keep it, it means:

$$soc_c^{p,t+1} = \begin{cases} new\_soc_c^{p,t}, & new\_fit_c^{p,t} < fit_c^{p,t} \\ soc_c^{p,t}, & \text{otherwise} \end{cases}. \tag{4.14}$$

Finally, the social condition of the coyote that best adapted itself to the environment is selected and is used as the global solution of the problem. The pseudo-code of the COA is described in Alg. 9, while the geometrical interpretation is drawn in Fig. 4.1, where the circles represent the coyotes and the star represents the cultural tendency. In this representation, the δ_1 and the δ_2 can be better interpreted, where the first component forces the coyote to the direction of the best and the second one to the direction of the center of the group. The new solutions are more likely to be generated inside the group space and it tends to converge along the iterations. Combined with the pack exchange, the whole population slowly converges to a promising region.

Algorithm 9 Pseudo code of the COA

```
Initialize N_p packs with N_c coyotes each (Eq. 4.2)
Verify the coyote's adaptation (Eq. 4.3)
while stopping criterion is not achieved do
    for each p pack do
        Define the alpha coyote of the pack (Eq. 4.5)
        Compute the social tendency of the pack (Eq. 4.6)
        for each c coyotes of the p pack do
            Update the social condition (Eq. 4.12)
            Evaluate the new social condition (Eq. 4.13)
            Adaptation (Eq. 4.14)
        end for
        Birth and death (Eq.4.7 and Alg. 8)
    end for
    Transition between packs (Eq. 4.4)
    Update the coyotes' ages
end while
Select the best adapted coyote
```

4.2 WHITE-FACED CAPUCHIN MONKEYS OPTIMIZER (WFCMO)

The *Cebus capucinus* species, also known as white-faced capuchin monkeys, white-throated capuchin or white-headed capuchin dwells in Central and South America and it performs an important role to ecology by dispersing pollen and seeds. This species lives in groups from 4 to 40 members (Fragaszy et al., 2004a), usually around 20, and its maximum lifespan is 54 years, which is considerably high compared to other primate's species (Schaik and Isler, 2012). The life

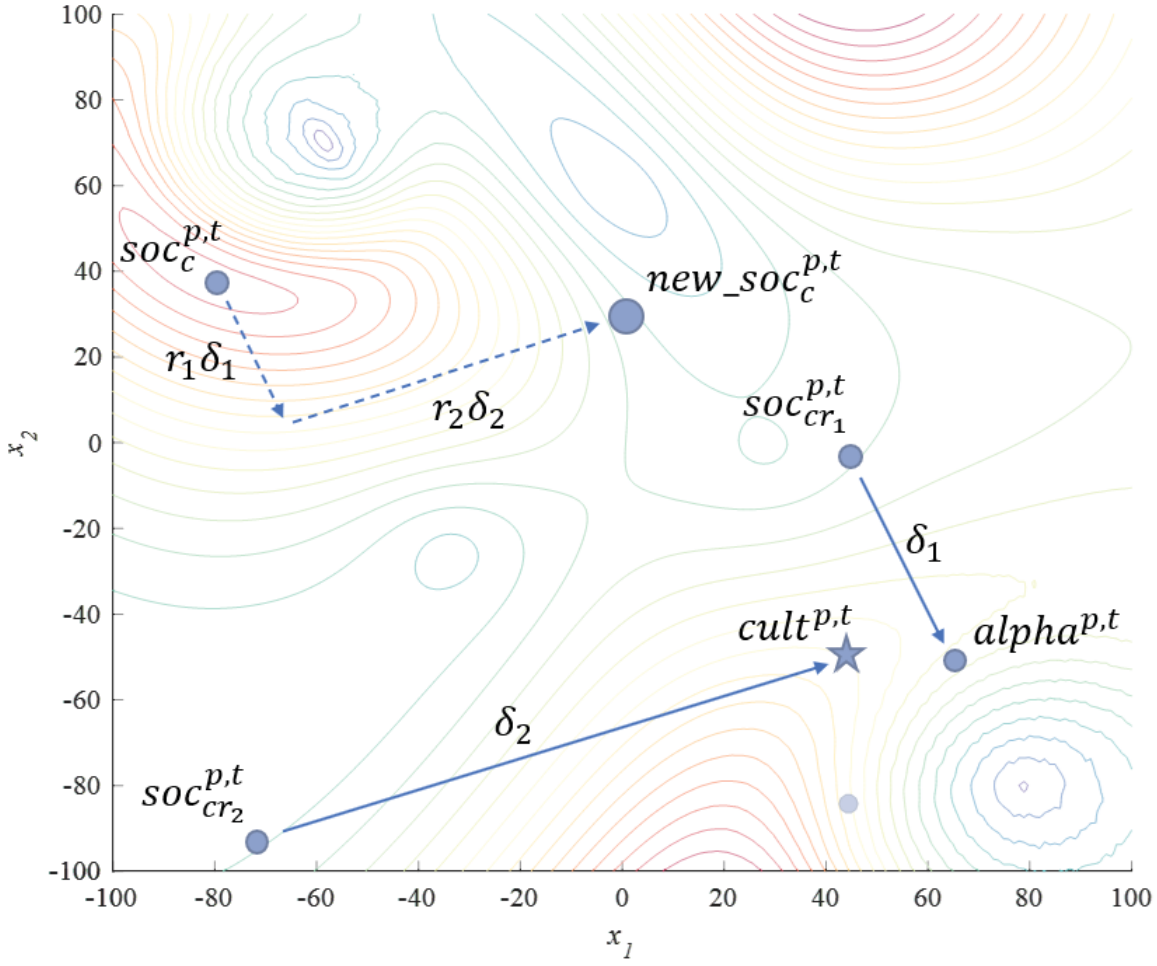

Figure 4.1: Geometrical interpretation of the COA.

maintenance of this species occurs though the reproduction and death, as well as it happen in the *Homo sapiens* species.

According to (Schaik and Isler, 2012), living in a cohesive groups causes food competition and reduces growth and reproduction. On the other hand, it enables individuals to develop long-term cooperative relationships. In fact, it has been observed that groups formed *Cebus capucinus* species fight with groups from the same species for food and other resources (Vogel et al., 2007).

In contrast with the SMO algorithm (Bansal et al., 2014), which is based on the fission–fusion social system of the spyder-monkey species and aims to reduce the foraging competition, the proposed WfCMO has the completely opposite purpose. It is inspired on the grouping and fighting behaviour of this species (Fragaszy et al., 2004b). Yet, while the SMO considers a global leader and sub groups led by a female, the WfCMO considers the decentralized leadership observed in the white-faced capuchins, where the initiation of group movements are not concentrated into a single individual (Leca et al., 2003).

Hence, the WfCMO can be classified as a nature-inspired population based and evolutionary heuristic and its population is divided into $N_g \in \mathbb{N}^*$ groups with $N_m \in \mathbb{N}^*$ monkeys each. In this first proposal, the number of monkeys per pack is static and similar for all groups. Hence, the total population in the algorithm is obtained by the multiplication of N_g and N_m. To facilitate the reader's understanding, each monkey's position is a possible set of variables ($\vec{x}$) for the global optimization problem and its adaptation to the environment is the cost of the

objective function. Thus, the position of the m^{th} monkey of the g^{th} group in the t^{th} instant of time is written as

$$pos_m^{g,t} = \vec{x} = (x_1, x_2, ..., x_D) \tag{4.15}$$

and it implies in the monkeys adaptation to the environment $fit_m^{g,t} \in \mathbb{R}$.

The first step in the WfCMO is to initialize the global population of monkeys. As the WfCMO is a stochastic algorithm, the initial positions are set randomly for each monkey. It happens by assigning random values inside the search space for $t = 0$ in the j^{th} dimension, such that:

$$pos_{m,j}^{g,0} = x_{j,min} + r_j \cdot (x_{j,max} - x_{j,min}), \tag{4.16}$$

wherein $x_{j,min}$ and $x_{j,max}$ represents, respectively, the lower and upper bounds of the j^{th} decision variable, D is the search space dimension and r_j is a real random number generated inside the range [0,1] using uniform probability function. After that, the monkeys' adaptations in the respective current position are evaluated:

$$fit_m^{g,t} = f(pos_m^{g,t}) \tag{4.17}$$

Initially, the coyotes are randomly assigned to the packs. It has been observed that the males migrate from a group to another (Vogel et al., 2007), however this feature is not considered in the WfCMO. In this first proposal, the males and females are redefined in every iteration of the algorithm - after some tests, it has achieved best results with this setup. To perform this, a control parameter has been set, the *male probability*, denoted ρ. Therefore, the definition of males and females in the t^{th} iteration is performed by:

$$male_m^{g,t} = \begin{cases} true, & \{m = i\} \cup \{rnd_m \leq \rho \cap m \neq j\} \\ false, & \{m = j\} \cup \{rnd_m > \rho \cap m \neq i\} \end{cases} \tag{4.18}$$

for $g = 1, 2, \ldots, N_g$ and $m = 1, 2, \ldots, N_m$, where $male$ stores the genre of the monkeys (true for males, false for females), i and j are random numbers inside $1, 2, \ldots, N_m$ with $i \neq j$ and rnd_m is a random number inside [0,1] generated with uniform probability. Note that, with this mechanism at least one male and one female are guaranteed in each group.

At each iteration of the algorithm, every group fight with another group for the competition for resources. In this version of the WfCMO, it occurs randomly, which means that each group fight with another random group. As observed by (Perry, 1996), in the most cases the males fight while the females run to defense the resources.

Considering that, the WfCMO considers distinct males and females movements initiated by the g group in a fight against the g_a group. The male movement is composed by two components with different purposes. The first (Δ_1) is to advance against the opponent to fight. The second (Δ_1) is to lure the opponent away from their own group to increase the safety of the kin females. The complete male movement is described as:

$$\Delta_1 = (pos_{r_m}^{g_a,t} - pos_m^{g,t}) \tag{4.19}$$

$$\Delta_2 = (pos_m^{g,t} - C_g) \tag{4.20}$$

$$\widehat{pos}_m^{g,t} = pos_m^{g,t} + r_1 \times \Delta_1 + r_2 \times \Delta_2 \tag{4.21}$$

where r_1 and r_2 are random numbers in the range [-1,1] generated by uniform probability distribution function, r_m is a random male of the opponent group and C_g is the geometrical center of the group g.

The geometrical interpretation of the males movements is drawn in Fig. 4.2, where the stars, the circles and the triangles represent the center of the groups, the male monkeys and the female monkeys, respectively. Note that the new solution tends to be generated around a solution from another group, promoting the information exchange between the groups.

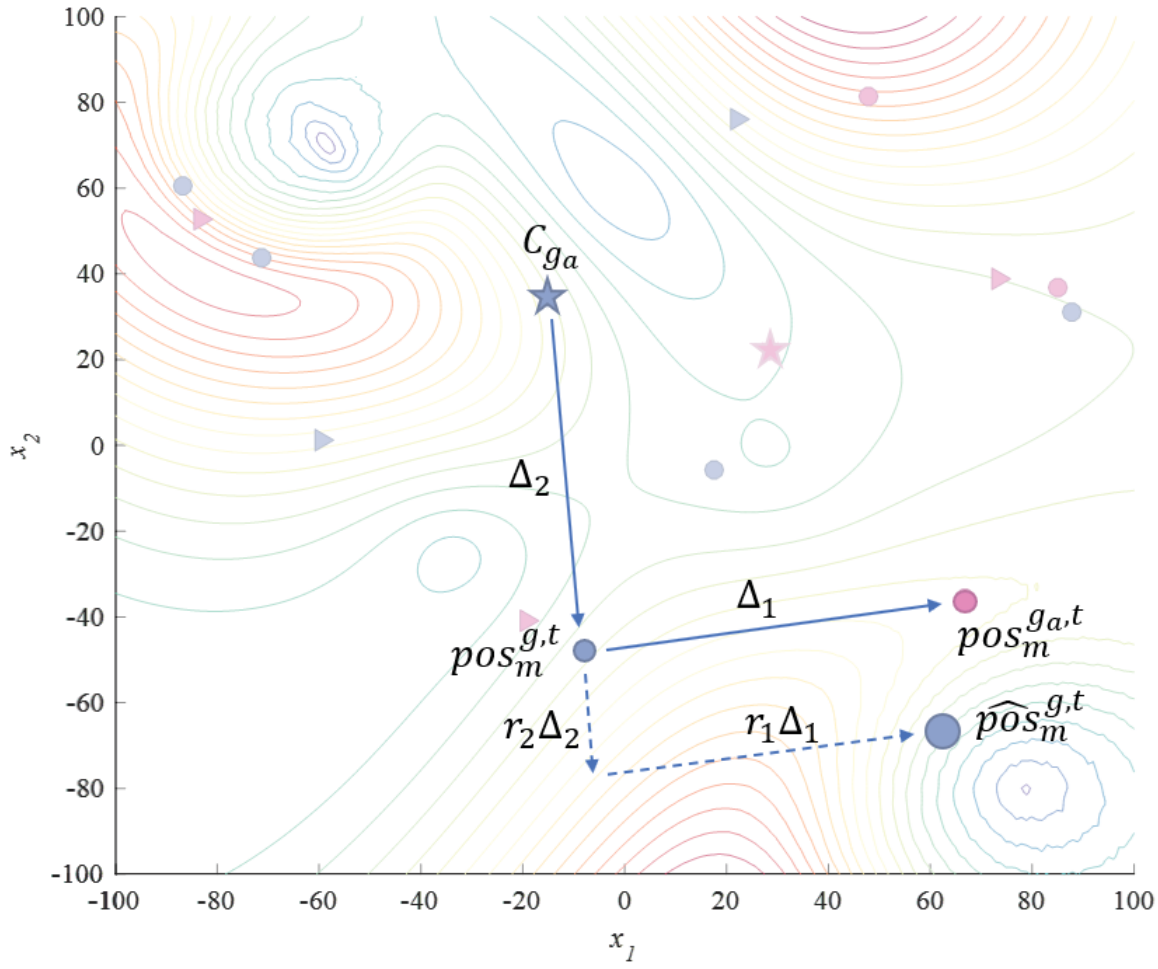

Figure 4.2: Geometrical interpretation of the males movements of WfCMO.

On the other hand, the females movements consists only into depart from the center of the opponent group (Δ_3), which is computed as:

$$\Delta_3 = (pos_m^{g,t} - C_{g_a}) \tag{4.22}$$

$$\widehat{pos}_m^{g,t} = pos_m^{g,t} + r_3 \times \Delta_3 \tag{4.23}$$

where r_3 is a random number in the range [-1,1] generated by uniform probability distribution function and C_{g_a} is the geometrical center of the opponent group. The geometrical interpretation of the females movements is drawn in Fig. 4.3, note that the female monkey moves away from the group, improving the exploration of the algorithm.

It is important to highlight that, as mentioned before, due to the decentralized leadership all monkeys can initiate an action and, therefore, all males and females perform one trial movement

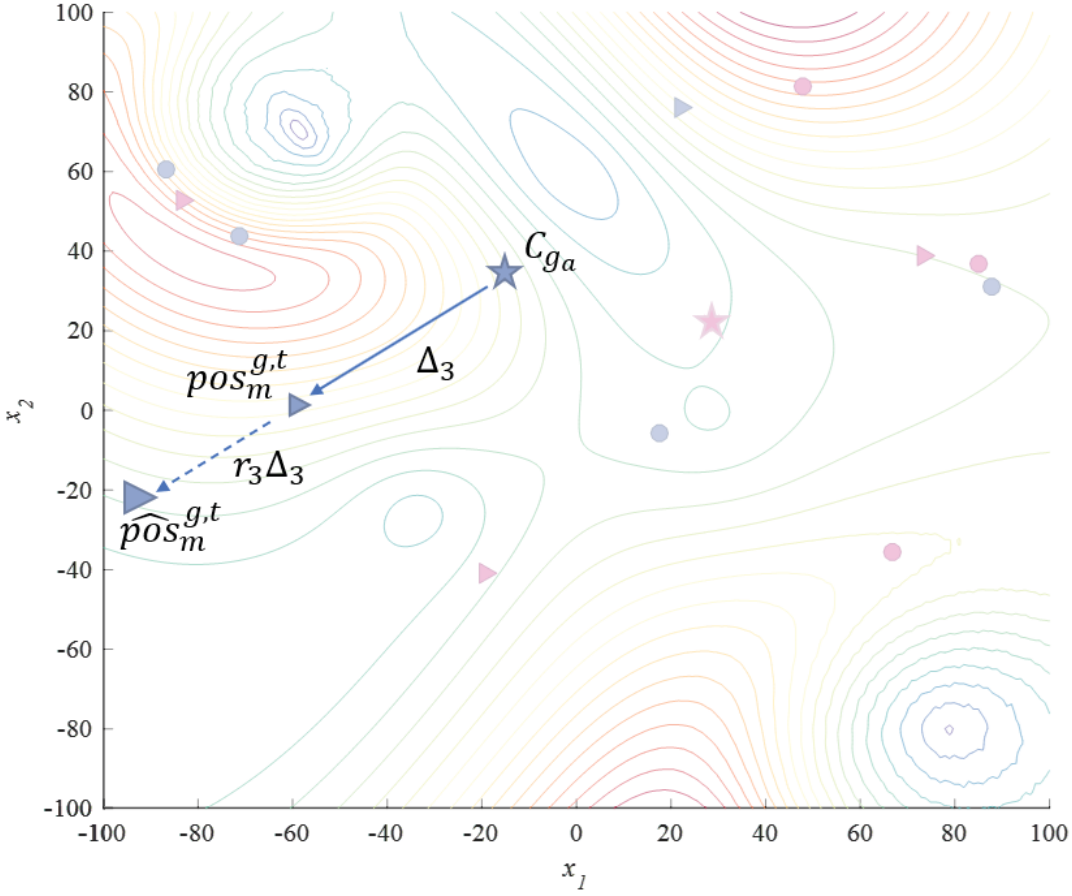

Figure 4.3: Geometrical interpretation of the females movements of WfCMO.

at each iteration. Moreover, a clip mechanism is included to maintain the monkeys inside the search space.

After that, the monkey check its adaptation to decide if it is a better or worse position. For males, it means a better position to fight, while for females it means better protection conditions. It means:

$$pos_m^{g,t+1} = \begin{cases} \widehat{pos}_m^{g,t}, & \widehat{fit}_m^{g,t} < fit_m^{g,t} \\ pos_m^{g,t}, & \text{otherwise} \end{cases}, \tag{4.24}$$

where $\widehat{fit}_m^{g,t} = f(\widehat{pos}_m^{g,t})$.

In order to take into account the two main biological events of life, the birth and the death, the WfCMO computes the age of the monkeys, which is denoted as $age_m^{g,t} \in \mathbb{N}$. Unlike most NiM that generates offspring from parents, the WfCMO must locate the new monkeys in the space. Thus, the birth of an young occurs by placing it as a combination of the position of the monkeys of the group, which is defined as:

$$young_{m,j}^{g,t} = pos_{r_{m,j},j}^{g,t} \tag{4.25}$$

for $j = 1, 2, \ldots, D$, where $r_{m,j} \in \{1, 2, \ldots, N_m\}$ is chosen randomly with uniform probability an represents a random monkey from the group. If $r_{m,j}$ is equal for all j, then the process is repeated until the young borns in a different location of all monkeys of the group.

Aiming to keep the population size static, the birth and death are synchronized in the WfCMO. Whenever a young is born, its position is compared to the monkeys of the group. If the young is better adapted than any other monkey, it survives. If there are multiples monkeys worse adapted than the oldest dies (the ages are computed as $age_c^{p,t} \in \mathbb{N}$). If the young is not better adapted, then it dies.

The Alg. 10 shows the birth and death process, where ω and φ represent, respectively, the set of monkeys worse adapted than the young and the number of monkeys in this set. Note that it is possible that two or more monkeys have similar age (in line 5). In this case, the monkey that presents the worst condition is the one who dies.

Algorithm 10 Birth and death inside a group of capuchins.

```
1: Compute ω and φ
2: if φ = 1 then
3:     The young survives and the only monkey in ω dies.
4: else
5:     if φ > 1 then
6:         The young survives and the oldest monkey in ω dies.
7:     else
8:         The young dies.
9:     end if
10: end if
```

Another important events observed in the white-faced capuchins are the immigration and emigration (Wikberg et al., 2014). However, these events have not been considered in this initial proposal of the WfCMO. Therefore, the pseudo-code of the WfCMO is shown in Alg. 11.

Algorithm 11 Pseudo code of the WfCMO

```
Initialize N_g groups with N_m monkeys each (Eq. 4.16)
Verify the monkeys adaptation (Eq. 4.17)
while stopping criterion is not achieved do
    Define all males and females (Eq. 4.18)
    for each g group do
        Assign a random group to fight against g_a
        Compute the geometrical centers of the groups g and g_a
        for each m monkey of the p group do
            if the monkey is male then
                Male fighting movement (Eq. 4.21)
            else
                Female running away movement (Eq. 4.23)
            end if
            Evaluate the new position and choose the best one (Eq. 4.24)
        end for
        Birth and death (Eq.4.25 and Alg. 10)
    end for
    Update the monkeys' ages
end while
Select the monkey in the best position as the solution of the problem
```

4.3 NATURE-INSPIRED METAHEURISTICS PARAMETERS

The three main factors considered for selecting the algorithms for comparison are (i) the natural inspiration adopted for designing the algorithm; (ii) the diffusion and relevance in this research area; (iii) the use of industrial applications. For comparison purposes, the population size (i.e. number of food sources (S) for ABC, population size (N_p) for BA and FA, number of wolves (N) for GWO, swarm size for PSO (N_p), and ecosystem size (N) for SOS) has been set as 100 for all problems dimensions. It also gives a perspective about the performance of the algorithms regarding the trade-off between the problem's dimension and the population size.

Considering that, the ABC has been chosen mainly because of the intelligent dancing bee's behavior. Further, it has been applied to numerous applications as bioinformatics, scheduling image processing, economic dispatch, engineering design, clustering, and data mining (Bolaji et al., 2013), and its performance has been proved in literature (Karaboga and Basturk, 2008). In this thesis, the ABC parameters *limit*, % of employed bees (N_e) , % of onlooker bees (N_o) and number of scouts (N_s) have been set respectively as $D \times S$, 50%, 50% and 1 (Karaboga and Akay, 2009).

The BA presents a dissimilar design based on the bat's echolocation. Further, it has a variety of applications, such as continuous optimization; combined optimization and scheduling; inverse problems and parameter estimation; classifications, clustering and data mining; image processing, and fuzzy inference systems (Hasançebi et al., 2013; Yang and He, 2013a). In this thesis, the optimal parameters suggested by (Xue et al., 2015) have been employed, such that: loudness (A), pulse rate (r) and γ equal to 0.9, minimum frequency (f_{min}) equals to 0, maximum frequency (f_{max}) equals to 5 and α equals to 0.99.

The FA design is based on the light intensities that depend on the distance between the fireflies. This NiM has been adopted for multimodal problems, continuous and combinatorial optimization, classification, and engineering applications as image processing, antenna design, robotics, and chemistry (Fister et al., 2013). Its parameters randomness (α) and absorption coefficient (γ) have been set as 0.2 and 1, respectively (b. Mo et al., 2013).

The GWO is more recent than the other NiM mentioned and it is inspired by the hierarchy and the hunting behavior of the grey wolfs. In the few years of its existence, it has already been applied to machine learning purposes (clustering and features selection) (Fahad et al., 2018; Emary et al., 2016), economic load dispatch (Pradhan et al., 2018), and some constrained problems (Kohli and Arora, 2017). The GWO's parameter a has been set as linearly decreasing from 2 to 0.

The PSO is one of the most widespread NiM and it is inspired by the synchronized movement observed in the species. It has been used for many real-life applications, such as clustering (Alam et al., 2014), economic dispatch (Mahor et al., 2009), and solar photovoltaic system (Khare and Rangnekar, 2013). Its parameters cognitive constant (c_1) and social constant (c_2) have been both set 2. The inertia weight (w) has been set up from 0.9 to 0.4 with linear decreasing (Poli et al., 2007).

The SOS presents an interesting inspiration that includes different species coexisting in nature. It has already been used in applications as hydrothermal scheduling (Das and Bhattacharya, 2018), economic dispatch (Secui, 2016), truss structures (Tejani et al., 2018), and machine learning purposes (Liao and Kuo, 2018). The only SOS's parameter is the ecosystem size N.

To perform a fair comparison, the proposed NiM has been set accordingly. The COA's number of coyotes(N_c) per pack has been tested as 5 and 10, resulting in, respectively, the COA5 and the COA10 versions. Hence, the resulting number of packs (N_p) is, respectively, 20 and 10. On the other hand, the WfCMO parameter number of monkeys (N_m) has been tested as 5

(WfCMO5), 10 (WfCMO10), and 20 (WfCMO20). The resulting number of groups (N_g) then is, respectively, 20, 10, and 5. The male probability (ρ) has been defined as 0.7. For simplification, let Ψ be the set of all algorithms tested, which means that Ψ = {COA5, COA10, ABC, BA, FA, GWO, PSO, SOS, WfCMO5, WfCMO10, WfCMO20}.

4.4 EXPERIMENTAL DESIGN

The algorithms have been tested on a series of 29[1] benchmark functions from the Institute of Electrical and Electronics Engineers Congress on Evolutionary Computation (IEEE-CEC) 2017 Special Session and Competition on Single Objective Real-Parameter Numerical Optimization (Suganthan et al., 2016). The detailed description of the IEEE-CEC-2017 benchmarks and evaluation criteria are presented in Appendix A. Each benchmark has been tested with dimensions 10, 30, 50, and 100, resulting in a total of 116 cases, summarized in Tab. 4.1, where D means the dimension of the problem, F_{CEC} is the respective function from IEEE-CEC-2017 and the search space is [-100,100]^D for all cases tested.

These cases are classified according to some features (Suganthan et al., 2016), resulting in the group δ = {Overall, Unimodal, Composition, Hybrid, D=10, D=30, D=50, D=100, Multimodal}. It provides a diversified functions landscape and implies in a richer analysis of the algorithms' advantages and disadvantages.

As the NiMs are stochastic algorithms, the validation of the results occurs by the analysis of the repeatability and reliability, which occurs through the statistical information from a series of experiments. It means that the algorithms are tested N_{exp} times with different initial conditions for each optimization problem. Although in some competitions the N_{exp} is set as 51, in this thesis it has been set as 30, which is a suitable value for a reliable statistical comparison with lower computational cost (Suganthan et al., 2005; Chen et al., 2014b).

To perform the fairest comparison possible, the stopping criteria have been defined as the total number of function evaluations N_f^{Max}. As not all algorithms evaluate the objective function at the same time in an iteration [2], it would not be relevant to use the number of iterations as the stopping criteria. The N_f^{Max} has been defined as $10000 \times D$.

The score evaluation from the IEEE-CEC 2017 has also been employed, which is up to 100 and equally considers two criteria, denoted SE and SR. The first one represents the sum of the errors, while the second one is the sum of the ranks. Each index results in a score of up to 50, which is S_1 and S_2, respectively.

Furthermore, the complexity of the algorithms has been evaluated based on the IEEE-CEC 2017 definitions. This analysis is based on the time spent to optimize objective functions with dimensions D = 10, D = 30 and D = 50. Thus, it provides not only the computational cost comparison among the algorithms but also how the algorithm's sensitivity to the dimensions of the problems.

To improve this analysis, two modifications have been implemented in the complexity estimator from IEEE-CEC 2017. First, the dimension D = 100 has been included in the analysis. Second, the objective function computational time (denoted T_0 by definition) has been measured five times instead of only one, as suggested in (Suganthan et al., 2016). The benchmark function used is the F_{18} and the number of function evaluations is 200000. The entire description of the IEEE-CEC 2017 performance analysis is written in Appendix A.

[1] A set of 30 functions has been initially proposed, however, one of these functions has been suspended from the competition because of technical problems.

[2] For example, the SOS evaluates the objective function four times each iteration. If it would be considered the stopping criteria, it would have up to four times more evaluations than the other algorithms.

F	F_{CEC}	D	F	F_{CEC}	D	F	F_{CEC}	D	F	F_{CEC}	D
F_1	1	10	F_{30}	9	30	F_{59}	16	50	F_{88}	23	100
F_2	1	30	F_{31}	9	50	F_{60}	16	100	F_{89}	24	10
F_3	1	50	F_{32}	9	100	F_{61}	17	10	F_{90}	24	30
F_4	1	100	F_{33}	10	10	F_{62}	17	30	F_{91}	24	50
F_5	3	10	F_{34}	10	30	F_{63}	17	50	F_{92}	24	100
F_6	3	30	F_{35}	10	50	F_{64}	17	100	F_{93}	25	10
F_7	3	50	F_{36}	10	100	F_{65}	18	10	F_{94}	25	30
F_8	3	100	F_{37}	11	10	F_{66}	18	30	F_{95}	25	50
F_9	4	10	F_{38}	11	30	F_{67}	18	50	F_{96}	25	100
F_{10}	4	30	F_{39}	11	50	F_{68}	18	100	F_{97}	26	10
F_{11}	4	50	F_{40}	11	100	F_{69}	19	10	F_{98}	26	30
F_{12}	4	100	F_{41}	12	10	F_{70}	19	30	F_{99}	26	50
F_{13}	5	10	F_{42}	12	30	F_{71}	19	50	F_{100}	26	100
F_{14}	5	30	F_{43}	12	50	F_{72}	19	100	F_{101}	27	10
F_{15}	5	50	F_{44}	12	100	F_{73}	20	10	F_{102}	27	30
F_{16}	5	100	F_{45}	13	10	F_{74}	20	30	F_{103}	27	50
F_{17}	6	10	F_{46}	13	30	F_{75}	20	50	F_{104}	27	100
F_{18}	6	30	F_{47}	13	50	F_{76}	20	100	F_{105}	28	10
F_{19}	6	50	F_{48}	13	100	F_{77}	21	10	F_{106}	28	30
F_{20}	6	100	F_{49}	14	10	F_{78}	21	30	F_{107}	28	50
F_{21}	7	10	F_{50}	14	30	F_{79}	21	50	F_{108}	28	100
F_{22}	7	30	F_{51}	14	50	F_{80}	21	100	F_{109}	29	10
F_{23}	7	50	F_{52}	14	100	F_{81}	22	10	F_{110}	29	30
F_{24}	7	100	F_{53}	15	10	F_{82}	22	30	F_{111}	29	50
F_{25}	8	10	F_{54}	15	30	F_{83}	22	50	F_{112}	29	100
F_{26}	8	30	F_{55}	15	50	F_{84}	22	100	F_{113}	30	10
F_{27}	8	50	F_{56}	15	100	F_{85}	23	10	F_{114}	30	30
F_{28}	8	100	F_{57}	16	10	F_{86}	23	30	F_{115}	30	50
F_{29}	9	10	F_{58}	16	30	F_{87}	23	50	F_{116}	30	100

Table 4.1: Description of the 116 optimization problems based on the IEEE-CEC 2017 benchmark functions described in Appendix A

4.5 CHAPTER RESULTS

This section is devoted to showing the experimental results, which are separated in i) the ranking analysis, ii) the scores according to the IEEE-CEC 2017 competition, and iii) the statistical significance tests, iv) the algorithms complexity analysis and v) the convergence and diversity graphics. Considering all these approaches the performance analysis becomes more reliable. The descriptive statistic is presented in Appendix B.

4.5.1 The ranking analysis

The first metric computed is the percentage of victories achieved by the algorithms, which is based on the smallest average error found compared to the global optimal. This metric has been evaluated for each class in δ, as shown in Tab. 4.2.

Overall, the COA10 has won in 22.4% of the cases tested followed by the WfCMO5, which has found the smallest average error in 20.7% of the cases. The ABC has outperformed the other variants of the WfCMO and the COA5 with 19% of victories. The other algorithms have not achieved significant performance in terms of victories.

Table 4.2: Percentage of smallest average error separated by the classes in δ (where Alg.: Algorithm. Uni.: Unimodal. Comp.:Composition and Multi.: Multimodal).

Alg.	Overall	Uni.	Comp.	Hybrid	D=10	D=30	D=50	D=100	Multi.
COA5	12.9%	12.5%	27.5%	7.5%	13.8%	**20.7%**	6.9%	10.3%	13.0%
COA10	**22.4%**	0.0%	17.5%	25.0%	**24.1%**	10.3%	17.2%	**37.9%**	**24.1%**
ABC	19.0%	12.5%	5.0%	**30.0%**	20.7%	**20.7%**	17.2%	17.2%	19.4%
BA	5.2%	0.0%	0.0%	12.5%	0.0%	3.4%	6.9%	10.3%	5.6%
FA	0.0%	0.0%	0.0%	0.0%	0.0%	0.0%	0.0%	0.0%	0.0%
GWO	0.0%	0.0%	0.0%	0.0%	0.0%	0.0%	0.0%	0.0%	0.0%
PSO	0.0%	0.0%	0.0%	0.0%	0.0%	0.0%	0.0%	0.0%	0.0%
SOS	6.9%	12.5%	0.0%	15.0%	10.3%	10.3%	6.9%	0.0%	6.5%
WfCMO5	20.7%	**37.5%**	**30.0%**	5.0%	**24.1%**	17.2%	**27.6%**	13.8%	19.4%
WfCMO10	11.2%	25.0%	15.0%	5.0%	6.9%	13.8%	13.8%	10.3%	10.2%
WfCMO20	1.7%	0.0%	5.0%	0.0%	0.0%	3.4%	3.4%	0.0%	1.9%

Considering the unimodal functions, the WfCMO5 has presented the best performance with 37.5% of victories, while the WfCMO10 has achieved 25%. The COA5, the ABC, and the SOS have all presented 12.5% of victories and the other algorithms have not scored.

Further, the WfCMO5 has outperformed the other algorithms for the composition functions, with 30% of victories against 27.5%, 17.5%, and 15% achieved by the COA5, COA10, and WfCMO10 respectively. The ABC and the WfCMO20 both have won in 5% of the cases and the other algorithms have not won in any case.

Nevertheless, the proposed algorithms have presented a more reticent performance for the hybrid functions. The ABC has achieved 30% of victories against 25% of COA10, 7.5% of COA5, and 5% of WfCMO5 and WfCMO10. The BA has achieved 12.5% and the other algorithms have not won any case.

Considering the different dimensions tested, the COA10 has achieved the best performance for D=10 and D=100, with 24.1% and 37.9% of victories, respectively. Among the WfCMO variants, the WfCMO5 has achieved the best performance for D=50, 27.6% of victories. For D=30, the COA5 and the ABC have found the best solution in 20.7% of the cases tested.

For multimodal functions, the COA10 has achieved the first position with 24.1% of victories against 19.4% of ABC and WfCMO5. The COA5, the WfCMO10, the WfCMO20, the BA, and the SOS have achieved, respectively, 13%, 10.2%, 1.9%, 6.5%, and 5.6% of victories. The other algorithms have not won any case.

To evaluate how suitable the algorithms are for each class in δ, the average rankings (LaTorre et al., 2015) have been computed and described in Tab. 4.3 and illustrated by the Radar plot in Fig. 4.4. Although COA5 and WfCMO10 have not achieved a high number of victories overall, both have presented a good average ranking, 3.89 and 3.87, respectively. It means that in many cases these algorithms have not won, they have been well-ranked anyway. The same can be said considering the multimodal functions, where the COA5 has achieved the lowest average ranking, 3.78. Again, the WfCMO5 and WfCMO10 have achieved the lowest average ranking for problems with dimension equals 30.

In Fig. 4.4, where the smaller ranks are around the center of the Radar plot, it is easier to see that the proposed algorithms are concentrated nearest to the center. Regardless of the ABC and the SOS, which have shown competitive performance, the proposed algorithms have outperformed the other state-of-the-art algorithms for the experimental design employed.

Table 4.3: Average ranking separated by the classes in δ (where Alg.: Algorithm, Uni.: Unimodal., Comp.:Composition and Multi.: Multimodal).

Alg.	Overall	Uni.	Comp.	Hybrid	D=10	D=30	D=50	D=100	Multi.
COA5	3.89	5.38	3.30	3.98	3.41	4.28	4.14	**3.72**	**3.78**
COA10	4.07	5.88	4.85	3.75	**3.28**	4.76	4.28	3.97	3.94
ABC	4.66	6.50	5.80	**3.25**	4.34	4.24	5.00	5.03	4.52
BA	8.35	6.50	8.78	8.13	9.21	8.21	8.10	7.90	8.49
FA	11.00	11.00	11.00	11.00	11.00	11.00	11.00	11.00	11.00
GWO	8.02	8.50	8.43	7.95	8.28	8.07	7.83	7.90	7.98
PSO	8.79	7.38	8.88	8.98	8.93	9.00	8.72	8.52	8.90
SOS	4.38	5.38	4.80	3.58	5.00	4.28	4.21	4.03	4.31
WfCMO5	3.91	3.25	**2.83**	5.03	3.83	**3.62**	**3.76**	4.45	3.96
WfCMO10	**3.87**	**2.50**	3.08	4.75	3.86	**3.62**	3.93	4.07	3.97
WfCMO20	5.06	3.75	4.28	5.63	4.86	4.93	5.03	5.41	5.16

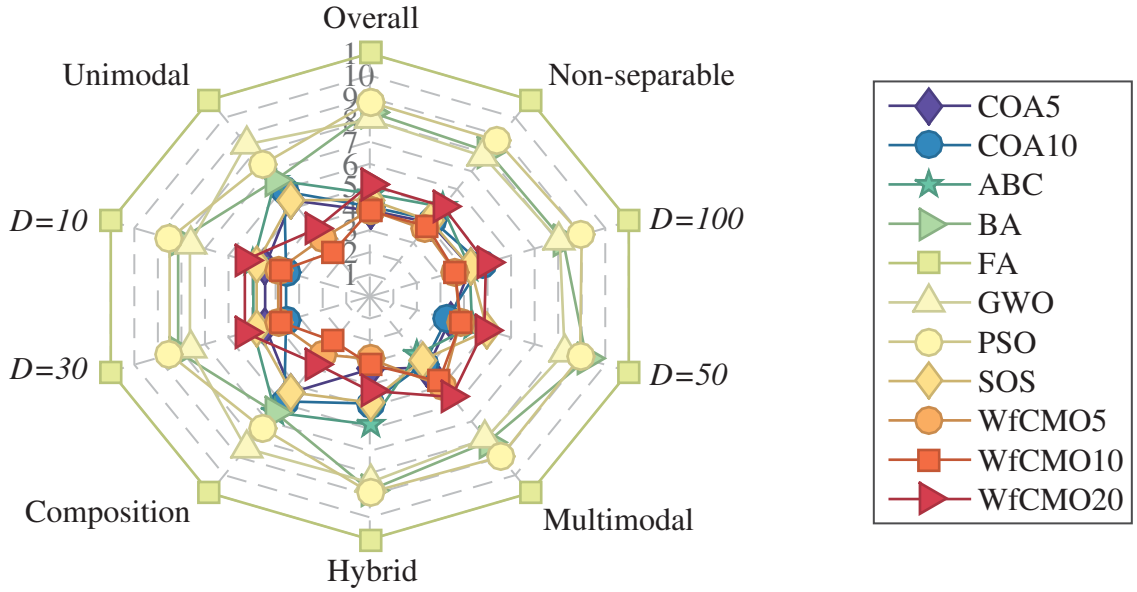

Figure 4.4: Average ranking separated by the classes in δ.

4.5.2 The performance scores

In this section, the score analysis is provided (Suganthan et al., 2016), which considers both the sum of the errors and the ranks weighted by the problems' dimensions. This analysis helps to evaluate the general performance of each algorithm due to the combination of those two criteria.

The Tab. 4.4 shows the scores achieved by the algorithm, where the resulting rank is computed in the last column. The COA5 has achieved the best performance in this criterion, followed by the COA10, the SOS, the WfCMO10, the WfCMO5, the WfCMO20, the ABC, the BA, the GWO, the PSO, and finally the FA.

Considering only the sum of the errors (S_1), the COA5 has achieved the best score, the COA10 the second best, and the SOS the third-best one. The WfCMO20, the WfCMO10,

Table 4.4: Scores according to the IEEE-CEC 2017.

Algorithm Name	S_1	S_2	Final Score	Rank
COA5	50.00	49.87	99.87	1
COA10	45.58	47.22	92.80	2
ABC	11.73	40.83	52.57	7
BA	1.98	24.03	26.00	8
FA	0.00	17.81	17.81	11
GWO	0.01	24.64	24.65	9
PSO	0.02	22.47	22.49	10
SOS	27.54	46.29	73.83	3
WfCMO5	11.70	48.80	60.50	5
WfCMO10	18.08	50.00	68.08	4
WfCMO20	20.34	38.04	58.39	6

the ABC, and the WfCMO5 have achieved lower scores, but still relevant values. The other algorithms have not achieved competitive performance for (S_1).

On the other hand, the WfCMO10 has presented the best score considering only the sum of the ranks (S_2), followed by the COA5, the WfCMO5, the COA10, the SOS, the ABC, the WfCMO20, the GWO, the BA, the PSO, and the FA, respectively. As the scores are weighted by the dimension of the problem (which tends to increase the complexity of finding the global optimal), it is not possible to say that the algorithms that presented lower scores can not be good options for low dimensional (10 and 30, for example) optimization problems.

4.6 STATISTICAL SIGNIFICANCE TESTS

In this section, a deeper analysis of the significance of the results is provided. Due to the high number of benchmark functions with different domains in terms of objective costs, the median values have been computed and converted to rankings to represent the set of experiments (García et al., 2010; Derrac et al., 2011; Gibbons and Wolfe, 2003). The null hypothesis H_0 states that the medians of all algorithms belong to the same population and the statistical confidence considered is $\alpha = 0.5$.

According to the Friedmann Rank sum test, the resulting p-value is neatly equal to zero (3.4343e-138) and the null hypothesis is rejected. It means that there is at least one algorithm significantly different from the others. In other to achieve a more complete analysis, multiple $1xN$ comparisons with the proposed algorithms as the control method are presented. In this context, the one-tailed Wilcoxon-Mann-Whitney's test has been applied and the Holm-Bonferroni post-hoc method is used to correct the p-values found. The null hypothesis H_0 states that the median error of the control method is not smaller than the median of the opponent, while H_1 states that the median error achieved by the control method is smaller than the other algorithms.

The results of the $1xN$ comparisons are exposed in Table 4.5, where the corrected p-values are presented and the null hypothesis is rejected if the p-value is smaller than α. The H_0 has been rejected for all comparisons with the BA, the FA, the GWO, and the PSO. Then, it can be said that all variations of COA and WfCMO have outperformed these algorithms. On the other hand, the H_0 has not been rejected in any comparison with the ABC and the SOS. It means that these two algorithms have not been outperformed by the proposed algorithms. Considering the comparison between the proposed algorithms, there is no significant difference in the results.

Algorithm	COA5		COA10		WfCMO5		WfCMO10		WfCMO20	
	p-value	H_1?	p-value	H_1?	p-value	H_1?	p-value	H_1?	p-value	H_1?
COA5	-	-	1.00E+00	No	1.00E+00	No	1.00E+00	No	1.00E+00	No
COA10	1.00E+00	No	-	-	1.00E+00	No	1.00E+00	No	1.00E+00	No
WfCMO5	1.00E+00	No	1.00E+00	No	-	-	1.00E+00	No	1.00E+00	No
WfCMO10	1.00E+00	No	1.00E+00	No	1.00E+00	No	-	-	1.00E+00	No
WfCMO20	1.00E+00	No	1.00E+00	No	1.00E+00	No	1.00E+00	No	-	-
ABC	3.24E-01	No	5.43E-01	No	2.13E-01	No	2.19E-01	No	6.07E-01	No
BA	3.75E-07	**Yes**	2.09E-06	**Yes**	1.36E-07	**Yes**	1.86E-07	**Yes**	1.30E-06	**Yes**
FA	5.40E-19	**Yes**	1.82E-17	**Yes**	1.36E-19	**Yes**	2.44E-19	**Yes**	1.75E-18	**Yes**
GWO	9.77E-04	**Yes**	2.73E-03	**Yes**	4.11E-04	**Yes**	4.71E-04	**Yes**	2.27E-03	**Yes**
PSO	1.98E-04	**Yes**	1.00E-03	**Yes**	9.82E-05	**Yes**	1.30E-04	**Yes**	6.87E-04	**Yes**
SOS	6.28E-01	No	1.00E+00	No	4.67E-01	No	5.40E-01	No	1.00E+00	No

Table 4.5: The one-tailed Wilcoxon-Mann-Whitney non-parametric test using the proposed algorithms as control methods individually for a significance level of $\alpha = 0.05$ combined with the post-hoc method of Holm-Bonferroni.

4.6.1 The metaheuristics complexity

This analysis provides a point of view that contrasts the performances based on the quality of the solutions achieved, which is the computational cost required by the algorithms. The computational complexities are described in Tab. 4.6, where a higher value indicates high computational cost and vice-versa. Moreover, the percent growth according to the problem's dimension is also shown for a clearer understanding. For a better view, these values are drawn side by sidebars on Fig. 4.5, where the complexity axis is set to a logarithmic scale.

Algorithms	D=10	D=30		D=50		D=100	
COA5	95.33	101.06	(+6.02 %)	106.15	(+5.03 %)	113.98	(+7.38 %)
COA10	81.10	85.67	(+5.63 %)	92.34	(+7.78 %)	99.66	(+7.93 %)
ABC	305.03	307.69	(+0.87 %)	312.55	(+1.58 %)	312.47	(-0.02 %)
BA	20.83	24.72	(+18.70 %)	25.95	(+4.96 %)	26.57	(+2.38 %)
FA	121.11	678.09	(+459.89 %)	862.33	(+27.17 %)	1101.04	(+27.68 %)
GWO	24.02	42.82	(+78.25 %)	61.20	(+42.93 %)	98.91	(+61.62 %)
PSO	18.45	21.41	(+16.06 %)	24.43	(+14.12 %)	28.24	(+15.58 %)
SOS	85.56	88.50	(+3.44 %)	91.86	(+3.80 %)	99.53	(+8.34 %)
WfCMO5	177.00	182.75	(+3.25 %)	188.26	(+3.02 %)	197.94	(+5.14 %)
WfCMO10	116.10	123.58	(+6.44 %)	128.41	(+3.91 %)	133.58	(+4.02 %)
WfCMO20	82.27	87.87	(+6.81 %)	93.25	(+6.12 %)	100.60	(+7.88 %)

Table 4.6: Algorithms complexity and the respective percent growth according to the problem dimension.

The first insight is that the WfCMO presents a notable difference in complexity according to the number of monkeys per group. The smaller this number, the higher is the computational cost. Considering that the population size is constant, this difference suggests that the complexity growth is caused by the group's management. It means the operations executed inside each group excepting those related to the monkey itself, like the male/female definition, the choice of groups to fight, and the birth and death.

On the other hand, the COA presents a smaller difference according to the number of packs, which suggests that COA has operators computationally simpler than WfCMO. The complexities presented by the COA5 and the COA10 are generally smaller than WfCMO variants.

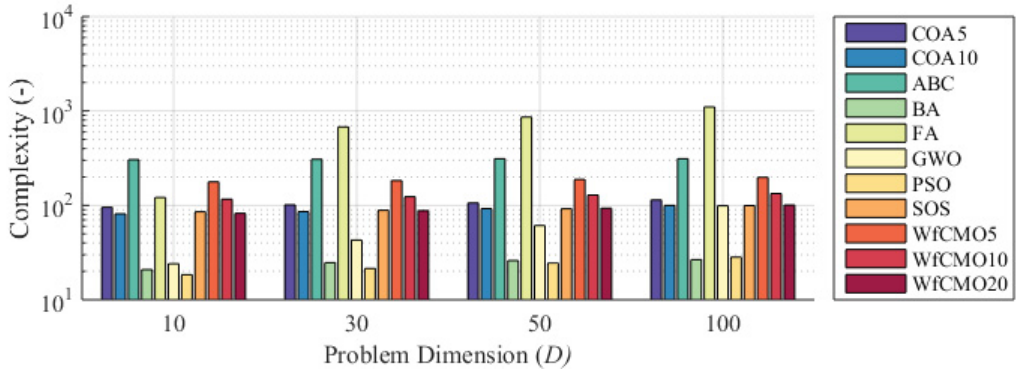

Figure 4.5: Complexity analysis based on the IEEE-CEC 2017 definitions.

The only exception is that the COA5 is slower than WfCMO20 due to the packs' management, however, it tends to be closer as the dimension increases.

Moreover, both COA and WfCMO variants present a linear computational cost growth, with values from 3.02% (WfCMO5 from $D = 30$ to $D = 50\%$) to 7.93% (COA10 from $D = 50$ to $D = 100\%$). In fact, the only algorithm that achieves a nearly constant computational cost from $D = 50$ to $D = 100\%$ is the ABC, where the variation is very close to zeros (0.02%).

Comparing the complexity values from the COA and the WfCMO variants with the other algorithms, it is notable that ABC and FA required more computational power, while BA and PSO are the fastest algorithms in the set. Regarding the SOS, the values are close to the COA variants and WfCMO20, while WfCMO5 and WfCMO10 present more costly values. Considering GWO, the costs presented are smaller than COA and WfCMO variants for all dimensions. However, the results present a growth tendency as the dimension increases, suggesting a higher cost than the proposed algorithms for dimensions higher than $D = 100$.

4.6.2 Convergence and diversity analysis

This analysis is devoted to correlate the convergence and diversity curves of the COA and the WfCMO among the optimization process. As stated, the balance between exploration and exploitation is an important factor to achieved good performance.

Overall, the COA versions have presented a more diverse population during the process compared to the WfCMO versions. As an example, Fig. 4.6 illustrates these curves for a unimodal function with dimension equals to 10, where the COA has kept higher diversity and still could converge as well as the WfCMO versions. Further, the COA5 and COA10 have presented similar behavior of convergence and diversity, as well as the WfCMO variants. Considering the unimodal functions, the difference can be considered wispy.

Nevertheless, this gap becomes notable for the other type of functions, as the example drawn in Fig. 4.7, which represents a multimodal function with dimension equals to 50. The resulting curves of the WfCMO variants are slightly different, where the higher the number of monkeys per group, the higher the diversity and the average error. On the other hand, the COA5 has presented higher diversity than the COA10, as well as higher average errors. The COA10 has present the best trade-off between diversity and convergence for this case.

Considering hybrid functions, otherwise, the algorithms have presented continuous convergence curves with steady diversity ones. As an example, Fig. 4.8 contains the results of a hybrid function with the dimension equals to 100. Again, the COA10 has achieved an intermediate diversity with the best convergence compared to the other algorithms. The WfCMO variants have shown similar curves in both cases.

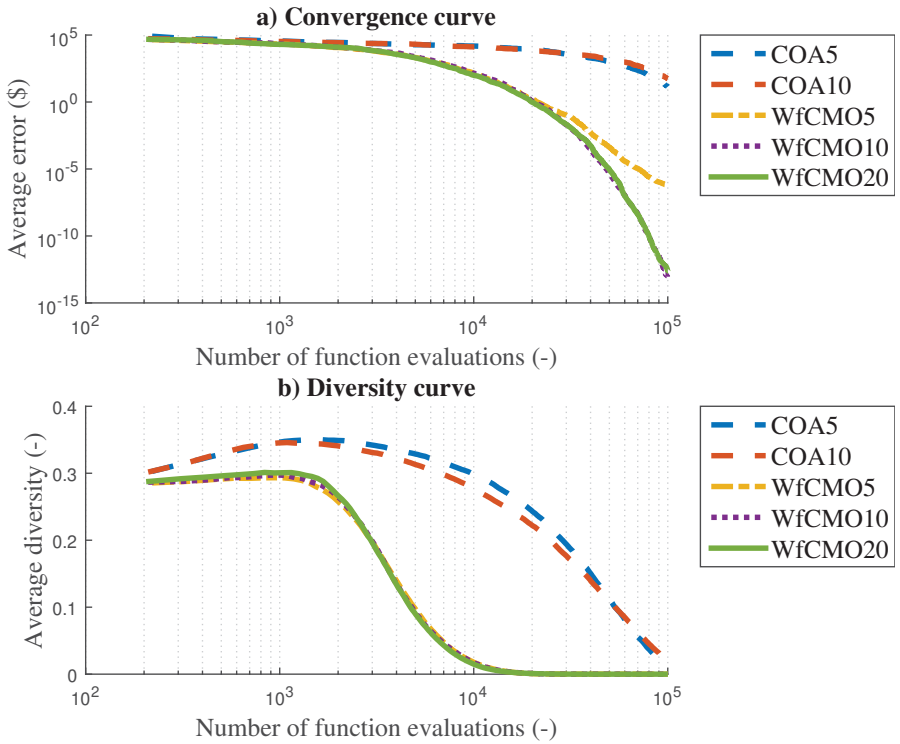

Figure 4.6: Convergence and diversity graphics of a unimodal function with dimension equals to 10 (f_5).

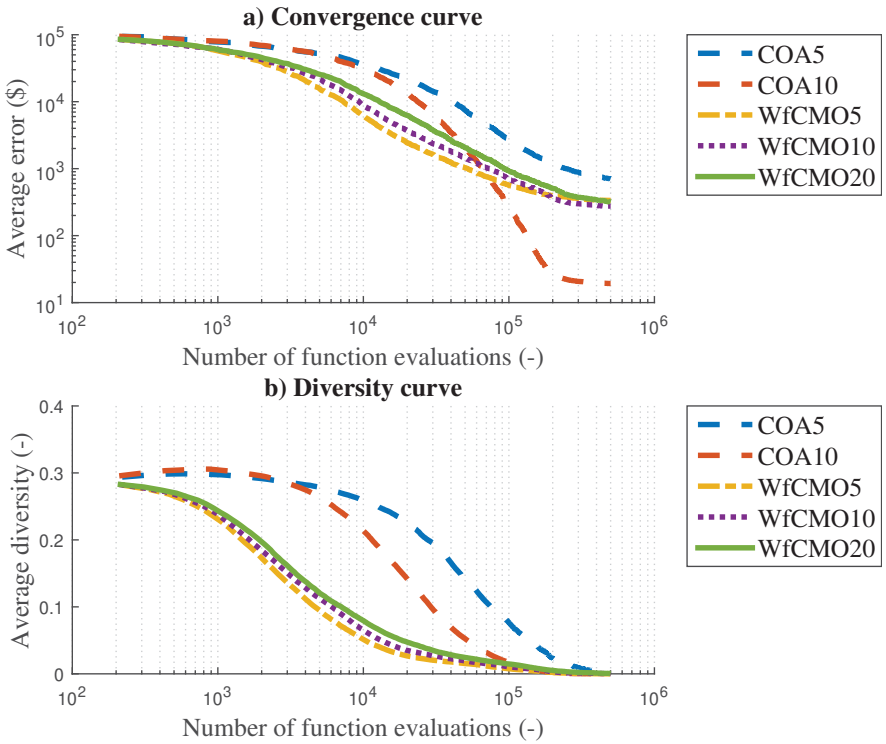

Figure 4.7: Convergence and diversity graphics of a simple multimodal function with dimension equals to 50 (f_{31}).

In the case of composition functions, all algorithms have presented similar convergence curves, however the diversity is notably different. In the example illustrated in Fig. 4.9, the COA10‘s diversity curve is bounded by the other algorithms, closer to the WfCMO variants.

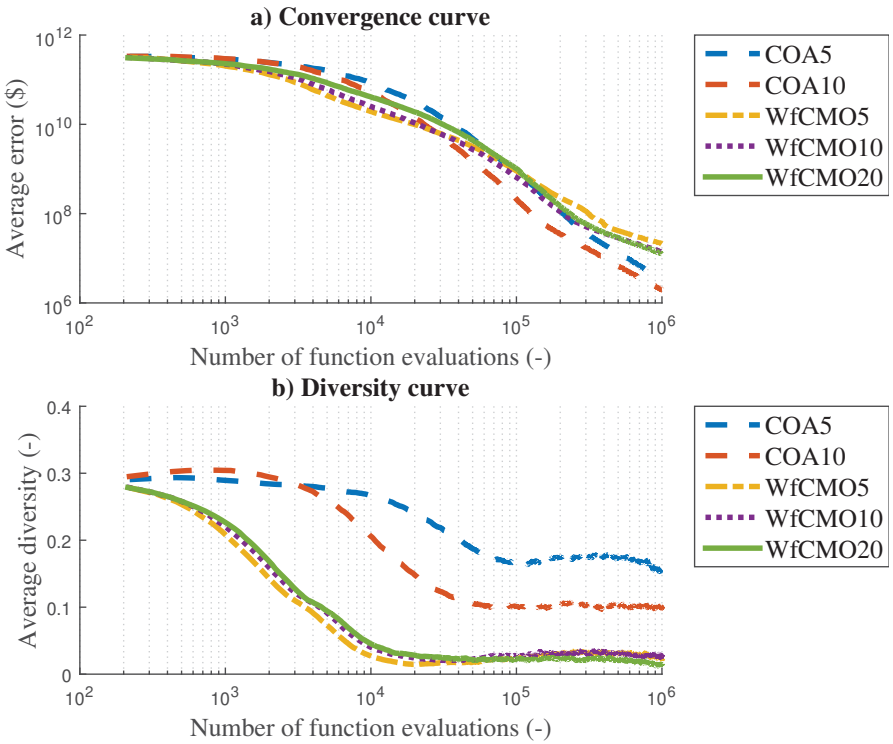

Figure 4.8: Convergence and diversity graphics of a hybrid function with dimension equals to 100 (f_{44}).

The WfCMO with fewer monkeys per group has resulted in a less spread population during the optimization process.

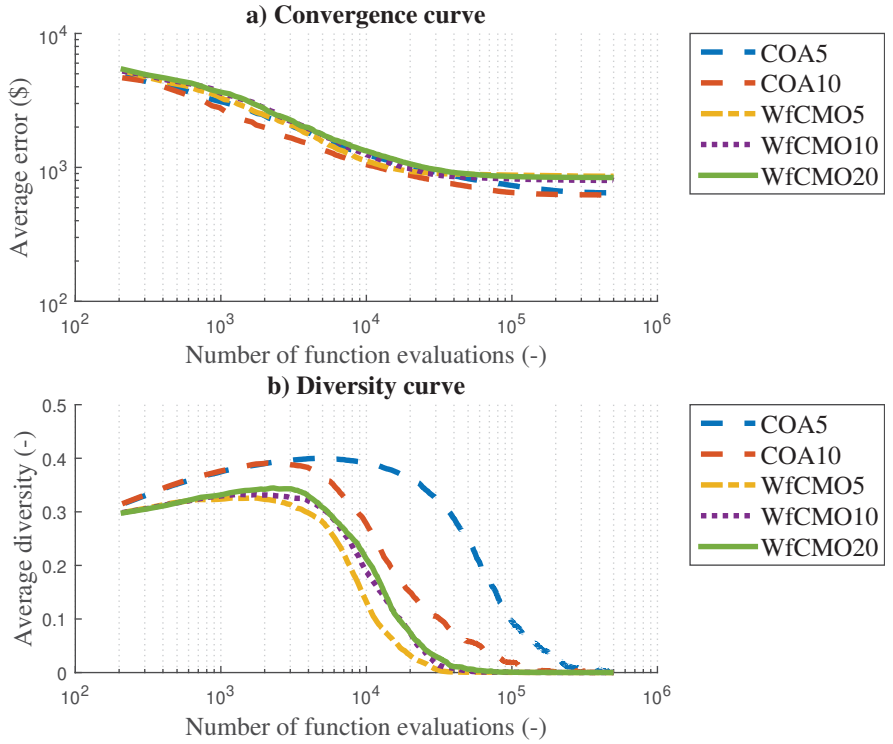

Figure 4.9: Convergence and diversity graphics of a composition function with dimension equals to 50 (function number 27 of the IEEE-CEC2017).

4.7 CHAPTER DISCUSSION

According to the analysis provided in this chapter, the proposed algorithms have presented competitive or better performance when compared to other state-of-the-art NiMs. The different performance metrics and classes of problems employed provided a complete view of the best cases for the algorithms. The high dimensional and multimodal problems have been included, which are the two more explored classes in the global optimization research area.

Considering the IEEE-CEC 2017 performance analysis, the COA variants have achieved the best performance in most cases. The COA10 has found the best solutions in almost a quarter of the cases tested, with the significant 37.9% of first place for the problems with dimension equals to 100 and 24.1% for multimodal ones. For hybrid functions, it has won a quarter of the cases, which is an important contribution considering that the proposed algorithms have not performed well for this class. It has also achieved low average rankings overall, which means that it could be employed for any desired problem class.

Moreover, the COA5 has presented good performance mainly for composition functions, which has won in 27.5% of the cases and it has achieved a lower average ranking. Although it has not been the best winner for high dimensional and multimodal problems, it has presented the lowest average ranking for both classes. It means that it could be reliably employed for these classes too.

Regarding the WfCMO variants, the main result is the performance gap between the WfCMO20 compared to the other variants. This one could not perform well for most cases tested and it could easily be replaced by the WfCMO5 of the WfCMO10, which has achieved better performance for the percentage of first place and average ranking. Even though it has presented higher diversity values during the optimization process, it could no converge better than the other variants.

On the other hand, the WfCMO5 and the WfCMO10 have presented competitive performance. Both have outperformed the BA, the FA, the GWO, and the PSO with a statistical confidence of 95%, while the ABC and the SOS have not been outperformed. The WfCMO10 has achieved the lowest overall average ranking and for unimodal problems, which is a class that the proposed algorithms have not shown expressive performance. It is more likely to be applied for unimodal and composition problems, not for hybrid functions though. The WfCMO10 has also achieved the best score among the WfCMO variants according to the IEEE-CEC competition criteria.

Nevertheless, the WfCMO5 has shown good performance in terms of victories mainly for composition, unimodal, and D=50 problems, in which it has won in a quarter or more of the cases tested. Overall, where it has won in 20.7% of the problems, it has only been outperformed by the COA10. It also appears as a good option for multimodal problems, while it is not the right choice for hybrid functions. Although it is not in the top rank of the final scores, it has achieved the best average ranking at all for composition functions and very good values for D=30 and D=50 problems. There might exist a correlation between the population size and the problem dimension not only for the WfCMO5 but for all WfCMO variants.

Considering the convergence and diversity graphics exposed, which are the best examples of the general behavior of the algorithms, the COA10 has shown a better ability to keep high diversity and convergence simultaneously. Although the WfCMO variants have presented small diversity values in the optimization process, the results presented have not been significantly worst than the COA variants. Hence, it is not possible to affirm that the balance between exploration and exploitation has not been achieved because of the low diversity presented.

5 IMPROVED COA FOR A GAS TURBINE OPTIMIZATION

Because of the promising results presented by the COA for IEEE CEC 2017 benchmarks, this algorithm has been chosen to be further explored. An improved version of the COA based on cultural algorithms is proposed and applied to the constrained optimization of a heavy-duty gas turbine operation. The results for five variations of the optimization problem are presented.

It is important to highlight that part of the content presented in this chapter has been published in the "Energy Conversion and Management" journal in the article entitled "Cultural coyote optimization algorithm applied to a heavy-duty gas turbine operation".

5.1 PROPOSED CULTURAL COA

The cultural algorithm is a methodology responsible for gathering knowledge to any optimization method based on populations(Ribeiro and Aguiar, 2011). According to (Peng et al., 2003; Ali et al., 2018) there are five types of knowledge sources: normative, situational, topographic, domain, and historical. Though the authors indicated that not all of them must be applied to all situations. Thus, once COA has good exploratory behavior, as mentioned in the previous chapter, the normative space is included, as it has the potential to restrict the search space when it is suitable.

The normative belief constrains the search space to a promising region, which is defined by the minimum (l) and maximum (u) values. The minimum and maximum costs, L and U, respectively, are also defined. These values are set from a subgroup (x) from the total population formed by $nAccepted$ best individuals. The number of individuals accepted is defined by the parameter ψ, which represents a percentage of the population, and the belief space of the t^{th} iteration is updated as follows:

$$l_j^t = \begin{cases} x_{i,j} & x_{i,j} \leq l_j^{t-1} \text{or} f(x_i) < L_j^{t-1} \\ l_j^{t-1} & \text{otherwise} \end{cases} \tag{5.1}$$

$$L_j^t = \begin{cases} f(x_i) & x_{i,j} \leq l_j^{t-1} \text{or} f(x_i) < L_j^{t-1} \\ L_j^{t-1} & \text{otherwise} \end{cases} \tag{5.2}$$

$$u_j^t = \begin{cases} x_{i,j} & x_{i,j} \geq u_j^{t-1} \text{or} f(x_i) < U_j^{t-1} \\ u_j^{t-1} & \text{otherwise} \end{cases} \tag{5.3}$$

$$U_j^t = \begin{cases} f(x_i) & x_{i,j} \geq u_j^{t-1} \text{or} f(x_i) < U_j^{t-1} \\ U_j^{t-1} & \text{otherwise} \end{cases} \tag{5.4}$$

for $i = \{1, 2, ..., nAccepted\}$ and $j = \{1, 2, ..., D\}$.

In the CCOA, the normative knowledge is employed in the coyote's social condition update. The mechanism is inspired by the suggestions of (Ma et al., 2008; Yan et al., 2012), and can be written as follows:

$$new\_soc_{c,j}^{p,t} = \begin{cases} soc_{c,j}^{p,t} + \gamma \times |r \times (u_j - l_j)|, & soc_{c,j}^{p,t} < l_j \\ soc_{c,j}^{p,t} - \gamma \times |r \times (u_j - l_j)|, & soc_{c,j}^{p,t} > u_j \\ ct_j^{p,t} + \gamma \times r \times (u_j - l_j), & \text{otherwise} \end{cases} \tag{5.5}$$

for $p = 1, 2, ..., N_p$, $c = 1, 2, ..., Nc$ and $j = 1, 2, ..., D$, where r represents a random number generated by normal distribution of probability with average and variance equal to 0 and 1, respectively, and γ is the step weight, which can be initially defined in the range]0,1]. The γ setup is discussed in the next sections.

It means that when outside, the coyotes are conducted to the cultural promising region defined by the normative belief among all population members. On the other hand, when inside, the coyotes are influenced by the social tendency of the respective pack. The pseudocode of the proposed CCOA is shown in the Algorithm 12, where r is a random number inside the range [0,1] generated by a uniform distribution of probability.

Algorithm 12 Pseudo code of the CCOA

```
Define the control parameters N_p, N_c, ψ, P_n and γ
Initialize N_p packs with N_c coyotes each (Eq. 4.2)
Verify the coyote's adaptation (Eq. 4.3)
while stopping criterion is not achieved do
    Update normative knowledge (Eqs. 5.1, 5.2, 5.3 and 5.4)
    for each p pack do
        Define the alpha coyote of the pack (Eq. 4.5)
        Compute the social tendency of the pack (Eq. 4.6)
        for each c coyotes of the p pack do
            if r < P_n then
                Update the social condition (Eq. 5.5)
            else
                Update the social condition (Eq. 4.12)
            end if
            Evaluate the new social condition (Eq. 4.13)
            Adaptation (Eq. 4.14)
        end for
        Birth and death (Eq.4.7 and Alg. 8)
    end for
    Transition between packs (Eq. 4.4)
    Update the coyotes' ages
end while
Select the best adapted coyote
```

5.2 PROBLEM FORMULATION

The heavy-duty GT studied in this research is the Siemens Westinghouse W501FD, as illustrated in Fig. 5.1. This equipment performs the Brayton cycle, the technical specifications of the system are written in Tab. 5.1 and the six subsystems of the heavy-duty GT are:

1. Admission system. The air intake system provides clean and cool atmospheric air to the compressor through the use of filters and an air cooling system, and it is composed of a weather protection cover, double barrier air filter, evaporative cooler, muffler, ducts, and vane control of intake air.

2. Compression system. The compressor has sixteen stages, or set of vanes mounted on a single shaft and is of the axial type, which guarantees a virtually constant flow at pressures variables.

3. Combustion system. The combustion system consists of sixteen low-emission Nitrogen Oxides (NO_x) in a circular arrangement, each combustion consisting of a combustion chamber cylindrical. Each set of combustors is composed of four subsets that have independent firing nozzles. The central nozzle is denoted the Pilot stage. It is surrounded by eight nozzles, which are four of stage A and four of stage B. There is also stage C, called the dispersion ring, which calibrates holes that disperse the gas inside the chamber.

4. Turbine system. The turbine of this equipment is a simple flow and internal combustion machine. It is a reaction type, it has four stages and is assembled with curved discs, which are responsible for transforming the flow of the working fluid (air) into torque.

5. Exhaust system. The temperature of the hot gases generated by the fuel burning in the primary section is cooled in the secondary section. The spaces along the combustion chamber allow cool air to pass and refrigerate its walls.

6. Fuel manifold system. It is a chamber that has a number of outlets for distributing the resulting gases to the outside.

The Pilot differs from the other stages since it injects an air-gas mixture instead of only gas. The power generated by the turbine relies on the combination of the gas inputs through those injection stages, and as they have different positions in the combustor design, the right combination of gas in the injectors can produce more power and emit fewer pollutants (Yamao et al., 2017a). Once pollutant emissions from combustion processes is a major public concern because of their impact on health and the environment (Lefebvre and Ballal, 2010), the set of values to the fuel injectors must be less than a predefined value. In concern to Brazilian regulations, the most critical pollutant in GT operations are the NO_x, which cannot exceed the value of 25 ppm (Brasil, 2018).

Nominal load	173 MW
Heat Rate (single cycle)	9360 Btu/kWh
Heat Rate (combined cycle)	5595 Btu/kWh
Air flow mass	449 kg/s
Efficiency using Natural Gas (NG)	36 %
Nominal speed	3600 rpm
Number of burners	16
Compressor stages (axial flow)	16
Turbine stages (reaction type)	04
Compression ratio	15:1
Turbine inlet temperature	2350 ºF / 1288 ºC
Exhaust temperature	1076 ºF / 580 ºC

Table 5.1: W501F technical specifications.

The GT has also two main operation restrictions due to its physical characteristics. The first is the maximum exhaust temperature, chosen in order to avoid damaging the chimney

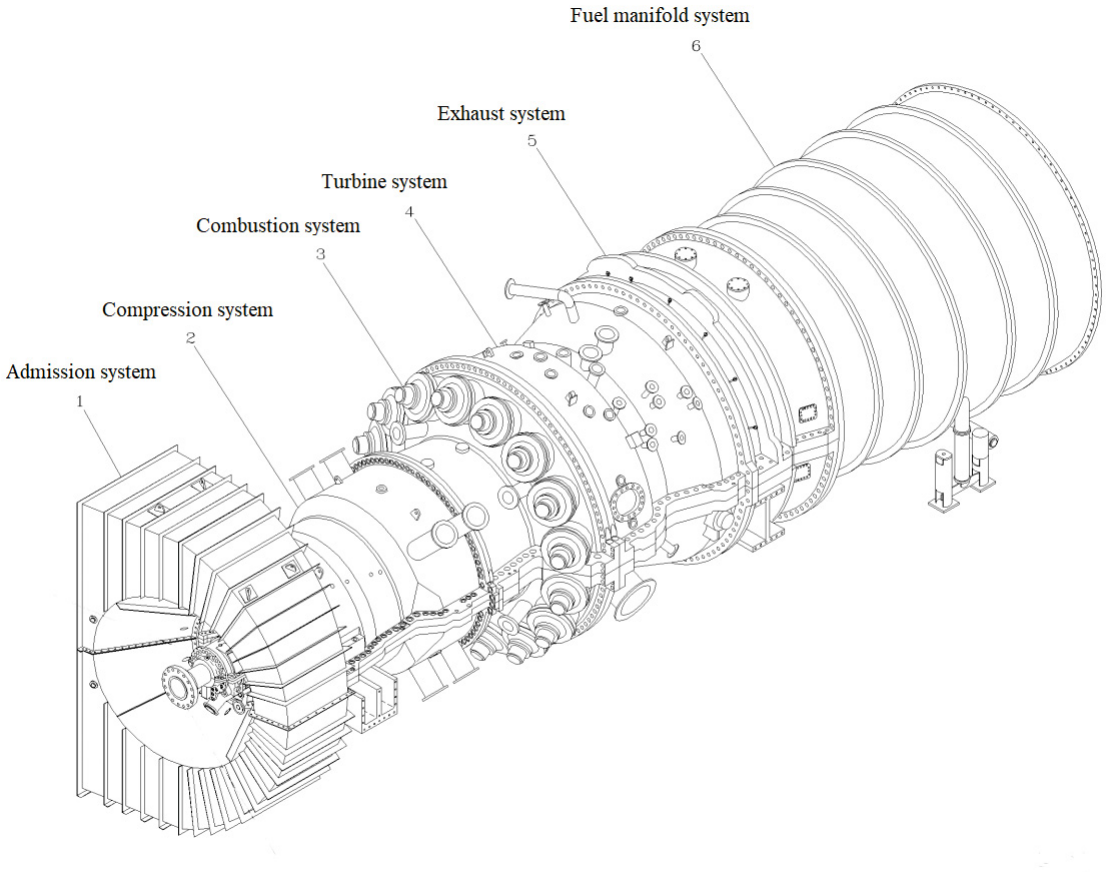

Figure 5.1: Heavy-duty gas turbine Siemens Westinghouse W501FD

materials, the highest allowed exhaust temperature (ET) is 600 ^oC. And the second critical restriction is the maximum value of Pressure Oscillations (PO) inside the combustion chamber, caused by the flame instability in combustor stages (Pierezan et al., 2017b; Iurashev et al., 2017).

The maximum value of PO is related to the frequency range, thus there are different threshold values to each frequency band. These constraints have been defined according to the equipment technical specifications and values allowed are exposed on Tab. 5.2.

Table 5.2: Frequency ranges and maximum pressure oscillations.

Ranges setup	f_1	f_2	f_3	f_4	f_5	f_6	f_7	f_8	f_9
From (KHz)	0	0.015	0.05	0.1	0.16	0.3	0.5	1	3
To (KHz)	0.015	0.05	0.1	0.16	0.3	0.5	1	3	4.2
Limit (PSI)	0.3	0.6	1.6	1.6	1.0	0.3	0.2	0.1	0.1

5.2.1 The simulation model

To simulate the GT, two different black-box modeling methods were employed using real data collected during the GT tuning procedure. At the tuning, a technician manually varies the gas inputs, called stages, until finding a sub-optimal adjustment to a given power range, thus generating a wide range of data to system identification.

As seen in the block diagram of Fig. 5.3, the ambient temperature and the gas flow in the fuel injectors A, B, C and $Pilot$ are common inputs to all the four modeled phenomena: the

GT power output, the estimated power output (Pot), the NO_x emission, the pressure oscillations in the combustion chamber, and the Exhaust temperature. The gas flow has been measured by the original gas turbine sensors at the combustion chamber stages entries. However, to the last three mentioned models, the output of the power model is also used as an input, in a cascade arrangement.

The values to the GT power output (Pot), the NO_x emission, and the ET are predicted through Radial Basis Function (RBF) feed-forward ANNs previously developed for this specific turbine in (Yamao et al., 2017a,b). Meanwhile, multilinear regression models are used to predict the maximum value of the pressure oscillations to each frequency range, in the same means of the model studied in (Pierezan et al., 2017b).

The models' accuracies are shown in Table 5.3, where the symmetric Mean Absolute Percentage Error (sMAPE) values, the Coefficient of Determination (R^2) and the Pearson's r (both indicators of the identification quality) to the validation data are presented. The validation set is composed of 16000 samples, corresponding to 50% of total samples. High correlation values are shown in the table, with a small percentage error. The NO_x model has shown the highest error, although it is within an acceptable value to assist in coping with the optimization problem treated in this work.

The real and predicted values to the Pot, NO_x, and ET are illustrated in Fig. 5.2, where it's possible to verify small errors and well-correlated models. The pressure oscillations model's accuracy is not shown once they are processed in a special method to guarantee a small error at the oscillation's peak, therefore this method is well detailed in (Pierezan et al., 2017b). All simulations mentioned in this research have been performed in the Mathworks Matlab 2015a platform.

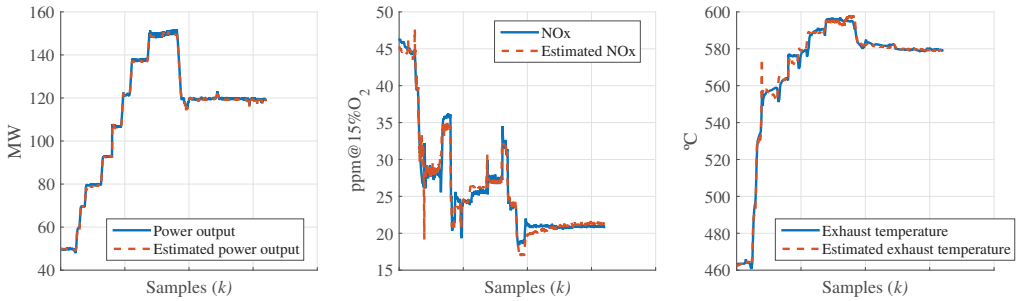

Figure 5.2: Comparison of the real data with the simulation of the identified data-driven models.

Table 5.3: Models errors evaluation.

Model	sMAPE	R^2	r
Pot	0.5396%	0.9997	0.9999
NO_x	2.3070%	0.9760	0.9879
ET	0.2935%	0.9947	0.9973

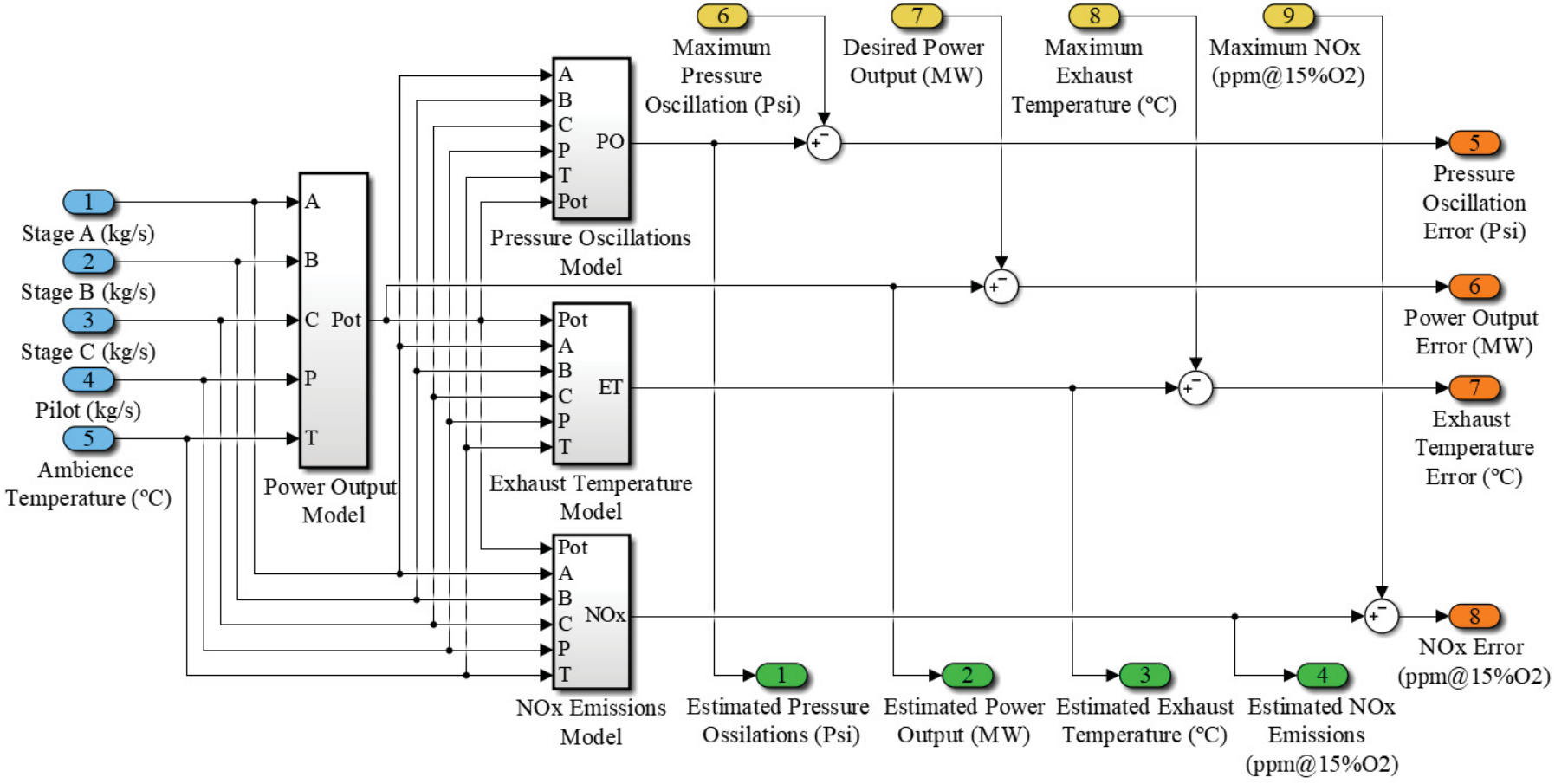

Figure 5.3: The block diagram of the simulation model.

5.2.2 Objective Function Design

Once the gas consumption is the highest operational cost in gas-Potered energy generation, the optimization problem aims to minimize the sum of stage's gas demands, also denoted the total gas demand (GD), to produce the desired power output ($dPow$) while coping with the constraints regarding the GT operation, such that:

$$\begin{aligned} \text{minimize} \quad & F(G) = G_A + G_B + G_C + G_P \\ \text{subject to} \quad & Pot = dPow, \\ & \text{NO}_x \leq NO_x limit, \\ & ET \leq ET_{max}, \\ & PO \leq PO_{max}, \end{aligned} \tag{5.6}$$

where G_A, G_B, G_C, and G_P are the gas flow in Kg/s in the inlet stages A, B, C, and Pilot, respectively. And its values are restricted to the following range:

$$\begin{aligned} 1.125 \leq G_A \leq 4.389, \\ 1.125 \leq G_B \leq 4.389, \\ 0 \leq G_C \leq 0.385, \\ 0.432 \leq G_P \leq 1.822, \end{aligned} \tag{5.7}$$

which are the minimum and maximum value from the data set used to train the models, and present the measured flow range in each valve.

In the optimization procedure, only the values to G_A, G_C, and G_P are manipulated, once G_B must be equal to G_A to avoid pressure instability inside the combustion chamber due to their geometrical positioning.

As mentioned, the operational constraints are the NO_x limit, the maximum exhaust temperature, ET_{max}, and the maximum pressure oscillation at each i^{th} frequency range, $PO_{max,i}$. However, carbon monoxide (CO) emissions are not included as a constraint once it is an issue only in low power generation of the heavy-duty GT, in a range below the studied in this work and which is not often used in practice.

Hence, the minimization objective functions J used as a metric to guide the optimizers is:

$$\begin{aligned} & J = F(G) + penalty, \\ \text{where} \quad & penalty = 1000 * (|Pot - dPow| + \sum_{n=1}^{N} C_n), \\ \text{such that} \quad & C_n = \begin{cases} |c_n - c_{n,limit}|, & \text{if } c_n > c_{n,limit} \\ 0, & \text{otherwise} \end{cases}. \end{aligned} \tag{5.8}$$

Thus, C_n is the value of the violation in the n^{th} constraint (c_n) over the limit $c_{n,limit}$ and the penalization constant equals to 1000 has been chosen arbitrarily without any previous study. There are twelve constraints, nine limit values to the nine different PO frequency ranges, the values to NO_x, ET, and $dPow$.

5.3 EXPERIMENTAL SETUP

The case studies tested in this work are a combination of an ambient temperature and the desired power output, which are independent variables in the simulation model. It means that these variables are treated as inputs that can be separately handled to obtain the desired outputs, which are the gas consumption, pressure oscillations, and pollutant emissions.

The values adopted have been selected from the available data set, as described in Tab. 5.4, to ease the process of comparison with the current GT setup. Further, five different combinations of parameters have been selected to analyze the CCOA's performance repeatability. These combinations have been chosen to cover differently values of each parameter (Because of the lack of data - only one day of operation - the temperature range could still be enlarged).

Table 5.4: Definition of the case studies in terms of power output and ambience temperature.

Independent Variables	Case 1	Case 2	Case 3	Case 4	Case 5
Power Output (MW)	130.020469	140.007642	145.012707	150.000516	149.979658
Ambient Temperature (^{o}C)	25.078574	21.910850	21.900713	21.985192	24.009801

The CCOA has been applied to the five case studies aforementioned and its performance has been compared to the original COA and also to the ABC (Karaboga and Basturk, 2007), the Backtracking Search Optimization Algorithm (BSA) (Civicioglu, 2013), the Self-adaptive Differential Evolution (SaDE) (Qin et al., 2009), the GWO (Mirjalili et al., 2014), the PSO (Kennedy and Eberhart, 1995) and the SOS (Cheng and Prayogo, 2014). The CCOA parameters γ, ψ and P_n have been arbitrarily defined as 0.3, 0.3 and 0.8, respectively.

The ABC, the GWO, the PSO, and the SOS have been selected because of the competitive results presented in Chapter 4. The BA and the FA have not been tested due to the performance demonstrated. The BSA and the SaDE have been selected considering the diffusion and relevance in this research area and the use of general industrial applications.

The BSA has presented a strong potential for solving numerical optimization and competitive performance toward several types of optimization problems (Hassan and Rashid, 2020). Besides, it has been successfully applied to many numerous industrial and energy-related research, including power dispatch, home energy management, wind speed forecasting, thermal power systems, hydroelectric generation, photovoltaic systems, and others (Chaib et al., 2016; Zhang et al., 2017; Bhattacharjee et al., 2015; Ahmed et al., 2017; Vitayasak et al., 2017; Madasu et al., 2017; Islam et al., 2017; Modiri-Delshad et al., 2016; Yan et al., 2018; Zhang et al., 2020b,c,a; Tsai, 2019; Kartite and Cherkaoui, 2017).

The SaDE is an adaptive version of the original Differential Evolution proposed in the '90s by Rainer Storn and Kenneth Price (Storn and Price, 1995, 1997). It has been designed to self-adapt to any optimization problem and a variety of researches have presented successful results for industrial and energy-related applications (Pierezan et al., 2017a; Acharjee, 2013; Ghimire et al., 2018; Beirami et al., 2015; Costa and Fichera, 2017; Fan and Zhang, 2016; Sivananaithaperumal et al., 2011; Moussa and Awotunde, 2018).

For comparison purposes, the population size (i.e. number of food sources (S) for ABC, population size (N_p) for BA and FA, number of wolves (N) for GWO, swarm size for PSO (N_p), and ecosystem size (N) for SOS) has been set as 30 (ten times the number of decision variables). Equivalently, the total population of COA and CCOA has been set as 30 by two combinations: six-packs with five coyotes each (denoted COA5 and CCOA5) and three packs with ten coyotes each (denoted COA10 and CCOA10).

The remaining parameters have been chosen from literature, as follows. The ABC parameters *limit*, number of employed bees (N_e), number of onlooker bees (N_o) and number of scouts (N_s) have been set respectively as $D \times S$, 15, 15 and 1 (Karaboga and Akay, 2009). The GWO's parameter a has been set as linearly decreasing from 2 to 0 (Mirjalili et al., 2014). The PSO parameters cognitive constant c_1 and social constant c_2 have been both set 2, while the inertia weight w has been setup from 0.9 to 0.4 with linear decreasing (Poli et al., 2007). The SaDE parameters learning period (LP) and crossover rate medians ($CRmk$) have been defined as 50 and 0.5, respectively (Qin et al., 2009). The only SOS's parameter is the ecosystem size (N), as well as the population size (N_p) for the BSA. The level of statistical significance considered in this research is 95% (i.e., the α has been defined as 0.05 and any p-value smaller than α indicates that exists significant difference with 95% of statistical confidence).

5.4 CHAPTER RESULTS

The results achieved by the algorithm are shown in Tabs. 5.5 to 5.9 considering the case studies 1 to 5, respectively. In these tables are presented the minimum, average, median, maximum, and standard deviation of the objective function, total gas demand obtained by CCOA. Moreover, the Wilcoxon-Mann-Whitney nonparametric statistical significance test combined with the post-hoc Bonferroni-Holm's method has been applied with α=0.05 using the CCOA5 and CCOA10 as the control method. In these cases, the null hypothesis H_0 states that the median error of the control method sample is equal or greater than the other algorithms compared. In contrast, the H_1 means that the median error of the control method is smaller than the other algorithms.

The proposed CCOA10 has found the smallest gas demand for all case studies, while the CCOA5 has not been found only for the case study 1. Considering the average objective function values, both algorithms have found the best values for 80% of the cases, while the other algorithms could not find as good results for this criterion. Moreover, the smallest maximum values have also been found by these algorithms, which reinforce the robustness of the proposed algorithm for the objective problem studied.

In addition, there is a significant difference between the CCOA versions and the other algorithms performances. Considering case study 4, the CCOA10 has outperformed all algorithms, including CCOA5, COA5, and COA10.

In order to improve the view, the results of the case study 1, 2, 3, 4, and 5 are drawn in Fig. 5.4 a), b), c), d) and e), respectively, where the percentiles are 25% and 75% and the whisker length is 1.5. The CCOA5 and CCOA10 have found the smallest gas demands with lower spreads after all experiments, for all case studies.

As a result of the experiments, the solutions that presented the smallest gas demands found by each algorithm have been selected for comparison. These solutions and the current power plant operation setup are all compared side by side in terms of power output, NOx emissions, exhaust temperature, and pressure oscillations, as shown in Tabs. 5.10 to 5.14. The constraints in the limit allowed are written in boldface.

Table 5.5: Statistical analysis of the results achieved by the algorithms after a set of 30 experiments for case study 1 using the Wilcoxon-Mann-Whitney non-parametric test combined with Bonferroni-Holm's method for $\alpha = 0.05$ (Min.: Minimum; Avg.: Average; Med.: Median; Max. Maximum; Std.: Standard Deviation)

Algorithm	Objective costs (gas demand in Kg/s)					Control: CCOA5		Control: CCOA10	
	Min.	Avg.	Med.	Max.	Std.	p-value	Reject H_0?	p-value	Reject H_0?
CCOA5	8.14251	8.14251	8.14251	8.14255	1.10E-05	-	-	1.11E-07	**Yes**
CCOA10	8.14251	8.14251	8.14251	8.14251	6.07E-07	1.00E+00	No	-	-
COA5	8.14251	8.14471	8.14251	8.17550	8.37E-03	1.00E+00	No	1.00E+00	No
COA10	8.14251	8.14581	8.14251	8.17550	1.01E-02	1.00E+00	No	1.00E+00	No
BSA	8.14257	8.14292	8.14286	8.14363	2.70E-04	1.36E-10	**Yes**	1.36E-10	**Yes**
PSO	8.14251	8.21876	8.17550	8.58358	1.46E-01	1.26E-04	**Yes**	9.47E-05	**Yes**
SOS	8.14257	8.14579	8.14487	8.15649	3.29E-03	1.36E-10	**Yes**	1.36E-10	**Yes**
ABC	8.14702	8.15479	8.15226	8.17852	7.54E-03	1.36E-10	**Yes**	1.36E-10	**Yes**
GWO	8.14540	8.16315	8.16144	8.18659	1.10E-02	1.36E-10	**Yes**	1.36E-10	**Yes**
SaDE	8.17467	8.22875	8.22404	8.33324	3.72E-02	1.36E-10	**Yes**	1.36E-10	**Yes**

Table 5.6: Statistical analysis of the results achieved by the algorithms after a set of 30 experiments for case study 2 using the Wilcoxon-Mann-Whitney non-parametric test combined with Bonferroni-Holm's method for $\alpha = 0.05$ (Min.: Minimum; Avg.: Average; Med.: Median; Max. Maximum; Std.: Standard Deviation)

Algorithm	Objective costs (gas demand in Kg/s)					Control: CCOA5		Control: CCOA10	
	Min.	Avg.	Med.	Max.	Std.	p-value	Reject H_0?	p-value	Reject H_0?
CCOA5	8.67551	8.67551	8.67551	8.67551	3.81E-07	-	-	4.78E-08	**Yes**
CCOA10	8.67551	8.67551	8.67551	8.67551	5.49E-09	1.00E+00	No	-	-
COA5	8.67551	8.68168	8.67551	8.73719	1.88E-02	1.00E+00	No	1.00E+00	No
COA10	8.67551	8.68168	8.67551	8.73719	1.88E-02	1.00E+00	No	1.00E+00	No
BSA	8.67551	8.67564	8.67561	8.67589	9.26E-05	1.36E-10	**Yes**	1.36E-10	**Yes**
PSO	8.67551	8.79085	8.73719	9.10153	1.59E-01	2.42E-06	**Yes**	1.56E-06	**Yes**
SOS	8.67568	8.67720	8.67658	8.68246	1.54E-03	1.36E-10	**Yes**	1.36E-10	**Yes**
ABC	8.67834	8.68742	8.68581	8.70560	7.20E-03	1.36E-10	**Yes**	1.36E-10	**Yes**
GWO	8.68444	8.70835	8.69913	8.75025	1.99E-02	1.36E-10	**Yes**	1.36E-10	**Yes**
SaDE	8.70679	8.78491	8.76682	8.97709	6.02E-02	1.36E-10	**Yes**	1.36E-10	**Yes**

Table 5.7: Statistical analysis of the results achieved by the algorithms after a set of 30 experiments for case study 3 using the Wilcoxon-Mann-Whitney non-parametric test combined with Bonferroni-Holm's method for $\alpha = 0.05$ (Min.: Minimum; Avg.: Average; Med.: Median; Max. Maximum; Std.: Standard Deviation)

Algorithm	Objective costs (gas demand in Kg/s)					Control: CCOA5		Control: CCOA10	
	Min.	Avg.	Med.	Max.	Std.	p-value	Reject H_0?	p-value	Reject H_0?
CCOA5	8.95459	8.95459	8.95459	8.95459	6.57E-08	-	-	3.04E-07	**Yes**
CCOA10	8.95459	8.95459	8.95459	8.95459	1.75E-09	1.00E+00	No	-	-
COA5	8.95459	8.98806	8.95459	9.36388	7.84E-02	1.00E+00	No	1.00E+00	No
COA10	8.95459	8.98310	8.95459	9.36388	7.80E-02	1.00E+00	No	1.00E+00	No
BSA	8.95461	8.95469	8.95465	8.95500	8.39E-05	1.36E-10	**Yes**	1.36E-10	**Yes**
PSO	8.95459	9.09848	9.02895	9.36388	1.50E-01	1.63E-08	**Yes**	1.63E-08	**Yes**
SOS	8.95498	8.95765	8.95619	8.97781	4.37E-03	1.36E-10	**Yes**	1.36E-10	**Yes**
ABC	8.95692	8.97695	8.97496	9.00274	1.18E-02	1.36E-10	**Yes**	1.36E-10	**Yes**
GWO	8.96425	8.98537	8.98351	9.02689	1.68E-02	1.36E-10	**Yes**	1.36E-10	**Yes**
SaDE	8.98937	9.10279	9.08812	9.27839	7.51E-02	1.36E-10	**Yes**	1.36E-10	**Yes**

Table 5.8: Statistical analysis of the results achieved by the algorithms after a set of 30 experiments for case study 4 using the Wilcoxon-Mann-Whitney non-parametric test combined with Bonferroni-Holm's method for $\alpha = 0.05$ (Min.: Minimum; Avg.: Average; Med.: Median; Max. Maximum; Std.: Standard Deviation)

Algorithm	Objective costs (gas demand in Kg/s)					Control: CCOA5		Control: CCOA10	
	Min.	Avg.	Med.	Max.	Std.	p-value	Reject H_0?	p-value	Reject H_0?
CCOA5	9.24091	9.24091	9.24091	9.24091	1.89E-07	-	-	8.19E-09	**Yes**
CCOA10	9.24091	9.24091	9.24091	9.24095	7.50E-06	1.00E+00	No	-	-
COA5	9.24091	9.36641	9.46014	9.46014	1.05E-01	7.45E-02	No	3.72E-02	**Yes**
COA10	9.24091	9.39405	9.46014	9.46014	9.22E-02	7.69E-05	**Yes**	5.13E-05	**Yes**
BSA	9.24093	9.24837	9.24103	9.46014	4.00E-02	1.36E-10	**Yes**	1.36E-10	**Yes**
PSO	9.24091	9.51485	9.46014	11.2893	3.40E-01	1.95E-10	**Yes**	1.95E-10	**Yes**
SOS	9.24116	9.2456	9.24227	9.30256	1.14E-02	1.36E-10	**Yes**	1.36E-10	**Yes**
ABC	9.24655	9.26528	9.26645	9.29992	1.25E-02	1.36E-10	**Yes**	1.36E-10	**Yes**
GWO	9.24794	9.28155	9.28370	9.31918	1.78E-02	1.36E-10	**Yes**	1.36E-10	**Yes**
SaDE	9.28444	9.38377	9.37034	9.54848	6.21E-02	1.36E-10	**Yes**	1.36E-10	**Yes**

Table 5.9: Statistical analysis of the results achieved by the algorithms after a set of 30 experiments for case study 5 using the Wilcoxon-Mann-Whitney non-parametric test combined with Bonferroni-Holm's method for $\alpha = 0.05$ (Min.: Minimum; Avg.: Average; Med.: Median; Max. Maximum; Std.: Standard Deviation)

Algorithm	Objective costs (gas demand in Kg/s)					Control: CCOA5		Control: CCOA10	
	Min.	Avg.	Med.	Max.	Std.	p-value	Reject H_0?	p-value	Reject H_0?
CCOA5	9.24241	9.24246	9.24241	9.24383	2.59E-04	-	-	1.65E-08	**Yes**
CCOA10	9.24241	9.24241	9.24241	9.24241	8.34E-09	1.00E+00	No	-	-
COA5	9.24241	9.35739	9.32899	9.46112	9.79E-02	3.97E-02	**Yes**	2.65E-02	**Yes**
COA10	9.24241	9.33840	9.32899	9.46112	9.50E-02	1.84E-01	No	9.22E-02	No
BSA	9.24243	9.24255	9.24253	9.24297	1.17E-04	1.11E-09	**Yes**	1.21E-10	**Yes**
PSO	9.24353	9.51954	9.46112	11.2684	3.34E-01	1.59E-11	**Yes**	1.42E-11	**Yes**
SOS	9.24279	9.24674	9.24379	9.29939	1.02E-02	3.66E-10	**Yes**	1.21E-10	**Yes**
ABC	9.24849	9.27093	9.26692	9.31737	1.95E-02	1.21E-10	**Yes**	1.21E-10	**Yes**
GWO	9.25183	9.27762	9.27979	9.30821	1.66E-02	1.21E-10	**Yes**	1.21E-10	**Yes**
SaDE	9.29595	9.37640	9.36486	9.58709	5.93E-02	1.21E-10	**Yes**	1.21E-10	**Yes**

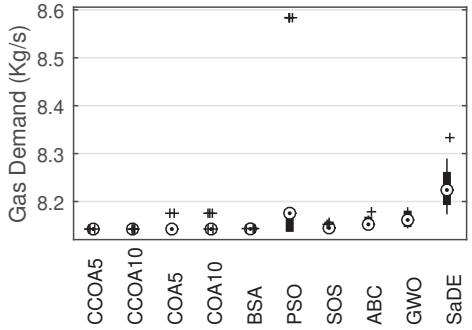

a) Case study 1

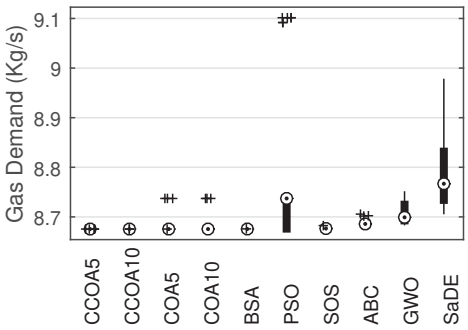

b) Case study 2

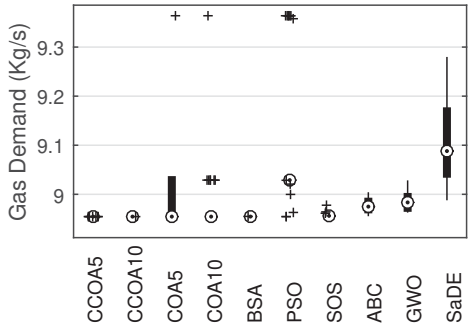

c) Case study 3

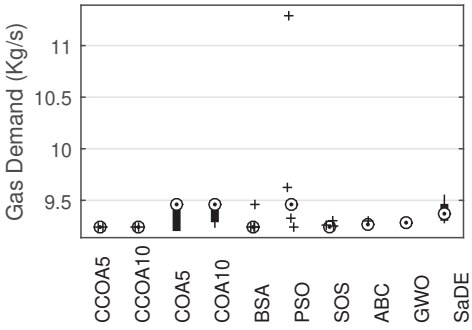

d) Case study 4

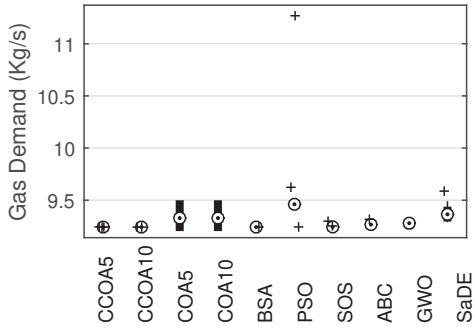

e) Case study 5

Figure 5.4: Boxplot of the best results achieved after a set of 30 independent experiments for all case studies.

Table 5.10: Comparison of the current operation setup with the simulated best solutions achieved by the algorithms for the case study 1.

Setup	Pot	GD	NO_x	ET	Pressure Oscillations (PSI)								
	(MW)	(Kg/s)	(ppm@15%O_2)	(^{o}C)	f_1	f_2	f_3	f_4	f_5	f_6	f_7	f_8	f_9
Current	130.020469	8.405638	23.957359	576.032873	0.15	0.19	0.35	0.22	0.07	0.06	0.09	0.01	0.02
CCOA5	130.020469	8.142507	24.999874	548.205783	0.11	0.19	**1.60**	0.30	0.08	0.18	0.11	0.02	0.03
CCOA10	130.020469	8.142506	24.999992	548.205674	0.11	0.19	**1.60**	0.30	0.08	0.18	0.11	0.02	0.03
COA5	130.020469	8.142506	**25.000000**	548.205667	0.11	0.19	**1.60**	0.30	0.08	0.18	0.11	0.02	0.03
COA10	130.020469	8.142506	**25.000000**	548.205667	0.11	0.19	**1.60**	0.30	0.08	0.18	0.11	0.02	0.03
BSA	130.020491	8.142544	24.974533	548.233427	0.11	0.19	**1.60**	0.30	0.08	0.18	0.11	0.02	0.03
PSO	130.020469	8.142506	**25.000000**	548.205667	0.11	0.19	**1.60**	0.30	0.08	0.18	0.11	0.02	0.03
SOS	130.020430	8.142527	24.988466	548.219868	0.11	0.19	**1.60**	0.30	0.08	0.18	0.11	0.02	0.03
ABC	130.020770	8.146718	24.574945	549.569186	0.12	0.19	1.54	0.30	0.08	0.17	0.12	0.02	0.03
GWO	130.020931	8.144940	24.320829	549.291624	0.12	0.19	1.57	0.30	0.08	0.18	0.11	0.02	0.03
SaDE	130.020045	8.174245	23.682949	556.147711	0.15	0.20	1.21	0.31	0.08	0.15	0.14	0.02	0.03

Table 5.11: Comparison of the current operation setup with the simulated best solutions achieved by the algorithms for the case study 2.

Setup	*Pot*	*GD*	NO_x	*ET*	Pressure Oscillations (PSI)								
	(MW)	(Kg/s)	(ppm@15%O_2)	(^{o}C)	f_1	f_2	f_3	f_4	f_5	f_6	f_7	f_8	f_9
Current	140.007642	8.970566	19.755550	590.862165	0.14	0.22	0.54	0.25	0.08	0.10	0.09	0.01	0.03
CCOA5	140.007642	8.675507	**25.000000**	571.640497	0.04	0.18	**1.60**	0.32	0.06	0.19	0.13	0.01	0.03
CCOA10	140.007642	8.675507	**25.000000**	571.640497	0.04	0.18	**1.60**	0.32	0.06	0.19	0.13	0.01	0.03
COA5	140.007642	8.675507	**25.000000**	571.640497	0.04	0.18	**1.60**	0.32	0.06	0.19	0.13	0.01	0.03
COA10	140.007642	8.675507	**25.000000**	571.640497	0.04	0.18	**1.60**	0.32	0.06	0.19	0.13	0.01	0.03
BSA	140.007642	8.675508	24.999902	571.640436	0.04	0.18	**1.60**	0.32	0.06	0.19	0.13	0.01	0.03
PSO	140.007642	8.675507	**25.000000**	571.640497	0.04	0.18	**1.60**	0.32	0.06	0.19	0.13	0.01	0.03
SOS	140.007604	8.675642	24.959648	571.615114	0.04	0.18	**1.60**	0.32	0.06	0.19	0.13	0.01	0.03
ABC	140.007151	8.677853	24.686303	571.607065	0.04	0.18	1.58	0.32	0.06	0.19	0.13	0.01	0.03
GWO	140.007200	8.684002	24.793131	572.415329	0.05	0.19	1.51	0.32	0.06	0.18	0.13	0.01	0.03
SaDE	140.002835	8.701981	19.126906	570.947182	0.09	0.20	1.54	0.34	0.07	0.20	0.16	0.02	0.03

Table 5.12: Comparison of the current operation setup with the simulated best solutions achieved by the algorithms for the case study 3.

Setup	*Pot*	*GD*	NO_x	*ET*	Pressure Oscillations (PSI)								
	(MW)	(Kg/s)	(ppm@15%O_2)	(^{o}C)	f_1	f_2	f_3	f_4	f_5	f_6	f_7	f_8	f_9
Current	145.012707	9.289385	22.344427	591.735929	0.15	0.21	0.57	0.27	0.08	0.10	0.09	0.01	0.03
CCOA5	145.012707	8.954590	**25.000000**	571.719768	0.04	0.19	**1.60**	0.34	0.07	0.20	0.14	0.01	0.03
CCOA10	145.012707	8.954590	**25.000000**	571.719768	0.04	0.19	**1.60**	0.34	0.07	0.20	0.14	0.01	0.03
COA5	145.012707	8.954590	**25.000000**	571.719768	0.04	0.19	**1.60**	0.34	0.07	0.20	0.14	0.01	0.03
COA10	145.012707	8.954590	**25.000000**	571.719768	0.04	0.19	**1.60**	0.34	0.07	0.20	0.14	0.01	0.03
BSA	145.012715	8.954598	24.999499	571.720172	0.04	0.19	**1.60**	0.34	0.07	0.20	0.14	0.01	0.03
PSO	145.012707	8.954590	**25.000000**	571.719768	0.04	0.19	**1.60**	0.34	0.07	0.20	0.14	0.01	0.03
SOS	145.012525	8.954801	24.949843	571.713459	0.04	0.19	**1.60**	0.34	0.07	0.20	0.14	0.01	0.03
ABC	145.014465	8.955162	24.886223	571.703093	0.04	0.19	**1.60**	0.34	0.07	0.20	0.14	0.01	0.03
GWO	145.012904	8.964050	23.117002	571.806971	0.06	0.20	1.58	0.34	0.07	0.20	0.15	0.02	0.03
SaDE	144.997014	8.973679	24.967091	573.584786	0.07	0.20	1.42	0.34	0.07	0.18	0.15	0.01	0.03

Table 5.13: Comparison of the current operation setup with the simulated best solutions achieved by the algorithms for the case study 4.

Setup	Pot	GD	NO_x	ET	Pressure Oscillations (PSI)								
	(MW)	(Kg/s)	(ppm@15%O_2)	(^{o}C)	f_1	f_2	f_3	f_4	f_5	f_6	f_7	f_8	f_9
Current	150.000516	9.577944	23.668806	594.548603	0.15	0.21	0.58	0.28	0.09	0.10	0.09	0.01	0.03
CCOA5	150.000516	9.240912	24.999999	572.691788	0.05	0.20	**1.60**	0.35	0.08	0.20	0.15	0.01	0.03
CCOA10	150.000516	9.240912	**25.000000**	572.691788	0.05	0.20	**1.60**	0.35	0.08	0.20	0.15	0.01	0.03
COA5	150.000516	9.240912	**25.000000**	572.691787	0.05	0.20	**1.60**	0.35	0.08	0.20	0.15	0.01	0.03
COA10	150.000516	9.240912	**25.000000**	572.691787	0.05	0.20	**1.60**	0.35	0.08	0.20	0.15	0.01	0.03
BSA	150.000501	9.240916	24.999177	572.692113	0.05	0.20	**1.60**	0.35	0.08	0.20	0.15	0.01	0.03
PSO	150.000516	9.240912	**25.000000**	572.691787	0.05	0.20	**1.60**	0.35	0.08	0.20	0.15	0.01	0.03
SOS	150.000595	9.241078	24.978085	572.704023	0.05	0.20	**1.60**	0.35	0.08	0.20	0.15	0.01	0.03
ABC	149.999633	9.245667	24.904626	573.136593	0.05	0.20	1.57	0.35	0.08	0.20	0.16	0.01	0.03
GWO	150.000078	9.247501	24.792897	573.292003	0.06	0.20	1.56	0.36	0.08	0.20	0.16	0.02	0.03
SaDE	150.014687	9.270267	23.369310	575.213566	0.08	0.21	1.47	0.36	0.08	0.20	0.17	0.02	0.03

Table 5.14: Comparison of the current operation setup with the simulated best solutions achieved by the algorithms for the case study 5.

Setup	*Pot*	*GD*	NO_x	*ET*	Pressure Oscillations (PSI)								
	(MW)	(Kg/s)	(ppm@15%O_2)	(^{o}C)	f_1	f_2	f_3	f_4	f_5	f_6	f_7	f_8	f_9
Current	149.979658	9.553761	26.831668	595.904596	0.15	0.19	0.51	0.27	0.09	0.07	0.08	0.01	0.03
CCOA5	149.979658	9.242412	**25.000000**	568.710598	0.08	0.21	**1.60**	0.37	0.09	0.20	0.15	0.02	0.03
CCOA10	149.979658	9.242412	**25.000000**	568.710598	0.08	0.21	**1.60**	0.37	0.09	0.20	0.15	0.02	0.03
COA5	149.979658	9.242412	**25.000000**	568.710598	0.08	0.21	**1.60**	0.37	0.09	0.20	0.15	0.02	0.03
COA10	149.979658	9.242412	**25.000000**	568.710598	0.08	0.21	**1.60**	0.37	0.09	0.20	0.15	0.02	0.03
BSA	149.979659	9.242429	24.997193	568.713697	0.08	0.21	**1.60**	0.37	0.09	0.20	0.15	0.02	0.03
PSO	149.979491	9.243358	24.999959	568.831769	0.08	0.21	1.59	0.37	0.09	0.19	0.15	0.02	0.03
SOS	149.979711	9.242737	24.958197	568.766651	0.08	0.21	**1.60**	0.37	0.09	0.20	0.15	0.02	0.03
ABC	149.978165	9.246994	24.717571	569.397632	0.08	0.21	1.58	0.37	0.09	0.19	0.16	0.02	0.03
GWO	149.980788	9.250699	24.339328	569.974582	0.09	0.21	1.57	0.37	0.09	0.19	0.16	0.02	0.03
SaDE	149.964828	9.281116	20.754265	574.989935	0.12	0.23	1.52	0.38	0.10	0.20	0.17	0.02	0.03

5.5 CONVERGENCE AND DIVERSITY ANALYSIS

In this section, the convergence and diversity curves of CCOA are analyzed and compared to the other algorithms tested. The resulting curves are drawn in Figs. 5.5 - 5.9 for all case studies, where the set of box plots represent the average values among all experiments inside each interval indicated in the x-axis. This view is focused on the beginning of the optimization process, where it is possible to evaluate the algorithms' ability to avoid premature convergence.

In general, the proposed algorithms demonstrated a similar behavior, mainly for case studies 1, 2, and 3. Regarding the convergence curves, the COA and the CCOA variants have presented slow convergence at the beginning of the process, with medians and boxes higher than PSO, SOS, ABS, and GWO. It indicates that these methods have not converged prematurely, as well as the BSA and the SaDE that have presented similar characteristics of median and boxes sizes. However, the median and the boxes sizes of the proposed algorithms have decreased significantly along the optimization process. The CCOA has demonstrated a promising ability to improve the search in the second half of the optimization process, mainly when compared to the COA. For case studies 4 and 5, this ability is evident in the convergence curve, where the most significant difference is in the last interval.

Considering the diversity curves, the initial values of median and boxes sizes presented by the CCOA variants are smaller than most of the algorithms. Along the process, these values decrease slower than PSO, faster than COA, SOS, ABC, GWO, and SaDE, and quite similar to the BSA. From 3% to 25% of the process, the median and the boxes sizes seem to be maintained and at the end of the process, these values have decreased.

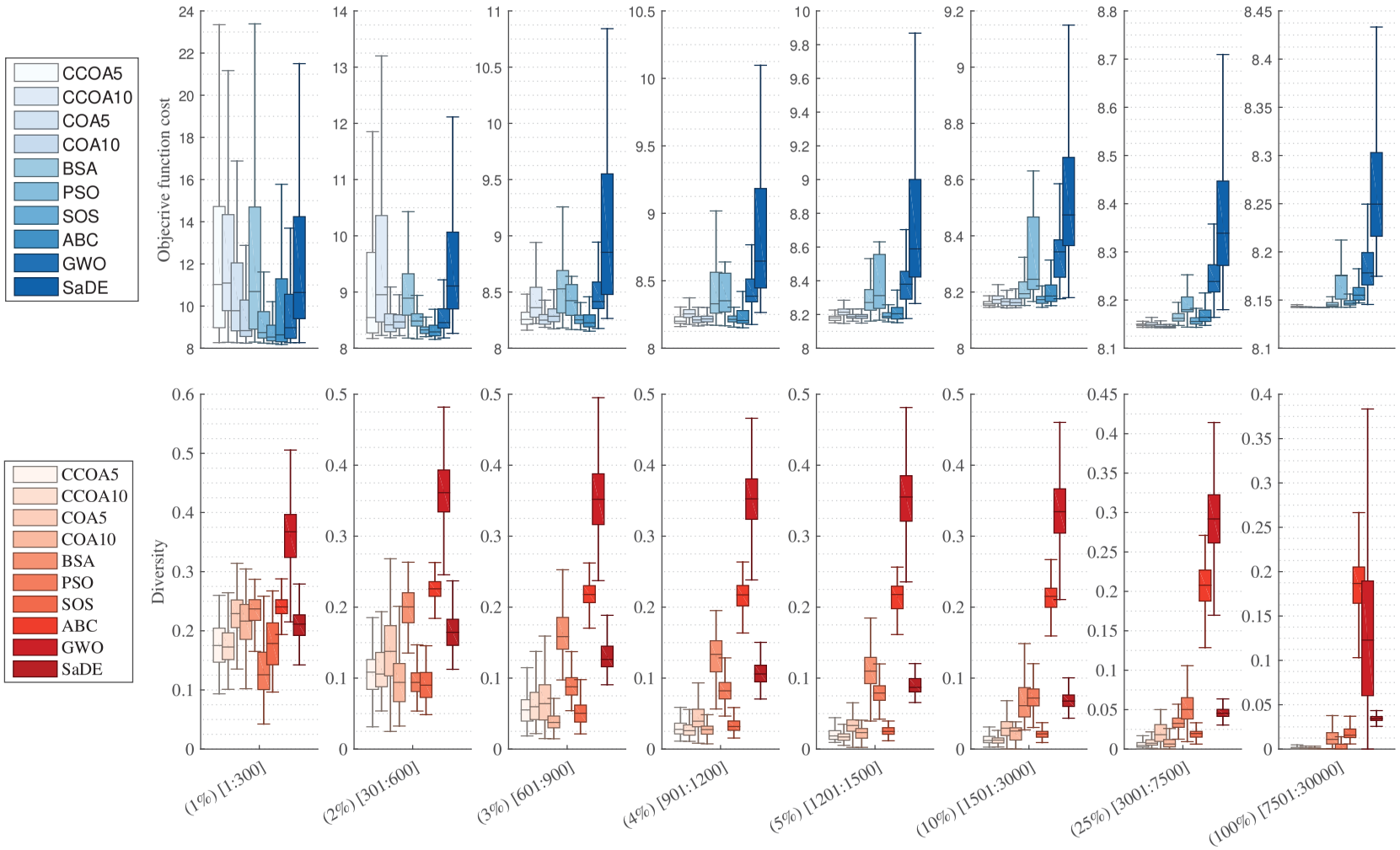

Figure 5.5: Convergence and diversity curves represented by box plots of different periods of the optimization process for case study 1, where the x-axis is written in the format (% of the optimization process) [Interval of function evaluations] and represents both curves.

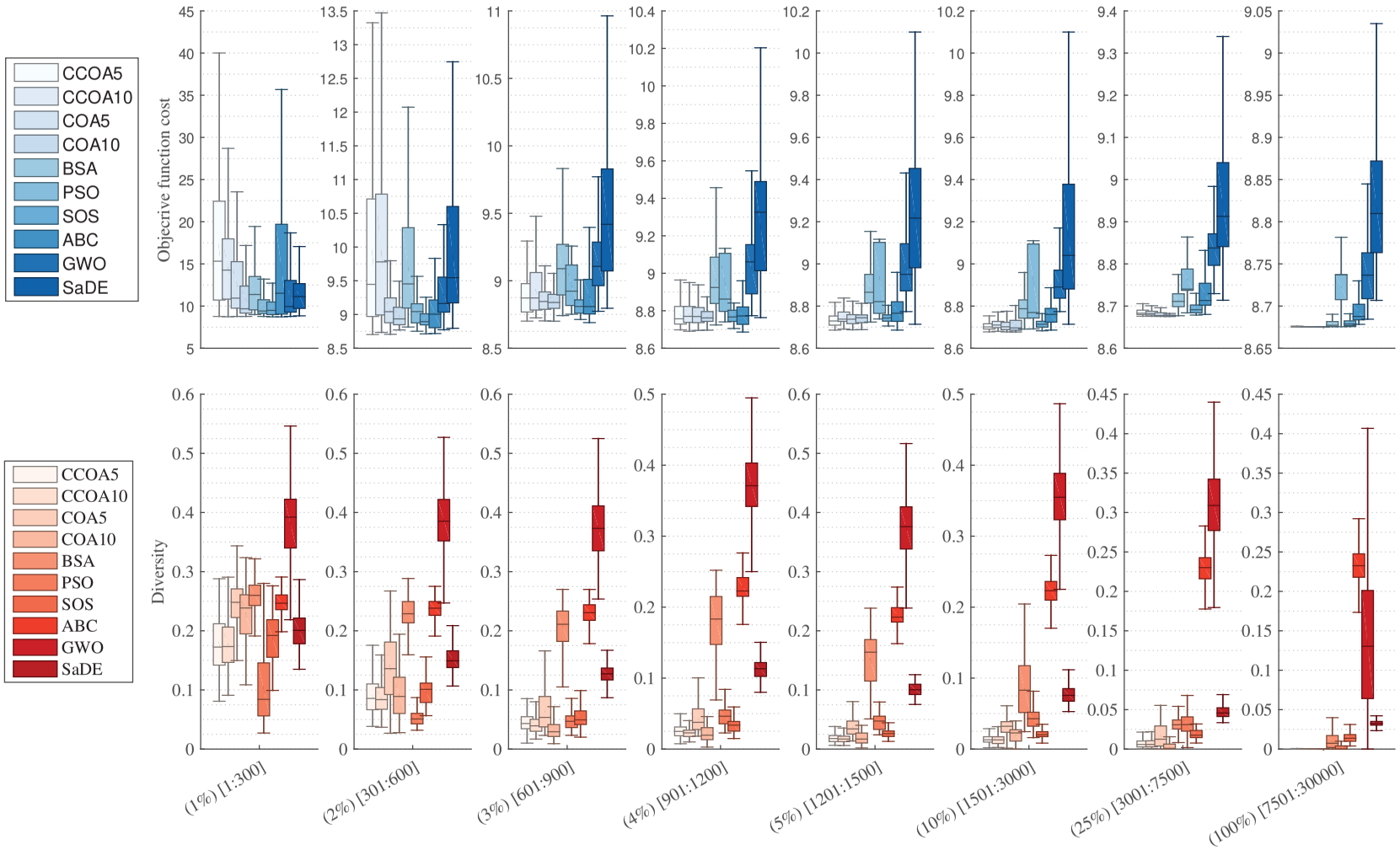

Figure 5.6: Convergence and diversity curves represented by box plots of different periods of the optimization process for case study 2, where the x-axis is written in the format (% of the optimization process) [Interval of function evaluations] and represents both curves.

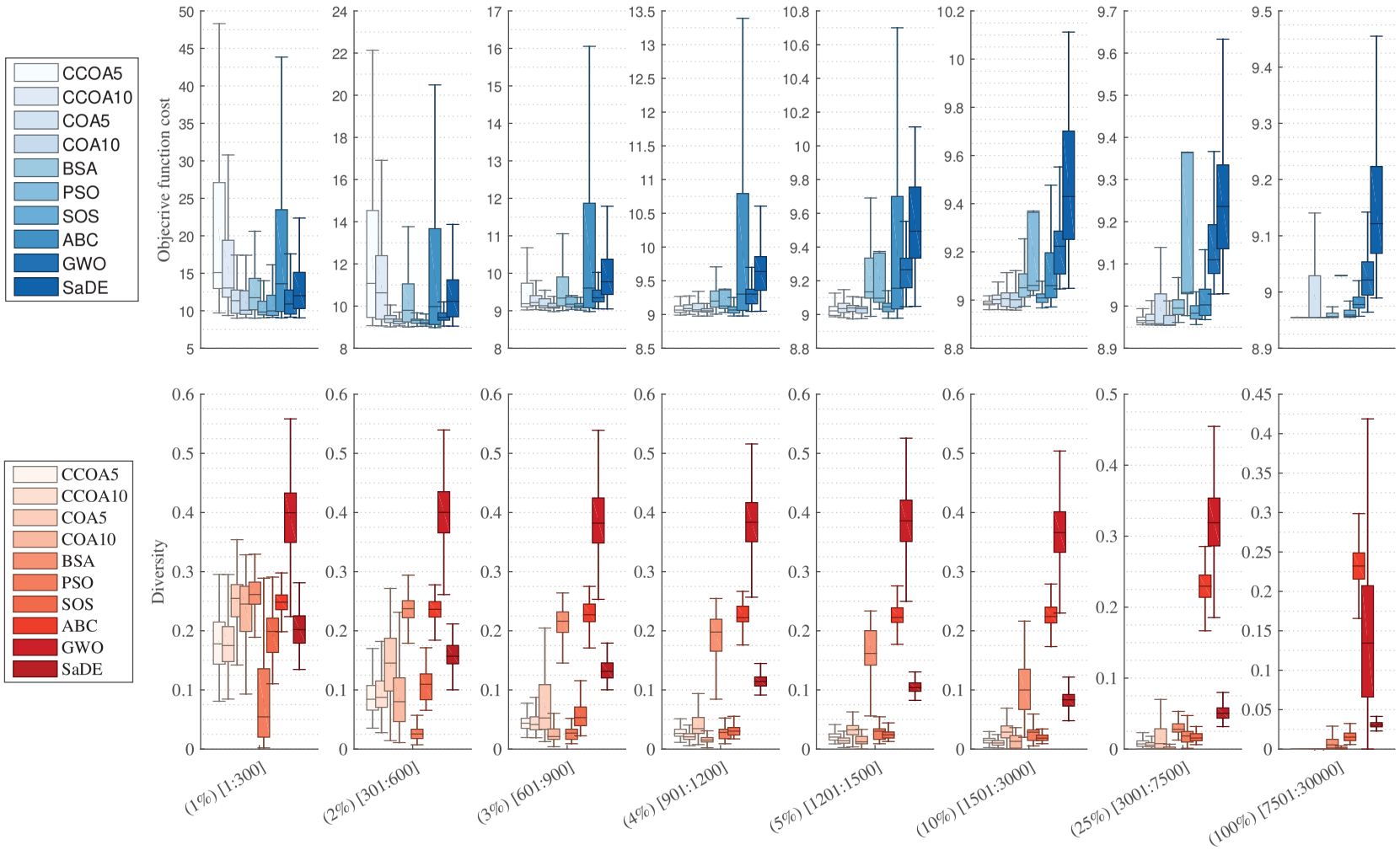

Figure 5.7: Convergence and diversity curves represented by box plots of different periods of the optimization process for case study 3, where the x-axis is written in the format (% of the optimization process) [Interval of function evaluations] and represents both curves.

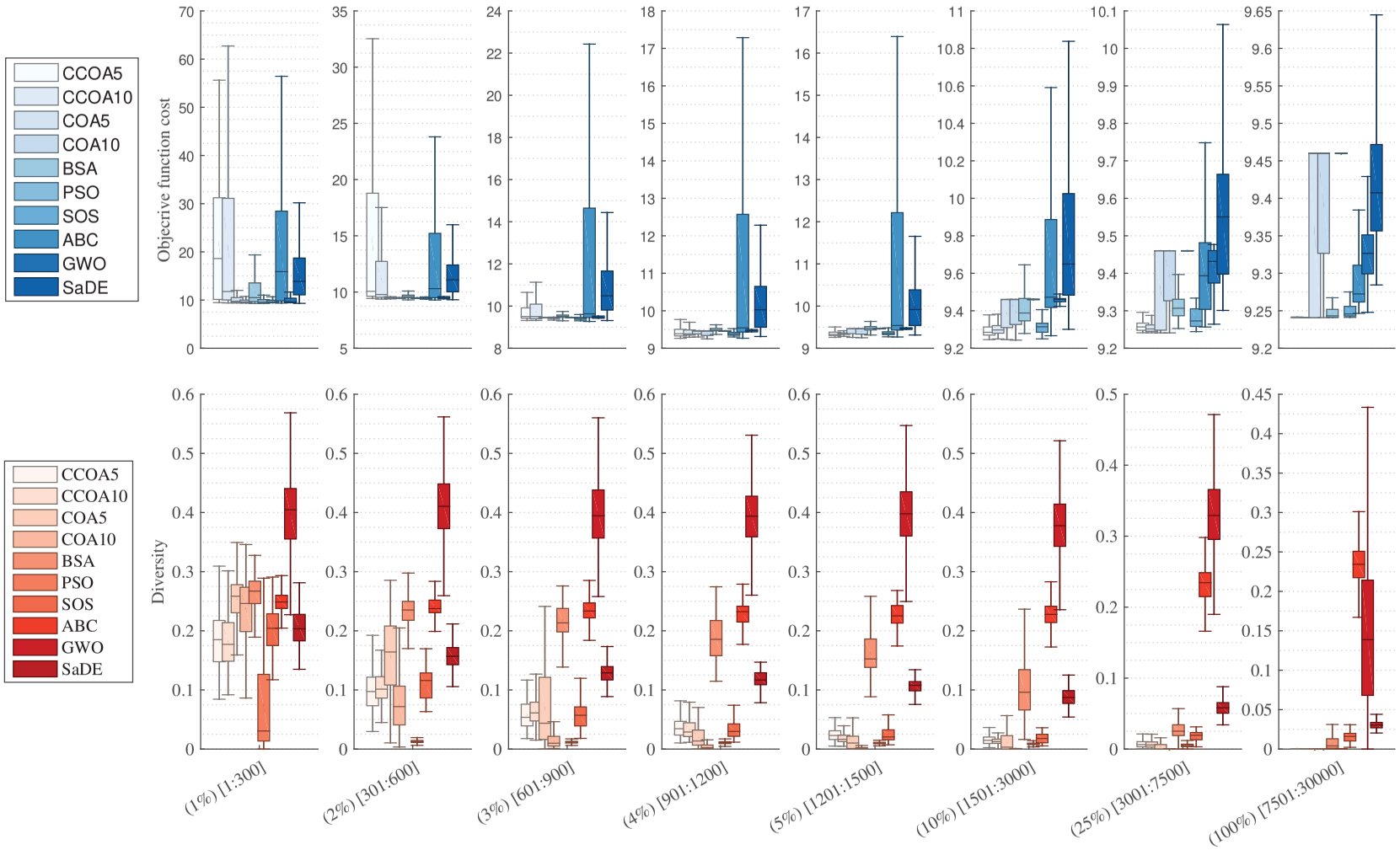

Figure 5.8: Convergence and diversity curves represented by box plots of different periods of the optimization process for case study 4, where the x-axis is written in the format (% of the optimization process) [Interval of function evaluations] and represents both curves.

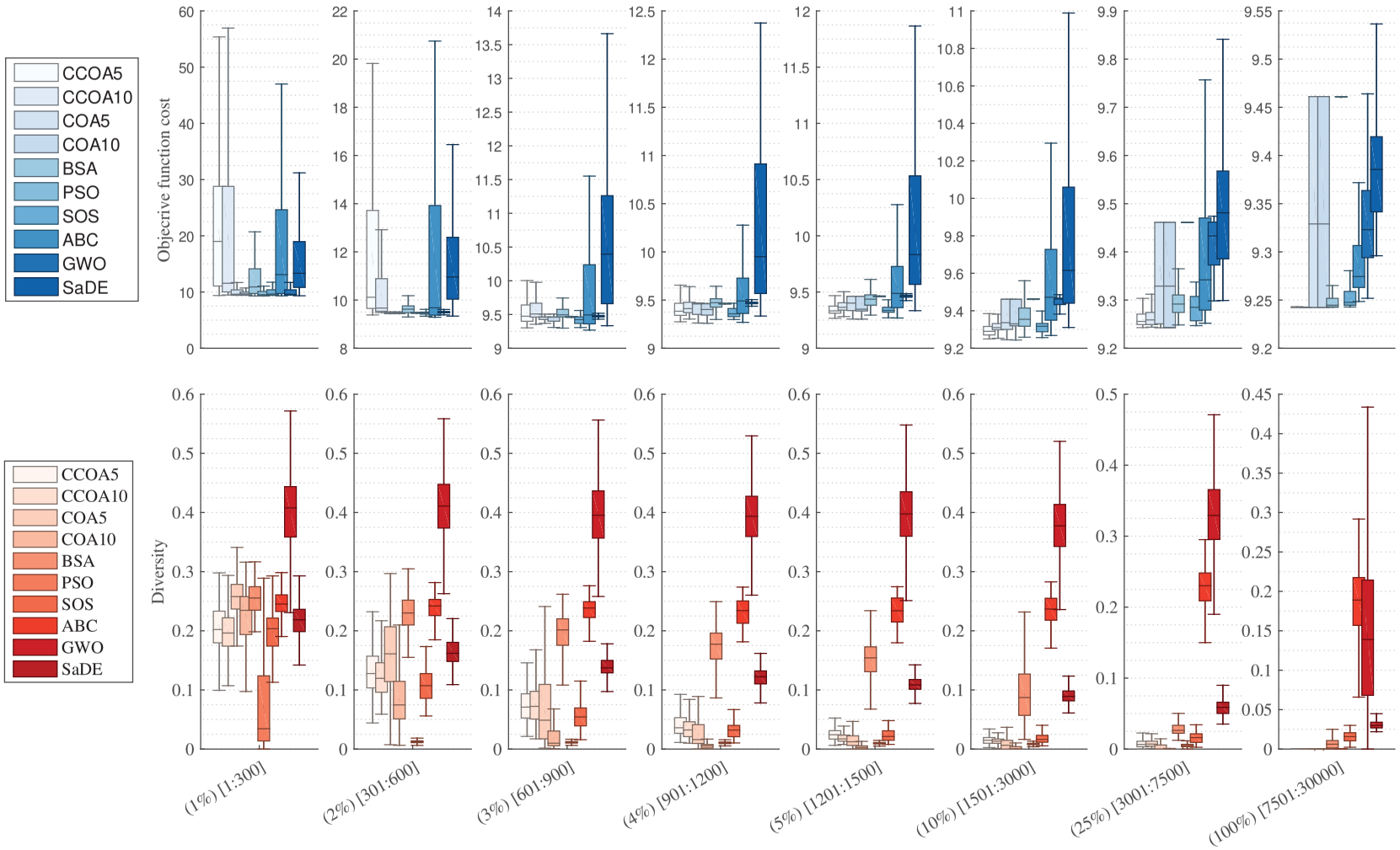

Figure 5.9: Convergence and diversity curves represented by box plots of different periods of the optimization process for case study 5, where the x-axis is written in the format (% of the optimization process) [Interval of function evaluations] and represents both curves.

5.6 CHAPTER DISCUSSION

In this chapter, a new metaheuristic combining the normative knowledge from cultural algorithms with COA has been proposed to optimize the operation of a heavy-duty GT. The objective function is composed of the stages of the GT as optimized variables and the pressure oscillations in the combustion can, the NO_x emissions, and the Power Output error as constraints. A set of experiments has been executed for five different operation points to evaluate the repeatability of results.

First, all algorithms have found better setups than the current one regarding the GD, with improvements up to 3.13%, 3.29%, 3.6%, 3.52%, and 3.26% for study cases 1 to 5, respectively. It might impact a considerable financial saving in the operations of the power plant. As a result of this improvement, the emissions and the pressure oscillations reached values close to the limits specified. The NOx constraint is most likely to achieve the limits, as it has happened in some cases, as well as the pressure oscillation in the f_3 range (which is the range 100Hz to 160Hz).

This is a result of the valves setups, where stage C is handled to reduce the total GD. It directly influences the amount of gas burnt, generating more/fewer NOx emissions. Similarly, it balances (or the opposite) the natural gas injection and influences the pressure oscillations. On the other hand, the exhaust temperature seems not to be as affected as the emissions and oscillations for different valves setup. The resulting values are even smaller considering the solutions achieved by the algorithms.

In general, the oscillations in the remaining frequency ranges seem a little bit higher than the current setup, except for f_1, f_2 and/or f_5 (in some cases). However, the differences seem not to be relevant considering the physical constraints defined by the manufacturer. Regarding the Power Output, which has been treated as an equality constraint, the results appeared very precise when compared to the real data. It proves that the penalization strategy was worth it and it reinforces the reliability of the identified data-driven mathematical models.

Regarding the performance achieved by the proposed CCOA, it has outperformed the BSA, the PSO, the SOS, the ABS, the GWO, and the SaDE in all case studies. It has been observed a small variance in the results achieved, it means solid repeatability of performance. It has also outperformed the original COA in some cases and the CCOA10 variant has presented better performance than the CCOA5 in all cases.

Besides, it has been noticed that the CCOA does not converge prematurely and it takes around 25% of the optimization process to find a promising region. After that, the CCOA variants have performed well for refining the solutions. It indicates a good versatility for a local search at the end of the process. Moreover, the CCOA spread of the population along the optimization process seems to be smaller than the COA. As a consequence of the cultural mechanism, it shows that the normative knowledge has reduced the search space to a promising region (comparing to the results achieved by all algorithms).

6 GENERAL CONCLUSION

In this thesis, two NiM have been proposed for global optimization. The first one is inspired in the *Canis latrans* species, while the second one is based on the behavior of the *Cebus capucinus* species. Both metaheuristics can be classified as swarm intelligence and evolutionary heuristic, once both are population-based and the animals that best adapt to the environment survive along with the iterations. These metaheuristics have been validated and under a set of 116 continuous benchmark functions with features as multimodality, high dimension, and non-separability, and the performances have been compared to the other six state-of-the-art NiM.

Besides, an optimization problem has been designed to improve the efficiency of a heavy-duty gas turbine of 173 MW of nominal load considering the maximum NOx emissions allowed and the pressure oscillations in the combustion chamber. A cultural version of the COA denoted CCOA has been applied to solve the designed problem. The performance achieved has been compared to the original COA and other state-of-the-art algorithms for five operation points described in terms of power output and ambient temperature.

6.1 PROPOSED METAHEURISTICS

The proposed COA and WfCMO have achieved a promising performance for a set of benchmark functions with different features as multimodality and dimension. Both COA and WfCMO have outperformed other state-of-the-art metaheuristics considering statistical confidence of 95%. On the other hand, neither the COA nor the WfCMO has presented superior performance when compared to each other. In addition, both COA and WfCMO have presented suitable computational complexity when increasing the dimension of the optimization problem and satisfactory convergence behavior. Because of the algorithmic structure, both COA and WfCMO are flexible and ready to be adapted to different applications. Both have few parameters to be adjusted and original social mechanisms when compared to other NiM.

Moreover, both are composed by original approaches inspired on nature. The fighting behavior between the same species developed in WfCMO has never been implemented in other NiM before. The death mechanisms as proposed is also an original contribution, considering the age of the animals according to the iterations. The birth mechanisms are also slightly different from the approaches found in literature.

Furthermore, both algorithms are ready to be combined with a local search method. Similarly to the NiM from literature, the output of these algorithms is a single-solution with the best objective function cost that can be further improved. The COA variants have achieved relevant scores (IEEE-CEC 2017 analysis) even without specific local search mechanisms. It highlights the COA's ability to refine the solutions (exploitation) after finding a suitable region (exploration).

6.2 THE ENGINEERING APPLICATION

The methodology used to design the constrained optimization problem has fulfilled the need of estimating the pollutant emissions, the pressure oscillations, and the exhaust temperature for each operation point. Thus, the exploration of different setups has been possible considering the system's constraints. This design and simulation would have probably not been viable using

white-box tools and simulation software, once part of the information needed was not even known, as the air-fuel ratio.

The results achieved with NiM presented a small improvement in the natural gas demand by exploring the limits of the constraints. It has been achieved by setting up the stages accordingly and observing the outputs from the models. Considering the dimension of the system, this improvement represents savings of thousands of hundreds of dollars a year, which is an outstanding achievement from a business perspective. However, the optimization methodology has been designed to explore the operation constraints limits, which does not necessarily mean that extra maintenance costs would not appear. To optimize the power plant costs, it would be necessary to expand the approach and to include the whole combined cycle and its costs.

Furthermore, there are two important attention points considering the methodology used in this research. The first one is that the black-box models have been designed from a very limited data set, which does not answer how much the simulation model generalizes the real system. The second one is that the black-box models identified present validation errors, which influence the optimization results. It means that part of the improvement presented could be a consequence of the black-box models (especially the constraints). Therefore, the setups found in this research should be reviewed by the expert engineers from the power plant before it is carefully and supervised tested in the real system.

6.3 PUBLICATIONS

Along with the development of this research, many results have been obtained and published in national and international engineering events, as well as in a peer-reviewed international journal. Some have been contemplated in the scope of the present document, but all of them present some scientific contributions in the optimization of real engineering problems.

6.3.1 Peer-reviewed Journals

1. S. R. Moreno, **J. Pierezan**, L. S. Coelho and V. C. Mariani. Multi-objective lightning search algorithm applied to wind farmlayout optimization, Energy, Vol. 216, Feb. 2021.

2. **J. Pierezan**, L. S. Coelho, V. C. Mariani, E. H. V. Segundo and D. Prayogo. Chaotic coyote algorithm applied to truss optimization problems, Computers & Structures, Vol. 242, Jan. 2021.

3. A. D. Boursianis, M. S. Papadopoulou, **J. Pierezan**, V. C. Mariani, L. S. Coelho, P. Sarigiannidis, S. Koulouridis and S. K. Goudos. Multiband patch antenna design using nature-inspired optimization method. IEEE Open Journal of Antennas and Propagation, Vol. 2, pp 151-162, 2021.

4. R. C. T. de Souza, C. A. de Macedo, L. S. Coelho,**J. Pierezan** and V. C. Mariani. Binary coyote optimization algorithm for feature selection. Pattern Recognition, Vol. 107, Nov. 2020.

5. **J. Pierezan**, G. Maidl, E. M. Yamao, L. S. Coelho and V. C. Mariani. Cultural coyote optimization algorithm applied to a heavy duty gas turbine operation. Energy Conversion and Management, Vol. 199, Nov. 2019.

6. **J. Pierezan**, R. Z. Freire, L. Weihmann, G. Reynoso-Meza and L. S. Coelho. Static force capability optimization of humanoids robots based on modified self-adaptive differential evolution. Computers and Operations Research, Vol. 84, Aug. 2016.

6.3.2 Book Chapters

1. E. M. Yamao, **J. Pierezan**, J. P. S. Gonçalves, M. C. Gritti, L. G. T. Ribas, F. Chiesa, V. M. L. Santos, M. D. Freitas, A. D. S. Orlandi and L. S. Coelho (2018). Abordagem de inteligência computacional aplicada para modelagem preditiva de emissões de NO_x e CO de uma turbina a gás de uma usina termelétrica de ciclo combinado (*in portuguese*). Energia Elétrica e Sustentabilidade 2, chapter 7, Atena Editora, Belo Horizonte, Brazil.

6.3.3 Conference Proceedings

1. A. Ferrari, G. Leandro, L. S. Coelho, **J. Pierezan** and L. F. Manke. Algoritmo de otimização do coiote aplicado na identificação de um sistema multivariável (*in portuguese*). Anais do 14º Simpósio Brasileiro de Automação Inteligente, Campinas, Brazil, Oct. 2019.

2. **J. Pierezan**, L. dos Santos Coelho, V. C. Mariani and L. Lebensztajn. Multiobjective coyote algorithm applied to electromagnetic optimization. 22nd International Conference on the Computation of Electromagnetic Fields (COMPUMAG), Paris, France, Jul. 2019.

3. G. Maidl, E. M. Yamao, **J. Pierezan**, R. A. P. Neto, L. S. Coelho and C. C. Toledo. Extreme learning machine to a gas turbine emissions modelling. XXXIX Ibero-Latin American Congress on Computational Methods in Engineering (CILAMCE), Paris, France, Nov. 2018.

4. **J. Pierezan** and L. S. Coelho. Coyote optimization algorithm: a new metaheuristic for global optimization problems. IEEE Congress on Evolutionary Computation (CEC), Rio de Janeiro, Brazil, Jul. 2018.

5. R. C. T. de Souza, C. A. Macedo, **J. Pierezan** and L. S. Coelho. A v-shaped binary crow search algorithm for feature selection. IEEE Congress on Evolutionary Computation (CEC), Rio de Janeiro, Brazil, Jul. 2018.

6. L. S. Coelho, **J. Pierezan**, N. J. Batistela, J. V. Leite and S. K. Goudos. Multiobjective lightning search applied to Jiles-Atherton hysteresis model parameter. IEEE International Conference on Modern Circuits and Systems Technologies (MOCAST), Thessaloniki, Greece, May 2018.

7. L. S. Coelho, G. Maidl, **J. Pierezan**, V. C. Mariani, M. V. F. da Luz and J. V. Leite. Ant lion approach based on Lozi map for multiobjective transformer design optimization. International Symposium on Power Electronics, Electrical Drives, Automation and Motion (SPEEDAM). Amalfi Coast, Italy, Jun. 2018.

8. **J. Pierezan**, G. Maidl, E. M. Yamao, J. P. S. Gonçalves, F. Chiesa and L. S. Coelho. Robust identification of pressure oscillations in the combustion chamber of a heavy-duty turbine. 24th ABCM International Congress of Mechanical Engineering (COBEM), Curitiba, Brazil, Dec. 2017.

9. E. M. Yamao, **J. Pierezan**, J. P. S. Gonçalves, M. C. Gritti, L. G. T. Ribas, F. Chiesa, V. M. L. Santos, M. D. Freitas, A. D. S. Orlandi and L. S. Coelho. Abordagem de Inteligência Computacional aplicada para modelagem preditiva de emissões de NO_x e CO de uma turbina a gás de uma usina termelétrica de ciclo combinado (*in portuguese*).

XXIV Seminário Nacional de Produção e Transmissão de Energia Elétrica (SNPTEE), Curitiba, Brazil, Oct. 2017.

10. P. G. Inça, F. Chiesa, E. M. Yamao, **J. Pierezan**, F. T. R. Tovar and T. L. Peruscello. Simulação da emissão de NO_x de uma turbina a gás do tipo heavy duty utilizando redes neurais (*in portuguese*). Workshop de Pesquisa em Computação dos Campos Gerais (WPCCG), Ponta Grossa, Brazil, Oct. 2017.

11. E. M. Yamao, J. P. S. Gonçalves, **J. Pierezan**, L. G. T. Ribas, F. Chiesa and L. S. Coelho. Identificação caixa preta de uma turbina a gás usando redes neurais artificiais integradas a algoritmos evolutivos de otimização (*in portuguese*). Simpósio Brasileiro de Automação Inteligente (SBAI), Porto Alegre, Brazil, Oct. 2017.

6.4 FUTURE RESEARCH

During the development of the present work, a set of future research fronts has been discovered to improve the COA and the WfCMO performances and to use the mechanisms proposed in other NiM. Therefore, the topics for future research regarding the COA, the WfCMO, and other NiM are:

1. To test the COA and the WfCMO for other real-world engineering problems;
2. To implement and test adaptive versions of the COA and the WfCMO regarding the total population size, from the initial values to the dynamic flow along the optimization process (Morales-Castañeda et al., 2020);
3. To implement and test the multi and many-objective versions of the COA and the WfCMO;
4. To explore improvements on the COA and the WfCMO using quantum inspiration (Yu et al., 2020; Sun et al., 2012; Talbi and Draa, 2017);
5. To propose the binary (Thom de Souza et al., 2020) and chaotic (Pierezan et al., 2021) versions of the WfCMO;
6. To propose a hybrid NiM combining the COA and the WfCMO populations and mechanisms.

Regarding the heavy-duty gas turbine application scope, the following topics can be explored in future research:

1. To improve the black-box models using new acquired data to increase the reliability of the optimization results;
2. To explore a multiobjective optimization approach considering the gas consumption, the pressure oscillations, and the NO_x emissions as objectives to be minimized;
3. To design the other elements from the combined-cycle power plant to obtain and complete the operation model and optimize the Heat Rate.

REFERENCES

Abido, M. A. (2002). Optimal design of power-system stabilizers using particle swarm optimization. *IEEE Transactions on Energy Conversion*, 17(3):406–413.

Acharjee, P. (2013). Application of efficient self-adaptive differential evolutionary algorithm for voltage stability analysis under practical security constraints. *Applied Mathematics and Computation*, 219(23):10882–10897.

Ahmed, M. S., Mohamed, A., Khatib, T., Shareef, H., Homod, R. Z. and Ali, J. A. (2017). Real time optimal schedule controller for home energy management system using new binary backtracking search algorithm. *Energy and Buildings*, 138:215–227.

Alam, S., Dobbie, G., Koh, Y. S., Riddle, P. and Ur Rehman, S. (2014). Research on particle swarm optimization based clustering: A systematic review of literature and techniques. *Swarm and Evolutionary Computation*, 17:1–13.

Alblawi, A. (2020). Fault diagnosis of an industrial gas turbine based on the thermodynamic model coupled with a multi feedforward artificial neural networks. *Energy Reports*, 6:1083–1096.

Ali, M. Z., Awad, N. H., Reynolds, R. G. and Suganthan, P. N. (2018). A balanced fuzzy cultural algorithm with a modified levy flight search for real parameter optimization. *Information Sciences*, 447:12 – 35.

Amani, E., Akbari, M. R. and Shahpouri, S. (2018). Multi-objective cfd optimizations of water spray injection in gas-turbine combustors. *Fuel*, 227:267–278.

Amiri Rad, E. and Kazemiani-Najafabadi, P. (2019). Introducing a novel optimized dual fuel gas turbine (dfgt) based on a 4e objective function. *Journal of Cleaner Production*, 206:944–954.

Antoniou, A. and Lu, W. S. (2007). *Practical Optimization: Algorithms and Engineering Applications*. Springer, New York, United States of America.

b. Mo, Y., z. Ma, Y. and y. Zheng, Q. (2013). Optimal choice of parameters for firefly algorithm. In *IEEE Fourth International Conference on Digital Manufacturing & Automation*, pages 887–892, Shinan, China.

Back, T., Fogel, D. B. and Michalewicz, Z. (1997). *Handbook of Evolutionary Computation*. IOP Publishing Ltd., Bristol, United Kingdom, 1st edition.

Bansal, J. C., Sharma, H., Jadon, S. S. and Clerc, M. (2014). Spider monkey optimization algorithm for numerical optimization. *Memetic Computing*, 6:31–47.

Batayev, N. (2018). Gas turbine fault classification based on machine learning supervised techniques. In *IEEE 14th International Conference on Electronics Computer and Computation (ICECCO)*, pages 206–212, Kaskelen, Kazakhstan.

Beirami, H., Shabestari, A. Z. and Zerafat, M. M. (2015). Optimal pid plus fuzzy controller design for a pem fuel cell air feed system using the self-adaptive differential evolution algorithm. *International Journal of Hydrogen Energy*, 40(30):9422–9434.

Bekoff, M. (1977). *Canis latrans*. *Mammalian Species*, 1(79):1–9.

Ben Rahmoune, M., Hafaifa, A. and Guemana, M. (2015). Neural network monitoring system used for the frequency vibration prediction in gas turbine. In *IEEE 3rd International Conference on Control, Engineering and Information Technology (CEIT)*, pages 1–5, Tlemcen, Algeria.

Ben Rahmoune, M., Hafaifa, A., Kouzou, A., Guemana, M. and Abudura, S. (2017). Control and diagnostic of vibration in gas turbine system using neural network approach. In *Proceedings of the IEEE 8th International Conference on Modelling, Identification and Control (ICMIC)*, pages 573–577, Algiers, Algeria.

Benyounes, A., Hafaifa, A. and Guemana, M. (2016). Gas turbine modeling based on fuzzy clustering algorithm using experimental data. *Applied Artificial Intelligence*, 30(1):29–51.

Benyounes, A., Hafaifa, A., Kouzou, A. and Guemana, M. (2017). Gas turbine modeling using adaptive fuzzy neural network approach based on measured data classification. *Mathematics-in-Industry Case Studies*, 7(4).

Bhattacharjee, K., Bhattacharya, A. and Halder Nee Dey, S. (2015). Backtracking search optimization based economic environmental power dispatch problems. *International Journal of Electrical Power & Energy Systems*, 73:830–842.

Bolaji, A. L., Khader, A. T., Al-Betar, M. A. and Awadallah, M. A. (2013). Artificial bee colony algorithm, its variants and applications: A survey. *Journal of Theoretical and Applied Information Technology*, 47(2):434–459.

Boussaïd, I., Lepagnot, J. and Siarry, P. (2013). A survey on optimization metaheuristics. *Information Sciences*, 237:82–117.

Boyd, S. and Vandenberghe, L. (2004). *Convex optimization*. Cambridge University Press, Cambridge, United Kingdom.

Brasil (2018). *Resolução Nº 491, de 19 novembro de 2018 (in portuguese)*. Diário Oficial da União, Ministério do Meio Ambiente/Conselho Nacional do Meio Ambiente, Brasília, Brazil.

Brasil (2020). *Resenha Energética Brasileira (in portuguese)*. Technical report, Ministério de Minas e Energia, Brasília, Brazil.

Cao, Y., Ren, J., Sang, Y. and Dai, Y. (2017). Thermodynamic analysis and optimization of a gas turbine and cascade co_2 combined cycle. *Energy Conversion and Management*, 144:193–204.

Chacartegui, R., Sánchez, D., Muñoz, A. and Sánchez, T. (2011). Real time simulation of medium size gas turbines. *Energy Conversion and Management*, 52(1):713–724.

Chaib, A. E., Bouchekara, H. R., Mehasni, R. and Abido, M. A. (2016). Optimal power flow with emission and non-smooth cost functions using backtracking search optimization algorithm. *International Journal of Electrical Power and Energy Systems*, 81:64–77.

Chaibakhsh, A. and Amirkhani, S. (2018). A simulation model for transient behaviour of heavy-duty gas turbines. *Applied Thermal Engineering*, 132:115–127.

Chen, H., Niu, B., Ma, L., Su, W. and Zhu, Y. (2014a). Bacterial colony foraging optimization. *Neurocomputing*, 137:268–284.

Chen, Q., Liu, B., Zhang, Q. and Liang, J. (2014b). Evaluation criteria for cec 2015 special session and competition on bound constrained single-objective computationally expensive numerical optimization. Technical report, Computational Intelligence Laboratory, Zhengzhou University, Zhengzhou, China and Technical Report, Nanyang Technological University, Singapore.

Cheng, M. Y. and Prayogo, D. (2014). Symbiotic organisms search: A new metaheuristic optimization algorithm. *Computers and Structures*, 139:98–112.

Chi, Y., Sun, F., Jiang, L. and Yu, C. (2012). An efficient population diversity measure for improved particle swarm optimization algorithm. In *6th IEEE International Conference Intelligent Systems*, pages 361–367, Sofia, Bulgaria.

Chu, S.-C., Tsai, P.-w. and Pan, J.-S. (2006). Cat swarm optimization. In Yang, Q. and Webb, G., (eds), *PRICAI 2006: Trends in Artificial Intelligence*, pages 854–858, Berlin, Heidelberg. Springer Berlin Heidelberg.

Civicioglu, P. (2013). Backtracking Search Optimization Algorithm for numerical optimization problems. *Applied Mathematics and Computation*, 219(15):8121–8144.

Cohen, J. (1988). *Statistical power analysis for the behavioral sciences*. New York: Routledge, 2nd edition.

Colera, M., Soria, Á. and Ballester, J. (2019). A numerical scheme for the thermodynamic analysis of gas turbines. *Applied Thermal Engineering*, 147(9):521–536.

Conner, M. M., Ebinger, M. R. and Knowlton, F. F. (2008). Evaluating coyote management strategies using a spatially explicit, individual-based, socially structured population model. *Ecological Modelling*, 219(1-2):234–247.

Costa, A. and Fichera, S. (2017). Economic statistical design of arma control chart through a modified fitness-based self-adaptive differential evolution. *Computers and Industrial Engineering*, 105:174–189.

Das, S. and Bhattacharya, A. (2018). Symbiotic organisms search algorithm for short-term hydrothermal scheduling. *Ain Shams Engineering Journal*, 9(4):499–516.

Das, S., Maity, S., Qu, B.-Y. and Suganthan, P. N. (2011). Real-parameter evolutionary multimodal optimization - a survey of the state-of-the-art. *Swarm and Evolutionary Computation*, 1(2):71–88.

Delgado-Torres, A. M. (2018). Effect of ideal gas model with temperature-independent heat capacities on thermodynamic and performance analysis of open-cycle gas turbines. *Energy Conversion and Management*, 176(5):256–273.

Demirbas, A. (2009). *Biohydrogen: For Future Engine Fuel Demands*. Springer, London, United Kingdom, 1st edition.

Derrac, J., García, S., Molina, D. and Herrera, F. (2011). A practical tutorial on the use of nonparametric statistical tests as a methodology for comparing evolutionary and swarm intelligence algorithms. *Swarm and Evolutionary Computation*, 1(1):3–18.

Dokeroglu, T., Sevinc, E., Kucukyilmaz, T. and Cosar, A. (2019). A survey on new generation metaheuristic algorithms. *Computers & Industrial Engineering*, 137:106040.

Dorigo, M., Birattari, M. and Stutzle, T. (2006). Ant colony optimization. *IEEE Computational Intelligence Magazine*, 1(4):28–39.

Emary, E., Zawbaa, H. M. and Hassanien, A. E. (2016). Binary grey wolf optimization approaches for feature selection. *Neurocomputing*, 172:371–381.

Engelbrecht, A. P. (2005). *Fundamentals of Computational Swarm Intelligence*, volume 1. John Wiley & Sons, Inc., Hoboken, United States of America, 1st edition.

Entezari, A., Manizadeh, A. and Ahmadi, R. (2018). Energetical, exergetical and economical optimization analysis of combined power generation system of gas turbine and stirling engine. *Energy Conversion and Management*, 159:189–203.

Fahad, M., Aadil, F., ur Rehman, Z., Khan, S., Shah, P. A., Muhammad, K., Lloret, J., Wang, H., Lee, J. W. and Mehmood, I. (2018). Grey wolf optimization based clustering algorithm for vehicular ad-hoc networks. *Computers & Electrical Engineering*, 70:853–870.

Fan, Q. and Zhang, Y. (2016). Self-adaptive differential evolution algorithm with crossover strategies adaptation and its application in parameter estimation. *Chemometrics and Intelligent Laboratory Systems*, 151(1550):164–171.

Fister, I., Yang, X. S. and Brest, J. (2013). A comprehensive review of firefly algorithms. *Swarm and Evolutionary Computation*, 13:34–46.

Fragaszy, D. M., Visalberghi, E. and Fedigan, L. M. (2004a). *The Complete Capuchin*, chapter: Life History and Demography, pages 74–79. Cambridge University Press, Cambridge, United Kingdom.

Fragaszy, D. M., Visalberghi, E. and Fedigan, L. M. (2004b). *The Complete Capuchin*. Cambridge University Press, Cambridge, United Kingdom, 1st edition.

Gandomi, A. H., Yang, X. S., Alavi, A. H. and Talatahari, S. (2013). Bat algorithm for constrained optimization tasks. *Neural Computing and Applications*, 22(6):1239–1255.

García, S., Fernández, A., Luengo, J. and Herrera, F. (2010). Advanced nonparametric tests for multiple comparisons in the design of experiments in computational intelligence and data mining: Experimental analysis of power. *Information Sciences*, 180(10):2044–2064.

Gese, E. M., Ruff, R. L. and Crabtree, R. L. (1996). Foraging ecology of coyotes (*Canis latrans*): the influence of extrinsic factors and a dominance hierarchy. *Canadian Journal of Zoology*, 74(5):769–783.

Ghanaatpisheh, M. and Pakaein, M. (2015). Optimization and increase production and efficiency of gas turbines ge-f9 using media evaporative cooler in fars combined cycle power plant. In *30th International Power System Conference (PSC)*, pages 241–247, Tehran, Iran.

Ghimire, S., Deo, R. C., Downs, N. J. and Raj, N. (2018). Self-adaptive differential evolutionary extreme learning machines for long-term solar radiation prediction with remotely-sensed modis satellite and reanalysis atmospheric products in solar-rich cities. *Remote Sensing of Environment*, 212(11):176–198.

Gibbons, J. D. and Wolfe, D. A. (2003). *Nonparametric Statistical Inference*. Marcel Dekker, Inc., New York, United States of America, 4th edition.

Goldberg, D. E. (1989). *Genetic Algorithms in Search, Optimization, and Machine Learning*. Addison-Wesley, Boston, United States of America, 1st edition.

Gul, M., Kalam, M., Mujtaba, M., Alam, S., Bashir, M. N., Javed, I., Aziz, U., Farid, M. R., Hassan, M. T. and Iqbal, S. (2020). Multi-objective-optimization of process parameters of industrial-gas-turbine fueled with natural gas by using grey-taguchi and ann methods for better performance. *Energy Reports*, 6:2394 – 2402.

Gunnarsdottir, I., Davidsdottir, B., Worrell, E. and Sigurgeirsdottir, S. (2020). Review of indicators for sustainable energy development. *Renewable and Sustainable Energy Reviews*, 133:110294.

Guo, G. W. and Lihong (2013). A novel hybrid bat algorithm with harmony search for global numerical optimization. *Journal of Applied Mathematics*, 2013(696491):1–21.

Hackl, A., Magele, C. and Renhart, W. (2016). Extended firefly algorithm for multimodal optimization. In *2016 19th International Symposium on Electrical Apparatus and Technologies (SIELA)*, Bourgas, Bulgaria.

Hajer, F., Tahar, K. and Ben Brahim, A. (2014). Gas turbine cycle performance and no_x releases. In *IEEE 5th International Renewable Energy Congress (IREC)*, pages 1–5, Hammamet, Tunisia. IEEE.

Hanachi, H., Mechefske, C., Liu, J., Banerjee, A. and Chen, Y. (2017). Enhancement of prognostic models for short-term degradation of gas turbines. In *IEEE International Conference on Prognostics and Health Management (ICPHM)*, pages 66–69, Dallas, United States of America.

Hasançebi, O., Teke, T. and Pekcan, O. (2013). A bat-inspired algorithm for structural optimization. *Computers & Structures*, 128:77–90.

Hassan, B. A. and Rashid, T. A. (2020). Operational framework for recent advances in backtracking search optimisation algorithm: A systematic review and performance evaluation. *Applied Mathematics and Computation*, 370:124919.

Hassanin, M. F., Shoeb, A. M. and Hassanien, A. E. (2016). Grey wolf optimizer-based back-propagation neural network algorithm. In *IEEE 12th International Computer Engineering Conference (ICENCO)*, pages 213–218, Cairo, Egypt.

Hazi, A., Hazi, G., Grigore, R. and Vernica, S. (2011). Effects of deterioration equipment reliability in a gas turbine cogeneration power plant. In *IEEE 10th International Conference on Environment and Electrical Engineering*, pages 1–4, Rome, Italy.

Hogg, R. and Ledolter, J. (1987). *Engineering Statistics*. Mathematics & statistics. Macmillan, New York, United States of America.

Hollander, M. and Wolfe, D. A. (1999). *Nonparametric statistical methods*. John Wiley & Sons, Inc., Hoboken, United States of America, 3rd edition.

Holm, S. (1979). A simple sequentially rejective multiple test procedure. *Scandinavian Journal of Statistics*, 6(2):65–70.

Hu, W., Liu, J., Cui, J., Gao, Y., Cui, B. and Jiang, L. (2014). Fault diagnosis of gas turbine based on support vector machine. *IEEE 26th Chinese Control and Decision Conference (CCDC)*, pages 2853–2856.

Ibrahim, T. K., Basrawi, F., Awad, O. I., Abdullah, A. N., Najafi, G., Mamat, R. and Hagos, F. Y. (2017). Thermal performance of gas turbine power plant based on exergy analysis. *Applied Thermal Engineering*, 115:977–985.

IEA (2020). Iea key world energy statistics (kwes) 2020. Technical report, IEA, Paris, France.

Impram, S., Varbak Nese, S. and Oral, B. (2020). Challenges of renewable energy penetration on power system flexibility: A survey. *Energy Strategy Reviews*, 31:100539.

Iqbal, M., Azam, M., Naeem, M., Khwaja, A. S. and Anpalagan, A. (2014). Optimization classification, algorithms and tools for renewable energy: A review. *Renewable and Sustainable Energy Reviews*, 39:640–654.

Islam, N. N., Hannan, M. A., Shareef, H. and Mohamed, A. (2017). An application of backtracking search algorithm in designing power system stabilizers for large multi-machine system. *Neurocomputing*, 237(10):175–184.

Iurashev, D., Campa, G., Anisimov, V. V. and Cosatto, E. (2017). Two-step approach for pressure oscillations prediction in gas turbine combustion chambers. *International Journal of Spray and Combustion Dynamics*, 5:1–14.

Karaboga, D. (2005). An idea based on honey bee swarm for numerical optimization. Technical report, Technical Report TR06, Erciyes University, Kayseri, Turkey.

Karaboga, D. and Akay, B. (2009). A comparative study of artificial bee colony algorithm. *Applied Mathematics and Computation*, 214(1):108–132.

Karaboga, D. and Basturk, B. (2007). A powerful and efficient algorithm for numerical function optimization: artificial bee colony (abc) algorithm. *Journal of Global Optimization*, 39:459–471.

Karaboga, D. and Basturk, B. (2008). On the performance of artificial bee colony (abc) algorithm. *Applied Soft Computing*, 8(1):687–697.

Karande, A. S., Nigam, M. J. and Kadam, V. (2015). Design of a fuzzy pid controller for a gas turbine power plant. In *IEEE International Conference Communication, Control and Intelligent Systems (CCIS)*, pages 295–298, Mathura, India.

Kartite, J. and Cherkaoui, M. (2017). Improved backtracking search algorithm for renewable energy system. *Energy Procedia*, 141:126–130.

Kaveh, A. and Farhoudi, N. (2013). A new optimization method: Dolphin echolocation. *Advances in Engineering Software*, 59:53–70.

Kennedy, J. and Eberhart, R. (1995). Particle swarm optimization. In *Proceedings of the IEEE International Conference on Neural Networks (ICNN)*, volume 4, pages 1942–1948, Perth, Australia.

Khare, A. and Rangnekar, S. (2013). A review of particle swarm optimization and its applications in solar photovoltaic system. *Applied Soft Computing*, 13(5):2997–3006.

Khosravi, R., Khosravi, A., Nahavandi, S. and Hajabdollahi, H. (2015). Effectiveness of evolutionary algorithms for optimization of heat exchangers. *Energy Conversion and Management*, 89:281–288.

Kim, D. J., Moon, Y. H., Choi, B. S., Ryu, H. S. and Nam, H. K. (2018). Impact of a heavy-duty gas turbine operating under temperature control on system stability. *IEEE Transactions on Power Systems*, 33(4):4543–4552.

Kohli, M. and Arora, S. (2017). Chaotic grey wolf optimization algorithm for constrained optimization problems. *Journal of Computational Design and Engineering*, 5(4):458–472.

LaTorre, A., Muelas, S. and Peña, J.-M. (2015). A comprehensive comparison of large scale global optimizers. *Information Sciences*, 316:517–549.

Leca, J. B., Gunst, N., Thierry, B. and Petit, O. (2003). Distributed leadership in semifree-ranging white-faced capuchin monkeys. *Animal Behaviour*, 66(6):1045–1052.

Lefebvre, A. H. and Ballal, D. R. (2010). *Gas Turbine Combustion - Alternative Fuels and Emissions*. CRC Press, New York, United States of America, 3rd edition.

Lemma, T. A. and Hashim, F. B. M. (2011). Use of fuzzy systems and bat algorithm for exergy modeling in a gas turbine generator. In *IEEE Colloquium on Humanities, Science and Engineering*, pages 305–310, Penang, Malaysia.

Lemma, T. A., Hashim, F. M., Amin, M. and Abd, B. (2016). An integrated approach to industrial gas turbine diagnostics and reliability monitoring. *ARPN Journal of Engineering and Applied Sciences*, 11(12):7799–7805.

Li, J. and Ying, Y. (2018). A method to improve the robustness of gas turbine gas-path fault diagnosis against sensor faults. *IEEE Transactions on Reliability*, 67(1):3–12.

Li, M. D., Zhao, H., Weng, X. W. and Han, T. (2016). A novel nature-inspired algorithm for optimization: Virus colony search. *Advances in Engineering Software*, 92:65–88.

Liao, T. W. and Kuo, R. J. (2018). Five discrete symbiotic organisms search algorithms for simultaneous optimization of feature subset and neighborhood size of knn classification models. *Applied Soft Computing Journal*, 64:581–595.

Lisnianski, A., Laredo, D. and Haim, H. B. (2016). Multi-state markov model for reliability analysis of a combined cycle gas turbine power plant. In *2nd International Symposium on Stochastic Models in Reliability Engineering, Life Science and Operations Management (SMRLO)*, pages 131–135, Beer Sheva, Israel.

Liu, X. and Wang, S. (2011). Impact of aerodynamic performance by the heat value of fuel change on the turbine cascade of ground heavy duty gas turbine. In *IEEE Asia-Pacific Power and Energy Engineering Conference (APPEEC)*, pages 1–4, Wuhan, China.

Liu, Z. and Karimi, I. A. (2018). Simulating combined cycle gas turbine power plants in aspen hysys. *Energy Conversion and Management*, 171(2):1213–1225.

Lones, M. A. (2019). Mitigating metaphors: A comprehensible guide to recent nature-inspired algorithms. *SN Computer Science*, 1(49):1–12.

Long, W. and Xu, S. (2016). A novel grey wolf optimizer for global optimization problems. In *IEEE Advanced Information Management, Communicates, Electronic and Automation Control Conference (IMCEC)*, pages 1266–1270, Xi'an, China.

Ma, J., pei Zhang, J., Yang, J. and li Cheng, L. (2008). Research on cultural algorithm for solving routing problem of mobile agent. *The Journal of China Universities of Posts and Telecommunications*, 15(4):121–125.

Ma, L. and Cao, P. (2016). Comparative study of several improved firefly. In *IEEE International Conference on Information and Automation (ICIA)*, pages 910–914, Ningbo, China.

Madasu, S. D., Kumar, M. L. and Singh, A. K. (2017). Comparable investigation of backtracking search algorithm in automatic generation control for two area reheat interconnected thermal power system. *Applied Soft Computing Journal*, 55:197–210.

Mahdavi, S., Shiri, M. E. and Rahnamayan, S. (2015). Metaheuristics in large-scale global continues optimization: A survey. *Information Sciences*, 295:407–428.

Mahor, A., Prasad, V. and Rangnekar, S. (2009). Economic dispatch using particle swarm optimization: A review. *Renewable and Sustainable Energy Reviews*, 13(8):2134–2141.

Mehrpanahi, A. and Payganeh, G. H. (2017). Multi-objective optimization of igv position in a heavy-duty gas turbine on part-load performance. *Applied Thermal Engineering*, 125:1478–1489.

Mirjalili, S. (2015). How effective is the grey wolf optimizer in training multi-layer perceptrons. *Applied Intelligence*, 43:150–161.

Mirjalili, S. and Lewis, A. (2016). The whale optimization algorithm. *Advances in Engineering Software*, 95:51–67.

Mirjalili, S., Mirjalili, S. M. and Lewis, A. (2014). Grey wolf optimizer. *Advances in Engineering Software*, 69:46–61.

Modiri-Delshad, M., Aghay Kaboli, S. H., Taslimi-Renani, E. and Rahim, N. A. (2016). Backtracking search algorithm for solving economic dispatch problems with valve-point effects and multiple fuel options. *Energy*, 116:637–649.

Mohammed, H. J., Abdulsalam, F., Abdulla, A. S., Ali, R. S., Abd-Alhameed, R. A., Noras, J. M., Abdulraheem, Y. I., Ali, A., Rodriguez, J. and Abdalla, A. M. (2016). Evaluation of genetic algorithms, particle swarm optimisation, and firefly algorithms in antenna design. In *13th International Conference on Synthesis, Modeling, Analysis and Simulation Methods and Applications to Circuit Design (SMACD)*, pages 1–4, Lisbon, Portugal.

Molina, D., Poyatos, J., Ser, J. D., García, S., Hussain, A. and Herrera, F. (2020). Comprehensive taxonomies of nature- and bio-inspired optimization: Inspiration versus algorithmic behavior, critical analysis recommendations. *Cognitive Computation*, 12:897–939.

Montgomery, D. C. and Runger, G. C. (2011). *Applied Statistics and Probability for Engineers*. John Wiley & Sons, Inc., Hoboken, United States of America, 5th edition.

Morales-Castañeda, B., Zaldívar, D., Cuevas, E., Fausto, F. and Rodríguez, A. (2020). A better balance in metaheuristic algorithms: Does it exist? *Swarm and Evolutionary Computation*, 54(2).

Mosavi, M., Khishe, M. and Ghamgosar, A. (2016). Classification of sonar data set using neural network trained by gray wolf optimization. *Neural Network World*, 26(4):393–415.

Moussa, T. M. and Awotunde, A. A. (2018). Self-adaptive differential evolution with a novel adaptation technique and its application to optimize es-sagd recovery process. *Computers and Chemical Engineering*, 118:64–76.

Muangkote, N., Sunat, K. and Chiewchanwattana, S. (2014). An improved grey wolf optimizer for training q-gaussian radial basis functional-link nets. In *IEEE International Computer Science and Engineering Conference (ICSEC)*, pages 209–214, Khon Kaen, Thailand.

Muhuri, P. K., Shukla, A. K. and Abraham, A. (2019). Industry 4.0: A bibliometric analysis and detailed overview. *Engineering Applications of Artificial Intelligence*, 78:218–235.

Nikpey, H., Assadi, M. and Breuhaus, P. (2012). Development of an optimized artificial neural network model for combined heat and power micro gas turbines. *Applied Energy*, 108:137–148.

Omar, M., Ibrahim, R., Abdullah, M. F. and Tarik, M. H. M. (2018). Modelling and system identification of gas fuel valves in rowen's model for dry low emission gas turbine. In *IEEE Conference on Big Data and Analytics (ICBDA)*, pages 33–37, Langkawi, Malaysia.

Park, Y., Choi, M., Kim, K., Li, X., Jung, C., Na, S. and Choi, G. (2020). Prediction of operating characteristics for industrial gas turbine combustor using an optimized artificial neural network. *Energy*, 213:118769.

Parsopoulos, K. and Vrahatis, M. (2002). Recent approaches to global optimization problems through particle swarm optimization. *Natural Computing*, pages 235–306.

Peng, B., Reynolds, R. G. and Brewster, J. (2003). Cultural swarms. In *IEEE Congress on Evolutionary Computation (CEC)*, pages 1965–1971, Canberra, Australia.

Perpignan, A. A., Gangoli Rao, A. and Roekaerts, D. J. (2018). Flameless combustion and its potential towards gas turbines. *Progress in Energy and Combustion Science*, 69:28–62.

Perry, S. (1996). Intergroup encounters in wild white-faced capuchins (*Cebus capucinus*). *International Journal of Primatology*, 17:309–330.

Pierezan, J., dos Santos Coelho, L., Cocco Mariani, V., Hochsteiner de Vasconcelos Segundo, E. and Prayogo, D. (2021). Chaotic coyote algorithm applied to truss optimization problems. *Computers & Structures*, 242:106353.

Pierezan, J., Freire, R. Z., Weihmann, L., Reynoso-Meza, G. and dos Santos Coelho, L. (2017a). Static force capability optimization of humanoids robots based on modified self-adaptive differential evolution. *Computers & Operations Research*, 84:205–215.

Pierezan, J., Maidl, G., Yamao, E. M., Gonçalves, J. P. S., Chiesa, F. and Coelho, L. S. (2017b). Robust identification of pressure oscillations in the combustion chamber of a heavy duty turbine. In *24th ABCM International Congress of Mechanical Engineering (COBEM 2017)*, pages 1–10, Curitiba, Brazil.

Pitt, W. C., Box, P. W. and Knowlton, F. F. (2003). An individual-based model of canid populations: Modelling territoriality and social structure. *Ecological Modelling*, 166(1-2):109–121.

Plis, M. and Rusinowski, H. (2016). Modelling and simulation of the effect of ambient parameters on the performance of a combined cycle gas turbine power plant. *IEEE 17th International Carpathian Control Conference (ICCC)*, pages 590–595.

Poessel, S. A., Gese, E. M. and Young, J. K. (2014). Influence of habitat structure and food on patch choice of captive coyotes. *Applied Animal Behaviour Science*, 157:127–136.

Poli, R., Kennedy, J. and Blackwell, T. (2007). Particle swarm optimization. *Swarm Intelligence*, 1:33–57.

Pradhan, M., Roy, P. K. and Pal, T. (2018). Oppositional based grey wolf optimization algorithm for economic dispatch problem of power system. *Ain Shams Engineering Journal*, 9(4):2015–2025.

Qin, A. K., Huang, V. L. and Suganthan, P. N. (2009). Differential evolution algorithm with strategy adaptation for global numerical optimization. *IEEE Transactions on Evolutionary Computation*, 13(2):398–417.

Rao, S. S. (1996). *Engineering Optimization: Theory and Practice*. John Wiley & Sons, Inc., New York, United States of America, 3rd edition.

Ribeiro, M. R. and Aguiar, M. S. (2011). Cultural algorithms: A study of concepts and approaches. In *Workshop-School on Theoretical Computer Science*, pages 145–148, Pelotas, Brazil.

Saboohi, Z., Ommi, F. and Akbari, M. (2019). Multi-objective optimization approach toward conceptual design of gas turbine combustor. *Applied Thermal Engineering*, 148:1210–1223.

Salcedo-Sanz, S. (2016). Modern meta-heuristics based on nonlinear physics processes: A review of models and design procedures. *Physics Reports*, 655:1–70.

Sánchez, D., Melin, P., Carpio, J. and Puga, H. (2016). A firefly algorithm for modular granular neural networks optimization applied to iris recognition. In *IEEE International Joint Conference on Neural Networks (IJCNN)*, volume 10, pages 139–144, Vancouver, Canada.

Sánchez, D., Melin, P. and Castillo, O. (2017). A grey wolf optimizer for modular granular neural networks for human recognition. *Computational Intelligence and Neuroscience*, 2017:1–26.

Saremi, S., Mirjalili, S. and Lewis, A. (2017). Grasshopper optimisation algorithm: Theory and application. *Advances in Engineering Software*, 105:30–47.

Saria, A., Tahar, K. and Ammar, B. B. (2014). Thermodynamic and energy study of a regenerator in gas turbine cycle and optimization of performances. In *IEEE 5th International Renewable Energy Congress (IREC)*, pages 1–5, Hammamet, Tunisia.

Schaik, C. P. V. and Isler, K. (2012). *The Evolution of Primate Societies*, chapter: Life - History Evolution in Primates, pages 220–244. The University of Chicago Press, Chicago, United States of America.

Secui, D. C. (2016). A modified symbiotic organisms search algorithm for large scale economic dispatch problem with valve-point effects. *Energy*, 113:366–384.

Sergeyev, Y. D., Kvasov, D. E. and Mukhametzhanov, M. S. (2018). On the efficiency of nature-inspired metaheuristics in expensive global optimization with limited budget. *Scientific Reports*, 8(453):1–9.

Shukla, A. K., Janmaijaya, M., Abraham, A. and Muhuri, P. K. (2019). Engineering applications of artificial intelligence: A bibliometric analysis of 30 years (1988–2018). *Engineering Applications of Artificial Intelligence*, 85:517–532.

Simon, D. (2013). *Evolutionary optimization algorithms: Biologically-Inspired and Population-Based Approaches to Computer Intelligence*. John Wiley & Sons, Inc., Hoboken, United States of America.

Sina Tayarani-Bathaie, S. and Khorasani, K. (2015). Fault detection and isolation of gas turbine engines using a bank of neural networks. *Journal of Process Control*, 36:22–41.

Sivananaithaperumal, S., Amali, S. M. J., Baskar, S. and Suganthan, P. N. (2011). Constrained self-adaptive differential evolution based design of robust optimal fixed structure controller. *Engineering Applications of Artificial Intelligence*, 24(6):1084–1093.

Sorgenfrei, M. and Tsatsaronis, G. (2016). Detailed exergetic evaluation of heavy-duty gas turbine systems running on natural gas and syngas. *Energy Conversion and Management*, 107:43–51.

Storn, R. and Price, K. (1995). Differential evolution - a simple and efficient adaptive scheme for global optimization over continuous spaces. Technical Report TR-95-012, International Computer Science Institute, Berkeley, United States of America.

Storn, R. and Price, K. (1997). Differential evolution - a simple and efficient heuristic for global optimization over continuous spaces. *Journal of Global Optimization*, 11:341–359.

Suganthan, P. N., Hansen, N., Liang, J., Deb, K., Chen, Y., Auger, A. and Tiwari, S. (2005). Problem definitions and evaluation criteria for the cec 2005 special session on real-parameter optimization. Technical Report 2005005, Nanyang Technological University, Singapore.

Suganthan, P. N., Hansen, N., Liang, J. J., Deb, K., Chen, Y. P., Auger, A. and Tiwari, S. (2016). Problem definitions and evaluation criteria for the cec 2017 special session and competition on single objective real-parameter numerical optimization. Technical report, Nanyang Technological University, Singapore.

Sun, J., Lai, C.-H. and Wu, X.-J. (2012). *Particle swarm optimisation*. CRC Press, Boca Raton, United States of America, 1st edition.

Talbi, H. and Draa, A. (2017). A new real-coded quantum-inspired evolutionary algorithm for continuous optimization. *Applied Soft Computing*, 61:765–791.

Tarik, M. H. M., Omar, M., Abdullah, M. F. and Ibrahim, R. (2017). Modelling of dry low emission gas turbine using black-box approach. In *TENCON - IEEE Region 10 Conference*, pages 1902–1906, Penang, Malasya.

Tejani, G. G., Savsani, V. J., Patel, V. K. and Mirjalili, S. (2018). Truss optimization with natural frequency bounds using improved symbiotic organisms search. *Knowledge-Based Systems*, 143:162–178.

Thom de Souza, R. C., de Macedo, C. A., dos Santos Coelho, L., Pierezan, J. and Mariani, V. C. (2020). Binary coyote optimization algorithm for feature selection. *Pattern Recognition*, 107:107470.

Togni, S., Nikolaidis, T. and Sampath, S. (2020). A combined technique of kalman filter, artificial neural network and fuzzy logic for gas turbines and signal fault isolation. *Chinese Journal of Aeronautics*.

Tsai, H. C. (2019). Improving backtracking search algorithm with variable search strategies for continuous optimization. *Applied Soft Computing Journal*, 80:567–578.

Tsoutsanis, E. and Meskin, N. (2019). Dynamic performance simulation and control of gas turbines used for hybrid gas/wind energy applications. *Applied Thermal Engineering*, 147(9):122–142.

Udeh, G. T. and Udeh, P. O. (2019). Comparative thermo-economic analysis of multi-fuel fired gas turbine power plant. *Renewable Energy*, 133:295–306.

Vitayasak, S., Pongcharoen, P. and Hicks, C. (2017). A tool for solving stochastic dynamic facility layout problems with stochastic demand using either a genetic algorithm or modified backtracking search algorithm. *International Journal of Production Economics*, 190:146–157.

Vogel, E. R., Munch, S. B. and Janson, C. H. (2007). Understanding escalated aggression over food resources in white-faced capuchin monkeys. *Animal Behaviour*, 74(1):71–80.

Vyncke-Wilson, D. (2013). Advantages of aero-derivative gas turbines in industrial applications: technical, operational and financial considerations on equipment selection. In *20th Symposium of the Industrial Applications of Gas Turbines Committee*, pages 1–15, Banff, Canada.

Wang, C. J., Wang, D. D. and Wu, Z. Y. (2011). Tubulence combustion modeling in the gas turbine combustor. In *IEEE 3rd International Conference on Measuring Technology and Mechatronics Automation (ICMTMA)*, pages 1064–1067, Shanghai, China.

Wang, X., Yang, C., Huang, M. and Ma, X. (2018). Multi-objective optimization of a gas turbine-based cchp combined with solar and compressed air energy storage system. *Energy Conversion and Management*, 164:93–101.

Wikberg, E. C., Jack, K. M., Campos, F. A., Fedigan, L. M., Sato, A., Bergstrom, M. L., Hiwatashi, T. and Kawamura, S. (2014). The effect of male parallel dispersal on the kin composition of groups in white-faced capuchins. *Animal Behaviour*, 96:9–17.

Xu, J. and Zhang, J. (2014). Exploration-exploitation tradeoffs in metaheuristics: Survey and analysis. In *Proceedings of the 33rd Chinese Control Conference (CCC)*, pages 8633–8638, Nanjing, China.

Xue, F., Cai, Y., Cao, Y., Cui, Z. and Li, F. (2015). Optimal parameter settings for bat algorithm. *International Journal of Bio-Inspired Computing*, 7(2):125–128.

Yamao, E. M. et al. (2017a). Abordagem de inteligência computacional aplicada para modelagem preditiva de emissões de nox e co de uma turbina a gás de uma usina termelétrica de ciclo combinado (*in Portuguese*). In *XXIV Seminário Nacional de Produção e Transmissão de Energia Elétrica (SNPTEE)*, pages 1–10, Curitiba, Brazil.

Yamao, E. M., Pierezan, J., Gonçalves, J. P. S., Gritti, M. C., Ribas, L. G. T., Chiesa, F., Santos, V. M. L., Freitas, M., Orlandi, A. S. and Coelho, L. S. (2017b). Identificação caixa preta de uma turbina a gás usando redes neurais artificiais integradas a algoritmos evolutivos de otimização (*in portuguese*). In *XIII Simpósio Brasileiro de Automação Inteligente*, pages 1075–1082, Porto Alegre, Brazil.

Yamao, E. M., Pierezan, J., Gonçalves, J. P. S., Gritti, M. C., Ribas, L. G. T., Chiesa, F., Santos, V. M. L., Freitas, M., Orlandi, A. S. and Coelho, L. S. (2018). *Abordagem de inteligência*

computacional aplicada para modelagem preditica de emissões de NOx e CO de uma turbina a gás de uma usina termelétrica de ciclo combinado (in portuguese), chapter: 7, pages 70–81. Atena Editora, Belo Horizonte, Brazil.

Yan, S., Zhou, J., Zheng, Y. and Li, C. (2018). An improved hybrid backtracking search algorithm based t–s fuzzy model and its implementation to hydroelectric generating units. *Neurocomputing*, 275:2066–2079.

Yan, X., Li, W., Chen, W., Luo, W., Zhang, C. and Liu, H. (2012). Cultural algorithm for engineering design problems. *International Journal of Computer Science Issues (IJCSI)*, 9(2):53–61.

Yang, X.-S. (2009). Firefly algorithms for multimodal optimization. In Watanabe, O. and Zeugmann, T., (eds), *Stochastic Algorithms: Foundations and Applications*, volume 5792 of *Lecture Notes in Computer Science*, pages 169–178. Springer-Verlag, Berlin, Heidelberg.

Yang, X.-S. (2010). A new metaheuristic bat-inspired algorithm. In González, J. R., Pelta, D. A., Cruz, C., Terrazas, G. and Krasnogor, N., (eds), *Nature Inspired Cooperative Strategies for Optimization (NICSO)*, volume 284 of *Studies in Computational Intelligence*, pages 65–74. Springer-Verlag, Berlin, Heidelberg.

Yang, X.-S. (2012). Flower pollination algorithm for global optimization. In Durand-Lose, J. and Jonoska, N., (eds), *Unconventional Computation and Natural Computation*, volume 7445 of *Lecture Notes in Computer Science*, pages 240–249. Springer-Verlag, Berlin, Heidelberg.

Yang, X.-S. (2014). *Nature-Inspired Optimization Algorithms*. Elsevier Inc., Waltham, United States of America, 1st edition.

Yang, X.-S. and He, X. (2013a). Bat algorithm: literature review and applications. *International Journal of Bio-Inspired Computation*, 5(3):141–149.

Yang, X.-S. and He, X. (2013b). Firefly algorithm: recent advances and applications. *International Journal of Swarm Intelligence (IJSI)*, 1(1):1–14.

Yang, X.-S. and Koziel, S. (2011). Computational optimization and applications in engineering and industry. In Kacprzyk, J., editor, *Studies in Computational Intelligence*, volume 359, pages 1–5. Springer-Verlag, Berlin, Heidelberg.

Yang, X.-S., Koziel, S. and Leifsson, L. (2013). Computational optimization, modelling and simulation: Recent trends and challenges. *Procedia Computer Science*, 18:855–860.

Yu, C., Heidari, A. A. and Chen, H. (2020). A quantum-behaved simulated annealing algorithm-based moth-flame optimization method. *Applied Mathematical Modelling*, 87:1–19.

Yu, J. J. and Li, V. O. (2015). A social spider algorithm for global optimization. *Applied Soft Computing*, 30:614–627.

Zabihian, F. and Fung, A. S. (2013). Performance analysis of hybrid solid oxide fuel cell and gas turbine cycle: Application of alternative fuels. *Energy Conversion and Management*, 76:571–580.

Zang, H., Zhang, S. and Hapeshi, K. (2010). A review of nature-inspired algorithms. *Journal of Bionic Engineering*, 7:S232–S237.

Zelinka, I., Snasel, V. and Abraham, A. (2013). Handbook of optimization: from classical to modern approach. In Kacprzyk, J. and Jain, L. C., (eds), *Intelligent Systems Reference Library*, volume 38. Springer, Berlin, Heidelberg.

Zhang, C., Zhou, J., Li, C., Fu, W. and Peng, T. (2017). A compound structure of elm based on feature selection and parameter optimization using hybrid backtracking search algorithm for wind speed forecasting. *Energy Conversion and Management*, 143:360–376.

Zhang, Q., Ogren, R. M. and Kong, S.-C. (2018). Thermo-economic analysis and multi-objective optimization of a novel waste heat recovery system with a transcritical co2 cycle for offshore gas turbine application. *Energy Conversion and Management*, 172:212–227.

Zhang, X. (2017). Modeling and simulation of gas turbine engine based on object-oriented approach. In *IEEE 17th International Conference on Control, Automation and Systems (ICCAS)*, volume 10, pages 551–555, Jeju, South Korea.

Zhang, Y., Huang, C. and Jin, Z. (2020a). Backtracking search algorithm with reusing differential vectors for parameter identification of photovoltaic models. *Energy Conversion and Management*, 223(7):113266.

Zhang, Y., Jin, Z., Zhao, X. and Yang, Q. (2020b). Backtracking search algorithm with lévy flight for estimating parameters of photovoltaic models. *Energy Conversion and Management*, 208(1):112615.

Zhang, Y., Ma, M. and Jin, Z. (2020c). Backtracking search algorithm with competitive learning for identification of unknown parameters of photovoltaic systems. *Expert Systems with Applications*, 160:113750.

Zhang, Y., Martínez-García, M., Kalawsky, R. S. and Latimer, A. (2020d). Grey-box modelling of the swirl characteristics in gas turbine combustion system. *Measurement*, 151:107266.

APPENDIX A – DEFINITIONS OF THE BENCHMARK FUNCTIONS

This appendix is based on the definitions of the IEEE-CEC 2017 competition of single-objective optimization (Suganthan et al., 2016). A general description of the benchmark functions and the evaluation criteria are provided.

A.1 BENCHMARKS DESCRIPTION

A set of 30 benchmark functions has been proposed in the IEEE-CEC 2017 competition of single-objective real-parameter optimization. However, one function has presented technical issues and it has been removed from the set (the function 2). The remaining benchmark functions are presented in Tab. A.1, where an identification (F) assigned and main the features are presented, including the base functions and the global optima.

As it can be seen, the benchmark functions can be pure or a combination of more functions, called Base Functions. As consequence, the benchmark problems are labeled according to the resulting features. The features notations are:

- C: Composition;
- H: Hybrid;
- M: Multimodal;
- N-s: Non-separable;
- S: Separable;
- U: Unimodal.

By definition, the composition functions are written as:

$$F(\vec{x}) = \sum_{i=1}^{n} \{\omega_i \cdot [\lambda_i g_i(x) + bias_i]\} + F^*, \tag{A.1}$$

where $g_i(x)$ is the i^{th} basic function used to construct the composition function, n is the number of basic functions, ω_i and λ_i are used to normalize and to weight the composition, $bias_i$ is used to define the global optima position and $F*$ defines the optimal cost of the benchmark.

On the other hand, the hybrid functions are defined as:

$$F(\vec{x}) = \sum_{i=1}^{n} \{g_i(M_i z_i)\} + F^*, \tag{A.2}$$

where M_i is a component used to rotate the global optima and z_i is used to shift the global optima of g_i. Finally, the multimodal functions are those that present numerous local optima, while unimodal functions present only one region of convergence.

The search space of all benchmarks is defined as $[-100, 100]^D$, where D is the dimension of the function or, in other words, the number of design variables. The stopping criteria is the number of function evaluations, denoted N^{max}, set to $10000 \times D$.

F_{CEC}	Base Functions	Features	$F^* = F(\vec{x}^*)$
1	Bent Cigar	U, S	100
3	Zakharov	U, S	300
4	Rosenbrock	M, N-s	400
5	Rastrigin	M, N-s	500
6	Scaffer	M, N-s	600
7	Lunacek Bi-Rastrigin	M, N-s	700
8	Non-Continuous Rastrigin	M, N-s	800
9	Levy	M, N-s	900
10	Schwefel	M, N-s	1000
11	Zakharov, Rosenbrock, Rastrigin	M, H, N-s	1100
12	High Conditioned Elliptic, Modified Schwefel, Bent Cigar	M, H, N-s	1200
13	Bent Cigar, Rosenbrock, Lunache Bi-Rastrigin	M, H, N-s	1300
14	High Conditioned Elliptic, Ackley, Schaffer, Rastrigin	M, H, N-s	1400
15	Bent Cigar, HGBat, Rastrigin, Rosenbrock	M, H, N-s	1500
16	Expanded Schaffer, HGBat, Rocenbrock, Modified Schwefel	M, H, N-s	1600
17	Katsuura, Ackley, Expanded Griewank plus Rosenbrock, Modified Schwefel, Rastrigin	M, H, N-s	1700
18	High Conditioned Elliptic, Ackley, Rastrigin, HGBat, Discus	M, H, N-s	1800
19	Bent Cigar, Rastrigin, Expanded Griewank plus Rocenbrock, Weiertrass, Expanded Schaffer	M, H, N-s	1900
20	Happycat, Katsuura, Ackley, Rastrigin, Modified Schwefel, Schaffer	M, H, N-s	2000
21	Rosenbrock, High Conditioned Elliptic, Rastrigin	M, C, N-s	2100
22	Rastrigin, Griewank, Modified Schwefel	M, C, N-s	2200
23	Rosenbrock, Ackley, Modified Schwefel, Rastrigin	M, C, N-s	2300
24	Ackley, High Conditioned Elliptic, Griewank, Rastrigin	M, C, N-s	2400
25	Rastrigin, Happycat, Ackley, Discus, Rosenbrock	M, C, N-s	2500
26	Expanded Scaffer, Modified Schwefel, Griewank, Rosenbrock, Rastrigin	M, C, N-s	2600
27	HGBat, Rastrigin, Modified Schwefel, Bent-Cigar, High Conditioned Elliptic, Expanded Scaffer	M, C, N-s	2700
28	Ackley, Griewank, Discus, Rocwnbrock, Happycat, Expanded Scaffer	M, C, N-s	2800
29	F_{15}, F_{16}, F_{17}	M, C, N-s	2900
30	F_{15}, F_{18}, F_{19}	M, C, N-s	3000

Table A.1: Benchmarks definition from IEEE-CEC2017

To improve the readers understanding, some of the benchmark functions are drawn in Figs. A.1 and A.2, which contain the shape and the level plots for $D = 2$ and 50 points in each input axis.

A.2 EVALUATION CRITERIA

The evaluation criteria presented in this section is a tool for comparing the performance of a set of optimization algorithms, denoted Ψ. It is divided into two analyses: score evaluation and computational complexity.

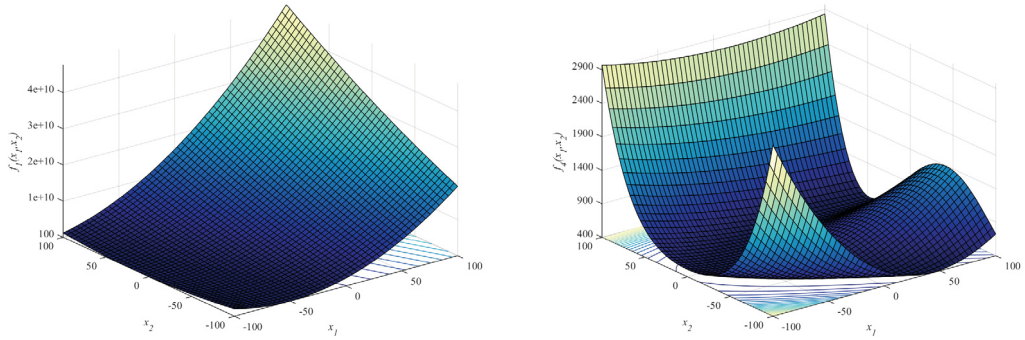

a) F_1

b) F_4

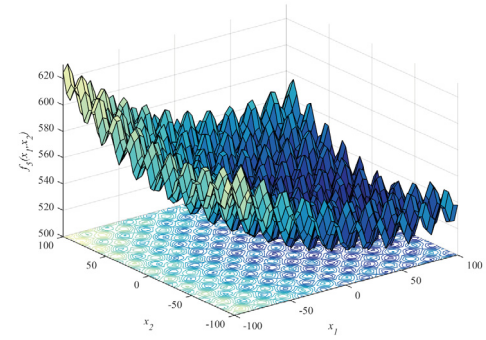

c) F_5

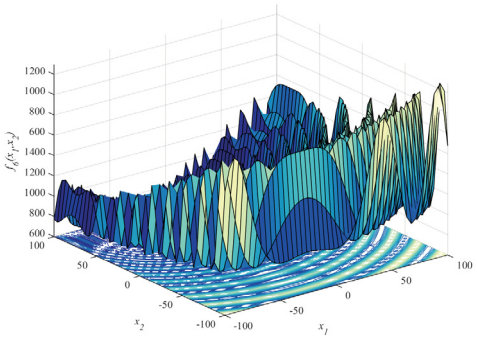

d) F_6

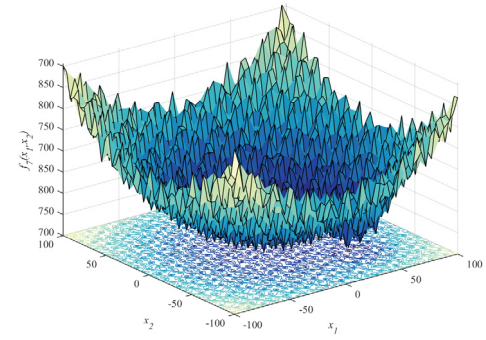

e) F_7

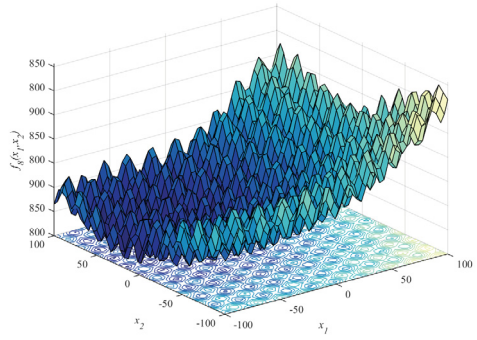

f) F_8

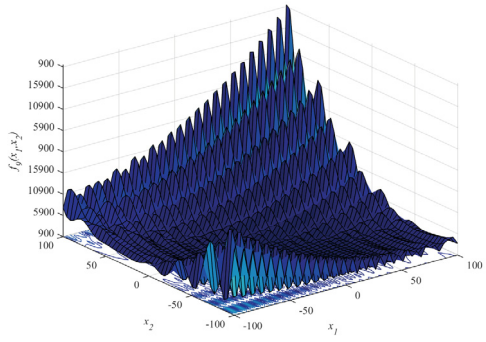

g) F_9

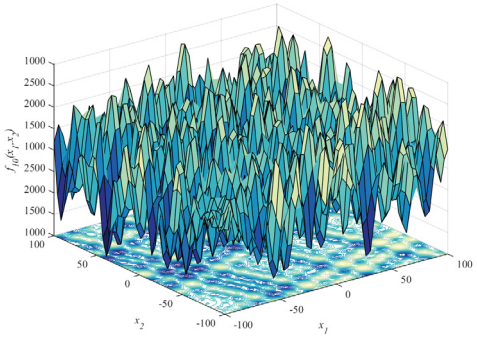

h) F_{10}

Figure A.1: 3D-view of some benchmark functions considering 2D - Part I

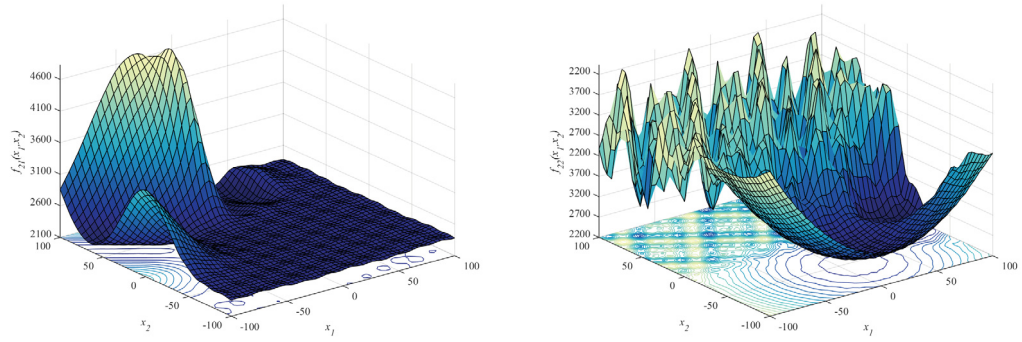

a) F_{21} b) F_{22}

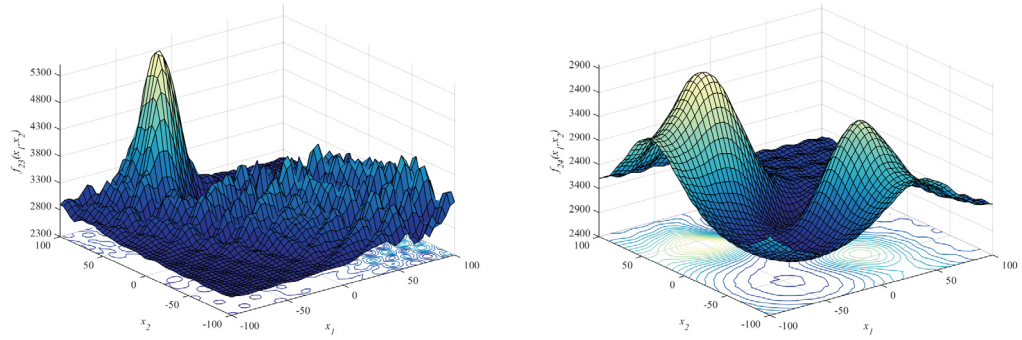

c) F_{23} d) F_{24}

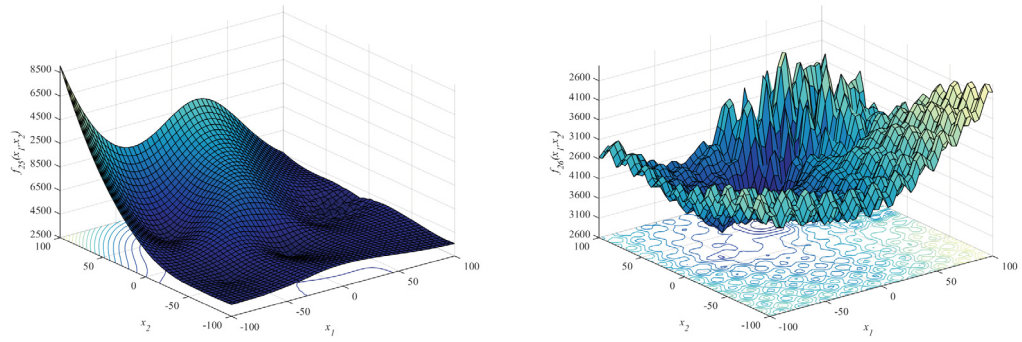

e) F_{25} f) F_{26}

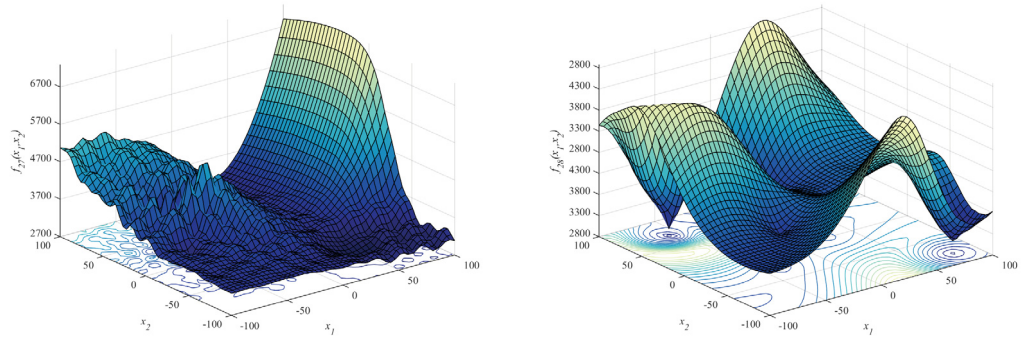

g) F_{27} h) F_{28}

Figure A.2: 3D-view of some benchmark functions considering 2D - Part II

The score evaluation is an index with values from 0 to 100 that equally considers two criteria. The first one is the sum of the errors between the optimal and the achieved cost (SE) for all dimensions, such that:

$$SE_a = \sum_{i=1}^{29} [(0.1 \times e_a^{10D}) + (0.2 \times e_a^{30D}) + (0.3 \times e_a^{50D}) + (0.4 \times e_a^{100D})] \tag{A.3}$$

for all $a \in \Psi$, where e_a^{10D}, e_a^{30D}, e_a^{50D} and e_a^{100D} contains the error values for the algorithm a and functions with dimensions 10, 30, 50 and 100, respectively. This sum is transformed into the first score S_1, which is defined as:

$$S_{1,a} = (1 - \frac{SE_a - SE^{Min}}{SE_a}) \times 50 \tag{A.4}$$

for all $a \in \Psi$, where SE^{Min} represents the minimum of the errors sum among all algorithms.

The second one considers the sum of ranks achieved by the algorithms for each benchmark function dimension, such that:

$$SR_a = \sum_{i=1}^{29} [(0.1 \times rank_a^{10D}) + (0.2 \times rank_a^{30D}) + (0.3 \times rank_a^{50D}) + (0.4 \times rank_a^{100D})] \tag{A.5}$$

for all $a \in \Psi$, which results in the second score (S_2), defined as:

$$S_{2,a} = (1 - \frac{SR_a - SR^{Min}}{SR_a}) \times 50 \tag{A.6}$$

for all $a \in \Psi$, where SR^{Min} represents the minimum of the rank sum among all algorithms. The final score of each algorithm is the combination of those two criteria, such that:

$$Score_a = S_{1,a} + S_{2,a} \tag{A.7}$$

for all $a \in \Psi$.

The computational complexity is calculated according to the time spent to execute the optimization, mitigating the influence of the benchmark function itself and the computer features. The complexity of the a^{th} algorithm regarding the dimension D is defined by the following equation:

$$C_a^D = \frac{(\hat{T}_{2,a}^D - T_1^D)}{T_0}, \tag{A.8}$$

where T_0 is the computer time calculated according to Alg. 13, T_1^D is a specific function time considering D and $\hat{T}_{2,a}^D$ is the time spent by the a^{th} algorithm to run the function for D.

According to the IEEE-CEC 2017 definitions, the time T_1^D is calculated based on one time run with N_e evaluations of the specific function for D. To mitigate possible oscillations in the Computer Processor Units (CPU) or even in the Random Access Memory (RAM), the time T_1^D is obtained through the average of N_t runs of N_e evaluations. Finally, the time $\hat{T}_{2,a}^D$ is obtained as the average time among N_t optimizations with N_e evaluations of the specific function with dimension D.

Algorithm 13 Computation of time T0

1: Initialize the time counter T0 and $x = 0.55$
2: **for** i from 1 to 1000000 **do**
3: $x = x + x$
4: $x = \frac{x}{2}$
5: $x = x \cdot x$
6: $x = \sqrt{x}$
7: $x = \ln x$
8: $x = \exp x$
9: $x = \frac{x}{(x+2)}$
10: Stop the time counter T_0 and store the resulting time.
11: **end for**

APPENDIX B – COMPLEMENTAR RESULTS

This appendix presents the complementary results from the IEEE-CEC 2017 116 benchmark functions. The descriptive statistic of the errors is presented in terms of minimum, average, median, maximum, and standard deviation values from Tabs. B.1 to B.29.

Algorithm	F_1					F_2				
	Minimum	Average	Median	Maximum	Standard Deviation	Mininum	Average	Median	Maximum	Standard Deviation
COA5	1.8813e+00	2.0652e+02	1.2405e+02	1.8545e+03	3.3504e+02	3.1119e+01	2.1487e+03	9.2876e+02	1.2337e+04	2.7798e+03
COA10	1.5369e+00	2.4548e+02	2.2766e+01	5.5320e+03	1.0046e+03	3.2176e+01	1.3605e+03	9.4148e+02	6.7402e+03	1.4832e+03
ABC	3.7790e+01	2.6218e+02	1.5553e+02	1.0401e+03	2.5484e+02	3.7580e+00	2.3407e+02	1.8012e+02	6.8525e+02	1.8907e+02
BA	9.5113e+04	2.9098e+05	2.8436e+05	4.4606e+05	8.3238e+04	2.1499e+06	3.4779e+06	3.4613e+06	4.5305e+06	4.3473e+05
FA	6.5693e+09	1.5588e+10	1.6413e+10	2.3471e+10	5.0643e+09	7.6685e+10	1.1358e+11	1.1548e+11	1.4401e+11	1.4302e+10
GWO	1.9804e+03	3.3162e+06	1.8339e+04	3.7893e+07	9.0749e+06	2.6405e+07	7.7968e+08	6.4521e+08	2.7297e+09	6.5876e+08
PSO	3.5012e+00	3.7943e+08	9.1293e+03	1.9429e+09	6.9468e+08	7.6233e+04	5.8923e+08	1.0012e+06	3.6892e+09	9.8299e+08
SOS	2.6630e+00	2.4720e+03	1.5430e+03	1.1954e+04	2.8848e+03	4.8029e+01	2.9982e+03	1.2764e+03	1.6299e+04	4.1399e+03
WfCMO5	2.6944e-11	4.6030e+02	8.1347e+01	2.9716e+03	7.1248e+02	1.1186e+01	2.1041e+03	1.4180e+03	8.1507e+03	2.3468e+03
WfCMO10	2.5024e-08	1.7176e+01	2.7806e-03	3.9632e+02	7.3091e+01	5.3958e-01	1.5121e+03	5.8796e+02	9.5596e+03	2.3558e+03
WfCMO20	5.7319e-08	1.9223e+01	1.7022e-01	2.3556e+02	4.5102e+01	3.0329e-01	2.4533e+03	1.6106e+03	1.3237e+04	2.8284e+03
Algorithm	F_3					F_4				
	Minimum	Average	Median	Maximum	Standard Deviation	Mininum	Average	Median	Maximum	Standard Deviation
COA5	1.9726e+01	2.2031e+03	1.2947e+03	1.0221e+04	2.7046e+03	6.3012e+01	4.0644e+03	2.0561e+03	1.7742e+04	4.4374e+03
COA10	3.0662e-03	3.6011e+03	1.7422e+03	1.8178e+04	4.5533e+03	1.8153e-02	4.3343e+03	2.4623e+03	2.5264e+04	5.8713e+03
ABC	3.9105e+01	2.4323e+03	9.5727e+02	1.1165e+04	2.9954e+03	4.3983e+01	5.4576e+03	3.3808e+03	1.8709e+04	5.0226e+03
BA	6.0440e+06	8.1137e+06	8.0326e+06	1.0476e+07	9.2615e+05	1.6661e+07	1.9911e+07	1.9536e+07	2.6539e+07	2.3797e+06
FA	1.8866e+11	2.3732e+11	2.4361e+11	2.7754e+11	2.1612e+10	5.0375e+11	5.9066e+11	5.9715e+11	6.6348e+11	3.9496e+10
GWO	1.0266e+09	4.3434e+09	4.1917e+09	9.7360e+09	2.0068e+09	1.2738e+10	2.7969e+10	2.7742e+10	4.9092e+10	7.6497e+09
PSO	9.7352e+06	1.8635e+09	8.8968e+08	7.1224e+09	2.2377e+09	7.0506e+08	3.6255e+09	2.6292e+09	1.6532e+10	3.6690e+09
SOS	6.4616e+01	4.3128e+03	2.2005e+03	2.4045e+04	5.4151e+03	5.0691e+01	7.2984e+03	3.7108e+03	5.9033e+04	1.1575e+04
WfCMO5	7.0006e+01	1.5577e+03	1.0890e+03	6.6392e+03	1.5634e+03	5.6864e+02	3.7945e+04	8.8686e+03	3.3929e+05	8.0092e+04
WfCMO10	7.0539e+00	3.4554e+03	2.3694e+03	1.3305e+04	3.5527e+03	7.2456e+00	6.6128e+03	2.8651e+03	3.0609e+04	8.8078e+03
WfCMO20	6.0927e+00	3.2845e+03	2.2600e+03	1.3321e+04	3.5192e+03	1.5507e+02	7.7185e+03	7.2569e+03	2.6492e+04	6.5150e+03

Table B.1: Descriptive statistics for IEEE-CEC 2017 benchmark functions considering the error measurements - Part I.

Algorithm	F_5					F_6				
	Minimum	Average	Median	Maximum	Standard Deviation	Mininum	Average	Median	Maximum	Standard Deviation
COA5	1.4562e+00	1.4048e+01	9.3979e+00	5.1327e+01	1.2354e+01	2.6382e+04	4.8214e+04	4.6736e+04	8.1923e+04	1.3928e+04
COA10	1.2599e+01	5.5402e+01	3.4384e+01	2.6285e+02	5.9595e+01	4.3675e+04	5.9835e+04	5.9725e+04	7.4440e+04	8.5583e+03
ABC	3.7565e+02	6.1980e+03	5.7062e+03	1.4071e+04	3.6509e+03	7.2546e+04	1.1690e+05	1.1463e+05	1.5051e+05	1.8101e+04
BA	1.7362e-01	5.3969e-01	5.0331e-01	9.0951e-01	1.8501e-01	1.6008e+01	5.2336e+02	1.5806e+02	2.6347e+03	7.5455e+02
FA	3.1098e+04	9.3556e+04	8.2509e+04	3.1804e+05	5.7745e+04	1.3733e+05	2.6713e+07	6.8496e+05	5.9840e+08	1.0974e+08
GWO	8.0019e+00	3.8895e+02	1.3001e+02	3.5717e+03	7.1842e+02	1.2305e+04	2.9457e+04	2.9091e+04	5.7163e+04	1.0324e+04
PSO	2.8422e-13	5.4330e+01	4.9297e-08	1.6299e+03	2.9757e+02	4.4687e+02	5.8375e+03	1.9275e+03	9.5597e+04	1.7194e+04
SOS	0.0000e+00	3.0316e-14	0.0000e+00	1.7053e-13	4.1513e-14	1.0611e+02	5.3017e+02	4.0480e+02	1.8425e+03	3.9429e+02
WfCMO5	5.6843e-14	4.9897e-07	4.5617e-11	1.3925e-05	2.5380e-06	4.7599e-05	4.5078e-02	3.6277e-03	1.0543e+00	1.9129e-01
WfCMO10	0.0000e+00	1.1748e-13	5.6843e-14	4.5475e-13	1.0758e-13	3.8607e-04	8.5293e-02	1.7867e-02	6.8740e-01	1.4999e-01
WfCMO20	0.0000e+00	3.0127e-13	5.6843e-14	7.0486e-12	1.2755e-12	7.0344e-02	3.6236e+00	6.9837e-01	6.0221e+01	1.0927e+01
Algorithm	F_7					F_8				
	Minimum	Average	Median	Maximum	Standard Deviation	Mininum	Average	Median	Maximum	Standard Deviation
COA5	1.2563e+05	1.9066e+05	1.9469e+05	2.3590e+05	2.9354e+04	5.4753e+05	6.2637e+05	6.2873e+05	7.1092e+05	4.2320e+04
COA10	1.2553e+05	1.7590e+05	1.7662e+05	2.0846e+05	1.9253e+04	4.8959e+05	5.6755e+05	5.6636e+05	6.4403e+05	4.4359e+04
ABC	2.2539e+05	2.6897e+05	2.6898e+05	3.3704e+05	2.9367e+04	4.5773e+05	6.5246e+05	6.6029e+05	7.3593e+05	5.3825e+04
BA	2.0610e+03	9.7662e+03	7.7466e+03	4.8607e+04	9.0424e+03	1.0884e+05	2.2957e+05	1.9046e+05	5.3519e+05	1.0989e+05
FA	3.6768e+05	1.7820e+10	9.4846e+05	5.3325e+11	9.7349e+10	8.7003e+05	4.0337e+09	1.9354e+08	4.0116e+10	8.3260e+09
GWO	4.3911e+04	6.8684e+04	6.8049e+04	1.0909e+05	1.8384e+04	1.6124e+05	2.0226e+05	2.0076e+05	2.4006e+05	2.3169e+04
PSO	4.2578e+03	1.4403e+04	1.3264e+04	3.9060e+04	7.9160e+03	3.9944e+04	5.9225e+04	5.6948e+04	9.7191e+04	1.2870e+04
SOS	8.4025e+03	1.6070e+04	1.5134e+04	2.5975e+04	4.3770e+03	1.0774e+05	1.2990e+05	1.2965e+05	1.6455e+05	1.2337e+04
WfCMO5	2.7658e-01	1.0163e+02	7.6468e+00	2.7947e+03	5.0872e+02	6.9754e+02	3.1028e+03	2.6459e+03	8.2038e+03	1.8623e+03
WfCMO10	8.5577e+00	9.0329e+01	4.1440e+01	6.0191e+02	1.2719e+02	2.5222e+03	9.9100e+03	9.6089e+03	2.0948e+04	4.4104e+03
WfCMO20	1.3116e+02	9.2017e+02	6.9017e+02	2.2737e+03	6.3692e+02	1.3434e+04	2.6801e+04	2.6407e+04	4.1402e+04	7.1193e+03

Table B.2: Descriptive statistics for IEEE-CEC 2017 benchmark functions considering the error measurements - Part II.

Algorithm	F_9					F_{10}				
	Minimum	Average	Median	Maximum	Standard Deviation	Mininum	Average	Median	Maximum	Standard Deviation
COA5	7.9518e-03	1.8123e+00	1.5949e+00	4.6215e+00	1.3874e+00	5.5584e-01	7.6090e+01	8.6175e+01	1.1798e+02	3.2208e+01
COA10	7.8465e-04	5.1681e-03	4.2240e-03	2.8622e-02	4.9532e-03	7.3576e+01	8.9135e+01	8.7286e+01	1.1695e+02	9.2811e+00
ABC	1.4804e-02	2.9508e-01	1.8360e-01	1.8065e+00	3.4722e-01	1.5655e+00	3.5730e+01	3.2284e+01	6.9697e+01	2.6854e+01
BA	6.9438e-02	2.8786e+00	2.9013e+00	9.5026e+00	1.6122e+00	4.4880e+00	4.6737e+01	2.7207e+01	1.0330e+02	3.0812e+01
FA	7.0398e+02	1.8059e+03	1.6798e+03	4.0859e+03	7.1167e+02	2.4055e+04	4.4107e+04	4.4572e+04	6.6996e+04	1.1361e+04
GWO	3.0529e+00	1.2056e+01	7.4778e+00	6.4678e+01	1.3823e+01	9.3553e+01	1.4976e+02	1.4165e+02	3.6071e+02	4.7678e+01
PSO	5.5854e-02	7.1540e+01	3.3476e+01	4.3303e+02	9.6501e+01	4.8239e+01	2.7004e+02	1.4941e+02	1.2712e+03	3.1310e+02
SOS	1.5255e-02	5.1621e-01	4.3337e-01	2.7069e+00	4.6442e-01	3.5901e-03	6.6013e+01	7.0554e+01	1.1463e+02	3.0803e+01
WfCMO5	3.4875e+00	6.3389e+00	6.6573e+00	7.6731e+00	1.0431e+00	4.6172e+00	8.9669e+01	8.4330e+01	1.6024e+02	2.8159e+01
WfCMO10	1.4607e-01	4.1567e+00	4.5015e+00	5.8222e+00	1.4039e+00	4.0683e+00	8.2861e+01	8.6963e+01	1.1764e+02	2.9895e+01
WfCMO20	6.8059e-09	1.2736e+00	1.0838e+00	3.5636e+00	1.0325e+00	5.7280e+01	9.4962e+01	8.8575e+01	1.4197e+02	2.5094e+01
Algorithm	F_{11}					F_{12}				
	Minimum	Average	Median	Maximum	Standard Deviation	Mininum	Average	Median	Maximum	Standard Deviation
COA5	3.1207e+01	1.1855e+02	1.2061e+02	2.0659e+02	3.7259e+01	1.6055e+02	2.9278e+02	2.9612e+02	3.7429e+02	5.0740e+01
COA10	2.9060e+01	1.2478e+02	1.1853e+02	2.2631e+02	5.0667e+01	1.5590e+02	2.5995e+02	2.5321e+02	3.4908e+02	4.2534e+01
ABC	3.1859e+00	4.2315e+01	4.5213e+01	7.5292e+01	1.3658e+01	1.6515e+02	2.1865e+02	2.2547e+02	2.5250e+02	2.3201e+01
BA	4.3858e+01	1.0853e+02	1.0236e+02	1.6545e+02	4.0778e+01	9.6447e+01	2.0521e+02	1.9125e+02	3.6681e+02	6.3450e+01
FA	5.6983e+04	1.0021e+05	1.0349e+05	1.2576e+05	1.6931e+04	2.1111e+05	2.7227e+05	2.6880e+05	3.3204e+05	2.9689e+04
GWO	2.8860e+02	4.8926e+02	3.8814e+02	1.5136e+03	2.7784e+02	1.0071e+03	2.1547e+03	2.0266e+03	3.8424e+03	6.3289e+02
PSO	1.4944e+02	4.7008e+02	3.3741e+02	1.5043e+03	3.0571e+02	3.7508e+02	1.2373e+03	9.2168e+02	3.2013e+03	7.9888e+02
SOS	1.9338e+01	9.1826e+01	7.7815e+01	2.1651e+02	5.6519e+01	1.6965e+02	2.5868e+02	2.5386e+02	3.8093e+02	5.4767e+01
WfCMO5	3.4444e+01	1.4976e+02	1.4240e+02	2.7185e+02	5.7301e+01	2.2713e+02	3.6019e+02	3.6470e+02	4.4716e+02	5.0718e+01
WfCMO10	2.9521e+01	1.3106e+02	1.4045e+02	2.2080e+02	4.8688e+01	1.7763e+02	3.2983e+02	3.3681e+02	4.3441e+02	5.8509e+01
WfCMO20	2.8529e+01	1.5299e+02	1.5327e+02	2.6401e+02	5.4674e+01	2.6383e+02	3.4986e+02	3.6300e+02	4.4355e+02	4.9741e+01

Table B.3: Descriptive statistics for IEEE-CEC 2017 benchmark functions considering the error measurements - Part III.

Algorithm	F_{13}					F_{14}				
	Minimum	Average	Median	Maximum	Standard Deviation	Mininum	Average	Median	Maximum	Standard Deviation
COA5	2.9854e+00	7.2594e+00	7.4622e+00	1.1947e+01	2.4609e+00	2.9849e+01	6.3520e+01	5.6714e+01	1.0564e+02	1.8669e+01
COA10	2.9931e+00	8.1262e+00	7.4676e+00	1.7909e+01	3.4961e+00	2.5869e+01	5.3300e+01	5.1240e+01	7.8697e+01	1.4043e+01
ABC	5.0243e+00	7.3968e+00	7.0266e+00	1.1800e+01	1.7686e+00	5.9587e+01	7.9066e+01	7.9639e+01	9.9651e+01	1.0701e+01
BA	1.4165e+01	6.1293e+01	6.1893e+01	1.0662e+02	2.5525e+01	2.1756e+02	3.3923e+02	3.2322e+02	5.1622e+02	6.6676e+01
FA	9.4702e+01	1.3821e+02	1.4295e+02	1.7355e+02	2.1727e+01	5.5761e+02	6.4136e+02	6.4569e+02	7.5499e+02	5.6986e+01
GWO	4.7682e+00	1.1056e+01	1.0026e+01	2.0328e+01	4.3879e+00	5.1553e+01	8.9973e+01	8.7029e+01	1.7693e+02	2.6383e+01
PSO	8.3322e+00	2.9509e+01	2.8919e+01	5.7512e+01	1.2274e+01	9.8228e+01	1.5541e+02	1.5122e+02	2.1615e+02	3.1781e+01
SOS	5.0171e+00	1.6508e+01	1.6575e+01	2.5121e+01	5.0699e+00	2.1946e+01	6.8421e+01	6.6110e+01	1.5929e+02	3.0112e+01
WfCMO5	9.0906e-06	3.8449e+00	3.7087e+00	8.9546e+00	1.8999e+00	1.4924e+01	4.1804e+01	4.1291e+01	6.9647e+01	1.1385e+01
WfCMO10	1.9899e+00	5.9759e+00	5.5265e+00	1.2596e+01	2.8511e+00	2.4874e+01	4.1271e+01	3.8804e+01	6.1687e+01	9.5247e+00
WfCMO20	2.8638e+00	1.0265e+01	1.0306e+01	1.8284e+01	3.9383e+00	2.4874e+01	4.9547e+01	4.6266e+01	1.3724e+02	2.0078e+01
Algorithm	F_{15}					F_{16}				
	Minimum	Average	Median	Maximum	Standard Deviation	Mininum	Average	Median	Maximum	Standard Deviation
COA5	8.7556e+01	1.3508e+02	1.2885e+02	2.4556e+02	3.3924e+01	2.9554e+02	3.7467e+02	3.5321e+02	5.0046e+02	5.8016e+01
COA10	6.3677e+01	1.1109e+02	1.0597e+02	2.0695e+02	2.8424e+01	1.9010e+02	2.7909e+02	2.7772e+02	4.3035e+02	5.9414e+01
ABC	1.5118e+02	1.8912e+02	1.9190e+02	2.2279e+02	1.8938e+01	5.6094e+02	6.7108e+02	6.7884e+02	7.6678e+02	4.6293e+01
BA	4.1163e+02	6.2574e+02	6.3641e+02	8.2831e+02	1.1064e+02	1.1147e+03	1.4653e+03	1.5269e+03	1.7232e+03	1.8317e+02
FA	9.9047e+02	1.1406e+03	1.1490e+03	1.2447e+03	5.8829e+01	2.3226e+03	2.5935e+03	2.6014e+03	2.7466e+03	9.2534e+01
GWO	1.3067e+02	1.7670e+02	1.7857e+02	2.0970e+02	2.2411e+01	4.6519e+02	5.3439e+02	5.3112e+02	6.1819e+02	4.0538e+01
PSO	1.8136e+02	2.9787e+02	3.0083e+02	3.8498e+02	4.8767e+01	5.7276e+02	7.2423e+02	7.2644e+02	8.7373e+02	7.4528e+01
SOS	7.0642e+01	1.2265e+02	1.2089e+02	1.6058e+02	2.4694e+01	3.1739e+02	4.0086e+02	3.8975e+02	6.7557e+02	7.6094e+01
WfCMO5	6.8652e+01	1.0440e+02	1.0547e+02	1.5322e+02	2.1909e+01	2.4775e+02	3.3848e+02	3.3679e+02	4.1490e+02	3.8236e+01
WfCMO10	5.7708e+01	1.0414e+02	1.0248e+02	1.4825e+02	2.3804e+01	2.7859e+02	3.5803e+02	3.5918e+02	4.8056e+02	4.8472e+01
WfCMO20	8.1587e+01	1.2828e+02	1.2138e+02	3.4124e+02	4.8139e+01	2.3680e+02	4.1877e+02	4.1738e+02	5.5817e+02	7.3584e+01

Table B.4: Descriptive statistics for IEEE-CEC 2017 benchmark functions considering the error measurements - Part IV.

Algorithm	F_{17}					F_{18}				
	Minimum	Average	Median	Maximum	Standard Deviation	Mininum	Average	Median	Maximum	Standard Deviation
COA5	8.8669e-04	7.4437e-03	4.8681e-03	3.5579e-02	7.2597e-03	6.6023e-03	5.0247e-02	2.5034e-02	2.5159e-01	5.7503e-02
COA10	1.5624e-05	3.1603e-05	2.8732e-05	1.0092e-04	1.4504e-05	7.2054e-06	2.5153e-05	1.5128e-05	2.4440e-04	4.2246e-05
ABC	3.9228e-05	1.1870e-04	1.1848e-04	2.1630e-04	5.2397e-05	1.0518e-04	2.2806e-04	2.1301e-04	3.7844e-04	6.4410e-05
BA	2.6923e+01	4.9704e+01	4.9945e+01	8.2974e+01	1.2215e+01	6.1754e+01	7.3590e+01	7.2433e+01	8.9015e+01	6.6818e+00
FA	4.8934e+01	8.6444e+01	8.6544e+01	1.0982e+02	1.4765e+01	1.0142e+02	1.3180e+02	1.3277e+02	1.5076e+02	1.2078e+01
GWO	1.9925e-02	2.6931e-01	7.0631e-02	1.8467e+00	4.3343e-01	1.0509e+00	3.9160e+00	3.1642e+00	9.6714e+00	2.2826e+00
PSO	3.4510e-01	3.4554e+00	2.4947e+00	1.3710e+01	3.1390e+00	1.2657e+01	2.5878e+01	2.4830e+01	4.3145e+01	8.0612e+00
SOS	4.6219e-06	1.4032e-05	1.2533e-05	4.4314e-05	8.3366e-06	3.3422e-03	3.2177e-02	1.4536e-02	1.7422e-01	3.9913e-02
WfCMO5	0.0000e+00	0.0000e+00	0.0000e+00	0.0000e+00	0.0000e+00	5.1001e-04	1.4434e-01	1.2581e-01	5.5154e-01	1.3445e-01
WfCMO10	0.0000e+00	7.5791e-15	0.0000e+00	1.1369e-13	2.8843e-14	2.1887e-04	9.7990e-02	1.6272e-02	1.8747e+00	3.4092e-01
WfCMO20	0.0000e+00	7.9581e-14	1.1369e-13	3.4106e-13	9.0310e-14	7.8115e-04	1.0506e-01	5.0371e-02	4.2503e-01	1.2661e-01
Algorithm	F_{19}					F_{20}				
	Minimum	Average	Median	Maximum	Standard Deviation	Mininum	Average	Median	Maximum	Standard Deviation
COA5	1.7712e-02	1.1184e-01	9.3932e-02	2.9327e-01	6.7404e-02	1.4789e-01	3.0431e-01	2.8731e-01	5.5435e-01	1.0508e-01
COA10	9.4856e-06	3.3126e-04	1.0840e-04	1.8821e-03	4.3084e-04	2.0709e-02	1.0474e-01	9.7122e-02	3.4863e-01	7.0948e-02
ABC	1.6014e-04	2.7580e-04	2.5361e-04	4.8137e-04	7.5785e-05	1.8164e-04	3.4917e-04	3.5421e-04	5.4879e-04	7.9654e-05
BA	5.7338e+01	8.2947e+01	8.4820e+01	1.0108e+02	9.5999e+00	7.8178e+01	8.9974e+01	9.1225e+01	1.0126e+02	6.8490e+00
FA	1.1043e+02	1.4763e+02	1.4924e+02	1.7188e+02	1.2373e+01	1.3260e+02	1.5999e+02	1.6021e+02	1.7556e+02	7.9510e+00
GWO	3.3314e+00	1.1088e+01	1.0720e+01	1.9189e+01	4.0421e+00	1.8917e+01	2.5977e+01	2.5722e+01	3.3283e+01	3.5874e+00
PSO	3.4411e+01	4.3472e+01	4.1060e+01	6.1896e+01	7.2334e+00	4.6130e+01	5.9096e+01	5.9608e+01	6.9590e+01	5.3259e+00
SOS	1.1704e-01	2.8348e-01	2.7899e-01	5.2825e-01	1.0932e-01	1.3416e+00	2.2734e+00	2.2303e+00	3.3983e+00	5.0994e-01
WfCMO5	8.8954e-01	2.2049e+00	2.1977e+00	3.6382e+00	9.1357e-01	7.3410e+00	1.2194e+01	1.2323e+01	1.6841e+01	2.0986e+00
WfCMO10	2.9316e-01	1.6473e+00	1.5627e+00	3.9664e+00	9.1136e-01	7.4501e+00	1.1060e+01	1.1586e+01	1.4119e+01	1.8649e+00
WfCMO20	3.2866e-01	1.7494e+00	1.7118e+00	4.7097e+00	9.7582e-01	8.4787e+00	1.2932e+01	1.2999e+01	1.7156e+01	2.2287e+00

Table B.5: Descriptive statistics for IEEE-CEC 2017 benchmark functions considering the error measurements - Part V.

Algorithm	F_{21}					F_{22}				
	Minimum	Average	Median	Maximum	Standard Deviation	Mininum	Average	Median	Maximum	Standard Deviation
COA5	9.4162e+00	1.7760e+01	1.8248e+01	2.5002e+01	3.4488e+00	5.9184e+01	9.6582e+01	9.5150e+01	1.1824e+02	1.4957e+01
COA10	9.8338e+00	1.7151e+01	1.6841e+01	2.9364e+01	3.3261e+00	5.0727e+01	8.0222e+01	8.1162e+01	1.0828e+02	1.3290e+01
ABC	7.3363e+00	1.6736e+01	1.7324e+01	2.2916e+01	3.7159e+00	7.1157e+01	1.0021e+02	1.0069e+02	1.1888e+02	1.2125e+01
BA	9.0891e+01	2.3818e+02	2.2917e+02	3.7134e+02	7.2600e+01	1.0821e+03	1.7865e+03	1.7529e+03	2.2852e+03	3.2659e+02
FA	2.4040e+02	4.0999e+02	3.9998e+02	6.0030e+02	7.9916e+01	1.8286e+03	2.5269e+03	2.5354e+03	3.0607e+03	2.3122e+02
GWO	1.4247e+01	2.7517e+01	2.5353e+01	4.8643e+01	8.8278e+00	8.9894e+01	1.3291e+02	1.2301e+02	2.1687e+02	3.0374e+01
PSO	1.2568e+01	3.1660e+01	2.9229e+01	6.5802e+01	1.1157e+01	1.4845e+02	2.3090e+02	2.3085e+02	3.2730e+02	4.3236e+01
SOS	2.1380e+01	3.3492e+01	3.3439e+01	4.4800e+01	5.2058e+00	1.0450e+02	1.7924e+02	1.7563e+02	2.5814e+02	3.5974e+01
WfCMO5	1.1504e+01	1.3409e+01	1.3412e+01	1.7246e+01	1.3383e+00	5.1745e+01	7.7566e+01	7.6313e+01	1.0732e+02	1.3742e+01
WfCMO10	1.2619e+01	1.6718e+01	1.6396e+01	2.2489e+01	2.9443e+00	5.1524e+01	8.2395e+01	8.0500e+01	1.7466e+02	2.3588e+01
WfCMO20	1.5366e+01	2.3218e+01	2.3230e+01	3.0037e+01	3.5416e+00	6.4202e+01	1.0844e+02	9.6188e+01	1.8255e+02	4.1002e+01
Algorithm	F_{23}					F_{24}				
	Minimum	Average	Median	Maximum	Standard Deviation	Mininum	Average	Median	Maximum	Standard Deviation
COA5	1.5851e+02	1.9071e+02	1.8970e+02	2.4899e+02	2.3623e+01	3.7977e+02	5.3672e+02	5.2361e+02	7.3192e+02	8.7419e+01
COA10	1.0606e+02	1.5367e+02	1.4953e+02	2.1681e+02	2.4163e+01	3.0801e+02	4.1711e+02	4.0037e+02	6.2741e+02	7.2635e+01
ABC	1.7743e+02	2.0974e+02	2.1093e+02	2.4233e+02	1.5390e+01	5.8760e+02	6.5903e+02	6.5936e+02	7.2669e+02	3.1186e+01
BA	1.9250e+03	3.5415e+03	3.5967e+03	4.9715e+03	7.9972e+02	6.6211e+03	8.2529e+03	7.9891e+03	1.0412e+04	1.1580e+03
FA	4.0638e+03	5.1661e+03	5.2556e+03	5.7024e+03	3.9742e+02	1.0624e+04	1.2220e+04	1.2273e+04	1.3332e+04	6.8002e+02
GWO	2.2917e+02	3.1104e+02	2.9290e+02	5.6402e+02	6.9647e+01	7.8000e+02	1.0168e+03	1.0128e+03	1.3231e+03	1.1408e+02
PSO	3.2869e+02	5.4141e+02	5.3032e+02	7.8652e+02	1.1083e+02	1.4321e+03	1.6891e+03	1.6447e+03	2.1030e+03	1.8553e+02
SOS	1.6201e+02	3.4724e+02	3.7421e+02	4.6746e+02	8.9366e+01	4.2433e+02	6.3404e+02	6.0066e+02	1.0929e+03	1.3326e+02
WfCMO5	1.6063e+02	2.1768e+02	2.2569e+02	2.9274e+02	3.6178e+01	6.1559e+02	8.6207e+02	8.3555e+02	1.2415e+03	1.3258e+02
WfCMO10	1.4633e+02	2.0512e+02	1.9846e+02	3.4762e+02	4.4601e+01	6.5732e+02	8.5480e+02	8.4834e+02	1.1301e+03	1.1801e+02
WfCMO20	1.6077e+02	2.1918e+02	2.1593e+02	2.8081e+02	3.3357e+01	5.5548e+02	8.4060e+02	7.9905e+02	1.1961e+03	1.6958e+02

Table B.6: Descriptive statistics for IEEE-CEC 2017 benchmark functions considering the error measurements - Part VI.

Algorithm	F_{25}					F_{26}				
	Minimum	Average	Median	Maximum	Standard Deviation	Mininum	Average	Median	Maximum	Standard Deviation
COA5	9.9541e-01	6.9531e+00	6.7207e+00	1.5919e+01	3.6004e+00	2.3924e+01	7.0607e+01	7.1637e+01	1.2217e+02	2.0400e+01
COA10	1.9899e+00	7.2964e+00	6.4674e+00	1.9899e+01	3.9827e+00	2.3879e+01	5.8212e+01	5.6610e+01	8.7556e+01	1.7503e+01
ABC	5.3028e+00	8.9556e+00	8.5624e+00	1.3097e+01	2.1241e+00	6.7726e+01	9.5785e+01	9.7579e+01	1.2227e+02	1.4379e+01
BA	2.6136e+01	5.7114e+01	5.6903e+01	1.0367e+02	1.8990e+01	1.5451e+02	2.8108e+02	2.9294e+02	3.9088e+02	6.3455e+01
FA	8.6023e+01	1.2628e+02	1.3018e+02	1.5469e+02	1.5829e+01	4.9257e+02	5.7468e+02	5.6806e+02	6.4492e+02	3.8350e+01
GWO	3.9820e+00	1.0541e+01	1.0286e+01	1.9273e+01	3.9704e+00	3.7508e+01	8.7524e+01	8.6758e+01	1.8293e+02	2.8419e+01
PSO	6.9647e+00	2.1153e+01	2.1392e+01	3.8825e+01	8.8262e+00	5.6755e+01	1.2791e+02	1.2759e+02	1.9350e+02	2.9143e+01
SOS	6.2648e+00	1.3418e+01	1.3727e+01	2.2265e+01	3.9093e+00	3.2109e+01	6.0362e+01	5.5976e+01	1.2193e+02	2.0996e+01
WfCMO5	1.6755e-06	3.5588e+00	3.9798e+00	6.9652e+00	1.6830e+00	2.7859e+01	4.0826e+01	4.0296e+01	6.1687e+01	9.4516e+00
WfCMO10	1.9899e+00	5.5694e+00	5.2518e+00	1.1944e+01	2.3888e+00	2.0894e+01	3.5122e+01	3.2834e+01	4.8753e+01	8.8150e+00
WfCMO20	3.9808e+00	1.0069e+01	1.0167e+01	1.6259e+01	3.8038e+00	2.5869e+01	4.5307e+01	4.1788e+01	1.3673e+02	2.0227e+01
Algorithm	F_{27}					F_{28}				
	Minimum	Average	Median	Maximum	Standard Deviation	Mininum	Average	Median	Maximum	Standard Deviation
COA5	9.0781e+01	1.3842e+02	1.3631e+02	1.8307e+02	2.1897e+01	2.7958e+02	3.7818e+02	3.6764e+02	5.0451e+02	5.7470e+01
COA10	6.6662e+01	1.0616e+02	9.9713e+01	1.9603e+02	3.1573e+01	1.8904e+02	2.6356e+02	2.5670e+02	4.0844e+02	4.9650e+01
ABC	1.4887e+02	2.1089e+02	2.1250e+02	2.5271e+02	2.0206e+01	5.8164e+02	6.9000e+02	6.9002e+02	7.9464e+02	4.9309e+01
BA	4.4584e+02	6.2962e+02	6.2762e+02	8.1229e+02	1.1269e+02	1.1673e+03	1.5773e+03	1.5835e+03	2.0024e+03	2.1117e+02
FA	1.0008e+03	1.1578e+03	1.1635e+03	1.2621e+03	6.6671e+01	2.4069e+03	2.6855e+03	2.7058e+03	2.9084e+03	1.2303e+02
GWO	1.2508e+02	1.9213e+02	1.8993e+02	2.6880e+02	2.6893e+01	4.4145e+02	5.5170e+02	5.4659e+02	6.9784e+02	7.0142e+01
PSO	2.2356e+02	2.8357e+02	2.7822e+02	3.6759e+02	3.4297e+01	6.7032e+02	8.0100e+02	8.0381e+02	9.3480e+02	7.1888e+01
SOS	8.6561e+01	1.3345e+02	1.2089e+02	3.1772e+02	4.7514e+01	2.9550e+02	3.9336e+02	3.8903e+02	5.2335e+02	5.6757e+01
WfCMO5	6.3677e+01	9.7663e+01	9.1039e+01	1.7810e+02	2.2988e+01	2.3780e+02	3.1233e+02	3.0396e+02	3.9997e+02	4.1110e+01
WfCMO10	5.5718e+01	9.9063e+01	9.7008e+01	1.3432e+02	1.9942e+01	2.8953e+02	3.4690e+02	3.4127e+02	4.2385e+02	3.6469e+01
WfCMO20	7.6612e+01	1.2816e+02	1.1989e+02	3.6386e+02	4.8211e+01	3.3431e+02	4.2939e+02	4.1727e+02	5.8603e+02	5.9055e+01

Table B.7: Descriptive statistics for IEEE-CEC 2017 benchmark functions considering the error measurements - Part VII.

Algorithm	F_{29}					F_{30}				
	Minimum	Average	Median	Maximum	Standard Deviation	Mininum	Average	Median	Maximum	Standard Deviation
COA5	3.5728e-05	4.3213e-02	6.2876e-03	5.5634e-01	1.2698e-01	1.6930e+01	7.9394e+01	6.0930e+01	3.5457e+02	6.2938e+01
COA10	2.3747e-09	8.1617e-09	5.6518e-09	5.0257e-08	9.2281e-09	2.8222e-09	3.8413e-01	3.1669e-01	2.8155e+00	5.5766e-01
ABC	7.1863e-04	1.7287e-01	8.6708e-02	7.9656e-01	2.2454e-01	2.2754e+02	7.1913e+02	6.5406e+02	1.9351e+03	4.1595e+02
BA	6.2616e+02	1.2803e+03	1.2014e+03	2.3645e+03	4.8177e+02	6.4875e+03	1.1658e+04	1.1472e+04	1.6192e+04	2.3552e+03
FA	1.9418e+03	3.5818e+03	3.5873e+03	4.8740e+03	7.3277e+02	1.8233e+04	3.3139e+04	3.4957e+04	4.2730e+04	6.2527e+03
GWO	1.8981e-03	4.5683e+00	5.9453e-01	5.8281e+01	1.1065e+01	8.0680e+01	4.1425e+02	3.1033e+02	1.0511e+03	2.8148e+02
PSO	8.9528e-02	6.7211e+00	3.9640e+00	2.5698e+01	7.3418e+00	2.3391e+02	1.4459e+03	1.3684e+03	4.3404e+03	8.0747e+02
SOS	0.0000e+00	0.0000e+00	0.0000e+00	0.0000e+00	0.0000e+00	7.2291e-01	9.0352e+00	6.0461e+00	7.0743e+01	1.2585e+01
WfCMO5	6.8212e-13	1.8151e-02	5.9857e-08	4.5438e-01	8.3993e-02	2.9945e+00	2.2888e+01	1.6891e+01	1.2140e+02	2.3652e+01
WfCMO10	0.0000e+00	1.8128e-02	2.2737e-13	4.5432e-01	8.3988e-02	2.7192e+00	1.9081e+01	1.2996e+01	7.3834e+01	1.5442e+01
WfCMO20	0.0000e+00	1.6674e-13	1.1369e-13	9.0949e-13	1.8581e-13	1.9897e+00	2.4971e+01	1.7878e+01	1.7962e+02	3.2397e+01
Algorithm	F_{31}					F_{32}				
	Minimum	Average	Median	Maximum	Standard Deviation	Mininum	Average	Median	Maximum	Standard Deviation
COA5	3.0723e+02	7.0796e+02	6.3875e+02	1.3150e+03	2.8400e+02	3.4481e+03	7.4929e+03	7.0855e+03	1.1776e+04	2.0467e+03
COA10	2.8155e+00	1.9254e+01	1.4131e+01	7.4988e+01	1.7318e+01	1.0494e+02	4.4603e+02	3.6203e+02	1.5413e+03	3.1966e+02
ABC	1.8494e+03	5.3219e+03	5.5885e+03	9.9514e+03	1.8051e+03	2.5332e+04	3.3001e+04	3.3666e+04	4.0906e+04	3.8285e+03
BA	2.3733e+04	3.9700e+04	3.9106e+04	5.7762e+04	9.2523e+03	7.3326e+04	1.0059e+05	9.7694e+04	1.3055e+05	1.8057e+04
FA	6.8894e+04	9.7715e+04	9.7154e+04	1.1854e+05	1.2742e+04	1.7242e+05	2.1564e+05	2.1432e+05	2.5383e+05	1.7800e+04
GWO	1.5204e+03	4.2454e+03	3.0891e+03	1.2906e+04	2.6257e+03	8.8748e+03	2.2623e+04	1.8856e+04	4.3417e+04	1.0089e+04
PSO	3.4564e+03	7.6194e+03	7.1358e+03	1.4824e+04	2.9485e+03	1.4517e+04	2.1911e+04	2.2679e+04	2.5899e+04	3.2236e+03
SOS	5.7732e+01	3.6222e+02	2.9305e+02	1.4950e+03	3.0780e+02	4.3646e+03	1.3539e+04	1.4297e+04	2.3849e+04	4.2812e+03
WfCMO5	7.0976e+01	3.3569e+02	3.2507e+02	7.7253e+02	1.6023e+02	2.1974e+03	4.1929e+03	3.7859e+03	8.1683e+03	1.5991e+03
WfCMO10	4.0640e+01	2.7613e+02	2.2625e+02	1.3537e+03	2.3783e+02	1.7938e+03	4.4985e+03	3.3828e+03	1.3081e+04	2.6915e+03
WfCMO20	2.6913e+01	3.1699e+02	2.8275e+02	1.0244e+03	2.1362e+02	1.7585e+03	6.2833e+03	5.3891e+03	1.7777e+04	3.7284e+03

Table B.8: Descriptive statistics for IEEE-CEC 2017 benchmark functions considering the error measurements - Part VIII.

Algorithm	F_{33}					F_{34}				
	Minimum	Average	Median	Maximum	Standard Deviation	Mininum	Average	Median	Maximum	Standard Deviation
COA5	3.7184e+01	2.2926e+02	2.4483e+02	4.7986e+02	1.0040e+02	1.5562e+03	2.3544e+03	2.3523e+03	3.2798e+03	4.0409e+02
COA10	3.4656e+01	3.0317e+02	3.2786e+02	6.2517e+02	1.4440e+02	1.8495e+03	2.6722e+03	2.6255e+03	3.5545e+03	4.8252e+02
ABC	3.7956e+01	2.6325e+02	2.6164e+02	4.4688e+02	1.0223e+02	1.6700e+03	2.2700e+03	2.2952e+03	2.7868e+03	2.7704e+02
BA	5.0013e+02	1.1671e+03	1.1914e+03	1.7762e+03	3.0982e+02	3.6385e+03	4.6148e+03	4.5522e+03	6.2807e+03	6.0252e+02
FA	2.0023e+03	2.2731e+03	2.3120e+03	2.5441e+03	1.6846e+02	8.2511e+03	9.0114e+03	9.0236e+03	9.4921e+03	2.6626e+02
GWO	1.3539e+02	5.3136e+02	4.5859e+02	1.3220e+03	2.6975e+02	1.8492e+03	3.1185e+03	2.9101e+03	6.5183e+03	1.0086e+03
PSO	4.2193e+02	8.8273e+02	9.0227e+02	1.4144e+03	2.4324e+02	3.0161e+03	5.1864e+03	5.0697e+03	7.1501e+03	1.1288e+03
SOS	1.2745e+02	4.8944e+02	5.2147e+02	8.4209e+02	1.9524e+02	1.5514e+03	3.0254e+03	2.9778e+03	4.4677e+03	7.8491e+02
WfCMO5	4.2630e+00	2.2548e+02	2.3461e+02	4.9098e+02	1.1834e+02	2.8508e+03	4.1695e+03	4.2755e+03	5.4009e+03	6.6762e+02
WfCMO10	1.3875e+02	4.1263e+02	4.1757e+02	7.5614e+02	1.6406e+02	3.3424e+03	6.1839e+03	6.3187e+03	7.0226e+03	6.8556e+02
WfCMO20	3.9020e+02	8.6710e+02	9.1197e+02	1.3256e+03	2.2092e+02	5.6651e+03	6.4494e+03	6.5103e+03	7.0389e+03	3.4913e+02
Algorithm	F_{35}					F_{36}				
	Minimum	Average	Median	Maximum	Standard Deviation	Mininum	Average	Median	Maximum	Standard Deviation
COA5	3.3931e+03	4.6557e+03	4.7516e+03	5.6456e+03	5.7956e+02	1.0014e+04	1.2610e+04	1.2620e+04	1.5249e+04	1.0698e+03
COA10	3.6252e+03	4.8265e+03	4.6503e+03	6.7764e+03	7.5413e+02	1.0669e+04	1.6808e+04	1.4073e+04	2.9114e+04	6.8778e+03
ABC	3.2293e+03	4.2147e+03	4.3579e+03	4.8378e+03	3.6407e+02	9.6746e+03	1.1113e+04	1.1129e+04	1.2214e+04	5.2131e+02
BA	5.2950e+03	7.8138e+03	7.7515e+03	9.6828e+03	1.0603e+03	1.3753e+04	1.5979e+04	1.5937e+04	1.8473e+04	1.0926e+03
FA	1.5057e+04	1.5934e+04	1.5985e+04	1.6895e+04	5.0092e+02	3.2294e+04	3.4020e+04	3.4121e+04	3.5229e+04	6.3744e+02
GWO	3.8535e+03	5.4832e+03	5.2091e+03	1.2663e+04	1.5375e+03	9.4847e+03	1.3134e+04	1.3091e+04	1.7104e+04	1.6861e+03
PSO	6.2159e+03	8.8106e+03	8.7139e+03	1.3358e+04	1.6348e+03	1.3481e+04	1.7864e+04	1.7315e+04	2.2778e+04	2.1780e+03
SOS	2.8306e+03	5.0303e+03	4.7562e+03	8.0027e+03	1.3783e+03	9.7172e+03	1.2036e+04	1.2118e+04	1.4314e+04	1.2287e+03
WfCMO5	5.2527e+03	7.7924e+03	7.5034e+03	1.0658e+04	1.7878e+03	1.1146e+04	2.1543e+04	2.4707e+04	2.7997e+04	6.1819e+03
WfCMO10	9.4802e+03	1.1969e+04	1.2108e+04	1.3050e+04	7.1390e+02	1.2038e+04	2.2625e+04	2.5089e+04	2.8297e+04	5.7567e+03
WfCMO20	4.9748e+03	1.1833e+04	1.2077e+04	1.2633e+04	1.3609e+03	1.1105e+04	2.2484e+04	2.6569e+04	2.8674e+04	6.3696e+03

Table B.9: Descriptive statistics for IEEE-CEC 2017 benchmark functions considering the error measurements - Part IX.

Algorithm	F_{37} Minimum	Average	Median	Maximum	Standard Deviation	F_{38} Mininum	Average	Median	Maximum	Standard Deviation
COA5	2.7392e-01	2.1577e+00	1.9924e+00	5.5541e+00	1.2446e+00	9.0272e+00	4.0848e+01	2.9214e+01	1.0065e+02	2.8819e+01
COA10	4.1387e-03	1.4359e+00	1.0861e+00	3.0009e+00	8.3636e-01	8.5461e+00	5.6026e+01	7.2007e+01	1.1526e+02	3.2764e+01
ABC	8.5209e-01	5.5461e+00	5.3355e+00	1.0119e+01	2.3548e+00	1.4908e+02	4.4482e+02	3.0911e+02	1.8174e+03	3.9076e+02
BA	1.8145e+01	1.0644e+02	8.8663e+01	3.3908e+02	7.9213e+01	1.2449e+02	2.2531e+02	2.1519e+02	3.4992e+02	5.3942e+01
FA	9.3712e+02	1.0522e+04	7.7742e+03	2.9098e+04	7.7525e+03	1.1836e+04	3.8212e+04	3.6248e+04	7.7387e+04	1.5030e+04
GWO	5.7274e+00	2.3218e+01	1.5708e+01	1.4832e+02	2.6352e+01	1.5927e+02	2.6091e+02	2.6021e+02	5.6752e+02	8.1962e+01
PSO	9.1107e+00	7.9069e+01	6.0518e+01	3.2951e+02	6.8621e+01	1.2018e+02	2.8475e+02	2.3912e+02	8.9200e+02	1.5108e+02
SOS	4.9728e-01	3.4806e+00	3.7207e+00	6.2462e+00	1.3921e+00	2.7104e+01	6.4258e+01	6.2081e+01	1.2067e+02	2.8721e+01
WfCMO5	1.1972e+00	4.4123e+00	4.1589e+00	1.0115e+01	2.1211e+00	4.9645e+01	1.0734e+02	1.1018e+02	1.5698e+02	3.0089e+01
WfCMO10	3.9449e-01	3.3679e+00	3.3871e+00	6.0874e+00	1.5954e+00	3.6922e+01	9.7375e+01	9.5053e+01	1.9732e+02	4.0366e+01
WfCMO20	1.0887e+00	3.2573e+00	3.1503e+00	8.6810e+00	1.7996e+00	5.2361e+01	1.2233e+02	1.1116e+02	2.9825e+02	5.5842e+01
Algorithm	F_{39} Minimum	Average	Median	Maximum	Standard Deviation	F_{40} Mininum	Average	Median	Maximum	Standard Deviation
COA5	6.1415e+01	9.4715e+01	8.8451e+01	1.4336e+02	2.2046e+01	3.4423e+02	5.2946e+02	5.3845e+02	6.6976e+02	8.0030e+01
COA10	3.9510e+01	8.4070e+01	7.1465e+01	1.8240e+02	3.6538e+01	9.4642e+02	1.3796e+03	1.3341e+03	2.6032e+03	3.7209e+02
ABC	1.8391e+02	1.2357e+03	1.2111e+03	3.8748e+03	8.5543e+02	2.3269e+04	6.5921e+04	6.6237e+04	9.7682e+04	1.8525e+04
BA	2.0751e+02	3.4353e+02	3.3367e+02	4.9175e+02	7.7580e+01	1.0380e+03	1.8923e+03	1.7883e+03	3.5328e+03	4.7927e+02
FA	3.1090e+04	9.5593e+04	9.2415e+04	2.4943e+05	4.2834e+04	3.0830e+05	8.0090e+06	1.9199e+06	5.7849e+07	1.4889e+07
GWO	6.2185e+02	1.9141e+03	1.4994e+03	4.7592e+03	1.1392e+03	1.9618e+04	3.5605e+04	3.4316e+04	5.5195e+04	9.4618e+03
PSO	2.6347e+02	4.3135e+02	3.9617e+02	7.9062e+02	1.1889e+02	1.9206e+03	4.0396e+03	2.6449e+03	2.4528e+04	4.3069e+03
SOS	7.3925e+01	1.5002e+02	1.4165e+02	2.3914e+02	4.5066e+01	4.7750e+02	7.4518e+02	6.9738e+02	1.0999e+03	1.7427e+02
WfCMO5	1.3934e+02	2.2670e+02	2.1993e+02	3.5657e+02	6.0026e+01	8.1615e+02	1.3270e+03	1.3364e+03	1.8296e+03	2.5073e+02
WfCMO10	1.2095e+02	2.1390e+02	2.1590e+02	3.5314e+02	6.3445e+01	6.7621e+02	1.2822e+03	1.2560e+03	2.0462e+03	2.8606e+02
WfCMO20	1.0681e+02	2.2678e+02	2.3016e+02	3.5833e+02	5.3954e+01	8.7837e+02	1.3227e+03	1.2804e+03	2.1410e+03	2.8243e+02

Table B.10: Descriptive statistics for IEEE-CEC 2017 benchmark functions considering the error measurements - Part X.

Algorithm	F_{41}					F_{42}				
	Minimum	Average	Median	Maximum	Standard Deviation	Mininum	Average	Median	Maximum	Standard Deviation
COA5	3.1093e+01	6.7971e+02	6.8114e+02	1.4895e+03	3.0029e+02	3.5699e+03	7.8283e+04	5.3175e+04	2.9093e+05	5.8748e+04
COA10	3.5043e+02	6.1316e+02	6.3900e+02	9.2704e+02	1.4833e+02	9.6713e+03	1.6857e+05	1.1623e+05	7.2518e+05	1.7153e+05
ABC	2.3471e+03	2.0957e+04	2.0526e+04	5.2489e+04	1.1317e+04	5.4197e+04	3.5896e+05	2.7077e+05	9.6734e+05	2.5234e+05
BA	2.3502e+04	1.0849e+06	8.3037e+05	4.1321e+06	1.0545e+06	7.7362e+05	5.5024e+06	4.6077e+06	1.8244e+07	3.6602e+06
FA	3.8602e+08	1.2556e+09	1.1786e+09	2.8731e+09	6.5211e+08	1.1530e+10	2.1844e+10	2.1677e+10	3.1754e+10	4.9610e+09
GWO	1.0228e+04	6.0965e+05	1.9101e+05	2.8377e+06	8.0108e+05	1.6618e+06	4.0183e+07	1.7147e+07	2.6908e+08	6.0593e+07
PSO	8.9813e+02	1.7614e+06	7.9447e+03	9.0899e+06	3.3281e+06	1.3854e+05	7.9359e+07	1.4253e+07	5.8671e+08	1.5121e+08
SOS	1.1157e+03	1.2664e+04	8.1318e+03	5.0847e+04	1.2104e+04	9.1829e+03	8.2312e+04	5.1249e+04	2.4344e+05	6.6415e+04
WfCMO5	8.1975e-01	2.8826e+02	2.8132e+02	6.9084e+02	1.5379e+02	2.3843e+04	1.1710e+06	1.0186e+06	3.8896e+06	8.8233e+05
WfCMO10	2.4564e+00	3.1544e+02	3.2944e+02	6.3609e+02	1.6296e+02	7.9079e+03	4.2724e+04	2.7562e+04	2.4233e+05	4.7328e+04
WfCMO20	2.0815e-01	3.1548e+02	3.3583e+02	6.8374e+02	1.9384e+02	5.3565e+03	3.8614e+04	2.7312e+04	1.0906e+05	2.6043e+04
Algorithm	F_{43}					F_{44}				
	Minimum	Average	Median	Maximum	Standard Deviation	Mininum	Average	Median	Maximum	Standard Deviation
COA5	2.5898e+05	9.6957e+05	7.4909e+05	2.4862e+06	5.7430e+05	1.4524e+06	3.2416e+06	3.0059e+06	5.8567e+06	1.2062e+06
COA10	9.5983e+04	7.6968e+05	5.9969e+05	2.9214e+06	6.7973e+05	6.0014e+05	1.9664e+06	1.7679e+06	4.0177e+06	8.7188e+05
ABC	4.5967e+05	2.9029e+06	2.7048e+06	7.8716e+06	1.5720e+06	6.8994e+06	1.3820e+07	1.4178e+07	2.2417e+07	4.3260e+06
BA	8.2704e+06	2.5659e+07	2.3232e+07	5.9023e+07	1.2571e+07	1.9715e+07	4.9628e+07	4.7693e+07	7.5766e+07	1.2690e+07
FA	9.4344e+10	1.2589e+11	1.2288e+11	1.5810e+11	1.6439e+10	2.8940e+11	3.3774e+11	3.3474e+11	3.9904e+11	2.7371e+10
GWO	1.4936e+07	2.7319e+08	1.1912e+08	2.9500e+09	5.2741e+08	1.3105e+09	4.9880e+09	4.4176e+09	1.2089e+10	2.7008e+09
PSO	7.9011e+06	1.9403e+09	1.4768e+09	1.2742e+10	2.4887e+09	1.1927e+08	4.6608e+09	3.8602e+09	1.4384e+10	4.3011e+09
SOS	1.6709e+05	1.1361e+06	8.9401e+05	3.7555e+06	9.4129e+05	1.5747e+06	7.8309e+06	6.7079e+06	1.7228e+07	4.2323e+06
WfCMO5	9.1183e+05	3.5549e+06	3.1322e+06	9.2245e+06	1.9494e+06	4.0445e+06	2.1314e+07	2.0047e+07	5.0081e+07	1.0316e+07
WfCMO10	4.8194e+05	2.2054e+06	2.0223e+06	4.1604e+06	1.0743e+06	4.3898e+06	1.3787e+07	1.4093e+07	2.1987e+07	5.1455e+06
WfCMO20	2.0668e+05	1.2274e+06	1.0478e+06	4.1963e+06	9.1150e+05	2.4354e+06	1.2574e+07	1.2247e+07	2.3236e+07	5.6660e+06

Table B.11: Descriptive statistics for IEEE-CEC 2017 benchmark functions considering the error measurements - Part XI.

Algorithm	F_{45} Minimum	Average	Median	Maximum	Standard Deviation	F_{46} Mininum	Average	Median	Maximum	Standard Deviation
COA5	4.7955e-01	6.2473e+00	6.9802e+00	1.0263e+01	2.6804e+00	1.2459e+02	8.6059e+02	4.7811e+02	7.5965e+03	1.3796e+03
COA10	6.4129e+00	9.3888e+00	9.1817e+00	1.3645e+01	1.8466e+00	3.6993e+02	1.9376e+04	6.4875e+03	6.1011e+04	2.5336e+04
ABC	2.7117e+01	4.3206e+02	3.6943e+02	1.4455e+03	3.4439e+02	2.4048e+02	8.8557e+03	6.9745e+03	4.2154e+04	8.3470e+03
BA	7.3074e+02	1.4418e+04	1.0620e+04	6.8264e+04	1.4501e+04	2.2202e+05	3.8035e+05	3.8580e+05	6.4793e+05	9.7203e+04
FA	4.6866e+06	1.2038e+08	8.7685e+07	7.2639e+08	1.4964e+08	9.4226e+09	2.2843e+10	2.1800e+10	3.7684e+10	6.1604e+09
GWO	2.0563e+03	1.1913e+04	1.1125e+04	2.9709e+04	7.1964e+03	1.8575e+04	9.4773e+06	7.0907e+04	2.6947e+08	4.9158e+07
PSO	2.4205e+01	4.7957e+03	1.0368e+03	3.7298e+04	1.0053e+04	1.8935e+03	2.8920e+08	1.8397e+05	2.9124e+09	7.5456e+08
SOS	1.1584e+01	1.2623e+03	6.9007e+02	6.9095e+03	1.8072e+03	1.2788e+02	1.9046e+04	8.6552e+03	6.0636e+04	2.1332e+04
WfCMO5	1.4887e+00	8.4651e+00	8.6830e+00	1.7782e+01	4.6692e+00	1.6295e+03	1.1254e+04	9.5856e+03	2.4388e+04	7.0461e+03
WfCMO10	1.9356e+00	1.1765e+01	1.2201e+01	2.2224e+01	5.7113e+00	1.0907e+02	1.1071e+04	1.1074e+04	2.5143e+04	7.1206e+03
WfCMO20	3.1356e+00	1.5467e+01	1.3714e+01	4.4821e+01	1.0409e+01	2.1317e+02	1.3139e+04	9.5324e+03	4.2753e+04	1.1049e+04
Algorithm	F_{47} Minimum	Average	Median	Maximum	Standard Deviation	F_{48} Mininum	Average	Median	Maximum	Standard Deviation
COA5	2.2619e+02	4.0414e+03	2.3653e+03	2.2359e+04	4.8449e+03	3.0061e+02	3.9089e+03	3.1881e+03	1.3551e+04	3.2065e+03
COA10	8.6271e+02	1.7526e+04	1.8100e+04	3.7484e+04	1.2859e+04	2.4756e+02	5.3623e+03	3.4129e+03	2.8705e+04	6.4871e+03
ABC	3.0387e+02	7.4741e+03	4.2233e+03	3.0844e+04	8.6379e+03	7.3432e+02	3.0352e+03	1.9323e+03	1.3678e+04	2.8083e+03
BA	8.5243e+05	1.2191e+06	1.2008e+06	1.6471e+06	2.2848e+05	1.2951e+06	1.9570e+06	1.9611e+06	2.3296e+06	2.4038e+05
FA	2.5026e+10	7.0492e+10	7.1532e+10	1.0513e+11	1.7073e+10	6.2826e+10	8.6911e+10	8.9044e+10	1.0981e+11	1.0807e+10
GWO	7.3147e+04	1.0425e+08	3.4106e+07	3.2372e+08	1.1698e+08	1.1761e+06	3.6656e+08	2.1690e+08	1.7672e+09	3.9186e+08
PSO	8.1525e+03	4.6229e+08	4.8026e+06	3.6204e+09	9.0099e+08	4.0815e+04	4.2443e+08	8.5447e+06	2.3492e+09	6.3123e+08
SOS	1.7538e+02	5.4288e+03	2.8688e+03	3.6908e+04	7.4642e+03	3.8975e+02	5.6814e+03	4.4664e+03	2.1414e+04	5.0919e+03
WfCMO5	1.9196e+02	1.9149e+03	9.9433e+02	9.4775e+03	2.2130e+03	2.2444e+03	5.2806e+03	4.6425e+03	1.3660e+04	2.7014e+03
WfCMO10	1.8373e+02	2.2188e+03	1.9846e+03	8.3682e+03	1.8617e+03	7.3190e+02	5.2310e+03	3.7204e+03	1.3715e+04	3.9662e+03
WfCMO20	3.8752e+02	3.2667e+03	2.5426e+03	1.1631e+04	2.8625e+03	6.4128e+02	6.3964e+03	5.2322e+03	1.7830e+04	4.3088e+03

Table B.12: Descriptive statistics for IEEE-CEC 2017 benchmark functions considering the error measurements - Part XII.

Algorithm	F_{49}					F_{50}				
	Minimum	Average	Median	Maximum	Standard Deviation	Mininum	Average	Median	Maximum	Standard Deviation
COA5	4.5098e-04	2.5192e+00	1.9932e+00	6.3230e+00	1.5728e+00	3.2812e+01	5.6035e+01	5.6298e+01	7.7241e+01	1.0921e+01
COA10	2.3452e-06	2.3578e+00	1.9912e+00	4.9755e+00	1.5097e+00	4.1296e+01	7.3521e+01	7.5163e+01	1.0712e+02	2.2058e+01
ABC	2.4569e+01	2.1035e+02	1.1717e+02	9.4748e+02	2.4617e+02	1.1221e+04	5.0809e+04	4.3897e+04	1.6925e+05	3.6046e+04
BA	6.5963e+01	1.7840e+03	8.3096e+02	1.2060e+04	2.7598e+03	7.5021e+02	1.4457e+04	1.0554e+04	4.2802e+04	1.1021e+04
FA	2.3950e+03	1.6750e+06	5.4851e+05	1.5246e+07	3.6891e+06	7.0563e+06	4.3788e+07	4.1984e+07	1.3279e+08	3.2570e+07
GWO	5.0648e+01	8.1552e+02	7.3977e+01	3.8515e+03	1.5070e+03	6.1727e+03	2.6446e+05	5.3840e+04	1.8709e+06	5.5673e+05
PSO	2.4924e+01	7.9398e+01	6.9250e+01	2.1158e+02	4.7852e+01	1.6877e+02	9.2283e+04	9.5131e+03	1.6716e+06	3.0721e+05
SOS	1.1064e+00	9.1459e+00	7.2268e+00	3.0564e+01	7.7006e+00	6.6625e+01	2.4868e+03	1.3753e+03	1.1385e+04	2.8786e+03
WfCMO5	0.0000e+00	2.2499e+00	1.5057e+00	2.0019e+01	3.5711e+00	5.2693e+01	1.1644e+02	1.1111e+02	2.3338e+02	3.8874e+01
WfCMO10	5.2590e-01	6.6230e+00	4.7929e+00	2.2913e+01	6.0876e+00	6.9761e+01	1.3397e+02	1.2820e+02	2.5986e+02	4.5442e+01
WfCMO20	1.2968e+00	1.3180e+01	9.3980e+00	2.4225e+01	7.4470e+00	6.7652e+01	1.2796e+02	1.1988e+02	2.6070e+02	4.2777e+01
Algorithm	F_{51}					F_{52}				
	Minimum	Average	Median	Maximum	Standard Deviation	Mininum	Average	Median	Maximum	Standard Deviation
COA5	1.3672e+02	6.1935e+02	3.5223e+02	2.7987e+03	6.4678e+02	7.1621e+03	6.8368e+04	6.4279e+04	1.8630e+05	3.9875e+04
COA10	3.2021e+02	6.6739e+02	5.8163e+02	2.8447e+03	4.5814e+02	1.5459e+04	2.0805e+05	2.0386e+05	4.1504e+05	1.0556e+05
ABC	1.7344e+05	5.8750e+05	5.5616e+05	1.0901e+06	2.6740e+05	7.5987e+05	3.4996e+06	3.4211e+06	6.1123e+06	1.2897e+06
BA	1.2246e+04	8.3432e+04	5.3432e+04	3.2377e+05	8.1106e+04	1.1766e+05	4.6937e+05	4.4513e+05	1.0140e+06	2.3130e+05
FA	8.0304e+07	2.4392e+08	2.5620e+08	4.9743e+08	1.0401e+08	1.2015e+08	6.5810e+08	6.6470e+08	1.3024e+09	2.9337e+08
GWO	1.3660e+04	2.5940e+05	1.3819e+05	9.1653e+05	2.7448e+05	5.9389e+05	3.5228e+06	2.8392e+06	1.2828e+07	2.7157e+06
PSO	3.0301e+03	1.1349e+06	1.8903e+05	5.5963e+06	1.5918e+06	8.8482e+03	3.0868e+05	9.6962e+04	4.9001e+06	8.8263e+05
SOS	6.8435e+03	5.1327e+04	3.4329e+04	2.9192e+05	5.4770e+04	6.3346e+04	3.3937e+05	2.6455e+05	1.0067e+06	2.3288e+05
WfCMO5	1.7129e+02	4.6895e+02	3.7708e+02	3.1179e+03	5.1315e+02	3.1940e+03	2.3705e+04	1.8745e+04	6.0123e+04	1.5364e+04
WfCMO10	1.5863e+02	4.4879e+02	3.6718e+02	2.3792e+03	3.8426e+02	4.9164e+03	5.6074e+04	4.6993e+04	2.0490e+05	4.5780e+04
WfCMO20	2.2648e+02	4.1835e+02	3.7442e+02	6.5522e+02	1.0939e+02	3.7670e+03	6.2178e+04	5.5823e+04	1.5011e+05	3.6240e+04

Table B.13: Descriptive statistics for IEEE-CEC 2017 benchmark functions considering the error measurements - Part XIII.

Algorithm	F_{53} Minimum	Average	Median	Maximum	Standard Deviation	F_{54} Mininum	Average	Median	Maximum	Standard Deviation
COA5	1.3091e-01	1.1282e+00	1.1092e+00	4.6274e+00	8.8478e-01	2.1241e+01	5.9958e+01	5.5673e+01	1.2904e+02	2.6820e+01
COA10	1.1817e-01	7.1486e-01	5.1791e-01	1.7562e+00	5.1062e-01	3.1143e+01	2.8826e+03	1.2727e+02	4.1314e+04	1.0438e+04
ABC	4.5000e+00	1.3531e+02	6.4002e+01	6.7510e+02	1.8686e+02	7.0859e+01	1.2443e+03	8.5544e+02	5.7507e+03	1.2817e+03
BA	4.8388e+02	1.7234e+04	1.6400e+04	4.4093e+04	1.1706e+04	3.4179e+04	1.0630e+05	9.6083e+04	2.3520e+05	4.6988e+04
FA	8.9604e+03	4.0074e+06	8.2626e+05	3.8094e+07	8.1071e+06	5.8892e+08	5.1338e+09	5.2629e+09	1.0150e+10	2.4221e+09
GWO	1.5054e+01	1.5307e+03	6.4304e+02	8.4064e+03	1.7649e+03	1.3264e+04	3.6861e+05	4.7678e+04	2.1023e+06	6.9599e+05
PSO	1.8458e+01	6.7218e+02	1.3856e+02	5.8327e+03	1.4721e+03	8.0650e+02	3.3699e+04	1.9935e+04	2.7354e+05	5.6075e+04
SOS	7.9599e-01	1.3667e+01	9.7922e+00	1.1406e+02	2.0064e+01	3.7430e+01	5.0504e+03	1.6453e+03	2.8128e+04	8.1263e+03
WfCMO5	7.8948e-02	1.9437e+00	1.2515e+00	9.2971e+00	2.2502e+00	2.1109e+02	4.4214e+02	4.0206e+02	8.9668e+02	1.8082e+02
WfCMO10	1.4310e-01	2.6836e+00	2.1643e+00	1.0198e+01	2.2240e+00	3.3518e+02	1.2920e+03	9.5090e+02	4.1810e+03	9.0805e+02
WfCMO20	7.8699e-01	6.1570e+00	4.2809e+00	2.1100e+01	5.0297e+00	3.8628e+02	1.5023e+03	1.1463e+03	5.9464e+03	1.1493e+03
Algorithm	F_{55} Minimum	Average	Median	Maximum	Standard Deviation	F_{56} Mininum	Average	Median	Maximum	Standard Deviation
COA5	7.4714e+01	1.8000e+03	5.4038e+02	1.7772e+04	3.5359e+03	2.3129e+02	3.1547e+03	1.5631e+03	1.9291e+04	4.3526e+03
COA10	1.0660e+02	2.0063e+04	3.0212e+04	3.1521e+04	1.3852e+04	1.9156e+02	5.2735e+03	2.8173e+03	2.7516e+04	6.0539e+03
ABC	3.4440e+02	9.3720e+03	7.7376e+03	1.8343e+04	7.3445e+03	4.7067e+02	2.1140e+03	1.5425e+03	7.7382e+03	1.6117e+03
BA	2.3429e+05	4.2328e+05	4.0969e+05	5.7968e+05	8.4646e+04	5.5644e+05	9.0917e+05	9.3072e+05	1.2246e+06	1.5631e+05
FA	1.4377e+10	2.9406e+10	2.9923e+10	4.5105e+10	6.8621e+09	2.9309e+10	4.4009e+10	4.4679e+10	5.5741e+10	7.5648e+09
GWO	6.6934e+03	6.5256e+06	7.4498e+04	7.2022e+07	1.7206e+07	5.3099e+05	7.5813e+07	3.2824e+07	3.4657e+08	9.7911e+07
PSO	1.2175e+03	3.5978e+04	2.9024e+04	1.1396e+05	2.6690e+04	1.0310e+04	5.3251e+07	5.7170e+04	7.1949e+08	1.8310e+08
SOS	7.6729e+01	5.5064e+03	2.9048e+03	2.6558e+04	6.6261e+03	3.8603e+02	2.4110e+03	1.7664e+03	8.5868e+03	2.1416e+03
WfCMO5	2.1547e+02	5.5074e+03	3.9397e+03	1.5863e+04	4.3130e+03	3.5905e+02	1.8649e+03	1.0835e+03	9.7118e+03	2.0249e+03
WfCMO10	4.1608e+02	5.6463e+03	4.2229e+03	1.4600e+04	4.5131e+03	2.9130e+02	1.5700e+03	9.2841e+02	6.9858e+03	1.5769e+03
WfCMO20	6.0656e+02	8.9580e+03	7.6323e+03	2.6304e+04	6.1254e+03	2.5464e+02	2.2827e+03	1.1247e+03	1.4863e+04	3.0070e+03

Table B.14: Descriptive statistics for IEEE-CEC 2017 benchmark functions considering the error measurements - Part XIV.

Algorithm	F_{57}					F_{58}				
	Minimum	Average	Median	Maximum	Standard Deviation	Mininum	Average	Median	Maximum	Standard Deviation
COA5	1.8745e-01	8.3701e+00	1.0012e+00	3.8505e+01	1.2771e+01	1.4164e+02	7.0640e+02	7.8384e+02	1.0743e+03	2.3300e+02
COA10	2.1901e-01	5.8929e+00	5.3572e+00	1.6422e+01	5.5054e+00	1.4562e+02	8.3357e+02	8.1184e+02	1.5491e+03	3.2083e+02
ABC	1.4434e+00	7.4781e+00	3.2111e+00	3.9623e+01	8.7833e+00	2.5678e+02	6.0790e+02	6.5146e+02	9.2293e+02	1.6320e+02
BA	5.2753e+01	4.3223e+02	4.0888e+02	7.8073e+02	1.9389e+02	1.1541e+03	1.9888e+03	1.9147e+03	2.8187e+03	4.3966e+02
FA	6.9396e+02	1.0152e+03	1.0543e+03	1.2566e+03	1.3124e+02	4.5146e+03	6.3790e+03	6.2823e+03	1.1643e+04	1.4843e+03
GWO	7.2645e+00	7.7256e+01	4.3089e+01	2.7240e+02	7.3494e+01	3.8509e+02	7.2638e+02	6.7184e+02	1.3131e+03	2.3134e+02
PSO	2.9645e+00	1.2721e+02	1.2192e+02	4.2467e+02	1.2089e+02	6.6322e+02	1.3800e+03	1.3818e+03	2.8914e+03	4.2663e+02
SOS	1.2547e-01	3.3379e+00	9.5591e-01	3.8357e+01	7.3916e+00	1.4359e+02	5.4987e+02	4.9202e+02	1.0355e+03	2.5518e+02
WfCMO5	2.4418e-01	5.7210e+00	1.7344e+00	1.2054e+02	2.1701e+01	3.1046e+01	4.1442e+02	4.4723e+02	8.4537e+02	2.3402e+02
WfCMO10	7.7032e-01	2.0142e+00	1.5883e+00	1.1670e+01	2.0524e+00	4.4177e+01	5.7870e+02	4.9699e+02	1.2808e+03	3.7583e+02
WfCMO20	7.8123e-01	1.1378e+01	3.0339e+00	1.3193e+02	2.5427e+01	6.0270e+00	7.1161e+02	7.8742e+02	1.1514e+03	3.2293e+02
Algorithm	F_{59}					F_{60}				
	Minimum	Average	Median	Maximum	Standard Deviation	Mininum	Average	Median	Maximum	Standard Deviation
COA5	8.5700e+02	1.3958e+03	1.3366e+03	2.0102e+03	3.0366e+02	2.7360e+03	3.7447e+03	3.7503e+03	5.3028e+03	5.8066e+02
COA10	1.0308e+03	1.5356e+03	1.4977e+03	2.1732e+03	3.1263e+02	2.7671e+03	4.7135e+03	4.1891e+03	7.4188e+03	1.5601e+03
ABC	7.4806e+02	1.1772e+03	1.2073e+03	1.5560e+03	2.0830e+02	2.2954e+03	3.2246e+03	3.2776e+03	3.7576e+03	3.6462e+02
BA	1.9858e+03	2.7937e+03	2.7275e+03	3.9192e+03	5.0459e+02	4.3718e+03	5.7409e+03	5.6204e+03	7.1929e+03	7.8417e+02
FA	8.5987e+03	1.1627e+04	1.1359e+04	1.6983e+04	1.9907e+03	2.6153e+04	3.5840e+04	3.5730e+04	4.3633e+04	4.6043e+03
GWO	7.0859e+02	1.2332e+03	1.2262e+03	1.9326e+03	2.3615e+02	2.3820e+03	3.6324e+03	3.6449e+03	5.2195e+03	7.0154e+02
PSO	1.3292e+03	2.1265e+03	2.1880e+03	2.7329e+03	4.1770e+02	4.1324e+03	5.5279e+03	5.3786e+03	7.4073e+03	8.5010e+02
SOS	6.5271e+02	1.1903e+03	1.1170e+03	2.0119e+03	3.6282e+02	1.9983e+03	3.2047e+03	3.2579e+03	4.4333e+03	5.7422e+02
WfCMO5	3.7542e+02	9.1409e+02	8.4592e+02	1.7260e+03	2.9973e+02	1.8009e+03	3.0056e+03	3.0348e+03	3.9155e+03	5.7890e+02
WfCMO10	5.3023e+02	1.0575e+03	9.3149e+02	1.9489e+03	4.2111e+02	2.0355e+03	3.0012e+03	3.0509e+03	4.3095e+03	5.7121e+02
WfCMO20	5.7481e+02	1.0488e+03	9.7949e+02	2.0097e+03	3.2306e+02	1.7025e+03	3.1375e+03	3.1469e+03	4.3605e+03	6.5226e+02

Table B.15: Descriptive statistics for IEEE-CEC 2017 benchmark functions considering the error measurements - Part XV.

Algorithm	F_{61} Minimum	Average	Median	Maximum	Standard Deviation	F_{62} Mininum	Average	Median	Maximum	Standard Deviation
COA5	7.6514e-02	2.0243e+00	1.4417e+00	1.9688e+01	3.4331e+00	7.4012e+01	2.6262e+02	2.6551e+02	4.5971e+02	1.1154e+02
COA10	1.0736e-01	5.4501e+00	2.3034e+00	2.1955e+01	7.1002e+00	5.8735e+01	2.7817e+02	2.8258e+02	5.6122e+02	1.3629e+02
ABC	5.1750e-01	3.2692e+00	3.1152e+00	8.5924e+00	1.7790e+00	5.1577e+01	2.1335e+02	2.1090e+02	3.5573e+02	7.5471e+01
BA	7.3335e+01	2.3459e+02	2.0650e+02	4.5618e+02	1.1178e+02	5.7964e+02	1.1103e+03	1.1053e+03	1.7644e+03	3.0963e+02
FA	2.9913e+02	5.5667e+02	5.8753e+02	9.3464e+02	1.7280e+02	1.9391e+03	1.2672e+04	9.9276e+03	4.1457e+04	1.0061e+04
GWO	4.0771e+00	5.4903e+01	4.3809e+01	1.6338e+02	3.7883e+01	8.3222e+01	2.0872e+02	1.9528e+02	5.4808e+02	1.1983e+02
PSO	2.5615e+01	6.7442e+01	5.9426e+01	1.8454e+02	3.1930e+01	1.3792e+02	6.1621e+02	6.5561e+02	1.3867e+03	3.0676e+02
SOS	1.5628e+00	1.1214e+01	1.0869e+01	2.4789e+01	6.7046e+00	3.5618e+01	1.0294e+02	6.4520e+01	2.8821e+02	7.1860e+01
WfCMO5	9.1306e-02	4.4848e+00	2.3264e+00	2.3192e+01	6.2441e+00	3.4244e+01	1.0136e+02	7.8889e+01	2.3803e+02	5.9701e+01
WfCMO10	8.9553e-01	9.4232e+00	3.4286e+00	2.7311e+01	9.4142e+00	3.2968e+01	1.0795e+02	7.9096e+01	2.2749e+02	5.9755e+01
WfCMO20	1.8343e+00	1.6455e+01	1.5061e+01	3.9161e+01	9.9570e+00	3.7630e+01	1.3833e+02	8.9960e+01	3.7588e+02	9.1177e+01
Algorithm	F_{63} Minimum	Average	Median	Maximum	Standard Deviation	F_{64} Mininum	Average	Median	Maximum	Standard Deviation
COA5	3.2635e+02	9.8804e+02	9.4639e+02	1.4814e+03	2.9166e+02	1.5904e+03	2.5615e+03	2.4468e+03	3.5548e+03	5.1794e+02
COA10	3.1195e+02	1.0176e+03	1.0126e+03	1.6021e+03	2.9495e+02	1.6582e+03	2.8057e+03	2.6898e+03	4.7128e+03	7.5425e+02
ABC	5.2621e+02	9.3105e+02	9.5514e+02	1.1928e+03	1.5643e+02	1.8736e+03	2.5744e+03	2.5530e+03	3.1971e+03	3.0754e+02
BA	1.5546e+03	2.3547e+03	2.3996e+03	3.0061e+03	3.3417e+02	3.7222e+03	4.5709e+03	4.5535e+03	5.9050e+03	5.4072e+02
FA	3.3977e+04	6.7045e+05	4.2509e+05	2.6187e+06	7.1986e+05	8.5732e+06	6.7468e+07	5.5753e+07	1.6740e+08	4.3245e+07
GWO	5.9189e+02	9.9705e+02	1.0104e+03	1.9541e+03	3.0168e+02	1.7431e+03	2.7884e+03	2.6973e+03	3.8293e+03	5.0268e+02
PSO	1.1034e+03	1.7266e+03	1.6886e+03	2.6086e+03	3.9285e+02	3.0445e+03	5.0633e+03	5.0450e+03	6.6314e+03	8.5260e+02
SOS	2.3833e+02	8.4597e+02	8.1935e+02	1.7369e+03	3.5793e+02	1.8136e+03	2.5753e+03	2.4993e+03	3.4965e+03	4.2845e+02
WfCMO5	3.3623e+02	7.0835e+02	7.0020e+02	1.0412e+03	1.7567e+02	1.5370e+03	2.2298e+03	2.2158e+03	3.1919e+03	4.2181e+02
WfCMO10	2.6831e+02	6.8397e+02	6.2350e+02	1.2973e+03	2.3995e+02	1.7582e+03	2.3960e+03	2.3613e+03	3.1941e+03	3.7056e+02
WfCMO20	3.1517e+02	7.4545e+02	7.1291e+02	1.2525e+03	2.5329e+02	1.7158e+03	2.4550e+03	2.4717e+03	3.3171e+03	3.8953e+02

Table B.16: Descriptive statistics for IEEE-CEC 2017 benchmark functions considering the error measurements - Part XVI.

Algorithm	F_{65}					F_{66}				
	Minimum	Average	Median	Maximum	Standard Deviation	Mininum	Average	Median	Maximum	Standard Deviation
COA5	2.6862e-01	1.4690e+00	1.4891e+00	3.2440e+00	8.5340e-01	2.3797e+03	1.9159e+04	1.8628e+04	5.3566e+04	1.1796e+04
COA10	3.2667e-01	2.4070e+00	1.8477e+00	5.8059e+00	1.5148e+00	6.4176e+03	5.6783e+04	4.7625e+04	2.7687e+05	6.1029e+04
ABC	6.5158e+01	1.2663e+03	1.0592e+03	2.9602e+03	7.2929e+02	7.0942e+04	1.6645e+05	1.2803e+05	5.4588e+05	1.0712e+05
BA	6.3268e+02	2.0000e+04	1.7454e+04	6.2196e+04	1.6720e+04	5.5795e+04	2.9456e+05	2.2835e+05	1.9289e+06	3.3506e+05
FA	1.8172e+07	3.5231e+08	2.2515e+08	1.2431e+09	3.0980e+08	1.6250e+07	3.7999e+08	2.9859e+08	1.0436e+09	2.6050e+08
GWO	6.0214e+02	2.6487e+04	3.1600e+04	5.1302e+04	1.5359e+04	1.0659e+05	8.0622e+05	3.6080e+05	5.8231e+06	1.1534e+06
PSO	4.2302e+01	1.5305e+04	6.5232e+03	5.4005e+04	1.9216e+04	3.4926e+02	9.2952e+05	3.8125e+04	1.5247e+07	2.8949e+06
SOS	5.4979e+01	3.6980e+03	2.6402e+03	1.9096e+04	4.1100e+03	1.5888e+04	1.1138e+05	7.9577e+04	9.4751e+05	1.6666e+05
WfCMO5	2.3258e-01	9.2788e+00	4.6034e+00	2.2535e+01	9.2372e+00	1.9659e+02	7.2276e+02	5.4680e+02	3.5018e+03	6.2842e+02
WfCMO10	1.5397e+00	1.7988e+01	2.1173e+01	3.7499e+01	8.8086e+00	2.7862e+02	2.3146e+03	8.7471e+02	1.5763e+04	3.9066e+03
WfCMO20	3.6371e-01	1.9559e+01	2.2048e+01	3.4729e+01	8.9358e+00	2.6547e+02	2.2248e+03	9.5225e+02	1.0166e+04	2.5669e+03
Algorithm	F_{67}					F_{68}				
	Minimum	Average	Median	Maximum	Standard Deviation	Mininum	Average	Median	Maximum	Standard Deviation
COA5	2.5085e+04	9.6105e+04	6.8695e+04	3.2104e+05	7.3734e+04	1.4694e+05	3.8767e+05	3.4537e+05	9.6360e+05	2.0909e+05
COA10	5.5097e+04	3.1134e+05	2.7184e+05	9.4760e+05	1.8035e+05	6.3161e+05	2.0148e+06	1.7771e+06	4.2621e+06	1.1132e+06
ABC	2.3925e+05	8.7808e+05	8.2452e+05	2.1150e+06	4.4127e+05	1.0831e+06	2.9978e+06	2.9743e+06	5.3823e+06	1.0784e+06
BA	2.1603e+05	6.3320e+05	5.7875e+05	1.3009e+06	3.1048e+05	3.0251e+05	7.3116e+05	6.8673e+05	1.1915e+06	2.5470e+05
FA	3.5210e+08	9.8137e+08	9.5510e+08	2.3483e+09	5.0940e+08	4.3580e+08	1.0972e+09	1.0810e+09	2.0989e+09	4.1625e+08
GWO	1.8508e+05	3.1188e+06	1.5840e+06	1.4028e+07	3.5659e+06	7.8006e+05	3.2853e+06	3.1331e+06	6.4672e+06	1.7890e+06
PSO	7.6023e+03	1.1551e+06	3.1556e+05	1.0537e+07	2.1234e+06	1.2570e+05	1.2630e+06	4.4486e+05	1.0418e+07	2.0873e+06
SOS	2.9736e+04	2.2441e+05	1.9220e+05	7.5637e+05	1.6304e+05	8.1164e+04	5.5605e+05	4.9743e+05	2.0282e+06	3.8045e+05
WfCMO5	8.6943e+03	3.8124e+04	2.7414e+04	1.0651e+05	2.5802e+04	3.0989e+04	1.4456e+05	1.3472e+05	3.3309e+05	7.2644e+04
WfCMO10	3.8845e+03	4.2930e+04	4.0802e+04	9.5457e+04	2.2740e+04	7.3139e+04	1.7501e+05	1.4098e+05	4.8471e+05	8.9861e+04
WfCMO20	1.5902e+04	7.3315e+04	6.3916e+04	1.7394e+05	4.1188e+04	9.0761e+04	2.0456e+05	1.8333e+05	4.0066e+05	7.6910e+04

Table B.17: Descriptive statistics for IEEE-CEC 2017 benchmark functions considering the error measurements - Part XVII.

Algorithm	F_{69}					F_{70}				
	Minimum	Average	Median	Maximum	Standard Deviation	Mininum	Average	Median	Maximum	Standard Deviation
COA5	3.7677e-02	2.2337e-01	1.0875e-01	1.1994e+00	3.0606e-01	1.3566e+01	2.4782e+01	2.2564e+01	5.3975e+01	8.5027e+00
COA10	2.9247e-02	1.0076e-01	7.7748e-02	2.0789e-01	5.2755e-02	1.3421e+01	2.1360e+03	4.3155e+01	1.5705e+04	5.4116e+03
ABC	3.2606e+00	1.0518e+02	8.1074e+01	4.6963e+02	1.1699e+02	1.2345e+02	1.2816e+03	9.7717e+02	4.3287e+03	1.0218e+03
BA	3.5218e+01	6.8458e+03	2.3634e+03	2.4819e+04	7.9266e+03	3.9664e+04	1.3054e+06	1.3619e+06	2.5064e+06	6.0886e+05
FA	5.6466e+04	8.1473e+06	3.2163e+06	3.7895e+07	1.0839e+07	1.1387e+09	6.5890e+09	6.2136e+09	1.3525e+10	3.3377e+09
GWO	1.0799e+01	3.1745e+03	4.6027e+01	1.2679e+04	5.1274e+03	1.5299e+04	3.4273e+05	9.8559e+04	1.7659e+06	4.5699e+05
PSO	5.7977e+00	1.0971e+02	8.6541e+01	8.9415e+02	1.6748e+02	5.5425e+01	3.6707e+06	1.8543e+03	1.0192e+08	1.8581e+07
SOS	2.6045e-01	9.3053e+00	4.0400e+00	4.7882e+01	1.2043e+01	1.0730e+01	8.9936e+03	1.7298e+03	5.4113e+04	1.4331e+04
WfCMO5	1.0326e-02	2.2196e-01	6.1035e-02	1.0540e+00	3.5241e-01	4.2439e+01	2.0806e+02	1.8652e+02	9.2292e+02	1.5252e+02
WfCMO10	2.8073e-02	8.4538e-01	9.3573e-01	2.9681e+00	6.6335e-01	8.3368e+01	3.1958e+02	2.6207e+02	6.8770e+02	1.7481e+02
WfCMO20	5.2171e-01	1.8235e+00	1.5907e+00	3.3814e+00	6.8465e-01	1.1695e+02	3.6039e+02	2.6550e+02	1.4121e+03	2.7153e+02
Algorithm	F_{71}					F_{72}				
	Minimum	Average	Median	Maximum	Standard Deviation	Mininum	Average	Median	Maximum	Standard Deviation
COA5	3.4971e+01	1.7552e+02	1.2778e+02	8.5629e+02	1.6727e+02	1.0719e+02	3.8356e+03	1.2790e+03	2.7452e+04	5.7304e+03
COA10	8.8130e+01	3.5567e+03	1.8392e+03	3.3741e+04	6.8958e+03	1.6451e+02	6.8665e+03	2.8377e+03	3.7997e+04	9.8150e+03
ABC	4.9396e+02	6.5425e+03	5.7370e+03	2.4868e+04	4.8454e+03	3.8151e+02	1.8432e+03	1.1344e+03	9.8243e+03	1.9449e+03
BA	3.1368e+05	2.3624e+06	2.4145e+06	3.9549e+06	1.1474e+06	2.8880e+06	9.0552e+06	8.6119e+06	1.7251e+07	3.6645e+06
FA	4.7984e+09	1.1603e+10	1.1175e+10	1.9759e+10	3.4373e+09	3.5784e+10	4.6812e+10	4.7214e+10	5.9692e+10	5.8396e+09
GWO	1.4391e+05	2.8160e+06	6.9179e+05	3.3620e+07	7.7103e+06	3.4275e+06	6.5432e+07	4.7313e+07	2.7480e+08	7.2144e+07
PSO	4.5887e+02	8.9720e+05	4.7528e+04	1.6161e+07	3.0836e+06	2.5171e+04	7.5015e+07	4.0827e+06	7.5509e+08	1.8251e+08
SOS	9.2972e+01	1.4933e+04	1.2272e+04	4.2523e+04	1.3672e+04	2.7233e+02	7.2162e+03	2.7550e+03	3.9487e+04	1.1329e+04
WfCMO5	5.1340e+03	1.3041e+04	1.2305e+04	2.4545e+04	4.5799e+03	2.1659e+02	2.0220e+03	1.6050e+03	7.2234e+03	1.8005e+03
WfCMO10	2.9887e+03	1.5178e+04	1.4328e+04	2.8537e+04	7.5808e+03	2.1331e+02	2.2951e+03	9.8089e+02	1.4260e+04	3.3783e+03
WfCMO20	6.4942e+02	1.3861e+04	1.1630e+04	4.2394e+04	1.0137e+04	3.3662e+02	2.9583e+03	1.4232e+03	1.9656e+04	4.1225e+03

Table B.18: Descriptive statistics for IEEE-CEC 2017 benchmark functions considering the error measurements - Part XVIII.

Algorithm	F_{73}					F_{74}				
	Minimum	Average	Median	Maximum	Standard Deviation	Mininum	Average	Median	Maximum	Standard Deviation
COA5	7.0872e-07	5.0788e-01	1.4490e-01	1.9903e+00	5.8125e-01	3.5788e+01	2.2592e+02	1.8998e+02	4.3352e+02	1.0134e+02
COA10	7.5790e-09	3.6942e-01	1.6546e-05	2.6143e+00	6.1298e-01	1.3171e+01	2.7086e+02	2.0820e+02	7.0362e+02	1.9667e+02
ABC	1.1203e-02	9.6293e-01	1.0094e+00	2.0648e+00	6.2516e-01	6.6565e+01	2.3982e+02	2.1997e+02	4.0868e+02	8.0577e+01
BA	6.5924e+01	1.9646e+02	1.7209e+02	4.0017e+02	9.1508e+01	3.5117e+02	8.8230e+02	8.8026e+02	1.3297e+03	2.2934e+02
FA	2.3204e+02	4.2184e+02	4.3079e+02	6.3408e+02	9.3066e+01	1.2870e+03	1.6712e+03	1.7326e+03	1.9454e+03	1.8550e+02
GWO	1.4129e+01	5.8503e+01	4.4931e+01	1.4892e+02	4.0331e+01	1.3202e+02	3.2970e+02	2.9366e+02	6.4257e+02	1.5555e+02
PSO	2.1731e+01	8.6642e+01	5.8517e+01	2.3729e+02	6.0541e+01	1.1854e+02	4.9783e+02	4.8233e+02	9.2846e+02	1.7371e+02
SOS	7.4351e-11	7.2894e-01	6.2449e-01	2.3021e+00	5.9050e-01	2.6356e+00	1.9099e+02	1.6602e+02	4.7053e+02	1.2791e+02
WfCMO5	2.0441e-09	4.5669e+00	9.9496e-01	2.0996e+01	8.0906e+00	3.6128e+01	1.1855e+02	1.0121e+02	2.0943e+02	6.1072e+01
WfCMO10	4.0714e-09	1.2220e+00	3.1217e-01	2.0323e+01	3.6542e+00	2.8663e+01	1.0507e+02	6.3500e+01	3.2326e+02	8.3445e+01
WfCMO20	1.3224e-02	5.3791e+00	1.7049e+00	2.2647e+01	7.6771e+00	3.1856e+01	1.5359e+02	9.7206e+01	4.9326e+02	1.3688e+02
Algorithm	F_{75}					F_{76}				
	Minimum	Average	Median	Maximum	Standard Deviation	Mininum	Average	Median	Maximum	Standard Deviation
COA5	3.4317e+02	7.2352e+02	6.8842e+02	1.1103e+03	2.3041e+02	1.3444e+03	2.4995e+03	2.5070e+03	3.2911e+03	4.6276e+02
COA10	4.3765e+02	9.6414e+02	9.8539e+02	1.5697e+03	2.5260e+02	1.7534e+03	2.6622e+03	2.5689e+03	3.6868e+03	5.0675e+02
ABC	3.5085e+02	7.1274e+02	7.2122e+02	9.4342e+02	1.4785e+02	1.8472e+03	2.5162e+03	2.5262e+03	3.0998e+03	2.8990e+02
BA	9.6320e+02	1.8683e+03	1.9048e+03	2.7918e+03	4.9012e+02	3.2388e+03	4.2913e+03	4.1806e+03	5.2364e+03	5.0615e+02
FA	2.6562e+03	3.4156e+03	3.4171e+03	3.8562e+03	2.4975e+02	6.5866e+03	7.6508e+03	7.7054e+03	8.2112e+03	4.0159e+02
GWO	2.2441e+02	7.3418e+02	7.0077e+02	1.6243e+03	2.7247e+02	1.4406e+03	2.4290e+03	2.1941e+03	4.8960e+03	8.2276e+02
PSO	5.3440e+02	1.1608e+03	1.1160e+03	1.9469e+03	3.8476e+02	2.1597e+03	3.4009e+03	3.4082e+03	4.5708e+03	6.5002e+02
SOS	1.6910e+02	6.2549e+02	5.7489e+02	1.2058e+03	2.5493e+02	7.5418e+02	2.4958e+03	2.6204e+03	3.2738e+03	5.3382e+02
WfCMO5	1.1659e+02	4.4789e+02	3.7107e+02	9.5701e+02	2.3828e+02	1.2889e+03	2.2287e+03	2.1063e+03	3.7902e+03	6.2530e+02
WfCMO10	1.1051e+02	6.0243e+02	5.8336e+02	1.1015e+03	3.3432e+02	1.0263e+03	2.1742e+03	1.9727e+03	3.8971e+03	7.3960e+02
WfCMO20	1.8531e+02	7.5039e+02	8.1675e+02	1.2331e+03	3.3886e+02	1.0971e+03	2.4315e+03	2.4060e+03	3.6166e+03	7.0858e+02

Table B.19: Descriptive statistics for IEEE-CEC 2017 benchmark functions considering the error measurements - Part XIX.

Algorithm	F_{77}					F_{78}				
	Minimum	Average	Median	Maximum	Standard Deviation	Mininum	Average	Median	Maximum	Standard Deviation
COA5	1.0002e+02	1.4626e+02	1.0237e+02	2.2338e+02	5.6329e+01	2.3909e+02	2.6584e+02	2.6778e+02	2.9461e+02	1.4366e+01
COA10	1.0000e+02	1.4456e+02	1.0015e+02	2.1723e+02	5.5409e+01	2.2535e+02	2.5870e+02	2.6114e+02	2.9018e+02	1.4233e+01
ABC	6.4849e-01	1.0821e+02	1.1151e+02	1.2249e+02	2.0674e+01	1.1921e+02	2.2536e+02	2.6135e+02	3.1584e+02	7.5847e+01
BA	1.0005e+02	1.7341e+02	1.0541e+02	2.9103e+02	7.7765e+01	4.3275e+02	5.2843e+02	5.2329e+02	6.5370e+02	5.1874e+01
FA	1.7740e+02	2.9203e+02	3.0533e+02	3.8599e+02	6.1138e+01	6.9900e+02	8.0006e+02	7.9774e+02	9.0772e+02	4.8698e+01
GWO	1.0139e+02	1.9872e+02	2.1085e+02	2.5014e+02	3.9177e+01	2.3734e+02	2.7833e+02	2.7434e+02	3.7662e+02	2.6080e+01
PSO	1.0344e+02	2.1481e+02	2.2304e+02	2.5834e+02	3.8789e+01	2.7377e+02	3.3635e+02	3.2344e+02	4.1670e+02	3.9681e+01
SOS	1.0000e+02	1.0412e+02	1.0000e+02	2.1559e+02	2.1065e+01	2.3033e+02	2.5324e+02	2.4751e+02	3.2241e+02	2.0186e+01
WfCMO5	1.0000e+02	1.7151e+02	2.0605e+02	2.1207e+02	5.1457e+01	2.1911e+02	2.4033e+02	2.3825e+02	2.6056e+02	1.0964e+01
WfCMO10	1.0000e+02	1.3343e+02	1.0020e+02	2.1696e+02	5.1015e+01	2.1852e+02	2.3740e+02	2.3553e+02	2.7372e+02	1.2261e+01
WfCMO20	1.0000e+02	1.3427e+02	1.0000e+02	2.1579e+02	5.2261e+01	2.2212e+02	2.4221e+02	2.4104e+02	3.0818e+02	1.6601e+01
Algorithm	F_{79}					F_{80}				
	Minimum	Average	Median	Maximum	Standard Deviation	Mininum	Average	Median	Maximum	Standard Deviation
COA5	2.9649e+02	3.5022e+02	3.4772e+02	4.0416e+02	2.6077e+01	4.6645e+02	5.9935e+02	6.0325e+02	7.3750e+02	5.8052e+01
COA10	2.4622e+02	3.0572e+02	3.0718e+02	3.5620e+02	2.7734e+01	3.7971e+02	4.9372e+02	4.9135e+02	6.2798e+02	5.3696e+01
ABC	3.6029e+02	4.1664e+02	4.1696e+02	4.5648e+02	2.1507e+01	7.4762e+02	8.8817e+02	8.9660e+02	9.7103e+02	5.2238e+01
BA	6.8449e+02	8.8042e+02	8.9054e+02	1.0605e+03	9.2205e+01	1.7277e+03	2.1801e+03	2.1681e+03	2.5790e+03	2.0240e+02
FA	1.2323e+03	1.3939e+03	1.3753e+03	1.5336e+03	7.9196e+01	2.7405e+03	3.2174e+03	3.1954e+03	3.5817e+03	1.9605e+02
GWO	3.1477e+02	3.7618e+02	3.6383e+02	5.6900e+02	4.7628e+01	6.1310e+02	7.2581e+02	7.3151e+02	8.1654e+02	5.3917e+01
PSO	4.1495e+02	5.1744e+02	5.1525e+02	6.3988e+02	5.5988e+01	9.3312e+02	1.2063e+03	1.2061e+03	1.5660e+03	1.5082e+02
SOS	2.7680e+02	3.2337e+02	3.1562e+02	4.0552e+02	3.0066e+01	5.2508e+02	6.1553e+02	6.0628e+02	7.5546e+02	5.7450e+01
WfCMO5	2.5117e+02	2.8301e+02	2.7803e+02	3.4837e+02	2.3719e+01	4.8071e+02	5.4517e+02	5.4424e+02	6.2329e+02	3.8061e+01
WfCMO10	2.5860e+02	2.9106e+02	2.8812e+02	4.0296e+02	2.5703e+01	5.0770e+02	5.8200e+02	5.7634e+02	6.8383e+02	4.4985e+01
WfCMO20	2.6893e+02	3.0702e+02	3.0637e+02	3.6405e+02	2.4413e+01	5.1706e+02	6.5839e+02	6.5131e+02	8.2217e+02	6.4520e+01

Table B.20: Descriptive statistics for IEEE-CEC 2017 benchmark functions considering the error measurements - Part XX.

Algorithm	F_{81}					F_{82}				
	Minimum	Average	Median	Maximum	Standard Deviation	Mininum	Average	Median	Maximum	Standard Deviation
COA5	1.5182e+01	7.8119e+01	1.0097e+02	1.0217e+02	3.4527e+01	1.0001e+02	1.4181e+03	1.0005e+02	3.9831e+03	1.4795e+03
COA10	2.6164e-05	8.5703e+01	1.0043e+02	1.0195e+02	3.4169e+01	1.0000e+02	1.7436e+03	1.8751e+03	4.4953e+03	1.6427e+03
ABC	2.4929e+01	6.0621e+01	4.8152e+01	1.0243e+02	2.4566e+01	1.0115e+02	2.0126e+02	1.0521e+02	2.9477e+03	5.1874e+02
BA	5.4938e+01	1.1398e+02	1.1127e+02	2.0798e+02	2.1556e+01	3.8241e+03	5.0976e+03	4.9671e+03	6.7727e+03	7.1150e+02
FA	6.0628e+02	1.5497e+03	1.6160e+03	2.6717e+03	4.8050e+02	8.1951e+03	9.1451e+03	9.2392e+03	1.0281e+04	4.9543e+02
GWO	1.0059e+02	1.0577e+02	1.0531e+02	1.2273e+02	5.7912e+00	1.7066e+02	2.3636e+03	2.6044e+03	6.6810e+03	1.6450e+03
PSO	2.6013e+01	1.0933e+02	1.0828e+02	1.5405e+02	3.0639e+01	1.0538e+02	1.9785e+03	5.8495e+02	6.1462e+03	2.1326e+03
SOS	9.5497e-12	9.4380e+01	1.0124e+02	1.0394e+02	2.5738e+01	1.0000e+02	1.0049e+02	1.0000e+02	1.0250e+02	1.0046e+00
WfCMO5	1.0000e+02	1.0064e+02	1.0061e+02	1.0346e+02	7.1693e-01	1.0000e+02	2.4679e+02	1.0010e+02	4.4356e+03	7.9115e+02
WfCMO10	1.0000e+02	1.0048e+02	1.0050e+02	1.0189e+02	4.1350e-01	1.0000e+02	5.6589e+02	1.0123e+02	7.2549e+03	1.7664e+03
WfCMO20	1.0000e+02	1.0068e+02	1.0057e+02	1.0201e+02	5.4788e-01	1.0000e+02	3.1774e+02	1.0000e+02	6.5892e+03	1.1845e+03
Algorithm	F_{83}					F_{84}				
	Minimum	Average	Median	Maximum	Standard Deviation	Mininum	Average	Median	Maximum	Standard Deviation
COA5	3.8742e+03	5.2791e+03	5.2874e+03	6.5319e+03	6.6910e+02	1.1003e+04	1.3700e+04	1.3832e+04	1.5613e+04	1.1911e+03
COA10	3.9882e+03	5.6911e+03	5.7523e+03	6.9751e+03	7.3079e+02	1.0965e+04	1.4736e+04	1.4101e+04	2.9683e+04	3.1628e+03
ABC	4.3755e+03	5.1685e+03	5.2401e+03	5.9110e+03	3.9554e+02	1.1111e+04	1.2680e+04	1.2871e+04	1.3554e+04	5.6073e+02
BA	6.2536e+03	8.3527e+03	8.4871e+03	1.0170e+04	9.0492e+02	1.5635e+04	1.7357e+04	1.7159e+04	2.0072e+04	1.3247e+03
FA	1.4252e+04	1.6114e+04	1.6104e+04	1.7082e+04	6.4792e+02	3.2418e+04	3.4516e+04	3.4527e+04	3.6118e+04	8.4929e+02
GWO	4.0685e+03	6.2566e+03	5.9865e+03	1.1818e+04	1.4959e+03	1.2185e+04	1.5583e+04	1.5067e+04	3.1283e+04	3.1781e+03
PSO	1.5461e+03	7.9555e+03	7.9523e+03	1.1239e+04	1.8394e+03	1.7252e+04	2.0580e+04	2.0067e+04	2.8043e+04	2.4604e+03
SOS	1.0000e+02	3.9517e+03	4.5322e+03	8.6428e+03	2.8243e+03	9.1647e+03	1.2999e+04	1.2932e+04	1.5645e+04	1.4612e+03
WfCMO5	1.0478e+02	9.1229e+03	1.0096e+04	1.2294e+04	3.0050e+03	1.3193e+04	2.5542e+04	2.7753e+04	2.9973e+04	4.8310e+03
WfCMO10	1.0000e+02	1.1472e+04	1.2338e+04	1.3198e+04	3.1393e+03	1.2551e+04	2.4926e+04	2.7761e+04	3.0004e+04	5.5540e+03
WfCMO20	1.0000e+02	1.1901e+04	1.2248e+04	1.3244e+04	2.2942e+03	2.6934e+04	2.8543e+04	2.8632e+04	2.9553e+04	7.9329e+02

Table B.21: Descriptive statistics for IEEE-CEC 2017 benchmark functions considering the error measurements - Part XXI.

Algorithm	F_{85}					F_{86}				
	Minimum	Average	Median	Maximum	Standard Deviation	Mininum	Average	Median	Maximum	Standard Deviation
COA5	3.0553e+02	3.1364e+02	3.1375e+02	3.2364e+02	4.8747e+00	3.9554e+02	4.2109e+02	4.2419e+02	4.5518e+02	1.5693e+01
COA10	3.0799e+02	3.1250e+02	3.1218e+02	3.1818e+02	2.5482e+00	3.8405e+02	4.1733e+02	4.1305e+02	4.6597e+02	2.2953e+01
ABC	5.9628e+00	2.7467e+02	3.1386e+02	3.2065e+02	1.0242e+02	3.8073e+02	4.1139e+02	4.0433e+02	4.5691e+02	2.5980e+01
BA	3.5576e+02	4.0816e+02	4.0639e+02	4.9325e+02	3.3370e+01	7.5851e+02	1.0553e+03	1.0282e+03	1.3446e+03	1.3345e+02
FA	4.1741e+02	4.8492e+02	4.9218e+02	5.9007e+02	4.2726e+01	1.0524e+03	1.4327e+03	1.4341e+03	1.6677e+03	1.3575e+02
GWO	3.0426e+02	3.1613e+02	3.1370e+02	3.3215e+02	7.8614e+00	3.7662e+02	4.2998e+02	4.2805e+02	5.4322e+02	2.9982e+01
PSO	3.2161e+02	3.5690e+02	3.5620e+02	4.0874e+02	2.3328e+01	5.6207e+02	6.8988e+02	6.8637e+02	9.2665e+02	1.0308e+02
SOS	3.0799e+02	3.1517e+02	3.1449e+02	3.2975e+02	4.8594e+00	3.7854e+02	4.0894e+02	4.0157e+02	4.7007e+02	2.2919e+01
WfCMO5	3.0487e+02	3.0902e+02	3.0834e+02	3.1414e+02	2.5322e+00	3.7227e+02	3.9661e+02	3.9689e+02	4.3571e+02	1.3423e+01
WfCMO10	3.0487e+02	3.0911e+02	3.0907e+02	3.1325e+02	2.4655e+00	3.7411e+02	3.9324e+02	3.9099e+02	4.1776e+02	1.2101e+01
WfCMO20	3.0555e+02	3.1167e+02	3.1194e+02	3.1688e+02	3.4283e+00	3.7951e+02	4.0804e+02	4.0705e+02	4.8084e+02	2.2200e+01
Algorithm	F_{87}					F_{88}				
	Minimum	Average	Median	Maximum	Standard Deviation	Mininum	Average	Median	Maximum	Standard Deviation
COA5	5.2803e+02	5.9280e+02	5.8897e+02	6.5995e+02	3.1281e+01	6.8741e+02	7.9151e+02	7.9440e+02	9.0601e+02	4.8286e+01
COA10	4.7833e+02	5.5475e+02	5.4743e+02	6.3349e+02	3.9181e+01	6.6759e+02	7.4216e+02	7.4490e+02	8.0768e+02	3.8721e+01
ABC	4.4990e+02	6.2182e+02	6.5217e+02	6.9273e+02	7.8710e+01	7.8391e+02	8.7447e+02	8.6923e+02	9.3828e+02	3.1751e+01
BA	1.4302e+03	1.7900e+03	1.7766e+03	2.4687e+03	2.5198e+02	2.4506e+03	3.3609e+03	3.3578e+03	4.1376e+03	4.4415e+02
FA	2.2251e+03	2.6306e+03	2.5666e+03	3.0433e+03	2.1508e+02	3.9638e+03	4.3444e+03	4.3712e+03	4.8624e+03	1.7885e+02
GWO	5.4421e+02	6.1410e+02	6.0807e+02	8.3034e+02	5.3553e+01	9.8768e+02	1.1075e+03	1.1063e+03	1.2494e+03	5.3335e+01
PSO	9.5742e+02	1.1281e+03	1.1140e+03	1.5377e+03	1.2300e+02	1.8840e+03	2.1588e+03	2.1611e+03	2.4630e+03	1.6752e+02
SOS	4.9890e+02	5.5192e+02	5.4765e+02	6.4577e+02	2.8914e+01	7.5266e+02	8.2385e+02	8.1640e+02	9.3694e+02	5.0532e+01
WfCMO5	5.1238e+02	5.5470e+02	5.5137e+02	6.3389e+02	2.8979e+01	7.8600e+02	8.7789e+02	8.8038e+02	9.9610e+02	5.2532e+01
WfCMO10	5.0678e+02	5.4885e+02	5.4783e+02	5.9476e+02	2.6276e+01	7.8628e+02	8.7345e+02	8.6795e+02	9.8000e+02	4.2809e+01
WfCMO20	5.1296e+02	5.8692e+02	5.8124e+02	7.2368e+02	4.5293e+01	8.3281e+02	9.5568e+02	9.5302e+02	1.1192e+03	7.0678e+01

Table B.22: Descriptive statistics for IEEE-CEC 2017 benchmark functions considering the error measurements - Part XXII.

Algorithm	F_{89} Minimum	Average	Median	Maximum	Standard Deviation	F_{90} Mininum	Average	Median	Maximum	Standard Deviation
COA5	1.0004e+02	3.0880e+02	3.4525e+02	3.5878e+02	8.7465e+01	4.7894e+02	5.0892e+02	5.0609e+02	5.7073e+02	1.9744e+01
COA10	1.0000e+02	3.3504e+02	3.4219e+02	3.5268e+02	4.4595e+01	4.6579e+02	5.4871e+02	5.7558e+02	5.9451e+02	4.4518e+01
ABC	7.1328e+01	1.0727e+02	1.0398e+02	1.6278e+02	1.4433e+01	1.2385e+02	4.2973e+02	5.6410e+02	6.6659e+02	1.9572e+02
BA	1.0127e+02	4.3852e+02	4.5212e+02	5.2332e+02	7.3445e+01	1.0285e+03	1.2291e+03	1.2128e+03	1.5334e+03	1.0690e+02
FA	4.8763e+02	5.2595e+02	5.2819e+02	5.7601e+02	2.4418e+01	1.2271e+03	1.4307e+03	1.4541e+03	1.6312e+03	9.8742e+01
GWO	3.0006e+02	3.4496e+02	3.4537e+02	3.6318e+02	1.3074e+01	4.5471e+02	5.0019e+02	4.8849e+02	6.3139e+02	4.4123e+01
PSO	1.0000e+02	3.7335e+02	3.7164e+02	5.0461e+02	5.9144e+01	5.8345e+02	7.2822e+02	7.1676e+02	9.4913e+02	8.5841e+01
SOS	1.7651e-02	2.1783e+02	1.6771e+02	3.5768e+02	1.2471e+02	4.5408e+02	4.8498e+02	4.7980e+02	5.4699e+02	2.2910e+01
WfCMO5	1.0000e+02	3.0784e+02	3.3876e+02	3.4668e+02	8.2965e+01	4.4823e+02	4.7344e+02	4.7271e+02	5.2525e+02	1.4289e+01
WfCMO10	1.0000e+02	3.0075e+02	3.4012e+02	3.4812e+02	9.1375e+01	4.5554e+02	4.7550e+02	4.7417e+02	5.1395e+02	1.5936e+01
WfCMO20	2.8932e-07	2.8561e+02	3.4041e+02	3.4963e+02	1.0742e+02	4.4483e+02	4.8219e+02	4.7539e+02	5.5954e+02	2.7055e+01
Algorithm	F_{91} Minimum	Average	Median	Maximum	Standard Deviation	F_{92} Mininum	Average	Median	Maximum	Standard Deviation
COA5	6.0549e+02	6.7021e+02	6.6940e+02	7.4709e+02	3.3843e+01	1.1266e+03	1.2958e+03	1.3009e+03	1.4273e+03	6.9605e+01
COA10	6.1108e+02	7.8240e+02	8.1670e+02	8.4129e+02	7.5860e+01	1.0602e+03	1.2176e+03	1.2194e+03	1.3326e+03	5.6422e+01
ABC	2.2233e+02	9.6997e+02	9.9367e+02	1.0964e+03	1.5230e+02	1.3745e+03	1.4719e+03	1.4808e+03	1.5746e+03	4.1798e+01
BA	1.6901e+03	1.9344e+03	1.8613e+03	2.6908e+03	2.0550e+02	3.2985e+03	4.8707e+03	4.3428e+03	7.0503e+03	1.0745e+03
FA	2.1232e+03	2.4232e+03	2.4352e+03	2.6829e+03	1.2892e+02	6.9218e+03	7.7986e+03	7.8621e+03	8.6385e+03	5.5395e+02
GWO	6.1893e+02	6.9431e+02	6.6790e+02	9.6300e+02	8.5726e+01	1.3320e+03	1.5106e+03	1.5069e+03	1.6795e+03	7.6505e+01
PSO	9.7405e+02	1.2418e+03	1.2848e+03	1.5552e+03	1.4756e+02	2.3907e+03	3.3220e+03	3.2579e+03	5.0363e+03	5.3604e+02
SOS	5.8818e+02	6.3354e+02	6.1708e+02	7.5027e+02	4.1324e+01	1.1935e+03	1.3874e+03	1.3744e+03	1.5723e+03	1.0032e+02
WfCMO5	5.5455e+02	6.0547e+02	6.0716e+02	6.5064e+02	2.1899e+01	1.2670e+03	1.4301e+03	1.4163e+03	1.6717e+03	9.1396e+01
WfCMO10	5.6611e+02	6.1182e+02	6.1579e+02	6.6046e+02	2.4687e+01	1.3131e+03	1.4491e+03	1.4322e+03	1.6962e+03	9.6438e+01
WfCMO20	5.8587e+02	6.4674e+02	6.3879e+02	8.5588e+02	5.0644e+01	1.3760e+03	1.5928e+03	1.5835e+03	1.8214e+03	1.1996e+02

Table B.23: Descriptive statistics for IEEE-CEC 2017 benchmark functions considering the error measurements - Part XXIII.

Algorithm	F_{93} Minimum	Average	Median	Maximum	Standard Deviation	F_{94} Mininum	Average	Median	Maximum	Standard Deviation
COA5	1.0018e+02	3.4858e+02	3.9782e+02	3.9961e+02	1.1288e+02	3.8350e+02	3.8846e+02	3.8727e+02	4.2590e+02	7.1997e+00
COA10	3.9774e+02	3.9948e+02	3.9805e+02	4.4343e+02	8.3021e+00	3.8347e+02	3.8708e+02	3.8711e+02	3.8867e+02	7.7464e-01
ABC	6.0150e+01	1.5476e+02	1.2994e+02	3.2056e+02	6.2355e+01	3.8359e+02	3.8473e+02	3.8457e+02	3.8767e+02	8.9985e-01
BA	3.9785e+02	4.4207e+02	4.4590e+02	5.0955e+02	3.5528e+01	3.7568e+02	3.8198e+02	3.7926e+02	4.0274e+02	7.2605e+00
FA	7.5233e+02	1.5869e+03	1.5696e+03	2.6078e+03	5.1374e+02	7.6761e+03	1.3835e+04	1.3531e+04	2.0166e+04	3.1272e+03
GWO	3.9836e+02	4.2896e+02	4.4201e+02	4.4963e+02	1.9912e+01	4.0131e+02	4.5429e+02	4.5166e+02	5.1377e+02	2.6632e+01
PSO	3.9775e+02	4.4961e+02	4.4674e+02	6.4651e+02	5.2520e+01	3.8756e+02	4.1298e+02	4.0505e+02	5.0453e+02	2.7174e+01
SOS	3.9774e+02	4.1701e+02	3.9958e+02	4.4602e+02	2.2632e+01	3.8356e+02	3.9381e+02	3.8863e+02	4.4474e+02	1.4894e+01
WfCMO5	3.9790e+02	4.2650e+02	4.4352e+02	4.4668e+02	2.2453e+01	3.8679e+02	4.1360e+02	4.1333e+02	4.7073e+02	2.2343e+01
WfCMO10	3.9781e+02	4.1555e+02	3.9961e+02	4.4602e+02	2.2076e+01	3.8756e+02	4.0062e+02	3.8967e+02	4.4271e+02	1.8419e+01
WfCMO20	3.9774e+02	4.1378e+02	3.9961e+02	4.4583e+02	2.1618e+01	3.8455e+02	4.0092e+02	3.9124e+02	4.4391e+02	1.9081e+01
Algorithm	F_{95} Minimum	Average	Median	Maximum	Standard Deviation	F_{96} Mininum	Average	Median	Maximum	Standard Deviation
COA5	5.0090e+02	5.5992e+02	5.6266e+02	6.0617e+02	2.5758e+01	7.7705e+02	8.9497e+02	8.9725e+02	9.9624e+02	4.6722e+01
COA10	4.6034e+02	5.3029e+02	5.2837e+02	5.8213e+02	2.7158e+01	7.1870e+02	8.4418e+02	8.5366e+02	9.5455e+02	5.8836e+01
ABC	4.6873e+02	5.1599e+02	5.2020e+02	5.4326e+02	1.6079e+01	6.5166e+02	7.3826e+02	7.4417e+02	7.9491e+02	3.2054e+01
BA	4.3167e+02	4.5744e+02	4.3265e+02	5.8165e+02	3.6093e+01	6.2923e+02	7.3149e+02	7.1580e+02	8.5480e+02	6.3816e+01
FA	3.1457e+04	5.0888e+04	4.9629e+04	6.9642e+04	8.1911e+03	8.8823e+04	1.2650e+05	1.3029e+05	1.4541e+05	1.1796e+04
GWO	6.1289e+02	8.8251e+02	8.4312e+02	1.7044e+03	2.2044e+02	1.7756e+03	2.7652e+03	2.6213e+03	4.4764e+03	6.2365e+02
PSO	5.6624e+02	6.4128e+02	6.1908e+02	9.6655e+02	8.3222e+01	9.7818e+02	1.1517e+03	1.1124e+03	1.7083e+03	1.4975e+02
SOS	4.6683e+02	5.4663e+02	5.6176e+02	6.0052e+02	3.7908e+01	6.2042e+02	7.9850e+02	8.0382e+02	9.7415e+02	7.4989e+01
WfCMO5	5.5308e+02	5.9909e+02	6.0032e+02	6.3915e+02	1.8008e+01	8.1938e+02	9.4253e+02	9.4495e+02	1.0389e+03	5.6623e+01
WfCMO10	5.3202e+02	5.8696e+02	5.8617e+02	6.2701e+02	1.9511e+01	7.1384e+02	8.7363e+02	8.5740e+02	1.0086e+03	7.4899e+01
WfCMO20	4.7381e+02	5.7657e+02	5.7901e+02	6.1216e+02	2.5888e+01	7.2467e+02	8.9074e+02	8.7526e+02	1.0673e+03	7.2151e+01

Table B.24: Descriptive statistics for IEEE-CEC 2017 benchmark functions considering the error measurements - Part XXIV.

Algorithm	F_{97} Minimum	Average	Median	Maximum	Standard Deviation	F_{98} Mininum	Average	Median	Maximum	Standard Deviation
COA5	2.0002e+02	2.8742e+02	3.0002e+02	4.1638e+02	6.1853e+01	3.0020e+02	1.5617e+03	1.8362e+03	2.3977e+03	6.6168e+02
COA10	3.0000e+02	3.0662e+02	3.0000e+02	3.7573e+02	2.0661e+01	1.4017e+03	1.6962e+03	1.7067e+03	2.1280e+03	1.9909e+02
ABC	3.4994e+00	8.7475e+01	3.5873e+01	2.0793e+02	9.1612e+01	2.2386e+02	3.4759e+02	2.5538e+02	2.0443e+03	3.4301e+02
BA	3.0102e+02	1.2001e+03	1.1731e+03	2.1648e+03	5.6344e+02	2.2642e+03	7.6268e+03	7.4807e+03	9.5681e+03	1.4892e+03
FA	8.7011e+02	2.0938e+03	2.2459e+03	2.7858e+03	5.7852e+02	8.6614e+03	1.2406e+04	1.2471e+04	1.4819e+04	1.4305e+03
GWO	2.1161e+02	4.6424e+02	3.0011e+02	1.3110e+03	3.5195e+02	1.4960e+03	1.8843e+03	1.8585e+03	2.6701e+03	2.3663e+02
PSO	2.0000e+02	5.2546e+02	4.5686e+02	1.6782e+03	2.9010e+02	2.2052e+02	3.1973e+03	3.4586e+03	4.9859e+03	1.2285e+03
SOS	3.0000e+02	3.1829e+02	3.0000e+02	3.9299e+02	2.9698e+01	3.0000e+02	1.4057e+03	1.6080e+03	2.3079e+03	5.4344e+02
WfCMO5	3.6607e-10	3.1118e+02	3.0000e+02	4.3621e+02	9.3428e+01	3.0005e+02	1.5373e+03	1.5385e+03	1.9366e+03	2.8568e+02
WfCMO10	3.0000e+02	3.2756e+02	3.0000e+02	4.7287e+02	4.3305e+01	2.0000e+02	1.5298e+03	1.6240e+03	2.0002e+03	3.8063e+02
WfCMO20	3.0000e+02	3.0786e+02	3.0000e+02	3.4715e+02	1.7872e+01	2.0000e+02	1.4874e+03	1.6318e+03	2.1285e+03	5.0081e+02
Algorithm	F_{99} Minimum	Average	Median	Maximum	Standard Deviation	F_{100} Mininum	Average	Median	Maximum	Standard Deviation
COA5	1.9913e+03	2.7121e+03	2.7121e+03	3.3927e+03	3.2922e+02	6.2323e+03	7.6342e+03	7.6142e+03	9.2312e+03	7.7024e+02
COA10	2.0322e+03	2.5919e+03	2.4967e+03	3.5310e+03	3.8375e+02	5.9778e+03	7.0560e+03	7.0054e+03	8.7991e+03	6.7749e+02
ABC	3.3032e+02	1.0093e+03	4.8851e+02	3.8147e+03	1.0842e+03	4.7660e+02	9.2712e+03	9.9706e+03	1.0912e+04	2.3901e+03
BA	1.1938e+04	1.4155e+04	1.3782e+04	1.8447e+04	1.8631e+03	2.6273e+04	3.3748e+04	3.3028e+04	4.2376e+04	4.1993e+03
FA	1.9664e+04	2.6344e+04	2.6739e+04	3.1815e+04	2.7899e+03	6.4523e+04	8.1158e+04	7.9923e+04	9.7803e+04	8.1787e+03
GWO	2.3655e+03	3.2114e+03	3.1779e+03	4.0055e+03	3.8924e+02	8.2119e+03	9.9774e+03	1.0147e+04	1.1489e+04	8.5443e+02
PSO	4.1942e+03	6.3647e+03	6.3295e+03	8.2976e+03	1.1006e+03	5.6533e+03	2.1641e+04	2.2688e+04	3.0343e+04	5.1350e+03
SOS	1.9639e+03	2.7033e+03	2.6952e+03	4.6654e+03	4.6723e+02	3.0000e+02	8.8728e+03	8.9818e+03	1.3857e+04	2.2824e+03
WfCMO5	1.8523e+03	2.5467e+03	2.4779e+03	3.6040e+03	3.9878e+02	7.3402e+03	9.5112e+03	9.4094e+03	1.3616e+04	1.1281e+03
WfCMO10	3.4888e+02	2.6053e+03	2.6131e+03	3.6010e+03	5.4075e+02	7.5806e+03	9.5239e+03	9.6336e+03	1.0651e+04	7.4036e+02
WfCMO20	2.4047e+03	3.2868e+03	3.0651e+03	6.5556e+03	7.7116e+02	8.8166e+03	1.0479e+04	1.0527e+04	1.2244e+04	8.0435e+02

Table B.25: Descriptive statistics for IEEE-CEC 2017 benchmark functions considering the error measurements - Part XXV.

Algorithm	F_{101} Minimum	Average	Median	Maximum	Standard Deviation	F_{102} Mininum	Average	Median	Maximum	Standard Deviation
COA5	3.8898e+02	3.9016e+02	3.8991e+02	3.9268e+02	1.0414e+00	4.9045e+02	5.0795e+02	5.0966e+02	5.2578e+02	9.2642e+00
COA10	3.8898e+02	3.8962e+02	3.8964e+02	3.9033e+02	3.7617e-01	4.8560e+02	5.0108e+02	5.0251e+02	5.2084e+02	8.3257e+00
ABC	3.8895e+02	3.9470e+02	3.9472e+02	3.9942e+02	2.6520e+00	4.9796e+02	5.1158e+02	5.1227e+02	5.2096e+02	5.6646e+00
BA	3.9373e+02	4.6107e+02	4.5110e+02	5.7161e+02	4.6683e+01	4.7895e+02	1.0626e+03	1.0751e+03	1.7646e+03	3.5898e+02
FA	4.5378e+02	5.1962e+02	5.2399e+02	6.7284e+02	5.2642e+01	1.3406e+03	2.3129e+03	2.3103e+03	3.1405e+03	4.3906e+02
GWO	3.8947e+02	3.9655e+02	3.9480e+02	4.2100e+02	8.0453e+00	5.0729e+02	5.3939e+02	5.3636e+02	5.9455e+02	1.8737e+01
PSO	3.9501e+02	4.2833e+02	4.2130e+02	5.0256e+02	2.6981e+01	5.2435e+02	6.9449e+02	6.9121e+02	8.8761e+02	8.1521e+01
SOS	3.8898e+02	3.9001e+02	3.8966e+02	3.9519e+02	1.3547e+00	4.9532e+02	5.2126e+02	5.2079e+02	5.5558e+02	1.2682e+01
WfCMO5	3.8903e+02	3.9094e+02	3.9018e+02	3.9596e+02	2.0954e+00	5.0519e+02	5.2733e+02	5.2506e+02	5.6013e+02	1.2409e+01
WfCMO10	3.8901e+02	3.9069e+02	3.8971e+02	3.9527e+02	1.8438e+00	5.0269e+02	5.2965e+02	5.2557e+02	5.6230e+02	1.7454e+01
WfCMO20	3.8901e+02	3.9054e+02	3.8980e+02	3.9934e+02	2.0061e+00	4.9729e+02	5.2992e+02	5.2539e+02	5.9332e+02	1.9878e+01
Algorithm	F_{103} Minimum	Average	Median	Maximum	Standard Deviation	F_{104} Mininum	Average	Median	Maximum	Standard Deviation
COA5	5.3546e+02	6.4460e+02	6.3748e+02	7.5799e+02	5.3579e+01	6.8715e+02	7.9578e+02	7.9385e+02	8.9526e+02	4.9221e+01
COA10	5.0766e+02	6.2224e+02	6.0196e+02	7.8562e+02	7.3185e+01	6.6730e+02	7.4017e+02	7.3033e+02	8.9072e+02	5.3702e+01
ABC	5.9721e+02	6.4626e+02	6.4894e+02	7.0022e+02	2.5927e+01	6.9892e+02	7.5655e+02	7.5707e+02	7.9770e+02	2.3354e+01
BA	5.0001e+02	1.9619e+03	1.9479e+03	3.7720e+03	9.0252e+02	1.1701e+03	2.8017e+03	2.4838e+03	6.7276e+03	1.3751e+03
FA	2.6526e+03	4.8037e+03	4.8901e+03	6.3042e+03	9.0613e+02	1.0711e+04	1.3732e+04	1.4216e+04	1.5964e+04	1.4890e+03
GWO	6.3851e+02	7.6572e+02	7.5329e+02	9.3369e+02	6.5473e+01	9.2714e+02	1.1231e+03	1.1181e+03	1.4117e+03	1.0723e+02
PSO	1.0190e+03	1.4756e+03	1.4808e+03	1.9921e+03	2.5579e+02	1.1031e+03	2.4252e+03	2.4150e+03	3.6063e+03	5.7023e+02
SOS	5.8067e+02	7.2469e+02	7.2425e+02	9.2009e+02	9.5463e+01	7.3995e+02	9.3297e+02	9.2200e+02	1.3872e+03	1.1970e+02
WfCMO5	7.0952e+02	8.5907e+02	8.5638e+02	1.1291e+03	9.7311e+01	8.6277e+02	1.1115e+03	1.1167e+03	1.3612e+03	1.1547e+02
WfCMO10	6.7709e+02	7.9918e+02	7.7621e+02	1.0620e+03	8.9490e+01	8.4941e+02	1.1224e+03	1.1221e+03	1.3394e+03	1.1676e+02
WfCMO20	5.4545e+02	8.4007e+02	8.6809e+02	1.1244e+03	1.5971e+02	8.2883e+02	1.0966e+03	1.1236e+03	1.3328e+03	1.3063e+02

Table B.26: Descriptive statistics for IEEE-CEC 2017 benchmark functions considering the error measurements - Part XXVI.

Algorithm	F_{105} Minimum	Average	Median	Maximum	Standard Deviation	F_{106} Mininum	Average	Median	Maximum	Standard Deviation
COA5	3.0001e+02	3.3810e+02	3.3480e+02	3.9657e+02	3.7600e+01	3.3819e+02	4.2364e+02	4.1662e+02	4.6985e+02	2.5990e+01
COA10	3.0000e+02	3.4165e+02	3.0000e+02	5.8373e+02	6.4787e+01	3.1126e+02	4.1110e+02	4.0884e+02	4.6673e+02	3.7959e+01
ABC	2.8147e+01	2.6798e+02	3.0629e+02	3.7413e+02	9.8855e+01	4.0035e+02	4.0924e+02	4.0864e+02	4.1893e+02	4.6977e+00
BA	2.3220e+01	4.3538e+02	4.7726e+02	4.9028e+02	9.0746e+01	3.0076e+02	4.0483e+02	4.1001e+02	4.6400e+02	4.9563e+01
FA	9.3067e+02	1.0989e+03	1.1037e+03	1.2584e+03	8.4222e+01	6.6366e+03	9.7450e+03	9.9835e+03	1.1740e+04	1.4611e+03
GWO	3.6459e+02	5.6532e+02	6.0478e+02	6.1280e+02	8.3407e+01	4.8103e+02	5.4928e+02	5.2744e+02	6.4345e+02	5.1112e+01
PSO	3.0000e+02	5.7872e+02	6.0750e+02	1.1058e+03	1.5237e+02	4.2509e+02	5.7298e+02	5.4451e+02	1.1292e+03	1.3128e+02
SOS	9.0949e-13	3.2534e+02	3.0000e+02	6.1182e+02	9.8662e+01	3.0000e+02	3.5652e+02	3.1865e+02	4.6185e+02	6.0799e+01
WfCMO5	3.0000e+02	4.0905e+02	4.1575e+02	6.0269e+02	5.7234e+01	4.1586e+02	4.4863e+02	4.4999e+02	4.9711e+02	1.9294e+01
WfCMO10	3.0000e+02	3.9941e+02	3.9657e+02	6.1182e+02	6.8358e+01	3.9840e+02	4.2529e+02	4.2077e+02	4.6728e+02	1.9089e+01
WfCMO20	3.0000e+02	3.5212e+02	3.0001e+02	6.1182e+02	7.1696e+01	3.9762e+02	4.2843e+02	4.2407e+02	4.9158e+02	2.3621e+01
Algorithm	F_{107} Minimum	Average	Median	Maximum	Standard Deviation	F_{108} Mininum	Average	Median	Maximum	Standard Deviation
COA5	4.6391e+02	5.2479e+02	5.1954e+02	6.1906e+02	2.7909e+01	6.4681e+02	7.0240e+02	7.0180e+02	7.6947e+02	3.1327e+01
COA10	4.6157e+02	5.0867e+02	5.0807e+02	5.7901e+02	2.5061e+01	6.0217e+02	3.9114e+03	6.9474e+02	1.3205e+04	5.2392e+03
ABC	4.6460e+02	4.8910e+02	4.8991e+02	5.0491e+02	1.0783e+01	5.5097e+02	5.9857e+02	6.0046e+02	6.2080e+02	1.6527e+01
BA	4.4126e+02	4.7645e+02	4.7753e+02	5.8762e+02	2.6735e+01	4.7409e+02	5.1889e+02	5.2020e+02	5.6965e+02	2.0482e+01
FA	1.6441e+04	1.9320e+04	1.9003e+04	2.3203e+04	1.8960e+03	5.5507e+04	6.8557e+04	7.0199e+04	7.6719e+04	5.8941e+03
GWO	6.9158e+02	1.0325e+03	9.9795e+02	1.7592e+03	2.1329e+02	1.9227e+03	3.7374e+03	3.6236e+03	6.7723e+03	1.1081e+03
PSO	5.2271e+02	1.1141e+03	7.3858e+02	4.6763e+03	8.4702e+02	8.0170e+02	1.9316e+03	1.5665e+03	4.8177e+03	1.0979e+03
SOS	4.5885e+02	4.9034e+02	4.9931e+02	5.9677e+02	2.9388e+01	5.2741e+02	5.8816e+02	5.8666e+02	6.9671e+02	3.6754e+01
WfCMO5	5.0073e+02	5.5468e+02	5.5573e+02	6.2726e+02	2.7642e+01	6.6994e+02	7.5060e+02	7.5148e+02	8.1191e+02	3.2954e+01
WfCMO10	4.8614e+02	5.3616e+02	5.2749e+02	6.1846e+02	2.9176e+01	6.4582e+02	7.2952e+02	7.2091e+02	9.0035e+02	5.4993e+01
WfCMO20	4.7873e+02	5.4091e+02	5.3341e+02	6.1926e+02	3.3396e+01	6.4208e+02	7.1183e+02	7.1302e+02	7.8347e+02	3.2300e+01

Table B.27: Descriptive statistics for IEEE-CEC 2017 benchmark functions considering the error measurements - Part XXVII.

Algorithm	F_{109} Minimum	Average	Median	Maximum	Standard Deviation	F_{110} Mininum	Average	Median	Maximum	Standard Deviation
COA5	2.3162e+02	2.4133e+02	2.3904e+02	2.6238e+02	7.8742e+00	4.9370e+02	6.7309e+02	6.6309e+02	9.2054e+02	1.0847e+02
COA10	2.3210e+02	2.3989e+02	2.3834e+02	2.5793e+02	5.8428e+00	4.5522e+02	6.4477e+02	6.6175e+02	9.1294e+02	1.4120e+02
ABC	1.6441e+02	2.5500e+02	2.6371e+02	2.7920e+02	2.6610e+01	3.8156e+02	6.0310e+02	5.9878e+02	8.3853e+02	9.8219e+01
BA	2.7266e+02	4.8744e+02	4.6255e+02	8.4846e+02	1.3968e+02	1.3577e+03	1.9969e+03	1.8844e+03	2.6191e+03	3.3089e+02
FA	6.0121e+02	9.2714e+02	9.3930e+02	1.2798e+03	1.8265e+02	2.9276e+03	1.5924e+04	9.4735e+03	6.1917e+04	1.3035e+04
GWO	2.3707e+02	2.7631e+02	2.7057e+02	3.6585e+02	3.0673e+01	5.5222e+02	7.8492e+02	7.2919e+02	1.1437e+03	1.6178e+02
PSO	2.4609e+02	3.3629e+02	3.1793e+02	4.4864e+02	6.0638e+01	7.3418e+02	1.4534e+03	1.4097e+03	2.5525e+03	4.1524e+02
SOS	2.4533e+02	2.6780e+02	2.6934e+02	2.8792e+02	1.1453e+01	3.9409e+02	5.3587e+02	5.1942e+02	7.4887e+02	9.1842e+01
WfCMO5	2.4016e+02	2.5789e+02	2.5589e+02	2.8692e+02	1.2718e+01	4.7705e+02	5.9788e+02	5.7385e+02	8.5206e+02	8.6116e+01
WfCMO10	2.4223e+02	2.5678e+02	2.5673e+02	2.6999e+02	8.0285e+00	4.5157e+02	6.1432e+02	5.9728e+02	9.3209e+02	1.1332e+02
WfCMO20	2.4351e+02	2.5890e+02	2.5797e+02	2.7290e+02	7.8249e+00	5.3473e+02	7.3885e+02	6.6167e+02	1.2556e+03	1.9529e+02
Algorithm	F_{111} Minimum	Average	Median	Maximum	Standard Deviation	F_{112} Mininum	Average	Median	Maximum	Standard Deviation
COA5	5.4748e+02	1.0394e+03	1.1068e+03	1.4843e+03	2.4864e+02	2.1749e+03	2.9556e+03	2.9040e+03	3.7064e+03	3.9111e+02
COA10	5.5005e+02	1.2798e+03	1.2926e+03	2.1282e+03	4.5703e+02	2.3428e+03	3.0599e+03	3.0138e+03	4.2012e+03	4.2981e+02
ABC	7.7810e+02	1.0750e+03	1.0647e+03	1.3236e+03	1.3837e+02	3.2538e+03	3.8515e+03	3.8412e+03	4.2741e+03	2.3972e+02
BA	2.3885e+03	3.1853e+03	3.1438e+03	3.8921e+03	4.1313e+02	5.3505e+03	6.7086e+03	6.3688e+03	9.3429e+03	1.0848e+03
FA	5.7088e+04	1.3182e+06	5.4507e+05	5.2197e+06	1.5062e+06	8.7792e+05	1.1485e+07	9.7709e+06	3.1721e+07	7.8261e+06
GWO	8.4119e+02	1.3394e+03	1.3242e+03	1.9843e+03	2.7387e+02	2.7160e+03	4.3523e+03	4.3633e+03	5.3610e+03	5.9489e+02
PSO	1.8367e+03	3.0267e+03	2.7590e+03	6.0845e+03	9.1843e+02	4.7249e+03	5.9031e+03	5.7718e+03	7.8509e+03	7.7758e+02
SOS	4.7643e+02	7.5373e+02	7.3723e+02	1.0812e+03	1.6130e+02	2.2787e+03	3.0267e+03	2.9622e+03	4.0945e+03	5.1259e+02
WfCMO5	5.3712e+02	1.0183e+03	1.0416e+03	1.5084e+03	2.5094e+02	2.4312e+03	3.4861e+03	3.5013e+03	4.5929e+03	5.3479e+02
WfCMO10	7.5518e+02	1.0515e+03	9.5792e+02	1.9825e+03	2.7593e+02	2.3556e+03	3.4021e+03	3.4376e+03	4.4662e+03	5.6207e+02
WfCMO20	6.7013e+02	1.0070e+03	9.3071e+02	1.6169e+03	2.5673e+02	2.5741e+03	3.6951e+03	3.5324e+03	5.1447e+03	5.3605e+02

Table B.28: Descriptive statistics for IEEE-CEC 2017 benchmark functions considering the error measurements - Part XXVIII.

Algorithm	F_{113} Minimum	Average	Median	Maximum	Standard Deviation	F_{114} Mininum	Average	Median	Maximum	Standard Deviation
COA5	5.2977e+02	1.2281e+03	1.0876e+03	3.2277e+03	6.0843e+02	2.5040e+03	4.6536e+03	4.4827e+03	9.4516e+03	1.7012e+03
COA10	5.3449e+02	2.0842e+03	9.7078e+02	3.1412e+04	5.5617e+03	2.2965e+03	6.7722e+03	4.2529e+03	2.2124e+04	4.8595e+03
ABC	1.1606e+03	1.2015e+04	6.4077e+03	1.0422e+05	2.0268e+04	3.2664e+03	5.7785e+03	5.1885e+03	1.0751e+04	1.9198e+03
BA	4.4988e+03	4.1140e+04	3.5838e+04	2.3321e+05	4.1036e+04	5.3684e+05	2.5532e+06	2.6330e+06	5.4991e+06	1.3224e+06
FA	8.8286e+05	3.2936e+07	1.2025e+07	1.5245e+08	4.2167e+07	1.0651e+09	3.6591e+09	3.3295e+09	7.5292e+09	1.4890e+09
GWO	1.9223e+03	4.1627e+05	8.5531e+03	1.6895e+06	5.8840e+05	2.6936e+05	4.2598e+06	3.3679e+06	1.3697e+07	3.3802e+06
PSO	3.9451e+02	1.4518e+06	8.6406e+05	7.6281e+06	1.6503e+06	4.2867e+03	4.7339e+06	1.3888e+05	5.3764e+07	1.2048e+07
SOS	2.2297e+03	9.3716e+04	5.3350e+03	8.1777e+05	2.4825e+05	4.2872e+03	1.2995e+04	1.2289e+04	3.5554e+04	6.0573e+03
WfCMO5	3.9700e+02	4.2160e+03	4.5113e+02	1.1297e+05	2.0540e+04	3.3245e+03	7.4070e+03	6.3885e+03	1.5709e+04	3.5638e+03
WfCMO10	3.9522e+02	5.2366e+04	4.4633e+02	8.8243e+05	1.9654e+05	4.4114e+03	9.4988e+03	9.4140e+03	2.1204e+04	3.9577e+03
WfCMO20	3.9700e+02	5.7096e+04	4.7848e+02	8.8187e+05	2.1563e+05	4.4951e+03	1.8203e+04	1.4075e+04	5.5485e+04	1.3576e+04
Algorithm	F_{115} Minimum	Average	Median	Maximum	Standard Deviation	F_{116} Mininum	Average	Median	Maximum	Standard Deviation
COA5	5.9974e+05	7.2846e+05	6.8776e+05	9.3598e+05	1.1211e+05	2.7466e+03	7.0341e+03	5.2812e+03	1.6844e+04	4.1136e+03
COA10	5.8033e+05	7.6747e+05	6.5904e+05	1.5089e+06	2.6127e+05	2.5806e+03	6.1672e+03	5.2420e+03	1.6442e+04	3.5623e+03
ABC	6.1356e+05	7.2372e+05	7.3602e+05	8.3125e+05	5.0706e+04	3.4280e+03	1.1066e+04	1.0645e+04	1.8805e+04	4.3065e+03
BA	1.5856e+07	2.0533e+07	2.0641e+07	2.6381e+07	2.7747e+06	9.3333e+06	1.7092e+07	1.6757e+07	2.8309e+07	4.6293e+06
FA	6.7083e+09	1.6963e+10	1.6361e+10	2.5413e+10	5.4817e+09	4.9878e+10	7.3651e+10	7.4564e+10	9.9438e+10	1.1078e+10
GWO	3.5335e+07	7.1495e+07	6.3654e+07	1.5007e+08	2.9132e+07	2.8193e+07	3.7463e+08	2.3343e+08	1.7547e+09	3.9064e+08
PSO	1.0528e+06	7.4827e+06	3.2287e+06	7.1281e+07	1.3638e+07	2.3571e+06	9.2077e+08	5.2411e+08	4.2077e+09	1.0588e+09
SOS	5.8831e+05	9.0628e+05	9.1005e+05	1.7208e+06	2.5046e+05	2.6945e+03	6.3806e+03	3.6460e+03	1.7093e+04	4.8185e+03
WfCMO5	7.3540e+05	8.9572e+05	8.7124e+05	1.1186e+06	1.0357e+05	7.4398e+03	2.0359e+04	1.8344e+04	5.7926e+04	1.1765e+04
WfCMO10	7.5832e+05	9.0041e+05	8.5732e+05	1.3456e+06	1.2324e+05	4.5811e+03	1.0966e+04	9.3618e+03	1.9282e+04	4.0961e+03
WfCMO20	6.2343e+05	9.0237e+05	8.9484e+05	1.4075e+06	1.8931e+05	4.3786e+03	1.0764e+04	8.8821e+03	2.2039e+04	4.6466e+03

Table B.29: Descriptive statistics for IEEE-CEC 2017 benchmark functions considering the error measurements - Part XXIX.